

UNIVERSIDADE DE LISBOA
FACULDADE DE CIÊNCIAS
DEPARTAMENTO DE QUÍMICA E BIOQUÍMICA



**THE INTERPLAY BETWEEN HIV-1 gp41,
MEMBRANES AND PRE-FUSION ANTIVIRAL
AGENTS**

Ana Salomé Rocha do Nascimento Veiga

DOUTORAMENTO EM BIOQUÍMICA
(Especialidade de Biofísica Molecular)

2007

UNIVERSIDADE DE LISBOA
FACULDADE DE CIÊNCIAS
DEPARTAMENTO DE QUÍMICA E BIOQUÍMICA



**THE INTERPLAY BETWEEN HIV-1 gp41,
MEMBRANES AND PRE-FUSION ANTIVIRAL
AGENTS**

Ana Salomé Rocha do Nascimento Veiga

Tese orientada pelo Prof. Doutor Miguel Augusto Rico Botas Castanho

DOUTORAMENTO EM BIOQUÍMICA
(Especialidade de Biofísica Molecular)

2007

PREFÁCIO

Os estudos que resultaram nesta tese foram objecto dos seguintes artigos já publicados ou submetidos para publicação:

Veiga S, Henriques S, Santos NC, and Castanho M (2004) Putative role of membranes in the HIV fusion inhibitor enfuvirtide mode of action at the molecular level. *Biochem. J.* 377, 107-110.

Veiga AS, Santos NC, Loura LMS, Fedorov A, and Castanho MARB (2004) HIV fusion inhibitor peptide T-1249 is able to insert or adsorb to lipidic bilayers. Putative correlation with improved efficiency. *J. Am. Chem. Soc.* 126, 14758-14763.

Veiga S, Yuan Y, Li X, Santos NC, Liu G, and Castanho MARB (2006) Why are HIV-1 fusion inhibitors not effective against SARS-CoV? Biophysical evaluation of molecular interactions. *Biochim. Biophys. Acta* 1760, 55-61.

Veiga AS, Santos NC, and Castanho MARB (2006) An insight on the leading HIV entry inhibitors. *Recent Patents on Anti-Infective Drug Discovery* 1, 67-73.

Veiga AS and Castanho MARB (2006) The membranes' role in the HIV-1 neutralizing monoclonal antibody 2F5 mode of action needs re-evaluation. *Antiviral Res.* 71, 69-72.

Veiga AS and Castanho MARB (2007) The influence of cholesterol on the interaction of HIV gp41 membrane proximal domain derived peptides with lipid bilayers. *FEBS J.* 274, 5096-5104.

Veiga AS, Pattenden LK, Fletcher JM, Castanho MARB, and Aguilar M (2007) HIV-1 Monoclonal Antibodies 2F5 and 4E10 membranes interaction in the presence and absence of its epitopes. *Submetido*.

Um outro estudo envolvendo também proteínas virais, mas não directamente relacionado com o estudo aqui apresentado, é apresentado no anexo II:

Pérez-Berná AJ, Veiga AS, Castanho MARB, and Villalaín J. (2007) Hepatitis C virus core protein binding to lipid membranes: the role of domains 1 and 2. *J. Viral Hepatitis, in press*.

Gostaria de agradecer a todos os que de algum modo contribuíram para que a realização desta tese fosse possível.

À Fundação para a Ciência e a Tecnologia, pelo apoio financeiro concedido (bolsa SFRH/BD/14336/2003).

Ao Centro de Química e Bioquímica da Faculdade de Ciências da Universidade de Lisboa pelas condições de trabalho necessárias para a realização deste trabalho.

Ao meu orientador de trabalho, Professor Miguel Castanho, por me aceitar no seu laboratório e tornar possíveis as condições necessárias à realização dos trabalhos da tese. Agradeço ainda por toda a dedicação e apoio ao meu trabalho, mas principalmente pela amizade.

Aos meus colegas do grupo de Biofísica Molecular: Henri Franquelim, Marta Ribeiro e Manuel Melo pela amizade, companheirismo e boa disposição no dia-a-dia do laboratório. Um agradecimento especial à Sónia Henriques, companheira de licenciatura e doutoramento, pelo companheirismo e ajuda, por todos os momentos partilhados, pelas úteis discussões científicas, e não só, e principalmente pela amizade.

Um agradecimento especial ao Professor Manuel Prieto pelo constante encorajamento e discussões científicas, disponibilidade para a realização de alguns trabalhos experimentais no seu laboratório, e também pela sua amizade. Ao professor Luís Loura por toda a ajuda e disponibilidade, em especial na realização dos estudos de espectroscopia de fluorescência resolvida no tempo do inibidor de fusão T-1249. Aos restantes membros do grupo de Biofísica Molecular do Centro de Química-Física Molecular do Instituto Superior Técnico, por toda a ajuda e disponibilidade. Ao Doutor Alexander Fedorov, pela contribuição essencial para este trabalho através da realização das medidas de fluorescência resolvidas no tempo.

Ao Professor Nuno Santos, por toda a ajuda concedida e disponibilidade demonstrada ao longo de todo o doutoramento, mas também pela amizade.

À Professora Marie-Isabel Aguilar por me ter recebido no seu laboratório para os estudos de *Surface Plasmon Resonance* dos anticorpos 2F5 e 4E10, e por todo o apoio concedido. Ao Leonard Pattenden pelo seu apoio durante a realização do trabalho experimental, e pelo seu entusiasmo pelo trabalho. Ao Jordan Fletcher que tornou possível a síntese do péptido necessário à realização do trabalho experimental. Um agradecimento especial à Sharon Unabia por toda a assistência técnica, ajuda e

disponibilidade e por todos os momentos de diversão. Um agradecimento também aos restantes elementos do grupo por todas a ajuda e disponibilidade demonstradas.

À Roche (Palo Alto, CA, EUA) por ter facultado os inibidores de fusão T20 e T-1249.

Ao Professor Cláudio Soares pela ajuda nos modelos moleculares do T20 e T-1249.

Ao Professor João Pessoa, Instituto Superior Técnico, por me ter facultado a utilização do aparelho de difracção circular. Um agradecimento especial à Susana por toda a incassável ajuda na realização das medidas.

Ao Professor José Villalaín por me ter recebido no seu laboratório para a realização dos estudos de *FTIR* e por todo o apoio concedido. À Ana Joaquina Pérez-Berná pelo seu apoio durante a realização do trabalho experimental, e pela sua amizade. À Ana Isabel Gómez por toda a assistência técnica, ajuda, disponibilidade e pela amizade. Um agradecimento também aos restantes elementos do grupo por todas a ajuda e disponibilidade demonstradas.

À Virginia, companheira de licenciatura, por toda a amizade, partilha de muitos bons momentos, e pelo encorajamento constante no trabalho.

E finalmente gostava de agradecer aos meus pais pelo apoio e encorajamento sem os quais esta tese não seria possível.

RESUMO

O vírus da imunodeficiência humana (VIH) é o agente causador do síndrome da imunodeficiência adquirida (SIDA) e o seu modo de actuação consiste, sobretudo, em infectar e destruir células T CD4⁺ do organismo hospedeiro. Existem dois tipos do vírus, VIH-1 e VIH-2, mas é o VIH-1 o mais virulento e o responsável pela maior parte dos casos de SIDA no mundo.

O envelope do vírus consiste numa bicamada lipídica, derivada da célula hospedeira, que possui um complexo glicoproteico que confere ao vírus a capacidade para entrar nas células alvo. Este complexo é formado pelas subunidades gp120 (subunidade superfície) e gp41 (subunidade transmembranar), que se mantêm associadas de modo não covalente e oligomerizam sob a forma de trímeros na superfície do vírus. A gp41 é uma proteína transmembranar constituída por um domínio extracelular (ectodomínio), um domínio transmembranar e um domínio intracelular (endodomínio). O ectodomínio da gp41 contém várias regiões funcionais importantes para o processo de fusão viral. O péptido de fusão, localizado no terminal N da proteína, é uma região hidrófoba e rica em resíduos de glicina. Este domínio é essencial para o processo de fusão, nomeadamente para a penetração inicial da membrana da célula alvo. No seguimento do péptido de fusão encontram-se duas regiões que têm tendência para formar superenrolamentos de hélice α . A região adjacente ao péptido de fusão é chamada NHR e a região CHR é a que precede o segmento transmembranar. Os péptidos derivados destas regiões são chamados péptidos N- e C-, respectivamente. No terminal C da proteína, entre a região CHR e o domínio transmembranar, situa-se a chamada *região próxima da membrana* (MPR – membrane proximal region). Esta região é rica em resíduos de triptofano e parece ter também um papel chave na fusão viral.

O primeiro passo no processo de infecção consiste na ligação da gp120 ao receptor (CD4) e co-receptores (CXCR4 ou CCR5) na superfície das células alvo. Esta interacção induz alterações conformacionais na gp120 e modula as interacções gp120/gp41. A gp41 sofre então uma alteração conformacional e a sua estrutura nativa transita para uma estrutura intermediária de *pré-hairpin*. Estas variações na gp41 incluem a exposição do péptido de fusão e a sua inserção na membrana alvo. Posteriormente dá-se uma associação entre as regiões NHR e CHR levando à formação

da estrutura em *hairpin* (trímero em dímeros de hélices antiparalelas), activa para a fusão, o que leva à aproximação das membranas celular e viral. Na estrutura em *hairpin* a região NHR forma três hélices centrais arranjadas num superenrolamento trimérico, enquanto que a região CHR forma três hélices exteriores que encaixam de um modo antiparalelo em cavidades hidrófobas na superfície do superenrolamento. O que ocorre desde a aproximação das membranas até à fusão completa não está clarificado mas parece envolver a formação de agregados dos trímeros da proteína do envelope para formar poros de fusão.

O tratamento mais comum para os doentes com SIDA baseia-se na aplicação de combinações de drogas anti-VIH, nomeadamente inibidores do transcriptase reversa e do protease, dois enzimas virais com importância ao nível da replicação do vírus. Apesar dos benefícios do uso destas drogas, a sua utilização é limitada devido os seus efeitos tóxicos e aparecimento de estirpes resistentes. Assim, tornou-se óbvia a necessidade de desenvolvimento de drogas mais eficientes, menos tóxicas e que permitam eliminar os efeitos adversos associados à acção das drogas no interior das células.

Do trabalho científico desenvolvido nos últimos anos, resultaram fármacos que têm como objectivo actuar ao nível da entrada do vírus nas células, nomeadamente, na ligação da gp120 ao CD4, na ligação da gp120 aos co-receptores e na fusão do envelope do vírus com a membrana alvo. Apesar da enorme quantidade de compostos em desenvolvimento e até em fase de testes clínicos, o T20 (também chamado Enfuvirtide ou pelo nome comercial da marca Fuzeon), um inibidor de fusão, é o único já aprovado para aplicação clínica. No entanto, apesar da sua comprovada eficácia clínica, não há consenso sobre o seu modo de actuação ao nível molecular. O mecanismo de acção mais aceite envolve a interacção do T20 com a região NHR da gp41, na fase de pré-*hairpin*, impedindo a formação da estrutura em *hairpin* e deste modo a fusão viral com a membrana celular.

As membranas biológicas são entidades complexas, constituídas principalmente por lípidos e proteínas, que limitam as células, constituindo uma barreira entre o meio exterior e interior. A base estrutural das biomembranas é a bicamada lipídica. No entanto, a distribuição lipídica nas biomembranas pode ser assimétrica levando a que as duas camadas tenham uma composição lipídica diferente. Além disso, apesar de grande parte dos lípidos na bicamada formarem uma mistura uniforme e homogénea na

chamada fase fluida, podem ocorrer heterogeneidades laterais, ou domínios, com composições lipídicas distintas. Os *rafts* lipídicos, são domínios encontrados nas membranas plasmáticas que são enriquecidos em colesterol e esfingolípidos. Estes domínios existem numa fase de líquido ordenado que é mais ordenada e compacta que o resto da bicamada, em fase fluida. Tem sido proposto que os *rafts* podem funcionar como plataformas para a reunião de complexos macromoleculares associados a membranas com importância ao nível de vários processos celulares, entrada de vírus como o VIH-1 para as células (uma vez que receptores e co-receptores se encontram provavelmente associados a *rafts*) e a formação de vírus a partir da célula infectada. De resto, a membrana deste vírus é muito enriquecida em colesterol e esfingolípidos, relativamente aos níveis encontrados nas membranas das células alvo, sendo sugerido que isso se deve ao facto de a formação dos novos vírus se fazer através de *rafts* lipídicos. O colesterol possui um papel central uma vez que mantém os *rafts* num estado funcional.

O estudo da interacção entre péptidos e/ou proteínas e biomembranas é muitas vezes necessário de modo a clarificar alguns processos em que ambos estejam envolvidos. No entanto, as membranas biológicas são sistemas demasiado complexos para serem usadas como tal neste tipo de estudo. Uma alternativa viável é o estudo destas interacções em sistemas modelo de membranas, nomeadamente vesículas lipídicas unilamelares. Podendo ser preparadas em diferentes tamanhos, foram no presente trabalho utilizados na sua maioria vesículas unilamelares grandes com diâmetro aproximado de 100 nm. Estes sistemas miméticos de membranas biológicas permitem uma base de estudo simplificada em simultâneo com a manutenção das principais propriedades das biomembranas.

Os estudos realizados ao longo deste trabalho foram essencialmente biofísicos, baseados em técnicas de espectroscopia de fluorescência, dado o facto de os péptidos e proteínas estudados serem intrinsecamente fluorescentes sem necessidade de acoplamento de sondas.

O T20, um péptido sintético que corresponde a uma sequência linear da gp41 do VIH-1 (entre o terminal C da região CHR e o terminal N da MPR), é um potente inibidor da fusão deste vírus. Apesar de estar aprovado para uso clínico, não existe ainda consenso acerca da sua acção ao nível molecular. Investigou-se a possível existência de um papel para as membranas lipídicas no modo de acção do T20, sendo que este envolvimento é sugerido tanto pela estrutura secundária do péptido, como por

estudos de hidrofobicidade teórica e por trabalhos já publicados. Os resultados obtidos permitem inferir um modelo para descrever a acção do T20. O T20 insere-se na membrana principalmente nas zonas mais fluidas, ao nível da camada externa da bicamada lipídica. Devido ao elevado conteúdo em colesterol do envelope do vírus, o T20 não tem tendência a ligar-se a este. Assim, o T20 concentra-se na membrana celular podendo esta funcionar como um reservatório. No entanto, a concentração do T20 no ambiente aquoso pode ficar suficientemente elevada de modo a permitir ligação à gp41, inibindo deste modo o processo de fusão pelo modelo de acção mais aceite. Por outro lado, a ligação do T20 à membrana pode possibilitar a sua ligação a outras regiões da gp41, diferentes da ligação que ocorre em solução aquosa, e que também permitem o bloqueio da fusão.

O T-1249 é um péptido inibidor de fusão do VIH-1 de segunda geração, mais potente do que o T20 e activo em estirpes que apresentam resistência à inibição pelo T20. Este péptido foi obtido através de técnicas de *design* de drogas, sendo composto por sequências do VIH-1, VIH-2 e do vírus da imunodeficiência símio (VIS). Não havendo também consenso sobre o seu mecanismo de acção e tendo em conta os resultados obtidos com o T20, a interacção deste péptido com membranas lipídicas foi também investigada. Tal como o T20, o T-1249 insere-se na camada externa da bicamada lipídica, nas zonas fluidas da membrana. No entanto, ao contrário do T20, o T-1249 tem a capacidade de adsorver a domínios ricos em colesterol. Esta capacidade aumenta a concentração local de T-1249 quer nas zonas da célula onde ocorre a fusão, os *rafts* lipídicos, quer na membrana do vírus, também rica em colesterol. Assim, tanto a membrana da célula como a membrana do vírus podem funcionar como um reservatório de péptido. O aumento da eficácia clínica do T-1249 em relação ao T20 pode estar relacionada com as diferenças da interacção de ambos com as membranas, descritas para os dois inibidores.

O SARS-CoV é um novo coronavírus identificado como o agente causador do síndrome respiratório agudo. A glicoproteína S do envelope do vírus é responsável, à semelhança da gp120/gp41, pela entrada do vírus nas células alvo. Alguns estudos apontam para um mecanismo de entrada na célula semelhante ao usado pelo VIH-1. Sendo um novo vírus não estão ainda disponíveis medicamentos específicos para o inibir. Dadas as semelhanças entre os dois vírus e com base numa análise estrutural da gp41 e da proteína S2, foi proposto que o T20 poderia inibir a fusão do SARS-CoV, através de um mecanismo semelhante ao mais aceite, ou seja, a inibição da formação da

estrutura em *hairpin*. Num estudo efectuado no âmbito desta tese foi investigado o potencial do T20 e T-1249 para inibirem o SARS-CoV. Os resultados obtidos permitem concluir que apesar de ocorrer a interacção entre o T20 e o T-1249 e a região NHR do vírus, que pode levar à inibição do SARS-CoV, esta ligação pode não ser suficientemente forte para conseguir uma inibição efectiva.

A MPR no ectodomínio da gp41 do VIH-1 tem um papel chave no processo de fusão viral. Tem-se mostrado que esta região tem a capacidade de interactuar com membranas e provocar a sua destabilização, num processo semelhante à acção do péptido de fusão na membrana alvo. Dada a proximidade entre esta região e a membrana do vírus o efeito deve ser exercido sobre esta. Além disso, esta região contém uma pequena sequência normalmente definida como um domínio de ligação preferencial ao colesterol. Investigou-se a influência do colesterol na interacção com membranas de péptidos correspondentes à MPR como um todo e sem a sequência de ligação específica ao colesterol, e de um péptido correspondente apenas ao domínio de ligação ao colesterol. Propõe-se que a MPR pode ter uma função muito específica no processo de fusão viral de membranas, através da acção concertada de domínios de ligação ao colesterol e domínios que não ligam ao colesterol.

O 2F5 e o 4E10 são dois anticorpos com uma acção potente contra o VIH-1, cujos epitopos se encontram localizados na MPR no ectodomínio da gp41. Tem sido sugerido que as membranas lipídicas, mais concretamente a membrana do vírus, podem ter um papel no mecanismo de acção destes anticorpos, que ainda não é conhecido. Alguns estudos propuseram que estes anticorpos podem interactuar com a membrana viral através de uma superfície hidrófoba presente numa das cadeias pesadas. Estudou-se a interacção do 2F5 e do 4E10 com modelos de biomembranas, na presença e na ausência de um péptido que contempla o epitopo de ambos, de modo a investigar o possível papel das membranas no seu modo de acção. Tanto o 2F5 como o 4E10 têm a capacidade de interactuar com membranas, interacção mais fraca no caso do 2F5, e com o seu epitopo quando este está presente nas mesmas. Esta capacidade pode ser uma adaptação dos anticorpos para se ligarem a um epitopo que está tão próximo da membrana ou devido à existência de uma dependência da membrana na conformação do epitopo óptima para a ligação.

Palavras Chave: HIV-1; gp41; membranas; T20; CHR; MPR

SUMMARY

The HIV-1 envelope glycoprotein complex plays an important role in viral entry. Its surface subunit gp120 is responsible for virus binding to cellular receptors, and the transmembrane subunit gp41 mediates fusion of the virus with the target cell. Different functional regions can be identified in gp41, each one with importance in the fusion process.

T20 and T-1249 are two HIV-1 fusion inhibitor peptides, being T20 already approved for clinical application in AIDS treatment. The work here presented describes research on the role of biomembranes on their mode of action. A model for the role of biomembranes was proposed.

Given the similarities between the HIV-1 and SARS-CoV, and the urgency to obtain licensed drugs to treat SARS, the possibility that T20 and T-1249 can work as SARS-CoV inhibitors was investigated. The results obtained show that despite the hypothesis that T20 could inhibit SARS-CoV fusion is correct, the effect may not be strong enough for practical application.

A small sequence inside the HIV-1 gp41 ectodomain *membrane proximal region* (MPR) is commonly referred to as a cholesterol binding domain. As the MPR plays a key role in the HIV-1 fusion process and the viral envelope is rich in cholesterol, the influence of cholesterol on the interaction of the MPR derived peptides with membrane model systems was studied.

2F5 and 4E10 are two potent and broadly neutralizing antibodies against HIV-1, whose epitopes are localized in the gp41 MPR. It was proposed that these antibodies can interact with the viral membrane through a hydrophobic surface present on their third complementarity-determining region of the heavy chain. The 2F5 and 4E10 interactions with biomembranes models, in the absence and presence of its epitopes, were investigated in order to reveal the membranes role in the antibodies mechanism of action.

Key words: HIV-1; gp41; membranes; T20; CHR; MPR

CONTENTS

Prefácio	iii
Resumo	vii
Summary	xiii
Contents	xv
Abbreviations and Symbols List	xvii
I – INTRODUCTION	1
1. Human immunodeficiency virus (HIV)	1
1.1 HIV replication cycle and antiviral strategies	1
1.2 HIV entry and its inhibition	4
1.3 HIV fusion inhibitors	8
1.4 Anti-HIV antibodies	9
2. Biological membranes	11
2.1 Biological membranes lipid composition	11
2.2 Biological membranes asymmetry and heterogeneity	13
2.3 Lipid rafts	14
2.4 Cholesterol and rafts role on HIV infection	15
2.5 Membrane model systems	16
3. Peptides	18
3.1 Peptides as models	18
3.2 Peptide-membrane interactions	19
II – MEMBRANES ROLE ON THE MODE OF ACTION OF THE HIV-1 FUSION INHIBITORS T20 AND T-1249	21
1. Introduction	21
2. Putative role of membranes in the HIV fusion inhibitor enfuvirtide mode of action at the molecular level	25
3. HIV fusion inhibitor peptide T-1249 is able to insert or adsorb to lipidic bilayers. Putative correlation with improved efficiency	31

III – PUTATIVE INHIBITION OF SARS-CoV BY THE HIV-1 FUSION INHIBITORS T20 AND T-1249	49
1. Introduction	49
2. Why are HIV-1 fusion inhibitors not effective against SARS-CoV? Biophysical evaluation of molecular interactions	53
IV – THE gp41 MEMBRANE PROXIMAL REGION ROLE ON HIV-1 FUSION PROCESS	65
1. Introduction	65
2. The influence of cholesterol on the interaction of HIV gp41 membrane proximal region-derived peptides with lipid bilayers	69
V – THE ROLE OF MEMBRANES IN THE HIV-1 ANTIBODIES 2F5 AND 4E10 MODE OF ACTION	81
1. Introduction	81
2. The membranes' role in the HIV-1 neutralizing monoclonal antibody 2F5 mode of action needs re-evaluation	85
3. Real-time biosensor interactions of HIV-1 antibodies 2F5 and 4E10 with a gp41 epitope prebound to host cell and viral membrane mimetics	91
VI – FINAL CONCLUSIONS	129
VII – ANNEX I - An insight on the leading HIV entry inhibitors	137
VIII – ANNEX II - Hepatitis C virus core protein binding to lipid membranes: the role of domains 1 and 2.	147
IX – BIBLIOGRAPHY	161

ABBREVIATIONS AND SYMBOLS LIST

Ab	Antibody
AIDS	Acquired immunodeficiency syndrome
ACE-2	Angiotensin-converting enzyme 2
BLMs	Black lipid membranes
CDR H3	Third complementarity-determining region of the heavy chain
Chol	Cholesterol
CHR	C-terminal heptad repeat
CL	Cardiolipin
CoV	Coronavirus
CT	Cytoplasm tail
DNA	Deoxyribonucleic acid
DRMs	Detergent-resistant membranes
FDA	Food and drug administration
FP	Fusion peptide
GPI	Glycosylphosphatidylinositol
GUV	Giant unilamellar vesicle
HAART	Highly active antiretroviral therapy
6HB	Six helix bundle
HIV	Human immunodeficiency virus
HIV-1	Human immunodeficiency virus type 1
HIV-2	Human immunodeficiency virus type 2
HR	Heptad repeat
L	Lipid phase
L _d	Liquid-crystalline or fluid phase
L _α	Liquid-crystalline or fluid phase
L _β	Gel phase
L _{β'}	Tilted gel phase
L _o	Liquid-ordered phase
LR	Loop region
LUV	Large unilamellar vesicle
MAb	Monoclonal antibody
MLV	Multilamellar vesicle

MPR	Membrane proximal region
NHR	N-terminal heptad repeat
PA	Phosphatidic acid
PC	Phosphatidylcholine
PE	Phosphatidylethanolamine
PG	Phosphatidylglycerol
PI	Phosphatidylinositol
PIP	Phosphatidylinositol-4-phosphate
PIs	Protease inhibitors
PS	Phosphatidylserine
POPC	1-Palmitoyl-2-oleoyl- <i>sn</i> -glycero-3-phosphatidylcholine
RNA	Ribonucleic acid
RTIs	Reverse transcriptase inhibitors
SARS	Severe acute respiratory syndrome
SARS-CoV	Severe acute respiratory syndrome- associated coronavirus
SIV	Simian immunodeficiency virus
SM	Sphingomyelin
S _o	Ordered gel phase
SUV	Small unilamellar vesicle
TM	Transmembrane domain
UNAIDS	Joint United Nations programme on HIV/AIDS
W	Aqueous phase
WHO	World Health Organization
K _p	Partition coefficient
T _m	Melting temperature

Chapter I

INTRODUCTION

1. HUMAN IMMUNODEFICIENCY VIRUS (HIV)

Human Immunodeficiency Virus (HIV) is the causative agent of the acquired immunodeficiency syndrome (AIDS). There are two types of HIV, HIV-1 and HIV-2, being the HIV-1 the most virulent (Weiss, 2000; Janeway et al., 2001). HIV can be transmitted by blood and blood products, vertically (from mother to child), or through sexual activity. By the end of 2006 the United Nations Programme on AIDS (UNAIDS)/World Health Organization (WHO) epidemic update estimated 39.5 million (34.1-47.1 million) of people worldwide living with HIV (UNAIDS/WHO AIDS epidemic update, http://www.unaids.org/en/HIV_data/epi2006/default.asp). Despite the efforts, no curative treatment or effective vaccine has yet been achieved.

1.1 HIV replication cycle and antiviral strategies

HIV-1 is an enveloped virus (member of the Lentivirus subfamily of the retrovirus family (Weiss et al., 2000)) that infects CD4 T cells, dendritic cells and macrophages (Janeway et al., 2001). The viral envelope, derived from the host cell membrane, is composed of a lipid bilayer and has at the surface a glycoprotein complex that allows the virus to enter in target cells. The envelope glycoprotein complex is initially synthesized as a single chain glycoprotein precursor (gp160) which is proteolytically cleaved by a cellular protease to generate the gp120 (surface glycoprotein) and the gp41 (transmembrane glycoprotein) subunits. The virus contains also a viral capsid (constituted by the capsid protein), two copies of the viral genome and three essential enzymes: reverse transcriptase, integrase and protease (Figure I.1). Additionally the

virus has structural and accessory proteins important to the structural integrity and the virus replication process (reviewed in Vaishnav and Wong-Staal, 1991; Turner and Summers, 1999).

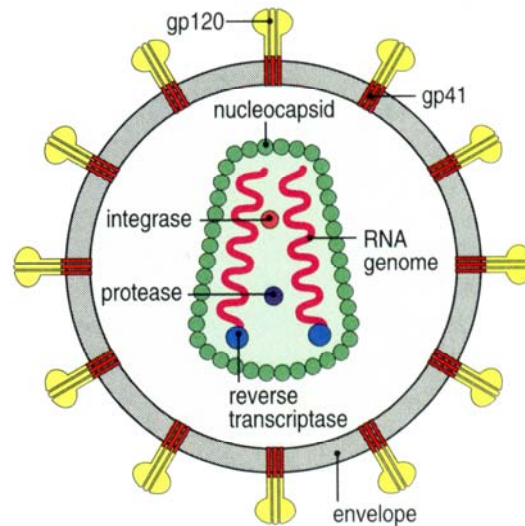


Figure I.1 – Simplified representation of the HIV-1. The reverse transcriptase, integrase, and viral protease enzymes are packed in the viral capsid (in reality, many molecules of these enzymes are contained in each virion). The glycoprotein complex, at the surface of the viral envelope, is composed by the subunits gp120 and gp41. For simplicity, the other virus proteins were omitted (from Janeway et al., 2001).

An outline of the HIV-1 replication cycle is shown in Figure I.2. The gp120 on the surface of the virus binds to the CD4 receptor on the surface of the target cells activating the process that leads to membrane fusion and subsequent viral entry. Once inside the cell the viral RNA genome is transcribed into viral DNA by the action of the viral reverse transcriptase. The later is inserted into the host cell genome by the viral integrase. The RNA transcripts produced from the integrated viral DNA serve both as mRNA to the synthesis of the viral proteins (in the form of polyprotein precursors) and as the RNA genome of new viral particles. New viral particles escape from the cell after budding at the plasma membrane. Then, the viral protease acts cleaving the polyproteins to produce independent and functional viral proteins. The final maturation process leads to the formation of infectious virions (reviewed in Vaishnav and Wong-Staal, 1991; Turner and Summers, 1999).

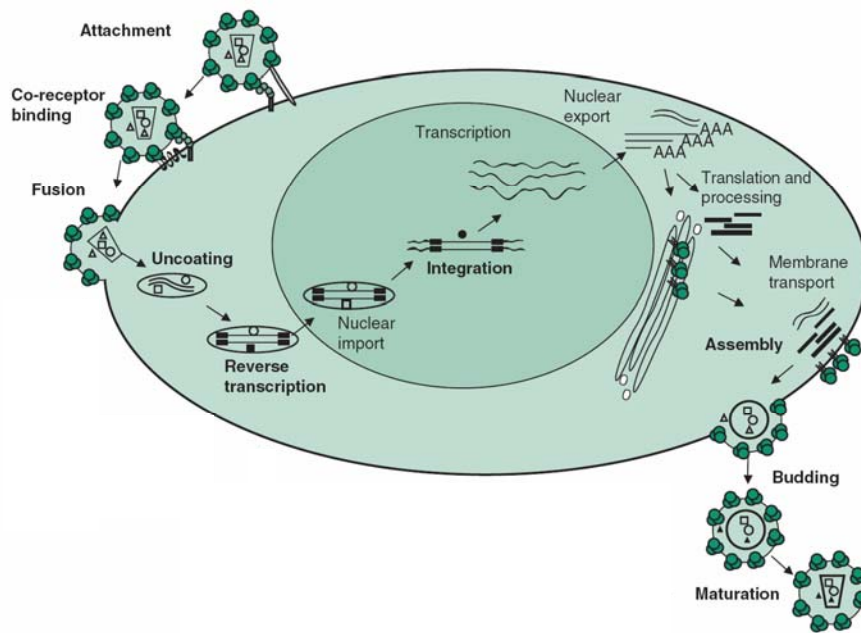


Figure I.2 – HIV replication cycle. The HIV life cycle presented shows the binding of the virus to CD4 and coreceptor on the surface of the target cell, followed by membranes fusion and viral entry; reverse transcription, integration and protein synthesis processes are also shown; processing, virus assembly, budding and maturation of nascent virions are the last steps (adapted from Reeves and Piefer, 2005).

Currently, there are three U.S. Food and Drug Administration (FDA)-approved classes of drugs to the treatment of HIV-1 infection: 1) reverse transcriptase inhibitors (RTIs), including nucleoside or nucleotide and non-nucleoside molecules; 2) protease inhibitors (PIs) and 3) entry inhibitors (only one drug was approved). Both RTIs and PIs act on post-entry steps of the virus on the cells. Combination therapy with RTIs and PIs (called highly active antiretroviral therapy, HAART), involving at least three drugs, is the most common current treatment of HIV-1 infection (reviewed in Gulick, 2003; Stolk and Lüers, 2004; Yeni, 2006). Despite the success of this therapy in reducing morbidity and mortality of HIV-1 infected patients (Palella et al., 1998; Mocroft et al., 2000; Li et al., 2000; Louie and Markowitz, 2002), the adverse effects and the emergence of drug resistant HIV-1 strains have limited its application (Brinkman et al., 1998; Carr et al., 1999; Yerly et al., 1999; Hirsh et al., 1998; Carr, 2003). In an attempt to overcome these problems a third class of antiviral agents, the entry inhibitors, are receiving a lot of attention and large development. These inhibitors act extracellularly, targeting the first step in the HIV-1 replication cycle, i.e. preventing viral entry into target cells (reviewed

in Eckert and Kim, 2001a; LaBranche et al., 2001; O'Hara and Olson, 2002; Moore and Doms, 2003).

1.2 HIV entry and its inhibition

The HIV-1 envelope glycoprotein, expressed on the surface of the viral membrane as a trimer (Center et al., 2002), is composed of two subunits noncovalently associated (gp120 and gp41). The gp120 subunit interacts with cellular receptors and the gp41 subunit is responsible for the fusion between the viral and cellular membranes (reviewed in Wyatt and Sodorski, 1998; Chan and Kim, 1998; Eckert and Kim, 2001a). The gp120/gp41 complex native conformation is not known in detail. Monomeric crystal structures of gp120 have been solved (Kwong et al., 1998; Wyatt et al., 1998) but no further information was achieved. Recent studies on the structure of the envelope glycoprotein complex showed contradictory results. For Zhu and colleagues a large globular domain comprises a gp120 trimer while the gp41 appears to form an open tripod (Zhu et al., 2006). The model derived by Zanetti et al. has the form of a mushroom with a more compact head domain and a gp41 stalk, rather than tripod legs (Zanetti et al., 2006). It was also proposed that the gp41 is folded in such way that brings the N- and C- terminal close to each other, stabilizing the native structure (Lorizate et al., 2006).

gp41 is composed of an ectodomain (extracellular domain), a transmembrane domain (TM) and an endodomain (intracellular domain or cytoplasm tail (CT)) (Figure I.3). Several functional domains have been identified in the ectodomain. The fusion peptide (FP) is located at the ectodomain N-terminal. This region, hydrophobic and rich in glycine residues, interacts with the target cell membrane and plays an important role in membrane fusion (reviewed in Tamm and Han, 2000; Epanand, 2003). Two heptad repeat regions (HR) are also included: the first (NHR or HR1) near the N-terminal is adjacent to the FP; the second (CHR or HR2) is located at the ectodomain C-terminal. As observed for other viral fusion proteins, the regions that follow the FP, NHR and CHR, have the tendency to form α -helical coiled-coils (Chambers et al., 1990), denoted respectively, N- and C-helices. Peptides derived from these regions are referred to as N- and C-peptides, respectively. The two HR are separated by a loop region (LR) that contains an intramolecular cysteine bridge. At the C-terminal between the CHR and the

TM is located a Trp-rich region, the *membrane proximal region* (MPR). Protein dissection combined with biophysical analysis demonstrated that the two HR regions within gp41 form a helical trimer of antiparallel dimers (Lu et al., 1995). The crystal structures of portions of the ectodomain (Chan et al., 1997; Tan et al., 1997; Weissenhorn et al., 1997) confirmed that the gp41 core tends to form a trimer of hairpins (or six-helix bundle (6HB)). Therefore, the N and C helices are arranged in a trimeric coiled coil. A central trimeric coiled coil formed by the N-peptide region is surrounded by three helical C-peptides that bind to conserved hydrophobic grooves on the coiled-coil surface in an antiparallel orientation. This structure represents the fusion-active conformation of gp41.

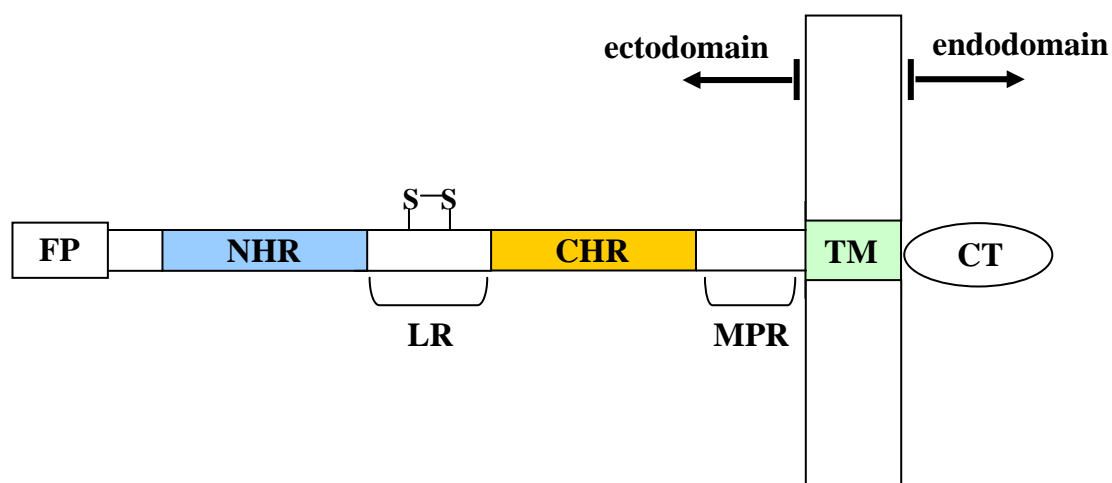


Figure I.3 – Schematic view of gp41 showing the location of the fusion peptide (FP), the N- and C-terminal heptad repeat regions (NHR and CHR), the loop region (LR), the *membrane proximal region* (MPR), the transmembrane domain (TM) and the cytoplasm tail (CT).

HIV-1 entry into target cells (Figure I.4) is believed to be a multi-step and complex process (reviewed in Chan and Kim, 1998; Eckert and Kim, 2001a). The first step is the binding of gp120 to the target cell surface molecule CD4, which serves as the main receptor for HIV-1 (Maddon et al., 1986). However, CD4 alone is not sufficient for HIV-1 to fuse with the cells (Chesebro et al., 1990; Clapham et al., 1991). Two chemokine receptors, known as CCR5 and CXCR4, are the major HIV-1 coreceptors and all strains can use one (R5 and X4 viruses) or both (R5X4 viruses). CCR5 is particularly important as a coreceptor because R5 viruses are responsible for almost all cases of HIV-1 transmission and predominate during the early events of infection. X4 and R5X4 viruses emerge in many but not all infected individuals in the late stages of the infection (reviewed in Moore et al., 1997; Berger et al., 1999; Clapham and

McKnight, 2002; Douek et al., 2003). The gp120-CD4 binding induces conformational changes in gp120 leading to the exposure or the formation of the coreceptor binding site. gp120 binding to the CD4 and coreceptor results in further conformational changes that lead to gp41 activation into its fusion-active state. The gp41 conformational changes leads to the insertion of its FP into the target cell membrane and the formation of a prehairpin intermediate that bridges the viral and cellular membranes. Subsequent changes within the gp41 ectodomain involve the interaction of CHR and NHR, and a 6HB structure (also called hairpin structure) is formed. The hairpin formation brings the viral and cell membrane into closed proximity, allowing fusion of the membranes and then entry of the virus. It is likely that the free energy released with the 6HB formation must be sufficient to membranes fusion to occur. In fact it was demonstrated that fusion is caused by the movement of the protein into the 6HB rather than by the 6HB itself (Melikyan et al., 2000). Despite this widely accepted viral entry model, accumulation of new data indicates the model needs revision. Gallo et al. proposed that the gp120-CD4 interaction triggers the prehairpin intermediate formation and that coreceptor binding leads to rapid 6HB formation (Gallo et al., 2001; Gallo et al., 2004). Also, the formation of the 6HB might not be complete until the fusion pore complex is formed. Some data suggest that the formation of some 6HB occur after a fusion pore has formed and in this way the essential role of this structure is to stabilize the fusion pore against collapse and ensure its growth (Markosyan et al., 2003).

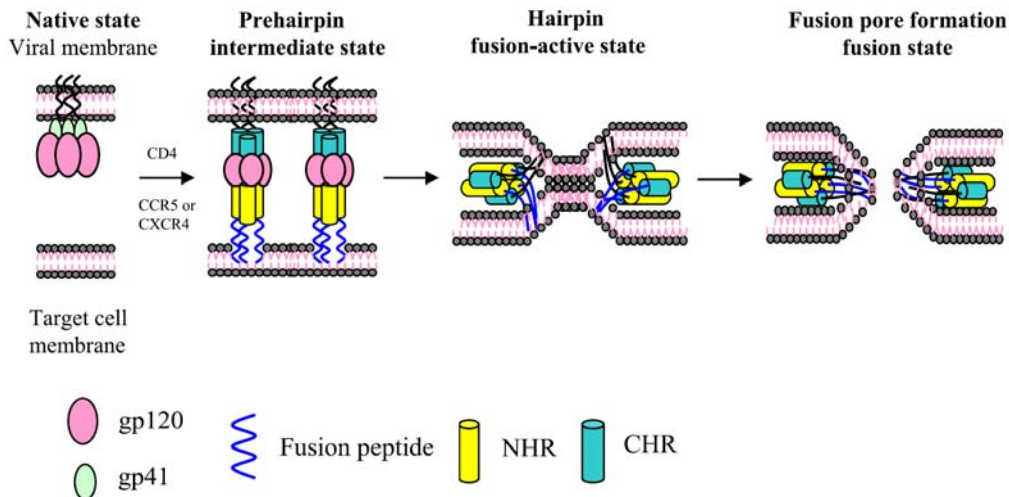


Figure I.4 – HIV entry process. The fusion process for the trimeric envelope glycoprotein complex is depicted in schematic form. The sequential binding of the gp120 to CD4 and a coreceptor on the cell membrane drives conformational changes in gp41. These changes cause the insertion of the FP into the cell membrane and the formation of the prehairpin intermediate. Subsequent gp41 conformational changes create the 6HB, and the viral and cellular membranes are brought into close proximity for fusion to occur (adapted from Liu et al., 2007b).

Each of the HIV-1 entry steps can be a target for entry inhibitors. The ones currently under development fall into three categories: gp120-CD4 binding inhibitors (or attachment inhibitors), gp120-coreceptors binding inhibitors (or chemokine coreceptors inhibitors) and fusion inhibitors (reviewed in De Clercq, 2004; Reeves and Piefer, 2005; Briz et al., 2006). Inhibitors that block the gp120-CD4 interaction include compounds that interact with the gp120 or CD4. PRO 542 (CD4-IgG2) is a recombinant tetrameric CD4-IgG2 fusion protein, which binds to gp120 (Allaway et al., 1995). BMS 806 (BMS 378806) is a small molecule inhibitor with potent antiviral activity. Firstly reported to binds directly to gp120 (Guo et al., 2003) it was proposed later that it should interfere with gp41 CD4-induced conformational changes (Si et al., 2004). TNX 355 (Hu5A8) is a CD4 specific MAb that binds to domain 2 of the CD4 receptor (Burkly et al., 1992). The antiviral agent cyclotriazadisulfonamide (CADA) exerts its effect by down-modulating the CD4 receptor (Vermeire et al., 2002). Several types of coreceptors inhibitors have been identified, namely low molecular weight CXCR4 and CCR5 antagonists. These include AMD 070 (Schols et al., 2003) and KRH-1636 (Ichiyama et al., 2003) for CXCR4 and Schering D (Tagat et al., 2004), TAK 220 (De Clercq, 2004) and AK602 (Maeda et al., 2004) for CCR5. Fusion inhibitors such as T20 (also known

as DP-178, Enfuvirtide, or Fuzeon) and T-1249 (Tifuvirtide) are compounds whose mode of action involves binding to gp41 and interfere with the conformational changes that lead to the 6HB formation and membrane fusion. These kinds of inhibitors are the leading compounds, being T20 the most advanced and already approved by the FDA (Kilby and Eron, 2003; Robertson, 2003).

1.3 HIV fusion inhibitors

Some synthetic C-peptides, such as C34 and T20, are potent inhibitors of HIV-1 infection (Wild et al., 1994a; Kilby et al., 1998). Despite being more potent, C34 is not a good candidate to a drug due to its low solubility (Otaka et al., 2002). C34 has been used in studies of HIV entry blocking by peptides, while T20 was developed as a novel anti-HIV drug. C34 sequence includes residues at the N-terminal that precede the T20 sequence (Figure I.5). These residues include those that pack into the hydrophobic pocket on the surface of the N-peptide coiled coil in the 6HB conformation, and are critical for its antiviral activity (Chan et al., 1998). C34 lacks the T20 C-terminal residues that are crucial to T20 inhibitory activity. It has been proposed that these C-peptides act by interfering with the formation of the 6HB in a dominant negative fashion, by binding to the NHR region exposed in the prehairpin intermediate (Lu et al., 1995; Chen et al., 1995; Furuta et al., 1998; Chan and Kim, 1998; Kilgore et al., 2003). Despite synthetic N-peptides exhibit also inhibitory activity against HIV, they are less potent inhibitors than the C-peptides (Wild et al., 1992; Lu et al., 1995; Eckert and Kim, 2001b). It was proposed that one of the main reasons for this behaviour is their tendency to aggregate in solution (Lu et al., 1995). N36 and DP107 are examples of N-peptide inhibitors (Figure I.5). In their mode of action, N-peptides may either target the CHR region (Lu et al., 1995) or intercalate with the NHR region (Wild et al., 1992; Wild et al., 1994b; Weng and Weiss, 1998). Based on the knowledge gathered on the structure, activity and function of these inhibitors, several modified peptides have been created, in an attempt to achieve better fusion inhibitors (reviewed in Liu et al., 2007a). One of these is the rationally designed, second generation fusion inhibitor T-1249, more potent than T20 and active against T20 resistant HIV-1 isolates (Greenberg et al., 2002). Another line of research is the design of recombinant proteins containing sequences of the gp41 NHR and/or CHR regions, which may act in a similar way as the N- and C-peptides. 5-Helix inhibitor, for instance, consists of three N-peptides and two C-

peptides connected by short linkers (Root et al., 2001). This inhibitor binds to the CHR region with high affinity and efficiently inhibits HIV-1 infection.

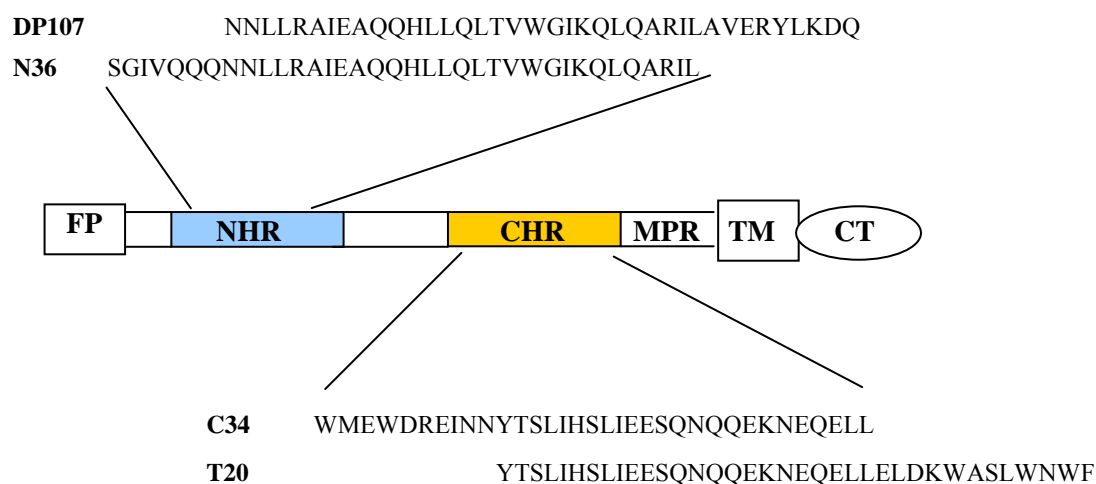


Figure I.5 – Peptide inhibitors from the NHR and CHR regions of gp41. The sequences of N-peptides N36 (residues 546-581) and DP107 (residues 553-590) are derived from the NHR region. The sequence of C-peptide C34 (residues 628-661) is derived from the CHR region, while that of T20 (residues 638-673) is derived from the CHR region and the MPR.

The potency of the antiviral activity of these fusion inhibitors peptides targeting the gp41 stimulated the search for small molecules with the same function (reviewed in Liu et al., 2007a). Non-peptidic small molecules can be used as an alternative and have the advantage of being easier to mass-produce and purify, and may be orally bioavailable. Peptides lack oral bioavailability, and need to be injectable since they are degraded in the digestive track. Moreover, they can be subjected to metabolic degradation and have a high cost of production.

1.4 Anti-HIV antibodies

The antibody (Ab) response to HIV is directed to several viral proteins. In HIV-1 infected individuals Abs against different proteins, including gp120 and gp41, are detectable (Pellegrin et al., 1996; Pilgrim et al., 1997; Richman et al., 2003; Aasa-Chapman et al., 2004). However, only a fraction of the Abs are neutralizing (Wyatt and Sodroski, 1998), i.e. Abs that neutralize HIV-1 prior to its entry into target cells. On HIV-1 the envelope glycoprotein complex gp120/gp41 is the only viral target available for neutralizing Abs (Figure I.6). Neutralizing Abs target in the gp120, the CD4 binding

domain, carbohydrate structures, the CD4-induced coreceptor binding domains and in the gp41, structures that are exposed during membrane fusion (Wyatt and Sodroski, 1998). Nevertheless, due to the envelope glycoprotein complex features, such as the extensive glycosylation, the occlusion of conserved domains within the oligomeric structure, and the transiently exposure during the viral entry process, potent neutralizing monoclonal Abs (MAbs) targeting these proteins are rare (reviewed in Wyatt and Sodroski, 1998; Ferrantelli and Ruprecht, 2002). Neutralizing MAbs against gp120 are directed predominantly to the CD4 binding domain and both the second and third hypervariable loops (V2 loop and V3 loop, respectively). Those that have been found to bind the gp41 ectodomain, target the MPR (reviewed in Zolla-Pazner, 2004). However, only few human MAbs with potent and broadly neutralizing activity have been isolated (Figure I.6). Of these, 2G12 and b12 bind to gp120 while 2F5, 4E10 and Z13 are directed to the MPR within gp41 (reviewed in Zolla-Pazner, 2004; Phogat et al., 2007).

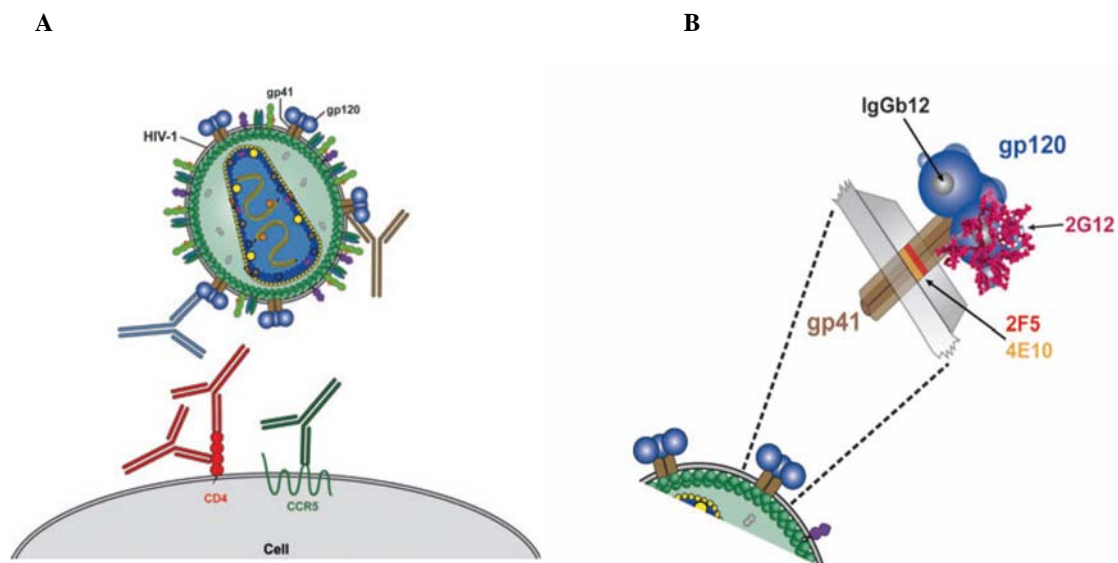


Figure I.6 – (A) The viral envelope glycoproteins gp120 and gp41 are targets for neutralizing Abs. Neutralizing Abs may also bind to cellular receptors sites implicated in HIV-1 entry as CD4 and CCR5. (B) The two broadly neutralizing MAbs to gp41, 2F5 and 4E10, bind to epitopes in the MPR; whereas 2G12 and b12 are the two broadly neutralizing gp120 Abs (adapted from Phogat et al., 2007).

2. BIOLOGICAL MEMBRANES

Biological membranes, consisting primarily of proteins and lipids, are essential for the integrity and functionality of cells, providing a barrier between the inside and outside environments. In eukaryotic cells internal membranes also form the boundaries of organelles. Despite the biomembranes complexity, a lipid bilayer is its primary structural element. Due to the amphipatic nature of the component lipids, the bilayer presents a hydrocarbon environment in the interior core with the polar groups oriented toward the water phase (Figure I.7). Biomembranes are not only physical barriers. They are highly selective permeability barriers that control the transfer of information and the transport of ions and molecules between the inside and the outside of the cell. Biomembranes serve as the matrix and support for several proteins, which are involved in important functions of the cell as energy and signal transduction, solute transport, protein targeting and trafficking (Edidin, 2003a).

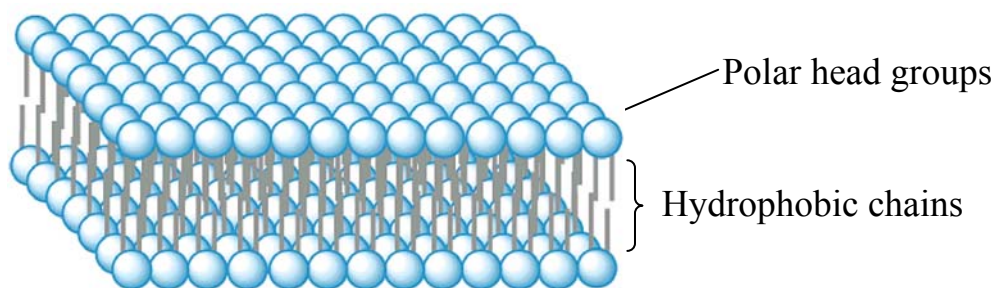


Figure I.7 – Schematic depiction of a lipid bilayer. The lipid bilayer surrounds and protects the cell from its environment. In a bilayer, the lipids hydrophilic head group of is oriented toward the water phase, while the hydrocarbon tails form the inner hydrophobic part (adapted from Menger et al., 2005).

2.1 Biological membranes lipid composition

Cell membranes are extremely complex having many different lipids. However, four main types of lipids occur in biological membranes: glycerophospholipids, phosphosphingolipids, sterols and glycolipids (reviewed in Gennis, 1989; Zubay, 1998; Loura and de Almeida, 2004).

Glycerophospholipids are the predominant class of lipids in biomembranes. Its hydrophobic section is composed of hydrocarbon chains esterified to *sn*-1 and *sn*-2 positions of the glycerol backbone. These hydrocarbon chains are diverse in length and unsaturation. The *sn*-3 position is esterified to phosphoric acid. If no more groups are linked to the molecule, the resulting compound is phosphatidic acid (PA). However, the phosphate group is generally linked to other group as choline (Figure I.8 A), ethanolamine, serine, glycerol, and inositol. The corresponding phospholipids are phosphatidylserine (PS), phosphatidylethanolamine (PE), phosphatidylcholine (PC), phosphatidylglycerol (PG), and phosphatidylinositol (PI). As the phosphate group is always negatively charged, the net charge of the molecule depends on the charge of the polar group moiety. In this way PG, PS, PI are negatively charged, while PC and PE have a net neutral charge. PC is the most abundant phospholipid of animal cell membranes, whereas PE is the major component in bacterial membranes (Gennis, 1989; Loura and de Almeida, 2004).

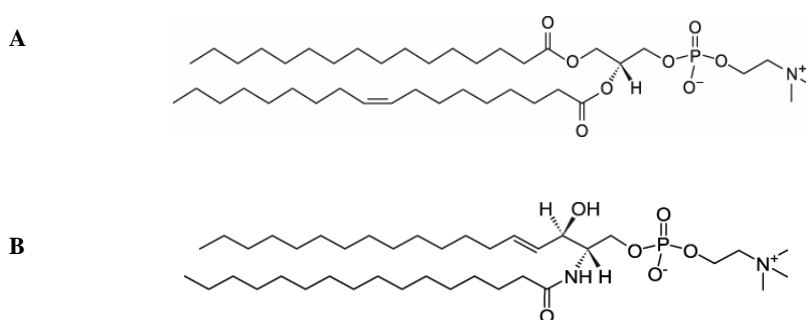


Figure I.8 – Structure of a phosphatidylcholine, 1-Palmitoyl-2-Oleoyl-*sn*-Glycero-3-Phosphocoline (POPC) (A) and sphingomyelin (Egg, chicken) (B) (from www.avantilipids.com).

In phosphosphingolipids the hydrophobic group is a ceramide. Sphingolipids are rich in long and saturated hydrocarbon chains. Rarely found in plants and bacteria, sphingomyelin (SM) is the most abundant phosphosphingolipid in animal cell plasma membranes (Figure I.8 B). SM is structurally similar to PC. Both molecules have two long hydrocarbon side chains and a negatively charged phosphate group esterified to a choline.

The basic structure of sterols is a four-ring hydrocarbon. In cholesterol (Chol), the most important sterol in animal membranes, the molecular structure includes a tetracyclic

fused ring skeleton, with a single hydroxyl group at carbon 3, a double bond between carbons 5 and 6, and a iso-octyl hydrocarbon side chain at carbon 17. The hydroxyl group gives Chol its slight amphipatic character and orients the molecule in membranes. Chol orients in a lipid bilayer with its polar hydroxyl group towards the aqueous phase and the hydrophobic ring system oriented parallel to, and buried in the hydrocarbon chains of the phospholipids. Other sterols are found in plant and yeast and other eukaryotic micro-organisms.

In glycoglycerolipids the *sn*-3 position of glycerol forms a glycosidic link to a carbohydrate. This kind of lipids is abundant in chloroplast membranes, blue algae and bacteria, but rarely found in animals. Glycosphingolipids have a glycosidic linkage to the terminal hydroxyl of ceramide. The simplest form of glycosphingolipid is a cerebroside that contains a single glycosidic residue. Glycosphingolipids are located in the outer surface of the plasma membrane and are particularly abundant in the nervous system.

2.2 Biological membranes asymmetry and heterogeneity

Lipids in the plasma membrane are asymmetrically distributed, i.e., the two membrane leaflets have a different lipid composition. The outer leaflet of an animal cell plasma membrane is mainly composed by SM and PC, while the inner leaflet has a mixture of predominantly PE and PS (Zachowski, 1993). Several functional roles for this asymmetric distribution have been suggested. These include several proteins that appear to localize in the cytoplasmic face of the membrane through their interaction with PS (Palfrey and Waseem, 1985; Meers and Mealy, 1993; MacDonald, 1993; O'Toole et al., 1999). Disruption of lipid asymmetry leads to exposure of PS on the outer surface of the plasma membrane that serves as a trigger for macrophage recognition of apoptotic cells (Fadok et al., 1992; Bratton et al., 1997; Shiratsuchi et al., 1997).

In the Singer-Nicolson fluid mosaic model of biological membranes, bilayer lipids form a uniform and homogeneous fluid mixture, where lipid and proteins could move freely. Proteins are free to diffuse laterally or to rotate about an axis perpendicular to the plane of the membrane (Singer and Nicolson, 1972). However, the Singer-Nicolson model is now regarded as a simplistic description of the complex interactions and

dynamics existent, namely by the presence of lateral heterogeneities like domains with distinct compositions. Examples of these are the apical and basolateral membranes of polarized epithelial cells that have distinct compositions, protein aggregation that result in domains that are enriched in a particular protein and lipid microdomains.

2.3 Lipid rafts

The fluidity of lipid bilayers is a function of temperature, pressure and lipid composition (length of the hydrocarbon chains and head group composition). The bulk of lipids in biomembranes are generally in the fluid liquid crystalline phase, and this state is essential for normal cell function (White et al., 2001). Pure phospholipid membranes show a temperature-dependent phase transition (Figure I.9). Phospholipid bilayers can exist in an ordered gel phase (S_o), where the lipid molecules are more condensed and the hydrocarbon chains highly ordered. Dependent on the head group composition the gel phase is L_β (for PE) or $L_{\beta'}$ (for PC). In the L_β and $L_{\beta'}$ phases, respectively, the chains are ordered parallel or show a tilt angle with the respect to the bilayer normal. Above a melting temperature (T_m), characteristic for each lipid, the bilayer is present in a phase termed liquid-crystalline or fluid phase (L_α , L_d), in which the phospholipid hydrocarbon chains are fluid and disordered (Gennis, 1989; Kranenburg and Smit, 2005). Chol has important effects on phase behaviour: decreases the order of the gel phase, increases the order of the fluid phase and stabilizes a new phase named liquid ordered (L_o). This L_o phase is characterized by high hydrocarbon chain order in combination with high lateral mobility in the bilayer, that is, has characteristics from both gel- and fluid-phase (Ipsen et al., 1990; Spink et al., 1996). In mixtures that comprise appropriate amounts of sphingomyelin, unsaturated phospholipids and cholesterol, L_o and L_d phases can co-exist (de Almeida et al., 2003; de Almeida et al., 2005).

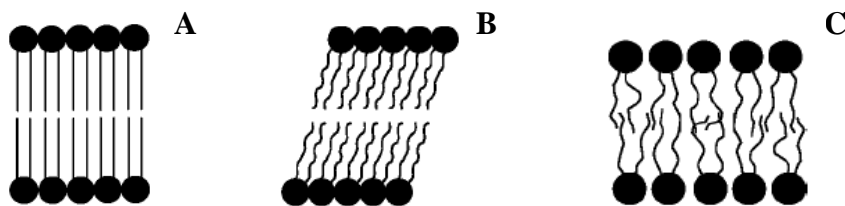


Figure I.9 – Lipid bilayer gel L_β (A) and $L_{\beta'}$ (B) phases and the fluid phase (C) (adapted from Kranenburg and Smit, 2005).

Lipid rafts are described as microdomains enriched in sphingolipids and Chol, that are present in the biological membranes organized in a way similar to a liquid ordered phase, more ordered than the surrounding fluid membrane (Simons and Ikonen, 1997; Edidin, 2003b; Simons and Vaz, 2004). It is believed that lipid rafts can facilitate selective protein-protein interactions, by excluding or including proteins. Examples of proteins that preferentially partition into raft domains are glycosylphosphatidylinositol (GPI)-anchored proteins and cholesterol-binding proteins such as caveolins (Rajendran and Simons, 2005). Raft domains are postulated to function as platforms involved in the lateral sorting of certain proteins during their trafficking within the cells and signal transduction events (Simons and Ikonen, 1997; Edidin, 2003b; Simons and Vaz, 2004). However, recent evidence points to an additional role of protein-lipid and protein-protein interactions in lipid rafts formation and stabilization. This evidence suggests that rafts are initially small and unstable but can be captured and stabilized by proteins (Jacobson et al., 2007; Hancock, 2007). Several methods have been used to study lipid rafts in model and cell membranes (Pike, 2004). Isolation of detergent-resistant membranes (DRMs) and disruption of the lipid rafts structure based on Chol-depletion are two of the most widely used. However, these methods have limitations and undesired effects (Lichtenberg et al., 2005), and despite growing evidence showing the rafts existence and importance for cell functions, the presence of these domains in biological membranes is still controversial (Munro, 2003). In spite of the possibility to visualize ordered domains in model membranes (Feigenson and Buboltz, 2001; Silvius, 2003; Veatch et al., 2004), visualize these domains in native cell membranes has proved difficult. The small rafts size, its dynamic and unstable nature in cell membranes makes them difficult to be resolved by conventional microscopy techniques. Several techniques have been used to study the size of lipid rafts and their stability in vivo (Schütz et al., 2000; Pralle et al., 2000; Dietrich et al., 2002; Bacia et al., 2004) but no conclusive results were obtained so far.

2.4 Cholesterol and rafts role on HIV infection

Increasing amount of evidence now suggests that lipid rafts are involved in both early and late phases of the HIV-1 replication cycle (reviewed in Campbell et al., 2001), as well as in its infectivity. The HIV envelope is enriched in Chol and sphingolipids, which are characteristic of lipid rafts (Aloia et al., 1993; Brügger et al., 2006). It was

shown that removal of Chol from viral particles almost completely eliminates HIV-1 infectivity (Campbell et al., 2002; Guyader et al., 2002; Graham et al., 2003; Campbell et al., 2004). The studies of the Chol and rafts role in viral entry have shown contradictory results. Some groups have shown that CD4 (Fragoso et al., 2003; Popik et al., 2002), CCR5 (Mañes et al., 1999; Popik et al., 2002) and, with reserve, CXCR4 (Popik et al., 2002) localize on lipid rafts. It was proposed that lipid rafts can serve as platforms for HIV entry, where the gp120 docking to receptors occurs (Mañes et al., 2000; Nguyen and Taub, 2002; Popik et al., 2002). However, coreceptors and CD4 may localize in different domains and it was suggested that initially HIV-1 binds to CD4 in rafts and subsequent interaction with CXCR4 requires the movement of the proteins complex out of the rafts (Kozak et al., 2002). A proposal based on Chol depletion of target cells indicates that although Chol is not required for viral entry, its depletion from cells with low coreceptor densities reduces the ability of gp120 to engage coreceptor clusters required to activate fusion (Viard et al., 2002). Additionally it was proposed that the presence of HIV-1 receptors in rafts is not required for viral infection and that Chol modulates the viral entry process independently of its ability to promote raft formation (Percherancier et al., 2003).

It has been suggested that viral budding occurs in cell membrane lipid raft domains (Nguyen and Hildreth, 2000, Ono and Freed, 2001; Pickl et al., 2001), what may explain the high level of Chol and sphingolipids in the viral membrane.

2.5 Membrane model systems

Given biomembranes complexity, the study of the lipid bilayer structure and properties is very important. The use of membrane model systems enables a simplified basis for these studies, while maintaining the main properties of the biomembranes. Models systems can be prepared with pure lipids or a mixture of lipids. There are different types of membrane model systems such as: lipid monolayers at an air-water interface; planar bilayers (also called black lipid membranes or BLMs); and lipid vesicles (or liposomes), which are probably the most popular models.

Liposomes preparation (Figure I.10) requires solubilization of lipids in organic solvents, followed by drying into a film and resuspension in an aqueous environment. Suspensions of liposomes prepared in this manner form multilamellar vesicles (MLVs). MLVs are constituted by a heterogeneous mixture of vesicular structures which contain

multiple bilayers forming groups of concentric shells. Due to the size of the MLVs particles light scattering is very significant, which could difficult its application in photophysical studies. In this way, different strategies were created in order to obtain unilamellar liposomes (Menger et al., 2005). The so called small unilamellar vesicles (SUVs), unilamellar vesicles of small diameter (30-50nm), are mainly obtained by sonication of MLVs suspensions. Regarding their small diameter, their light scattering activity is minimal. However, the small radius of curvature of SUVs results in packing difficulties of lipids. This curvature is much higher than the curvature of cell membranes, resulting in poor mimics of the properties of biomembranes. Additionally, SUVs are not stable and fusion occurs easily. Larger unilamellar vesicles (LUVs) can be produced by extrusion of MLVs through polycarbonate filters (with a defined pore size) that allow to obtain vesicles with a diameter near the pore size of the filter used. These vesicles closely resemble the lipid packing density and curvature of biomembranes. Giant unilamellar vesicles or GUVs (5-200 μ m) can be prepared by gentle hydration and electroformation (Rodriguez et al., 2005). These vesicles are particularly suitable for microscopy applications as their size enables visualization.

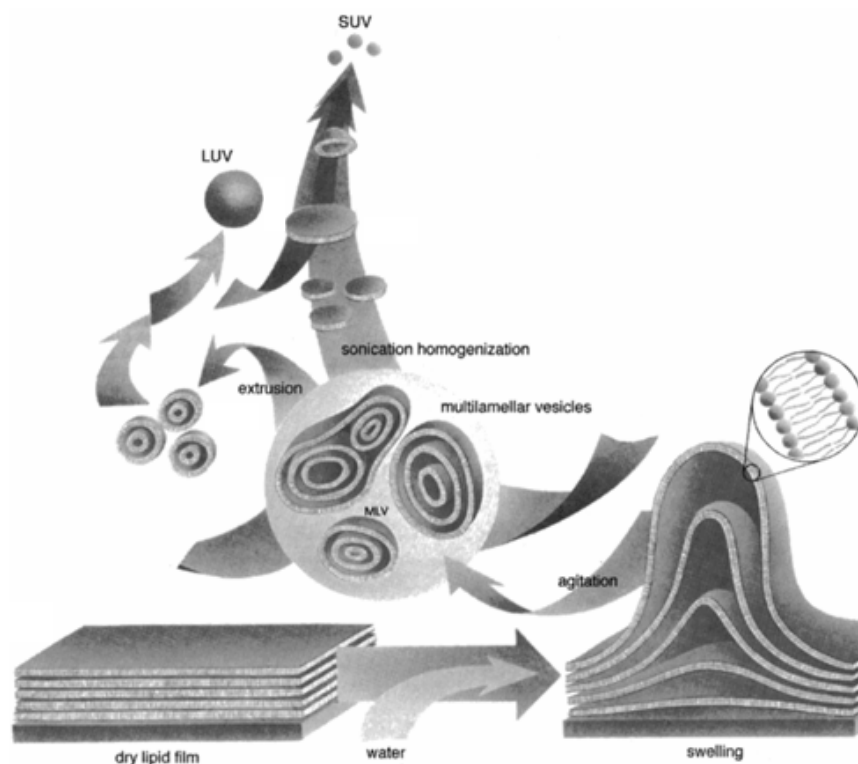


Figure I.10 – Schematic illustration of liposomes preparation that leads to MLVs, SUVs and LUVs (from www.avantilipids.com).

3. PEPTIDES

3.1 Peptides as models

Proteins complexity may difficult their functional and structural characterization as a whole. The study of protein-protein and protein-lipid interactions for instance is frequently important to understand the function of proteins and their role in supra-molecular systems. The use of a peptide, whose sequence derives from a specific protein region can be a valuable strategy to study that specific protein sequence. Synthetic peptides are easier to manipulate, to obtain in large quantities, and can be mutated in relation to the primary sequence with extensive mutation possibilities. These peptides can be used to the study of a particular protein characteristic and understand the role of a particular amino acids sequence.

In HIV-1 entry studies the envelope glycoprotein complex role is of crucial importance. Recently acquired knowledge of the gp41 and gp120 (Di Bello et al., 2004) function and behaviour was achieved by the study of the whole protein but also by the use of synthetic peptides derived from the proteins sequence. The study of gp41 synthetic derived peptides allows to identify and to study different functional domains. Namely, taking into account the importance of the gp41 in the membranes fusion process, several studies use different peptides to unravel the membrane-active regions (Mobley et al., 2001; Moreno et al., 2004; Moreno et al., 2006). As the gp41 FP is responsible for the initial insertion of the gp41 on target cells membrane, the use of synthetic peptides to study the membrane binding properties of this region is very common (reviewed in Nieva and Agirre, 2003). The identification of key residues was possible due to the use of synthetic FP with different lengths and amino acids mutations (Pécheur et al., 1999). The use of peptides derived from the gp41 NHR and CHR regions is widely used to study the interactions of both regions involved in the formation of the 6HB structure (Chan et al., 1997; Tan et al., 1997; Lu et al., 1999). Additionally these peptides are also frequently studied to assess the involvement of the correspondent regions in membrane binding and destabilization, and consequently in the fusion process (Rabenstein and Shin, 1995; Peisajovich et al., 2000; Kliger et al., 2000; Sackett and Shai, 2002; Sackett and Shai, 2003; Shnaper et al., 2004; Pascual et al., 2005a; Korazim et al., 2006). A direct role of the gp41 LR in the fusion process was also proposed based on studies with synthetic peptides (Santos et al., 1998; Contreras et

al., 2001; Pascual et al., 2005b). It has been proposed that the gp41 MPR is essential for the fusion process and the study with peptides has provided additional evidence for this function (Suárez et al., 2000a; Suárez et al., 2000b; Sáez-Cirion et al., 2002; Sáez-Cirion et al., 2003). Even the gp41 CT was shown to interact with membranes by the use of peptides derived from this region (Kliger and Shai, 1997).

3.2 Peptide-membrane interactions

Understanding the interactions between peptides and membranes is important since such interactions play a key role in many biological processes. Antimicrobial peptides interact with microbial membranes as part of their mechanism of action and selectivity (Epanand and Vogel, 1999; Hancock and Diamond, 2000; Zasloff, 2000), cell-penetrating peptides (CPPs) are able to translocate cell membranes non-endocytically (Derossi et al., 1998; Lindgren et al., 2000), and viral protein fragments are responsible for membranes fusion (Peisajovich and Shai, 2002; Tamm et al., 2002).

Both entropic, so called “hydrophobic” (Wimley and White, 1993) and electrostatic effects play a central role in peptide partition from water into membranes. Hydrophobic interactions are related with the energetic requirements for insertion of nonpolar residues in the aqueous environment. Electrostatic interactions occur because basic amino acid residues will be attracted electrostatically to the membrane surface containing negatively charged lipids. This effect is of particular importance for positively charged amphipatic peptides, such as antibacterial peptides, which interact and disrupt the negatively charged bacterial membrane (Matsuzaki, 1999; Epanand and Vogel, 1999). However, if the lipids are neutral the electrostatic influence is insignificant and if both lipids and peptides present negative charges, the electrostatic contribution becomes repulsive. The partition of peptides into membranes can promote changes on their conformation. It is frequent that peptides that in the aqueous environment have a random coil structure adopt an α -helical conformation when associated with the lipid bilayer (Ladokhin and White, 1999; Wieprecht et al., 1999). The change to an amphipatic structure at the membrane surface reduces the free energy and is in this way an important contribution for membrane binding. The aromatic amino acids Trp, Tyr and Phe are hydrophobic and important in defining the presence of the peptides in the bilayer. Trp amino acid residues have preference to being inserted into lipid bilayers at the membrane-water interface (Yau et al., 1998; Persson et al., 1998;

Killian and von Heijne, 2000; de Planque et al., 2003). Hydrophobicity scales (Wimley and White, 1996; White and Wimley, 1998) are composed of experimentally determined free energies of transfer between phases for each amino acid. These scales are a good tool in hydrophobicity analyses and in the prediction of peptide interactions with the bilayer. Two scales are used: one for partitioning from water to the bilayer interface and one for partitioning into *n*-octanol. The octanol scale appears to be a good measure of the partitioning to the bilayer interior (Wimley and White, 1996; White and Wimley, 1998). The parameter that describes the partition of a peptide between the lipid and water phases is the partition coefficient (K_p):

$$K_p = \frac{n_{S,L}/V_L}{n_{S,W}/V_W}$$

where $n_{S,i}$ are the moles of solute present in each phase ($i = W$, aqueous phase; $i = L$, lipid phase) and V_i is the phase volume (Santos et al., 2003).

Chapter II

MEMBRANES ROLE ON THE MODE OF ACTION OF THE HIV-1 FUSION INHIBITORS T20 and T-1249

1. INTRODUCTION

HIV infection most common treatment comprises RTIs and PIs. However, limitations such as treatment failure, toxicity, intolerance and HIV drug resistance, demand for new classes of antiviral agents. Entry inhibitors are a new class of drugs; the first antiviral agents that act extracellularly. Fusion inhibitors are the leading compounds of this class and T20 is the only approved so far by the FDA for clinical use (Robertson, 2003).

T20 is a synthetic 36 amino acids peptide derived from the C-terminal region of HIV-1 gp41 (Wild et al., 1994a; Wild et al., 1995). Its sequence contains residues from the CHR C-terminal and MPR N-terminal parts (Figure II.1). This fusion inhibitor is indicated for use as part of a combination therapy with other antiretroviral agents. Candidates for this therapy are treatment-experienced individuals with evidence of HIV-1 replication despite ongoing antiretroviral therapy, and is not generally applied in treatment-naïve patients. The recommended dosage of T20 in adults is 90mg twice daily, administered by subcutaneous injection (Dando and Perry, 2003). The addition of T20 to an optimized antiretroviral background regimen improved the virological

suppression and immunological benefit in treatment-experienced HIV-infected patients (Lalezari et al., 2003; Lazzarin et al., 2003). The most common adverse effects associated with its use are local injection sites reactions, but this does not seem to be a limitation to the treatment (Dando and Perry, 2003). Potent synergy was observed for T20 in combination with other entry inhibitors *in vitro* (Nagashima et al., 2001; Tremblay et al., 2002).

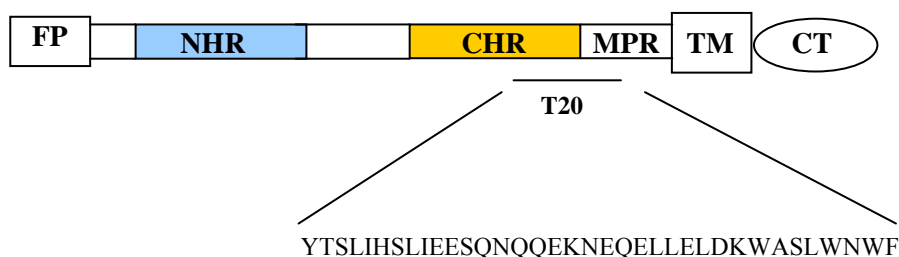


Figure II.1 – T20 sequence (residues 638-673) is derived from gp41 CHR and MPR.

The mode of action by which T20 inhibits viral fusion is still unclear, but several proposals have been presented involving different target sites in gp41 and gp120. The most currently accepted mechanism (Figure II.2) is the one proposed for C-peptides in general, involving interaction with the gp41 NHR region in an early intermediate of fusion, thus preventing the conformational changes that lead to the fusion-active arrangement (Wild et al., 1994a; Wild et al., 1995; Chen et al., 1995; Lawless et al., 1996; Rimsky et al., 1998; Kliger and Shai, 2000). In agreement, viral resistance to T20 is associated with mutations in the GIV sequence of the NHR region (Rimsky et al., 1998; Wei et al., 2002), and the LLSGIV sequence is important for the binding of T20 to gp41 (Trivedi et al., 2003). Nevertheless, T20 lacks some N-terminal residues present in other gp41 inhibitory C-peptides (e.g. C34) postulated as essential for the binding to the NHR region and inhibiting HIV-1 entry (Wild et al., 1994a, Chan et al., 1998). Blumenthal and co-workers (Muñoz-Barroso et al., 1998) proposed the existence of a second binding site for T20 on gp41, involving the contact site of gp41 oligomers cluster to form a fusion pore, which is required for the occurrence of the complete fusion process (Blumenthal et al., 1996; Chan and Kim, 1998). In fact, it was suggested that T20 binding affinity to the NHR region cannot justify its strong inhibitory activity and should have at least two different interactions modes with gp41 (Ryu et al., 1999). In addition Shai and colleagues (Kliger et al., 2001) showed that T20 can bind to membranes and oligomerize on its surface, at variance with aqueous solution, it cannot

interact with the NHR region in the membrane environment. Therefore there are two possible T20 target sites proposed in gp41, both contributing to fusion inhibition: interaction with the NHR region in aqueous solution prevents the formation of the 6HB structure while interaction with the gp41 C-terminal region in the membrane environment inhibits fusion pore formation (Ryu et al., 1999; Muñoz-Barroso et al., 1998; Kliger et al., 2001). When T20 is bound to membrane-anchored proteins expressed in genetically modified target cell of HIV-1 infection, replication of the virus was inhibited more than 100-fold (Hildinger et al., 2001). A less accepted, but also proposed T20 mode of action is its binding to the gp41 FP, preventing the insertion of the last into the target cell membrane and thus membrane fusion (Mobley et al., 2001; Jiang et al., 2002).

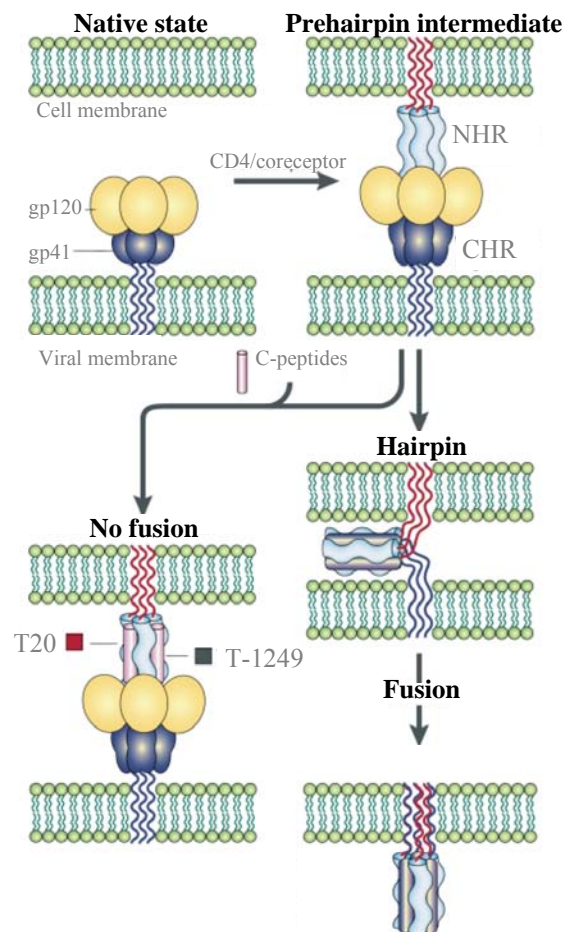


Figure II.2 – Mode of action of T20 and T-1249. Schematic of the most accepted mechanism by which T20 and T-1249 inhibit viral entry into target cells. Both inhibitor peptides bind to the NHR region in a prehairpin intermediate, preventing the formation of a fusion active structure and thereby fusion and viral entry (adapted from Moore and Stevenson, 2000).

Coreceptor specificity, that is determined by the gp120 V3 loop region, appears to be a factor that can also modulate sensitivity to T20 since X4 viruses are much more sensitive to T20 than R5 viruses (Derdeyn et al., 2000). It was proposed that both gp120/coreceptor binding affinity and coreceptor expression levels are related with this sensitivity (Derdeyn et al., 2001; Reeves et al., 2002). Assuming that T20 binds to gp41 after CD4 binding but prior to coreceptor binding (Furuta et al., 1998; Kliger and Shai, 2000), increased gp120/coreceptor affinity and higher coreceptor expression levels result in faster membrane fusion, reducing the time during which gp41 is sensitive to T20. In a different way, some studies suggest that gp120 can be an additional target site that contributes to T20 inhibitory activity. T20 may act through binding to CXCR4 (Xu et al., 2000) and/or interaction with the gp120 coreceptor binding site, blocking gp120 binding to the coreceptor (Yuan et al., 2004; Alam et al., 2004; Liu et al., 2005). This interaction with gp120 occurs in a CD4-induced manner (Yuan et al., 2004; Alam et al., 2004) with the gp120 of X4 viruses, which could explain the increased T20 sensitivity of these viruses (Yuan et al., 2004). However, different studies have not identified significant differences in T20 susceptibility for patients harbouring CCR5, CXCR4 or dual tropic viruses, indicating that viral tropism has no clinically relevant effect on the T20 therapy efficiency (e.g., Greenberg and Cammack, 2004; Matthews et al., 2004).

T-1249 is a second generation fusion inhibitor that follows T20. This 39 amino acids designed peptide is composed of sequences derived from HIV-1, HIV-2 and simian immunodeficiency virus (SIV) (Eron et al., 2004):

WQEWEQKITALLEQAQIQQEKNEYELQKLDKWASLWEWF

T-1249 is more potent than T20 and also retains activity against most T20-resistant HIV-1 strains (Gulick, 2003; Lalezari et al., 2005). Despite the need of clarification, it is believed that in its mechanism of action T-1249 (Figure II.2) acts like most C-peptides, interacting with NHR region preventing the 6HB formation (Kilby and Eron, 2003).

2. PUTATIVE ROLE OF MEMBRANES IN THE HIV FUSION INHIBITOR ENFUVIRTIDE MODE OF ACTION AT THE MOLECULAR LEVEL

I, Ana Salomé Veiga, declare that the experimental design and work, data analysis and discussion were carried out by me under the advisor of Prof. Miguel Castanho. Fluorescence life time experimental measurements were performed by Dr. Aleksandre Fedorov.

The manuscript was written by me and by my supervisor, Prof. Miguel Castanho. Prof. Nuno Santos collaborated in the discussion and preparation of the manuscript.

I, Miguel Castanho, as Ana Salomé Veiga supervisor, hereby acknowledge and confirm the information above is correct.

Ana Salomé Veiga

Miguel Castanho

Putative role of membranes in the HIV fusion inhibitor enfuvirtide mode of action at the molecular level

Salomé VEIGA*, Sónia HENRIQUES*, Nuno C. SANTOS† and Miguel CASTANHO*‡¹

*Centro de Química e Bioquímica, Faculdade de Ciências da Universidade de Lisboa, Campo Grande C8, 1749-016 Lisboa, Portugal, †Instituto de Bioquímica/Instituto de Medicina Molecular, Faculdade de Medicina de Lisboa, Av. Prof. Egas Moniz, 1649-028 Lisboa, Portugal, and ‡Centro de Química Física Molecular, Instituto Superior Técnico, Complexo I, 1049-001 Lisboa, Portugal

Partition of the intrinsically fluorescent HIV fusion inhibitor enfuvirtide into lipidic membranes is relatively high ($\Delta G = 6.6 \text{ kcal} \cdot \text{mol}^{-1}$) and modulated by cholesterol. A shallow position in the lipidic matrix makes it readily available for interaction with gp41. No conformational energetic barrier

prevents enfuvirtide from being active in both aqueous solution and lipidic membranes. Lipidic membranes may play a key role in the enfuvirtide biochemical mode of action.

Key words: AIDS, enfuvirtide, fusion inhibitor, fuzeon, HIV, T20.

INTRODUCTION

Despite the promising clinical studies and trials, which led to a fast and recent approval by the United States Food and Drug Administration [1] for clinical use, action of the HIV fusion inhibitor enfuvirtide (Fuzeon; Figure 1) at the molecular level is largely unknown. Unlike other peptides based on the C-region of gp41 (C-peptides), enfuvirtide lacks the eight-amino-acid sequence (628–635) thought to be essential for association with the N-region [2].

The sequence of enfuvirtide and its eventual arrangement in an α -helix (Figure 1), with amphipathic segments, clearly suggests that it may interact with biological membranes. A theoretical analysis (Membrane Protein Explorer, MPEx version 2.04; <http://blanco.biomol.uci.edu/mpex/>) on the hydrophobicity and interface affinity reinforces this idea (results not shown). Thus we were prompted to study (i) the extent of the partition of enfuvirtide into biological membrane models, (ii) its location in the lipidic matrix and (iii) the interplay between partition and conformation. The presence of tryptophan residues in enfuvirtide makes fluorescence techniques suitable tools to probe this molecule with no need for chemical derivatization.

EXPERIMENTAL

Materials

Enfuvirtide was a kind gift from Roche (Palo Alto, CA, U.S.A.). POPC (1-palmitoyl-2-oleyl-*sn*-glycero-3-phosphocholine), DPPC (1,2-dipalmitoyl-*sn*-glycero-3-phosphocholine) and POPG {1-palmitoyl-2-oleyl-*sn*-glycero-3-[phospho-*rac*-(1-glycerol)]} were purchased from Avanti Polar-Lipids (Alabaster, AL, U.S.A.), while cholesterol was from Sigma (St. Louis, MO, U.S.A.). 5NS (5-doxy-stearic acid) and 16NS (16-doxy-stearic acid) were from Aldrich Chem. Co. (Milwaukee, WI, U.S.A.). L-Tryptophan, acrylamide, Hepes and NaCl were from Merck (Darmstadt, Germany). The spectrofluorimeter used was an SLM Aminco 8100 (double monochromators; 450 W Xe lamp) and the CD spectrometer was a Jasco J720 (450 W lamp).

Methods

We used 10 mM Hepes, pH 7.4/150 mM NaCl buffer, and prepared lipidic LUVs (large unilamellar vesicles) by extrusion techniques [3]. Quenching studies were carried out by solubilization of the quenchers in ethanol followed by direct injection in the lipidic vesicles suspension (ethanol in the final sample was kept < 2%). Effective lipophilic quencher concentrations inside the membrane were calculated for data-analysis purposes. Excitation and emission wavelengths were 280 and 350 nm, respectively, in all fluorescence measurements. For details of transient-state fluorescence experiments, see [4]. We prepared enfuvirtide stock solutions in buffer (2.2×10^{-4} M), diluted to a final concentration of 7×10^{-6} M (fluorescence quenching), 1×10^{-5} M (partition coefficient calculation) or 7×10^{-5} M (CD experiments). Partition coefficient determination was carried out by successive addition of small aliquots of LUV (15 mM), with 10 min incubations in between. The dilution effect on fluorescence intensity was corrected.

RESULTS AND DISCUSSION

UV-visible absorption and fluorescence spectra in buffer of enfuvirtide are identical to those of Trp in aqueous solution (results not shown). No red-edge excitation effect (i.e. red shift of the emission spectrum) was detected, which indicates that all Trp residues sense similar local environments. Accordingly, the fluorescence quenching of enfuvirtide by acrylamide (a hydrophilic molecule) revealed that no hydrophobic pockets are present (linear Stern–Volmer plots; results not shown). Although the existence of hydrophobic pockets does not seem likely in a small peptide, aggregation or clustering could eventually take place. Aggregation is probably prevented by the intercalation of charged residues among hydrophobic ones (Figure 1a).

In the presence of LUV of POPC, the fluorescence intensity of enfuvirtide increases (Figure 2). Concomitantly, a fluorescence emission blue shift occurs (11 nm when [POPC] = 5 mM), which shows that the Trp residues in enfuvirtide are being incorporated progressively into the lipid and sensing a more hydrophobic

Abbreviations used: LUV, large unilamellar vesicles; POPC, 1-palmitoyl-2-oleyl-*sn*-glycero-3-phosphocholine; DPPC, 1,2-dipalmitoyl-*sn*-glycero-3-phosphocholine; POPG, 1-palmitoyl-2-oleyl-*sn*-glycero-3-[phospho-*rac*-(1-glycerol)]; 5NS, 5-doxy-stearic acid; 16NS, 16-doxy-stearic acid.

¹ To whom correspondence should be addressed, at the Centro de Química e Bioquímica, Faculdade de Ciências da Universidade de Lisboa (e-mail castanho@fc.ul.pt).

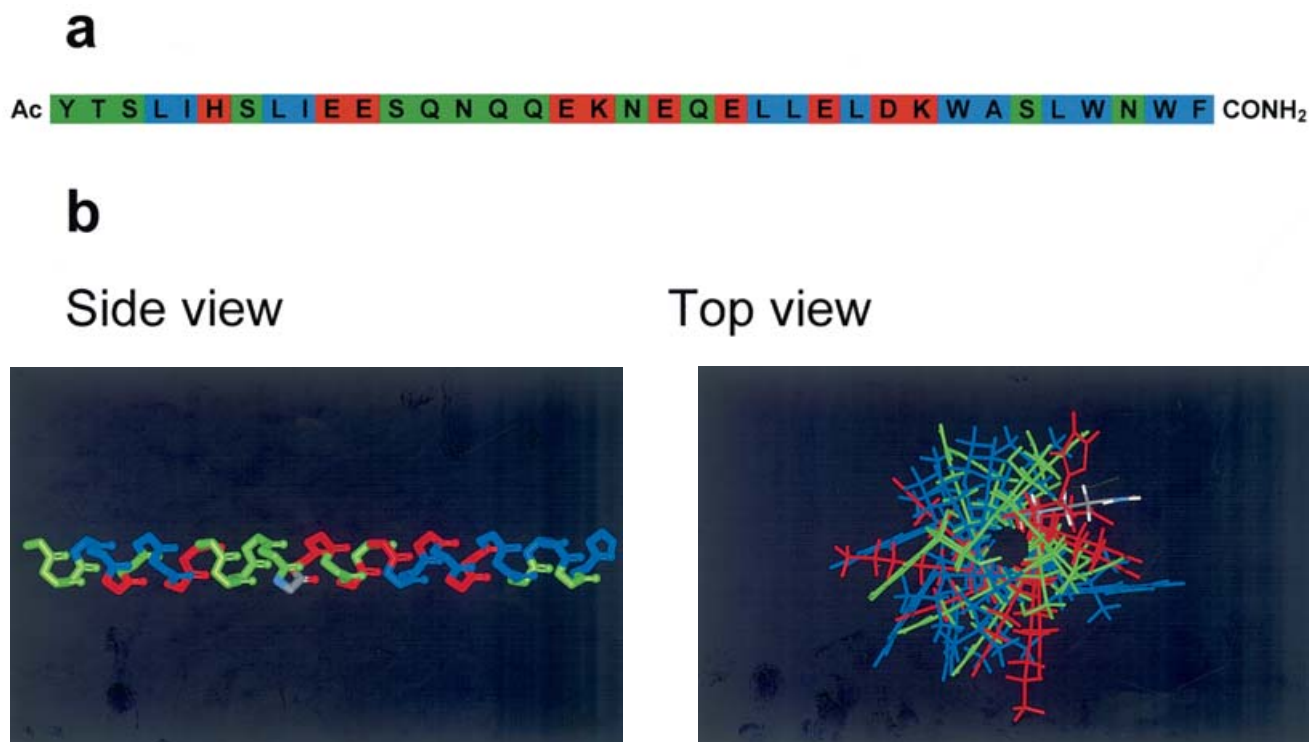


Figure 1 Amino acid sequence of enfuvirtide (a) and its arrangement in an α -helix (b), as it appears in the crystallographic structure of gp41

Hydrophobic (blue), non-charged polar (green) and charged polar (red) residues form amphipathic segments in the helix. The top view in (b) shows that the hydrophobic side chains point towards the same side of the chain. This is also apparent from the side view, when only the backbone is represented. Uncapped enfuvirtide at both ends is usually referred to as T20.

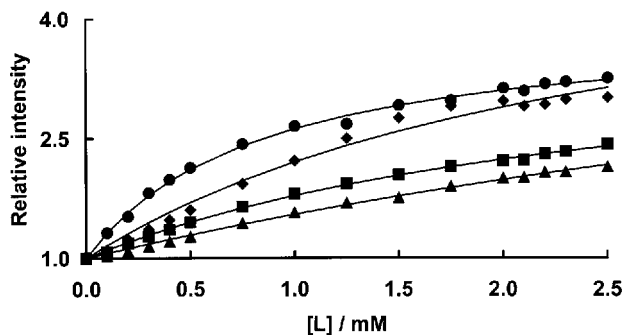


Figure 2 Partition coefficient determination

The fluorescence intensity of enfuvirtide increases upon addition of lipidic LUV as a result of a higher quantum yield of the molecules inserted into the lipidic matrix. POPC without added cholesterol (\bullet) is the most efficient in the uptake of the peptides, followed by DPPC (\blacklozenge). The differences are probably due to fluidity: POPC forms fluid bilayers (similar to biological membranes) while DPPC is in the gel state. POPC + cholesterol [33% cholesterol (in molarity); \blacktriangle] is the least efficient. The solid lines are fittings of eqn (1) to the experimental data [POPC, $K_p = (1.6 \pm 0.1) \times 10^3$; $\Delta G = 6.6 \text{ kcal} \cdot \text{mol}^{-1}$]. The presence of the negatively charged lipid POPG (20%; \blacksquare) mimics the inner leaflet of mammals' cell membranes and results in very weak incorporation. Outer leaflets are electrically neutral and mimicked by POPC. [L] is the outer leaflet lipidic (or lipid + cholesterol) concentration.

environment. The partition coefficient describing the distribution of enfuvirtide between aqueous and lipidic media is $K_p = [\text{enfuvirtide}]_L / [\text{enfuvirtide}]_w$, where $[\text{enfuvirtide}]_L$ and $[\text{enfuvirtide}]_w$ are the peptide concentrations in the lipidic and aqueous

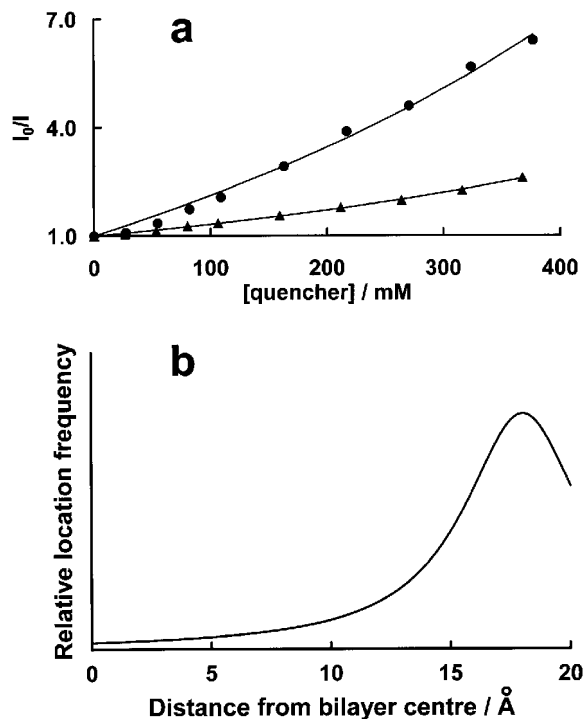


Figure 3 Location of enfuvirtide Trp residues inside the membrane

(a) Stern–Volmer plot for the quenching of enfuvirtide fluorescence by 5NS (\bullet) and 16NS (\blacktriangle) in POPC (5 mM) vesicles. 5NS is a better quencher; therefore Trp residues are located in a shallower position. (b) Quenching data (Table 1) were used to calculate the enfuvirtide Trp residues in-depth frequency distribution along the lipidic bilayer using the SIMEXDA method [9]. The shallow location is clear.

Table 1 Average fluorescence lifetimes (τ) of enfuvirtide

The mean fluorescence lifetime (τ) of enfuvirtide increases upon incorporation in lipidic membranes. Differential diffusional fluorescence quenching by 5NS and 16NS inside the lipidic matrix enables in-depth location of the Trp residues.

System	τ (ns)
Buffer	2.4
5 mM POPC	4.9
5 mM POPC/0.4 mM 5NS	3.0
5 mM POPC/0.4 mM 16NS	4.0

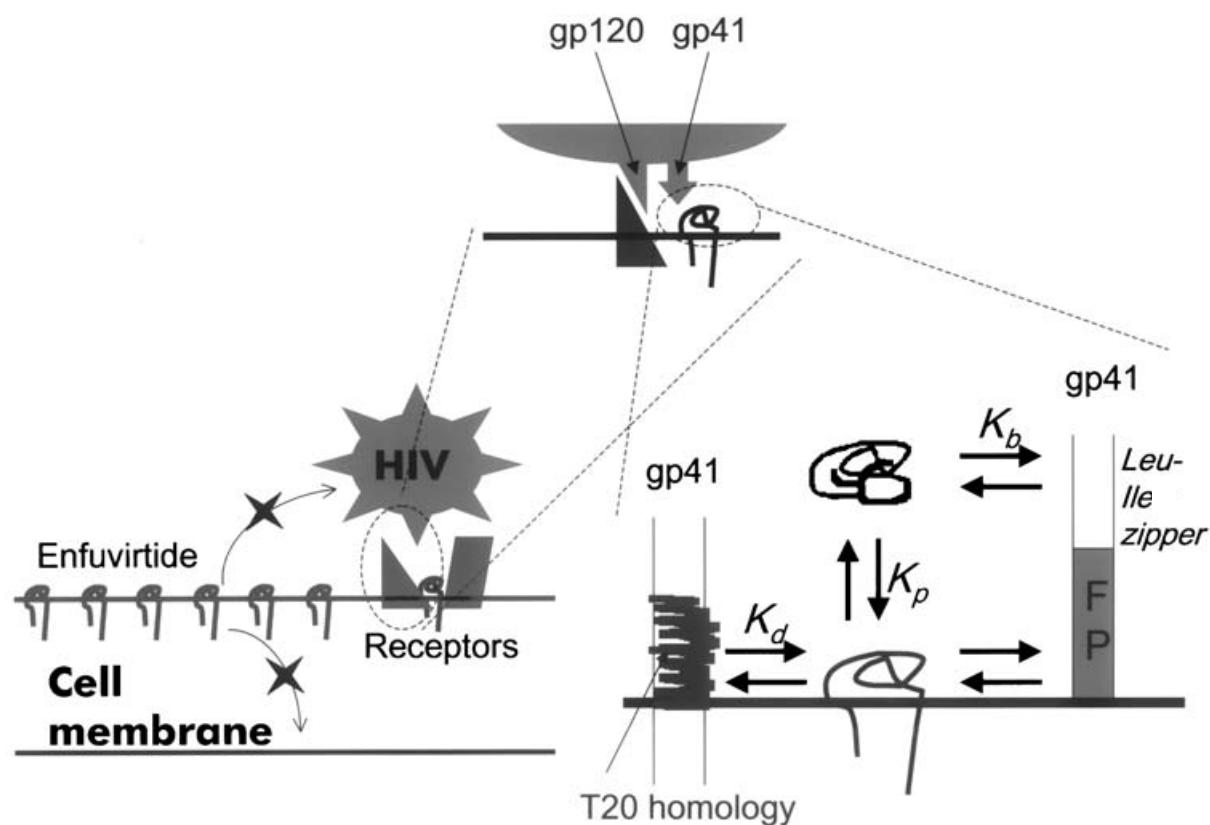
media, respectively. This can be calculated from the data (Figure 2) by fitting the following equation [5,6]:

$$\frac{I}{I_w} = \frac{1 + K_p \gamma_L [L] I_L / I_w}{1 + K_p \gamma_L [L]} \quad (1)$$

where I is the measured fluorescence intensity, I_w and I_L are the fluorescence intensities when all the molecules are in the aqueous or lipidic environment, respectively, γ_L is the lipidic molar volume [7] and $[L]$ is the molar concentration of the accessible lipid, i.e. that of the outer leaflet of the bilayer. For POPC, a lipid with packing density and fluidity properties similar to biological membranes, a K_p value of $(1.6 \pm 0.1) \times 10^3$ ($\Delta G =$

$6.6 \text{ kcal} \cdot \text{mol}^{-1}$) is obtained and this implies that, depending on the lipid concentration, the local concentration in the membrane can increase by several hundred- to thousand-fold relative to the bulk (≈ 700 -fold at $[\text{POPC}] = 4 \text{ mM}$; ≈ 1600 -fold at $[\text{POPC}] < 0.1 \text{ mM}$). However, this is severely reversed by the presence of cholesterol or physiological concentrations [8] of negatively charged lipids (Figure 2). The cholesterol effect does not seem totally caused by the condensation effect imposed by the sterol on the lipid because peptide partition into gel-phase membranes is more pronounced (Figure 2). The effect of negatively charged lipids is probably due to simple electrostatic repulsion (enfuvirtide has a overall negative net charge of -5).

The in-depth location of fluorescent molecules in lipidic membranes can be evaluated from quenching experiments with lipophilic molecules derivatized with quencher groups at selected sites [9]. Stearic acid, for instance, can be derivatized at carbon-5 or -16 with doxyl groups (5NS and 16NS, respectively). When placed in the membrane, the quencher group in 5NS locates at a shallow position, near the interface, whereas in 16NS it locates close to the hydrophobic core. 16NS is a better quencher for fluorescent molecules buried deeply in the membrane while 5NS is a better quencher for molecules near or at the interface. Enfuvirtide is better quenched by 5NS (Figure 3a), meaning that the Trp residues are located in a shallow position in the membrane. Fluorescence-lifetime quenching data (Table 1) enabled the application of the SIMEXDA method [9] to recover the Trp residues'

**Figure 4 Schematic representation of enfuvirtide action at the molecular level**

Enfuvirtide attaches to membranes in an interfacial position reaching local high concentrations. Translocation is prevented due to charge effects (among others). When the virus approaches the cell surface, its outer membrane will not compete for enfuvirtide uptake due to its high content of cholesterol. Therefore, enfuvirtide molecules remain as 'guardians' of the cell surface. The cell membrane is a reservoir of enfuvirtide; the gp41 fusiogenic approach exposes the Leu-Ile zipper-like region to the peptides, which binds them (K_b) [12]. However, local concentration of aqueous enfuvirtide is kept high due to partition equilibrium (K_p). Moreover, a high local concentration at the cell-membrane surface enables direct contact of the peptide with the gp41 C-region (K_d) when the enfuvirtide homologous sequence comes into contact with the lipidic matrix to form the fusion pore. Fusion peptide (FP) binding [2] also benefits from a high concentration of enfuvirtide at the cell surface.

in-depth distribution in the membrane (Figure 3B). A mean shallow location and a fairly narrow distribution were observed.

Like other HIV gp41 C-peptides [10], enfuvirtide is not an α -helix in solution (CD data not shown). It is known that several peptides go through a random-coil-to-helix transition upon binding to membranes [11]. However, this is not the case with enfuvirtide, which remains in a random-coil conformation when inserted in membranes (no alterations are detected in the CD spectra; results not shown).

Based on the data described above, one can depict in general terms what might be the action of enfuvirtide at the molecular level. As shown in Figure 4, enfuvirtide inserts into the external layer of the cell plasmalemma (non-charged lipids) and is prevented from translocation due to the repulsion caused by the negatively charged lipids of the inner layer, among other reasons. When the HIV approaches the cell, the virus lipidic membrane does not remove the enfuvirtide from the cell outer surface because of its high cholesterol content; i.e. enfuvirtide concentrates at cell surfaces and tends to stay there. Therefore, cell membranes are an enfuvirtide reservoir. The partition equilibrium tends to stabilize the enfuvirtide concentration in the aqueous environment when binding to gp41 occurs (i.e. improving fusion inhibition efficiency). Moreover, the high levels of enfuvirtide accumulated at the cell surface render the interaction with other segments of gp41 possible if they reach the cell surface (i.e. if enfuvirtide binding to the Leu-Ile-rich region fails and the fusion process proceeds). Binding of enfuvirtide and related molecules to the fusion peptide and other gp41-derived peptides has been reported [2,12].

Enfuvirtide was a kind gift from Roche (Palo Alto, CA, U.S.A.). We acknowledge Dr Cláudio Soares (ITQB, Lisbon, Portugal) for helping with molecular modelling, and Professor M. Prieto (Technical Univ. Lisbon) and Professor C. Saldanha (Univ. Lisbon) for valuable discussions. FCT (Portugal) funded this work.

REFERENCES

- Lalezari, J. P., Henry, K., O'Hearn, M., Montaner, J. S. G., Piliero, P. J., Trottier, B., Walmsley, S., Cohen, C., Kuritzkes, D. R., Eron, Jr, J. J. et al. (2003) Enfuvirtide, an HIV-1 fusion inhibitor, for drug-resistant HIV infection in North and South America. *N. Engl. J. Med.* **348**, 2175–2185
- Jiang, S., Zhao, Q. and Debnath, A. K. (2002) Peptide and non-peptide HIV fusion inhibitors. *Curr. Pharm. Design* **8**, 563–580
- Mayer, L. D., Hope, M. J. and Cullis, P. R. (1986) Vesicles of variable sizes produced by a rapid extrusion procedure. *Biophys. Biochim. Acta* **858**, 161–168
- Loura, L. M., Fedorov, A. and Prieto, M. (1996) Resonance energy transfer in a model system of membranes: application to gel and liquid crystalline phases. *Biophys. J.* **71**, 1823–1836
- Santos, N. C., Prieto, M. and Castanho, M. A. R. B. (1998) Interaction of the major epitope region of HIV protein gp41 with membrane model systems. A fluorescence spectroscopy study. *Biochemistry* **37**, 8674–8682
- Santos, N. C., Prieto, M. and Castanho, M. A. R. B. (2003) Quantifying molecular partition into model systems of biomembranes: an emphasis on optical spectroscopic methods. *Biochim. Biophys. Acta* **1612**, 123–135
- Chiu, S. W., Jakobsson, E., Subramanian, S. and Scott, H. L. (1999) Combined Monte Carlo and molecular dynamics simulation of fully hydrated dioleoyl and palmitoyl-oleoyl phosphatidylcholine lipid bilayers. *Biophys. J.* **77**, 2462–2469
- Gennis, R. B. (ed.) (1989) Introduction: the structure and composition of biomembranes. In *Biomembranes – Molecular Structure and Function*, pp. 22–35, Springer-Verlag, New York
- Fernandes, M. X., de La Torre, J. G. and Castanho, M. A. R. B. (2002) Joint determination by Brownian dynamics and fluorescence quenching of the in-depth location profile of biomolecules in membranes. *Anal. Biochem.* **307**, 1–12
- Lu, M., Blacklow, S. C. and Kim, P. S. (1995) A trimeric structural domain of the HIV-1 transmembrane glycoprotein. *Nat. Struct. Biol.* **2**, 1075–1082
- Wieprecht, T. and Seelig, J. (2002) Isothermal titration calorimetry for studying interactions between peptides and lipid membranes. In *Peptide-Lipid Interactions* (Simon, S. A. and McIntosh, T. J., eds.), pp. 31–56, Academic Press, New York
- Kliger, Y., Gallo, S. A., Peisajovich, S. G., Muñoz-Barroso, I., Avkin, S., Blumenthal, R. and Shai, Y. (2001) Mode of action of an antiviral peptide from HIV-1. Inhibition at a post-lipid mixing stage. *J. Biol. Chem.* **276**, 1391–1397

Received 4 September 2003/25 September 2003; accepted 26 September 2003
Published as BJ Immediate Publication 26 September 2003, DOI 10.1042/BJ20031350

3. HIV FUSION INHIBITOR PEPTIDE T-1249 IS ABLE TO INSERT OR ADSORB TO LIPIDIC BILAYERS. PUTATIVE CORRELATION WITH IMPROVED EFFICIENCY

I, Ana Salomé Veiga, declare that the experimental design and work, data analysis and discussion were carried out by me under the advisor of Prof. Miguel Castanho. The design and data analysis of the FRET experiments were done with the help of Prof. Luís Loura. Fluorescence life time experimental measurements were performed by Dr. Aleksandre Fedorov.

The manuscript was written by me and by my supervisor, Prof. Miguel Castanho. Theoretical deduction of simultaneous partition and adsorption presented in Appendix 1 was performed by Prof. Miguel Castanho. Theoretical deduction of fluorescence resonance energy transfer presented in Appendix 2 was performed by Dr. Luis Loura. Prof. Nuno Santos collaborated in the discussion and preparation of the manuscript.

I, Miguel Castanho, as Ana Salomé Veiga supervisor, hereby acknowledge and confirm the information above is correct.

Ana Salomé Veiga

Miguel Castanho

HIV Fusion Inhibitor Peptide T-1249 Is Able To Insert or Adsorb to Lipidic Bilayers. Putative Correlation with Improved Efficiency

A. Salomé Veiga,[†] Nuno C. Santos,[‡] Luís M. S. Loura,^{§,||} Aleksandre Fedorov,[§] and Miguel A. R. B. Castanho^{*,†}

Contribution from the Centro de Química e Bioquímica, Faculdade de Ciências da Universidade de Lisboa, Campo Grande C8, 1749-016 Lisboa, Portugal, Instituto de Biopatologia Química and Unidade de Biopatologia Vascular-Instituto de Medicina Molecular, Faculdade de Medicina de Lisboa, Av. Prof. Egas Moniz, 1649-028 Lisboa, Portugal, Centro de Química Física Molecular, Instituto Superior Técnico, Complexo I, 1049-001 Lisboa, Portugal, and Centro de Química e Departamento de Química, Universidade de Évora, Rua Romão Ramalho, 59, 7000-671 Évora, Portugal

Received July 6, 2004; E-mail: castanho@fc.ul.pt

Abstract: T-1249 is a HIV fusion inhibitor peptide under clinical trials. Its interaction with biological membrane models (large unilamellar vesicles) was studied using fluorescence spectroscopy. A gp41 peptide that includes one of the hydrophobic terminals of T-1249 was also studied. Both peptides partition extensively to liquid-crystalline POPC (1-palmitoyl-2-oleyl-*sn*-glycero-3-phosphocholine) ($\Delta G = -7.0$ kcal/mol and -8.7 kcal/mol, for T-1249 and terminal peptide, respectively) and are located at the interface of the membrane. T-1249 is essentially in a random coil conformation in this lipidic medium, although a small α -helix contribution is present. When other lipid compositions are used (DPPC, POPG + POPC, and POPC + cholesterol) (DPPC (1,2-dipalmitoyl-*sn*-glycero-3-phosphocholine) and POPG (1-palmitoyl-2-oleyl-*sn*-glycero-3-[phosphorac-(1-glycerol)]), partition decreases, the most severe effect being the presence of cholesterol. Partition experiments and fluorescence resonance energy transfer analysis show that T-1249 adsorbs to cholesterol-rich membranes. The improved clinical efficiency of T-1249 relative to enfuvirtide (T20) may be related to its bigger partition coefficient and ability to adsorb to rigid lipidic areas on the cell surface, where most receptors are inserted. Moreover, adsorption to the sterol-rich viral membrane helps to increase the local concentration of the inhibitor peptide at the fusion site.

Introduction

Human immunodeficiency virus type 1 (HIV-1) binding to the target cell and fusion of the membranes of both depend on the viral envelope glycoproteins complex formed by the transmembrane protein gp41, and the surface protein gp120, bounded to the external domain of gp41. The first step in the process of HIV-1 infection of a cell is mediated by gp120 binding to the CD4 receptor, present in the surface of some T-lymphocytes, macrophages, and other immune system cells.¹ This contact induces a conformational change in gp120, facilitating its connection to a second receptor, usually CCR5² or CXCR4³. The binding of gp120 to CD4 and CCR5 (or

CXCR4) triggers a conformational change in gp41, exposing a fusion peptide and allowing its insertion in the membrane of the target cell, leading to the fusion of the two membranes and mixing of the viral and cellular components.⁴

One feature of gp41 is the presence of two heptad repeat (HR1 and HR2) sequences.⁵ Enfuvirtide (T20: Fuzeon) is a synthetic 36-amino-acids peptide homologous to the C-terminal region of HR2 of HIV-1 gp41.^{6,7} This compound is currently the most advanced clinical drug for inhibiting HIV-1 entry⁶ and has recently received approval from the Food and Drug Administration.⁸ Despite the therapeutic potency of enfuvirtide, it has met with the emergence of resistant strains.^{6,8} T-1249 (a 39-amino-acids peptide) is a second-generation fusion inhibitor, composed of sequences derived from HIV-1, HIV-2, and simian immuno-

[†] Faculdade de Ciências da Universidade de Lisboa.

[‡] Faculdade de Medicina de Lisboa.

[§] Instituto Superior Técnico.

^{||} Universidade de Évora.

- (1) Lasky, L. A.; Nakamura, G.; Smith, D. H.; Fennie, C.; Shimasaki, C.; Patzer, E.; Berman, P.; Gregory, T.; Capon, D. J. *Cell* **1987**, *50*, 975–985.
- (2) Dragic, T.; Litwin, V.; Allaway, G. P.; Martin, S. R.; Huang, Y.; Nagashima, K. A.; Cayanan, C.; Maddon, P. J.; Koup, R. A.; Moore, J. P.; Paxton, W. A. *Nature* **1996**, *381*, 667–673.
- (3) Feng, Y.; Broder, C. C.; Kennedy, P. E.; Berger, E. A. *Science* **1996**, *272*, 872–877.

- (4) Klinger, Y.; Aharoni, A.; Rapaport, D.; Jones, P.; Blumenthal, R.; Shai, Y. *J. Biol. Chem.* **1997**, *272*, 13496–13505.
- (5) Trivedi, V. D.; Cheng, S.; Wu, C.; Karthikeyan, R.; Chen, C.; Chang, D. *Protein Eng.* **2003**, *16*, 311–317.
- (6) Baldwin, C. E.; Sanders, R. W.; Berkhout, B. *Curr. Med. Chem.* **2003**, *10*, 1633–1642.
- (7) Cooley, L. A.; Lewin, S. R. *J. Clin. Virol.* **2003**, *26*, 121–132.
- (8) Kilby, J. M.; Eron, J. J. *N. Engl. J. Med.* **2003**, *348*, 2228–2238.

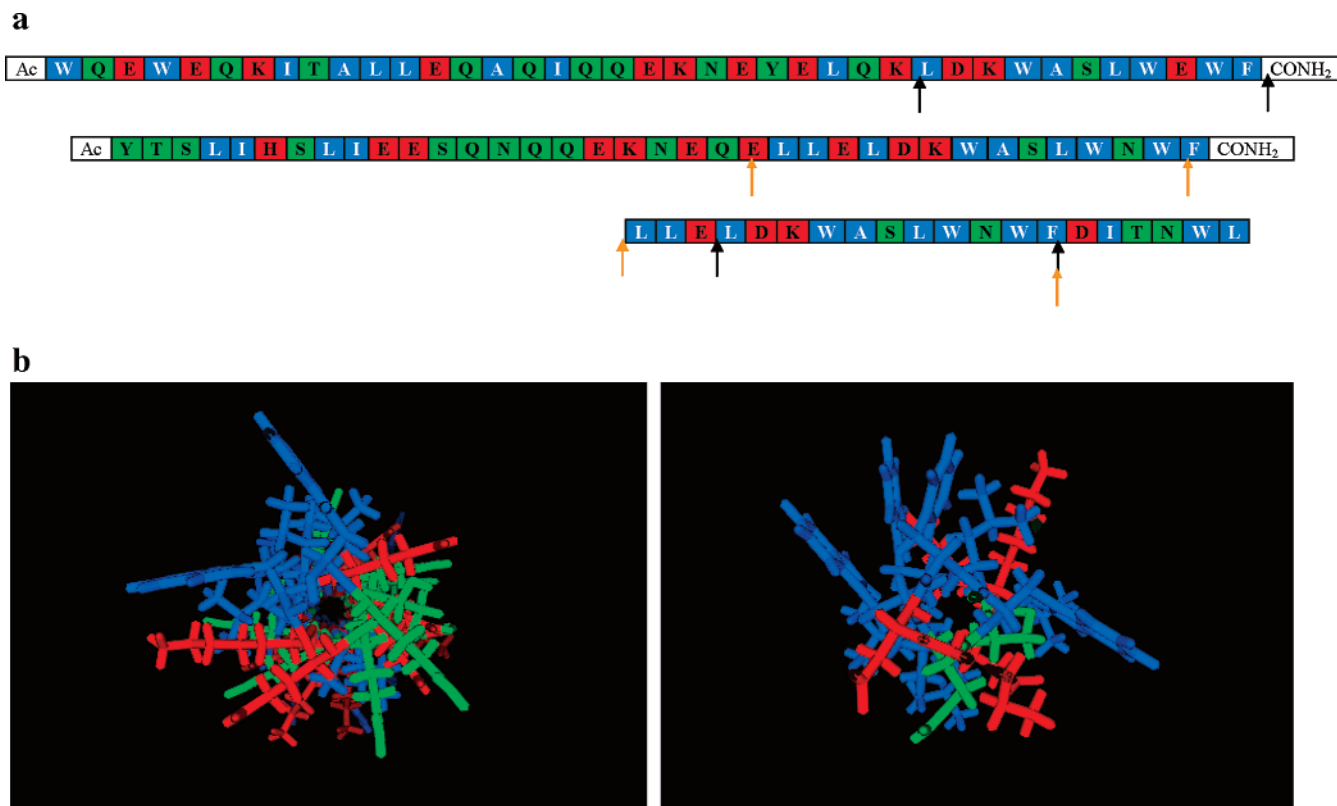


Figure 1. (A) Amino acids sequence of T-1249 (top), enfuvirtide (middle), and CTP (bottom). The arrows indicate the sequence homology between the CTP and the other peptides (black, T-1249; orange, enfuvirtide). (B) Top view of T-1249 (left) and CTP (right) arrangement in an α -helix. Hydrophobic residues are blue, noncharged polar are green, and charged polar are red.

deficiency virus (SIV).⁹ Initial phase I/II clinical trials with T-1249 have shown promising results; namely, it is a more potent inhibitor than enfuvirtide (even with a single daily administration instead of the two used for enfuvirtide) and retains activity against most enfuvirtide-resistant strains.^{6,7,9,10}

Similarly to enfuvirtide, the T-1249 sequence and presence of amphipathic segments (Figure 1, A and B) suggest that the peptide may interact with biological membranes. Theoretical analysis on the hydrophobicity of the amino acid residues sequence^{11,12} of the peptide further confirms this hypothesis. We were prompted to study the interaction of T-1249 with biological membrane models. A gp41 20-amino-acids peptide that includes the hydrophobic C-terminal sequence of enfuvirtide and T-1249 (hereafter named CTP-carboxyterminal peptide) was also studied, to conclude on the mode of insertion of these molecules in lipidic membranes.

Materials and Methods

Materials. Enfuvirtide and T-1249 were a kind gift from Roche (Palo Alto, CA), and the CTP fragment of enfuvirtide was purchased from AnaSpec, Inc. (San Jose, CA). 5NS (5-doxyl-stearic acid) and 16NS (16-doxyl-stearic acid) were from Aldrich Chem. Co. (Milwaukee, WI). L-Tryptophan, acrylamide, Hepes, and NaCl were from Merck (Darmstadt, Germany). POPC (1-palmitoyl-2-oleyl-*sn*-glycero-3-phospho-

choline), DPPC (1,2-dipalmitoyl-*sn*-glycero-3-phosphocholine), and POGG (1-palmitoyl-2-oleyl-*sn*-glycero-3-[phospho-rac-(1-glycerol)]) were purchased from Avanti Polar-Lipids (Alabaster, AL), while cholesterol and dehydroergosterol, DHE (ergosta-5,7,9(11),22-tetraen-3 β -ol), were from Sigma (St. Louis, MO). The spectrofluorimeter used was an SLM Aminco 8100 (double monochromators; 450 W Xe lamp), the UV–visible absorption spectrophotometer was a Jasco V-530, and the CD spectropolarimeter was a Jasco J720 (450 W lamp). The time-resolved instrumentation was previously described.¹³

Methods. All studied peptides contain tryptophan residues (Figure 1A), which make fluorescence techniques suitable tools to probe these molecules. In all fluorescence measurements, the excitation wavelength used was 280 nm (except time-resolved fluorescence experiments, 287 nm). 10mM Hepes, pH 7.4/150mM NaCl buffer was used throughout the studies. Enfuvirtide, T-1249, and CTP stock solutions (2.2×10^{-4} M, 1.985×10^{-4} M, and 3.9×10^{-4} M, respectively) in buffer were diluted to the final desired concentration. T-1249 and CTP solubilization required mild sonication. Remaining macroscopic aggregates of CTP were sometimes detected, although in very small quantities. In these cases, a centrifugation step was added to separate the aggregates. Large unilamellar vesicles (LUV) were prepared by extrusion techniques.¹⁴ Pure POPC and DPPC, POPC/POPG 80:20 (mol %), and POPC/cholesterol 67:33, 75:25, and 82:18 (mol %) were used on the studies of the interaction of the peptides with membrane models systems. Average fluorescence lifetimes, $\langle \tau \rangle$, were calculated from triexponential intensity decays (error estimates of the lifetime components ranged from 0.2% to 3.2%).

Membrane partition studies were performed by successive additions of small volumes of LUV (15mM) to the peptide samples (enfuvirtide 1×10^{-5} M, T-1249 6.7×10^{-6} M, or CTP 9.1×10^{-6} M) with a 10

- (9) Eron, J. J.; Gulick, R. M.; Bartlett, J. A.; Merigan, T.; Arduino, R.; Kilby, J. M.; Yangco, B.; Diers, A.; Drobnes, C.; DeMasi, R.; Greenberg, M.; Melby, T.; Raskino, C.; Rusnak, P.; Zhang, Y.; Spence, R.; Miralles, G. *J. Infect. Dis.* **2004**, *189*, 1075–1083.
- (10) Gulick, R. M. *Clin. Microbiol. Infect.* **2003**, *9*, 186–193.
- (11) White, S. H.; Wimley, W. C. *Annu. Rev. Biophys. Biomol. Struct.* **1999**, *28*, 319–365.
- (12) Jayasinghe, S.; Hristova, K.; White, S. H. *J. Mol. Biol.* **2001**, *312*, 927–934.

- (13) Loura, L. M.; Fedorov, A.; Prieto, M. *Biophys. J.* **1996**, *71*, 1823–1836.
- (14) Mayer, L. D.; Hope, M. J.; Cullis, P. R. *Biophys. Biochim. Acta* **1986**, *858*, 161–168.

min incubation in between. The emission wavelength used was 350 nm. Fluorescence intensity data were corrected for dilution effect.

Quenching studies were carried out by successive additions of small amounts of 5NS or 16NS in ethanol to samples of the peptide incubated with LUV (T-1249 4.5×10^{-6} M or CTP 6×10^{-6} M). Ethanol concentration in the sample was kept below 2% (v/v). After each addition of quencher, the sample was incubated for 10 min. The effective quencher concentration in the membrane was calculated from the partition coefficient of the quenchers to lipidic bilayers.¹⁵ The emission wavelength used was 340 nm.

Fluorescence resonance energy transfer studies between the tryptophan (donor) and fluorescently labeled vesicles with DHE (acceptor) were used to study the binding of T1249 to POPC/sterol (67:33 mol %) vesicles. The final concentration of T-1249 used was 2.2×10^{-6} M. The emission wavelength used to prevent interference of DHE emission was 320 nm. The critical distance for energy transfer, R_0 , was calculated according to Berberan-Santos and Prieto,¹⁶

$$R_0 = 0.2108[\kappa^2 \Phi_D n^{-4} \int_0^\infty I(\lambda) \epsilon(\lambda) \lambda^4 d\lambda]^{1/6} \quad (1)$$

where κ^2 is the orientation factor (the value $\kappa^2 = 2/3$, relative to the dynamic isotropic limit, was used in this study), Φ_D is the donor quantum yield in the absence of acceptor ($\Phi_D = 0.106$, the value measured in this study for high lipid concentration, was used), n is the refractive index ($n = 1.4$ was used in this study as the refractive index within the vesicles¹⁷), $I(\lambda)$ is the normalized donor emission spectrum, and $\epsilon(\lambda)$ is the acceptor molar absorption spectrum (expressed as $M^{-1} \text{cm}^{-1}$). If in eq 1 λ is in nm, the calculated R_0 will be in Å. Energy transfer efficiencies, E , were experimentally determined from

$$E = 1 - I_{DA}/I_D \quad (2)$$

where I_{DA} and I_D are the fluorescence intensities of the donor in the presence and absence of acceptor, respectively.

The final concentrations of T-1249 and enfuvirtide in the CD experiments were 6.6×10^{-5} M and 7.3×10^{-5} M, respectively. CD data are represented by the mean residue ellipticity, $[\theta]$, obtained from the observed ellipticity (θ) according to the equation $[\theta] = \theta/(Nlc)$ where l is the path length, c is the molar concentration, and N is the number of amino acid residues in the peptide.⁵

Inner filter effects were corrected¹⁸ in the fluorescence emission experiments.

Results and Discussion

Photophysical Characterization and Partition Coefficient Determination. Red edge excitation shift effects were not detected in the fluorescence emission of T-1249 and CTP tryptophan residues. Linear Stern–Volmer plots were obtained for peptides fluorescence quenching by acrylamide (not shown), revealing that the Trp residues are not localized inside hydrophobic pockets.

Figure 2 shows the result of a theoretical analysis^{11,12} of the hydrophobicity of T-1249. Enfuvirtide analysis is also shown for the sake of comparison. $\Delta G_{\text{oct}} < 0$ reveals the tendency of peptides to insert in the membrane.

As shown in Figure 3A and B, there is an increase in the fluorescence intensity of T-1249 and CTP in the presence of

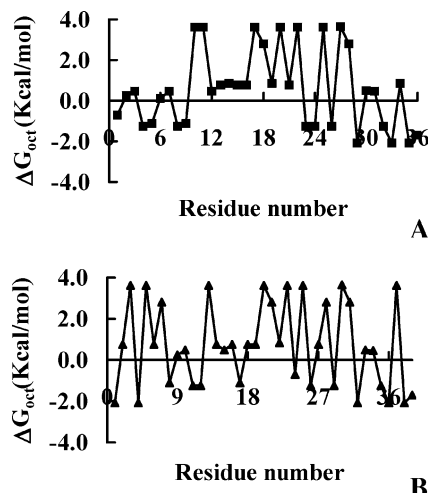


Figure 2. Theoretical analysis of partition into membranes of enfuvirtide (A) and T-1249 (B). Values of $\Delta G_{\text{oct}} < 0$ indicate the residues of the peptides with a higher tendency toward insertion in membranes. Figure 1 highlights the match of both peptides with CTP.

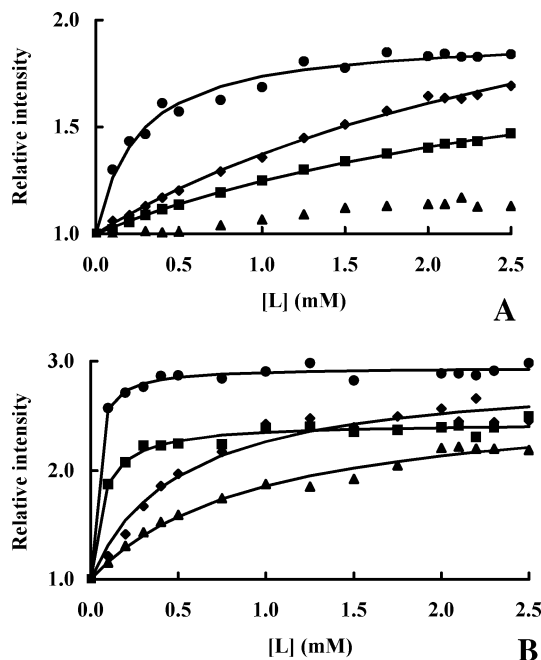


Figure 3. Partition coefficient determinations for T-1249 (A) and CTP (B). For both peptides, the largest increase in fluorescence intensity is detected in the presence of LUV of POPC (●). Although to a lesser extent, there is also an increase in the fluorescence intensity in the presence of gel state vesicles, DPPC (◆), and negatively charged lipid POPG (20% POPG in POPC; ■). The POPC/cholesterol mixture (33% mol cholesterol; ▲) is the least efficient; the increase of T-1249 fluorescence intensity is practically null. The solid lines are fittings of eq 3 to the experimental data. [L] is the concentration of the lipid available in the outer leaflet.

LUV of liquid-crystalline POPC. There is also a blue-shift of the emission spectra (3 and 12 nm for T-1249 and CTP, respectively, when $[\text{POPC}] = 5 \text{ mM}$). This spectral shift is further evidence of the interaction of the peptides with the membrane model system. The partition coefficient between the lipid and aqueous phases, $K_p = [\text{peptide}]_L/[\text{peptide}]_W$, was determined in order to quantify the extent of interaction of the peptides with the LUV. $[\text{peptide}]_L$ and $[\text{peptide}]_W$ are the peptide concentrations in the lipidic and aqueous environment, respectively. Since there is an increase in the fluorescence quantum

(15) Santos, N. C.; Prieto, M.; Castanho, M. A. R. B. *Biochemistry* **1998**, *37*, 8674–8682.

(16) Berberan-Santos, M. N.; Prieto, M. J. *Chem. Soc., Faraday Trans.* **1987**, *83*, 1391–1407.

(17) Davenport, L.; Dale, R. E.; Bisby, R. H.; Cundall, R. B. *Biochemistry* **1985**, *24*, 4097–4108.

(18) Coutinho, A.; Prieto, M. J. *Chem. Educ.* **1993**, *70*, 425–428.

yield upon membrane incorporation, K_p can be calculated from the fluorescence intensity data, I , by fitting eq 3¹⁹ to the data.

$$\frac{I}{I_W} = \frac{1 + K_p \gamma_L \frac{I_L}{I_W} [L]}{1 + K_p \gamma_L [L]} \quad (3)$$

(I_W and I_L are the fluorescence intensities expected when all the peptide is in water or in the lipidic phase, respectively; γ_L is the lipidic molar volume;²⁰ and $[L]$ is the molar concentration of the accessible lipid—outer leaflet of the bilayer.) K_p values of $(5.1 \pm 0.7) \times 10^3$ ($\Delta G = -7.0$ kcal/mol) and $(53 \pm 8.5) \times 10^3$ ($\Delta G = -8.7$ kcal/mol) were obtained for T-1249 and CTP, respectively, in POPC. Thus the K_p obtained for CTP is significantly larger than those obtained for T-1249 and enfuvirtide.²¹ This indicates that the hydrophobic segment of enfuvirtide and T-1249, which corresponds to CTP, is of major importance for lipidic membrane partition, while the hydrophilic segments tend to oppose them (theoretical expectations in Figure 2 are thus met). T-1249 has the hydrophobic amino acid moieties more evenly distributed than enfuvirtide, which concentrates the hydrophobic residues at both endings. This may explain the differences found in K_p (1.6×10^3 vs 5.1×10^3 for enfuvirtide and T-1249, respectively). When other lipid compositions are used, the K_p values of CTP and T-1249 decrease (Figure 3A and B). There is a decreased partition into gel phase membranes, due to the higher rigidity of DPPC bilayers. The presence of the 20% POPG-to-POPC ratio mimics the environment of the inner leaflet of mammal biomembranes. T-1249 and CTP have negative net formal charges of -4 and -2 , respectively. Decreased K_p in these systems can be related to electrostatic repulsion. However the most severe effect is related to the presence of sterol. For T-1249, the K_p is so small in cholesterol-rich membranes that the partition cannot be quantified ($K_p \approx 0$). At variance with T-1249 and enfuvirtide, CTP partition in these conditions occurs. Thus, the rigidity of the membrane is not the only factor that conditions the partition of the peptides.

Interaction of Enfuvirtide and T-1249 with Cholesterol-Containing Membranes. Lipidic rafts are plasma membrane domains that are enriched in cholesterol and sphingolipid.^{22,23} They are organized in a tightly packed, liquid ordered manner,²⁴ with cholesterol maintaining the rafts in a functional state.²⁵ It was proposed that rafts may function as platforms for the assembly of membrane-associated macromolecular complexes that are important in biological processes.²⁶ This prompted us to further investigate the interaction of HIV fusion inhibitor peptides with cholesterol-containing membranes. Vesicles with $\sim 33\%$ of cholesterol (i.e., ~ 2 phospholipids:1 sterol) are homogeneous²⁷ (liquid ordered phase). Considering its rigidity, this phase may be regarded as a crude mimic of lipid rafts.

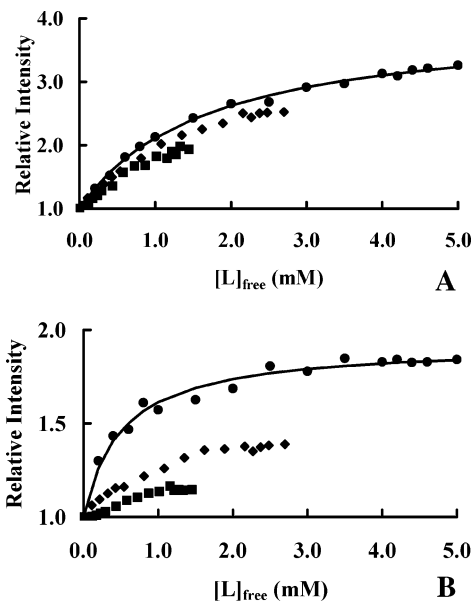


Figure 4. Partition plots of enfuvirtide (A) and T-1249 (B) to LUV of POPC/cholesterol. Fluorescence intensities dependence on $[lipid]_{free}$ (eq 4) for 0% (●), 18% (◆), and 25% (■) cholesterol. Data sets overlap for enfuvirtide (A) but not for T-1249 (B).

Although $K_p \approx 0$, adsorption of the peptides to the rigid bilayers surface cannot be discarded because adsorption can leave Trp residues exposed to the bulk aqueous environment, with unchanged fluorescence quantum yield (i.e., not contributing for K_p calculation). Vesicles with a lower content in cholesterol are heterogeneous, having cholesterol-rich and cholesterol-poor areas.²⁷ Thus, the liquid disordered phase and raft-like ordered phase coexist. If partition is only occurring to the disordered phase (cholesterol-poor) areas and no adsorption to the ordered phase (cholesterol-rich) is taking place, then one expects partition curves (I/I_W ; eq 3) to be only dependent on the lipid concentration which is involved in cholesterol-poor areas; i.e., partition plots against the concentration of POPC external to ordered areas should all coincide, regardless of the cholesterol content of the vesicles. “Free lipid” (i.e., in cholesterol-poor areas) concentration can be calculated from lipid/cholesterol phase diagrams²⁷ (namely the lower and upper limits of two-phase coexistence) using the lever rule (eq 4):

$$[lipid]_{free} = [lipid + sterol]_{total} \frac{33 - x}{33 - 5} \quad (4)$$

where x (5–33%) is the cholesterol mol % (18% and 25%, in our study, Figure 4A and B).

Partition curves for enfuvirtide are almost mutually overlapped, regardless of the cholesterol content, showing that enfuvirtide does not significantly adsorb to the cholesterol-rich areas. When K_p is calculated for 18% and 25% cholesterol in the $[lipid]_{free}$ domain, K_p is similar to those obtained with sterol-free membranes. However, T-1249 (Figure 4B) shows a different behavior: partition curves do not superimpose in the $[lipid]_{free}$ domain, and I/I_W decreases with cholesterol content. This may be due to adsorption of the peptide to the cholesterol-rich areas, without significant variation of the fluorescence quantum yield. This additional equilibrium (adsorption) competes with partition, decreasing the molar fraction of molecules embedded in the lipidic bilayers. With the increase of the percentage of chole-

(19) Santos, N. C.; Prieto, M.; Castanho, M. A. R. B. *Biochim. Biophys. Acta* **2003**, *1612*, 123–135.

(20) Chiu, S. W.; Jakobsson, E.; Subramaniam, S.; Scott, H. L. *Biophys. J.* **1999**, *77*, 2462–2469.

(21) Veiga, S.; Henriques, S.; Santos, N. C.; Castanho, M. *Biochem. J.* **2004**, *377*, 107–110.

(22) Campbell, S. M.; Crowe, S. M.; Mak, J. J. *Clin. Virol.* **2001**, *22*, 217–227.

(23) Silvius, J. R. *Biochim. Biophys. Acta* **2003**, *1610*, 174–183.

(24) Alonso, M. A.; Millán, J. J. *Cell Sci.* **2001**, *114*, 3957–3965.

(25) Simons, K.; Ehehalt, R. *J. Clin. Invest.* **2002**, *110*, 597–603.

(26) Guyader, M.; Kiyokawa, E.; Abrami, L.; Turelli, P.; Trono, D. *J. Virol.* **2002**, *76*, 100356–10364.

(27) Tauc, P.; Mateo, C. R.; Brochon, J.-C. *Biophys. J.* **1998**, *74*, 1864–1870.

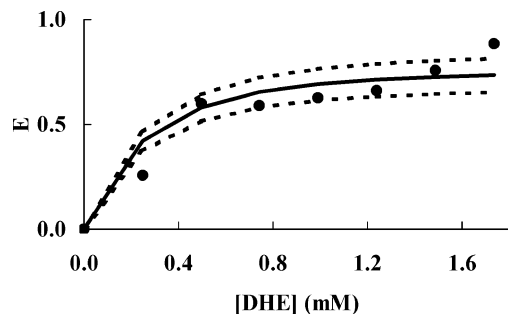


Figure 5. Energy transfer efficiency from Trp residues of T-1249 (donors) to DHE (acceptor) in POPC/cholesterol (33% mol cholesterol) vesicles (5 mM). Nonlinear regression (appendix 2) yields $A_1 = 0.3$ (molar fraction of nonadsorbed peptides). The boundaries $A_1 = 0.2$ and $A_1 = 0.4$ are also represented (dashed lines).

terol, a larger area is occupied by the domains and more adsorption of T-1249 occurs. Appendix 1 quantifies the equilibria balance and rationalizes the altered partition plots. This analysis takes into account partition of T-1249 to POPC and adsorption to the POPC/Cholesterol domains. Data fitting with eq A1.9 (appendix 1; Figure A1.2) leads to $K_a = 3.1 \times 10^3$ and $K_a = 4.6 \times 10^3$ for 18% and 25% of cholesterol, respectively (adsorption partition coefficient).

Interaction of T-1249 with Cholesterol-Rich Area Vesicles.

A FRET Study. To further confirm and quantify the adsorption of T-1249 to the cholesterol-rich areas, we used a fluorescence resonance energy transfer (FRET) methodology using DHE as an acceptor for T-1249 tryptophan fluorescence. LUV of POPC/cholesterol/DHE (33–9.9% cholesterol, 0–23.1% DHE) were used. Figure 5 shows an increase in the energy transfer efficiency with DHE content. Thus, the Trp moieties of T-1249 are in the vicinity of the sterol; i.e., adsorption occurs. To quantify the fraction of molecules adsorbed, we followed the methodology described in appendix 2. The fraction of nonadsorbed molecules, A_1 , is $A_1 = 0.3 \pm 0.1$, corresponding to 70% of adsorbed molecules when $[\text{POPC} + \text{cholesterol}] = 5 \text{ mM}$ (33% molar cholesterol). These values confirm that adsorption of T-1249 to sterol-rich membranes occurs. Equation A1.3 (appendix 1) relates the adsorption partition constant, K_a , lipid and sterol concentrations, and the molar fraction of the adsorbed peptide ($1 - A_1$). Therefore, $0.4 \times 10^3 < K_a < 1.0 \times 10^3$, which broadly concur to the values calculated in the previous section. K_a was calculated from the volumic concentration of the peptide in the membrane. The partition constant obtained from superficial concentration, $K_{a,\text{sup}}$, can be obtained from K_a from $K_{a,\text{sup}} = K_a h$, where h is the half-bilayer thickness.

In-Depth Location of the Peptides in Membranes and Secondary Structure Studies. Quenching methodologies were used to evaluate the in-depth location of the Trp residues of the peptides inserted in POPC vesicles. Stearic acid molecules derivatized with doxyl (quencher) groups at carbon-5 (5NS) and -16 (16NS) were used. 5NS is a better quencher for molecules near or at the interface, while 16NS is better for molecules buried deeply in the membrane.²⁸ Figure 6A shows the Stern–Volmer plots obtained for T-1249 (similar results were obtained with CTP, not shown) using the effective concentration of 5NS and 16NS in the bilayer matrix. The peptides are better quenched by 5NS. So, the Trp residues of the peptides are located near

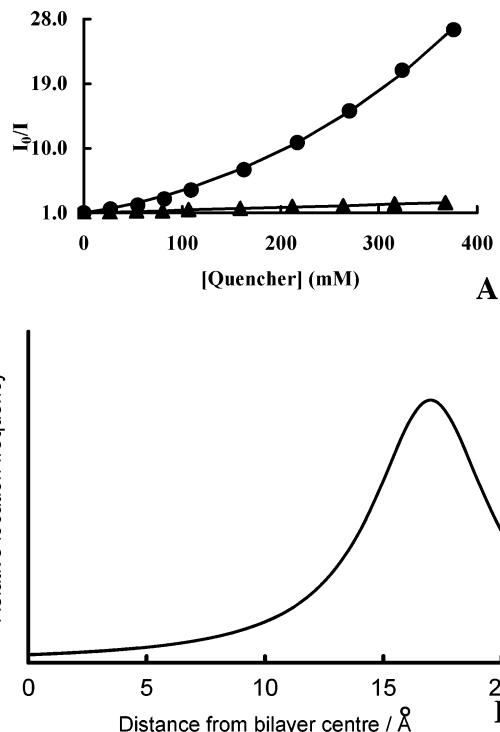


Figure 6. (A) Stern–Volmer plot for the quenching of T-1249 fluorescence by the derivatized lipophilic molecules 5NS (●) and 16NS (▲) in POPC vesicles (5 mM). Effective quencher concentration in the membrane was considered. (B) Using the SIMEXDA method²⁸ and fluorescence lifetime quenching data (Table 1), it was possible to determine the in-depth distribution of T-1249 Trp residues in the lipidic bilayer. The location is mainly interfacial.

Table 1. Average Fluorescence Lifetimes of T-1249 and CTP^a

system	$\langle \tau \rangle / \text{ns}$	
	T-1249	CTP
buffer	2.7	2.2
[POPC] = 5 mM	4.4	4.4
[POPC] = 5 mM, [5NS] = 0.4 mM	2.9	3.2
[POPC] = 5 mM, [16NS] = 0.4 mM	3.6	3.6

^a The average fluorescence life-time of peptides increases upon incorporation in lipidic membranes. Differential diffusional fluorescence quenching by 5NS and 16NS inside the lipidic matrix enables in-depth location of the Trp residues.

the interface of the membrane. Fluorescence lifetime quenching data (Table 1) enable the application of the SIMEXDA method²⁸ to obtain the in-depth distribution of the Trp residues of the peptides (Figure 6B; CTP distribution is similar; result not shown). This location distribution does not differ much from the one obtained previously with enfuvirtide.²¹ The Trp moieties are mainly located at the membrane interface.

CD experiments show that enfuvirtide and T-1249 are essentially in a random coil conformation in both aqueous and lipidic medium (POPC) (Figure 7). However, enfuvirtide has a negligible α -helix content ($\sim 8\%$ and $\sim 10\%$ in buffer and POPC, respectively), while a helix component can be detected in T-1249, albeit small ($\sim 30\%$ and $\sim 25\%$ in buffer and POPC, respectively). The obtained percentages of the α -helix content of the peptides are independent of the method applied to calculate them.^{29,30}

(28) Fernandes, M. X.; de la Torre, J. G.; Castanho, M. A. R. B. *Anal. Biochem.* **2002**, *307*, 1–12.

(29) Kligler, Y.; Shai, Y. *J. Mol. Biol.* **2000**, *295*, 163–168.

(30) Mobley, P. W.; Pilpa, R.; Brown, C.; Waring, A. J.; Gordon, L. M. *AIDS Res. Hum. Retroviruses* **2001**, *17*, 311–327.

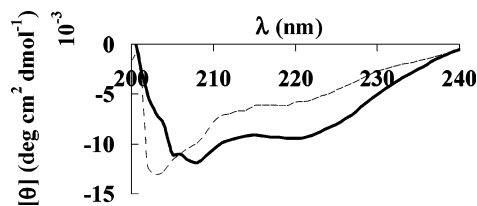


Figure 7. Far-UV CD spectra of enfuvirtide (dashed line) and T-1249 (solid line) in the presence of POPC vesicles ([POPC] = 2 mM; $X_{L, \text{Enfuvirtide}} = 0.54$; $X_{L, \text{T-1249}} = 0.8$). The increased helicity of T-1249 relative to enfuvirtide is noticeable. Spectra in buffer are similar.

Conclusions

T-1249 is a fusion inhibitor peptide under clinical trials but its mode of action is not totally understood. The use of fluorescence spectroscopy-based methodologies to study the interaction of the peptide with model membranes shows that (1) partition to LUV of POPC is very extensive and the peptide is located near the lipids polar heads level, mainly in random coil conformation; (2) in the presence of gel phase membranes (rigid DPPC bilayers), POPG-containing bilayers that mimic the environment of the inner leaflet of mammals biomembranes, and cholesterol-rich membranes, insertion in the lipidic environment is severely decreased; (3) however, there is a very significant adsorption of T-1249 to cholesterol-rich areas. Thus, lipidic membranes may play an important role in the mode of action of T-1249 (Figure 8). Namely, T-1249 can insert in the external layer of cell while it is prevented from translocation due to the repulsion caused by the negatively charged lipids of the inner layer. This way, T-1249 concentrates at the cell surfaces. Unlike enfuvirtide, T-1249 is able to adsorb to cholesterol-rich membranes. This ability raises the concentration of T-1249 in the surface of the cell directly at the fusion site because HIV-1 receptor CD4 and co-receptors CXCR4/CCR5 are considered to be localized within lipid rafts.³¹ It is possible that the coalescence of several small rafts, containing these proteins, would be necessary to form an active larger raft domain,²⁵ enabling receptors oligomerization, viral binding, and membrane fusion. Because the HIV membrane is very rich in cholesterol,^{26,31} the local concentration of T-1249 is further raised. Enfuvirtide inhibition occurs when target and viral membranes are near each other^(32 and references therein). The increased extension of partition of T-1249 relative to enfuvirtide,²¹ and the possibility to adsorb to cholesterol-rich membranes might be the main cause of its improved efficiency as HIV fusion inhibitor. Hydrophobic derivatives of enfuvirtide proved to be 100× more efficient than enfuvirtide itself in HIV-1 replication inhibition.³³ Gene therapeutic-based strategies are currently being developed with membrane-anchored en-

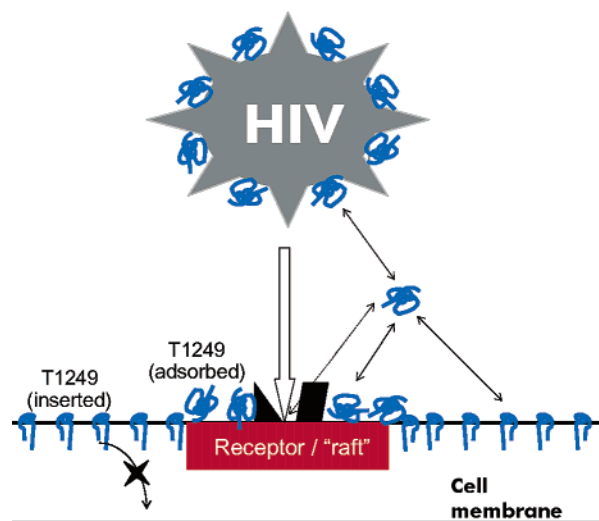


Figure 8. Schematic representation of the proposed involvement of lipidic membranes in T-1249 mode of action. T-1249 attaches to cell membranes in an interfacial position and adsorb to cholesterol-rich domains. Translocation is prevented due to charge effects. The virus outer membrane has loosely bound T-1249, contributing to the rise of the T-1249 local concentration at the fusion site. Moreover, the ability to loosely bind to lipid rafts in the direct vicinity of the receptors improves peptide action at the fusion site. The cell membrane and the virus are a reservoir of the peptide. gp41 fusogenic approach to the target membrane enables direct contact of the peptide with the gp41 C-region, which leads to fusion inhibition.

virtide.³⁴ T-1249's longer half-life in circulation (enabling a single daily administration, instead of the two daily administrations of enfuvirtide), together with its promising results in clinical trials, even with patients whose virus have reduced susceptibility to enfuvirtide,⁹ can be (at least partially) justified by T-1249 combination of hydrophobicity, membrane partition, and "selective" adsorption, a capability not shared with enfuvirtide.

Acknowledgment. This project was partially funded by FCT-MES (Portugal), including a grant (SFRH/BD/14336/2003) under the program POCTI to A.S.V. T-1249 and enfuvirtide were kind gifts from Roche (Palo Alto, CA).

Supporting Information Available: Appendix 1: simultaneous partition and adsorption. Appendix 2: fluorescence resonance energy transfer. This material is available free of charge via the Internet at <http://pubs.acs.org>.

JA0459882

(31) Campbell, S. M.; Crowe, S. M.; Mak, J. *AIDS* **2002**, *16*, 2253–2261.

(32) Bär, S.; Alizon, M. *J. Virol.* **2004**, *78*, 811–820.

(33) Hildinger, M.; Dittmar, M. T.; Schult-Dietrich, P.; Fehse, B.; Schnierle, B. S.; Thaler, S.; Stiegler, G.; Welker, R.; von Laer, D. *J. Virol.* **2001**, *75*, 3038–3042.

(34) Egelhofer, M.; Brandenburg, G.; Martinius, H.; Schult-Dietrich, P.; Melikyan, G.; Kunert, R.; Baum, C.; Choi, I.; Alexandrov, A.; von Laer, D. *J. Virol.* **2004**, *78*, 568–575.

Supporting Information Available (Veiga, AS et al.)

APPENDIX 1 – Simultaneous partition and adsorption

According to Figure A1.1, T-1249 is assumed to be distributed in 3 different locations: bulk aqueous media (W), ‘free’ POPC (L) and POPC/Cholesterol patches (LC). The total T-1249 fluorescence intensity is given by $I = I_W \cdot X_W + I_{LC} \cdot X_{LC} + I_L \cdot X_L$, where I_i and X_i are the fluorescence intensities that would be obtained if all the peptides were located in the environment i and the molar fractions of the peptide in that environment, respectively. Considering that the quantum yield of the peptide in water is equal to the quantum yield of the peptide adsorbed in POPC/Cholesterol patches, then $I_W = I_{LC}$ and:

$$I = I_W \cdot (1 - X_L) + I_L \cdot X_L \quad (\text{A1.1})$$

Considering the equilibria in Figure A1.1 (insertion in sterol-poor domains and adsorption to sterol-rich domains):

$$\frac{n_L}{n_W + n_L} = \frac{K_P \gamma_L [L]}{1 + K_P \gamma_L [L]} \quad (\text{A1.2})$$

$$\frac{n_{LC}}{n_w + n_{LC}} = \frac{K_a \gamma_{LC} ([L_C] + [C])}{1 + K_a \gamma_{LC} ([L_C] + [C])} \quad (\text{A1.3})$$

where n_i are the moles of the peptide in the environment i ; K_p and K_a are the partition and adsorption coefficients, respectively, of the peptide, as defined in Eq. A1.4 and A1.5; $[L]$, $[L_C]$ and $[C]$ are the molar concentration of ‘free’ POPC, POPC in the cholesterol domains and cholesterol, respectively; γ_L and γ_{LC} , are, respectively, the average lipidic molar volumes of the POPC and the cholesterol-rich domains. Combining Eq. A1.2 and A1.3, it is possible to calculate both the molar fraction of peptides inserted in the sterol-poor domains (X_L) and the molar fraction of peptides adsorbed to the sterol-rich domains (X_{LC}):

$$K_p = \frac{[T - 1249]_L}{[T - 1249]_w} \quad (\text{A1.4})$$

$$K_a = \frac{[T - 1249]_{LC}}{[T - 1249]_w} \quad (\text{A1.5})$$

$$X_L = (1 - X_{LC}) \frac{K_p \gamma_L [L]}{1 + K_p \gamma_L [L]} \quad (\text{A1.6})$$

$$X_{LC} = (1 - X_L) \frac{K_a \gamma_{LC} ([L_C] + [C])}{1 + K_a \gamma_{LC} ([L_C] + [C])} \quad (\text{A1.7})$$

Therefore,

$$X_L = \frac{(1 - U_a) U_p}{1 - U_a U_p} \quad (\text{A1.8})$$

where U_p and U_a are, respectively:

$$U_p = \frac{K_p \gamma_L [L]}{1 + K_p \gamma_L [L]} \quad (\text{A1.9})$$

$$U_a = \frac{K_a \gamma_{LC} ([L_C] + [C])}{1 + K_a \gamma_{LC} ([L_C] + [C])} \quad (\text{A1.10})$$

Eq. A1.1 can be rewritten as:

$$\frac{I}{I_w} = \frac{1 - U_p}{1 - U_a U_p} + \frac{I_L}{I_w} \frac{U_p (1 - U_a)}{1 - U_a U_p} \quad (\text{A1.11})$$

which describes the fluorescence intensity-dependence on lipid and sterol concentration. However, $[C]$ and $[L_C]$ are not practical variables to work with. Therefore, they were related to a single independent variable. If f_c is the cholesterol fraction and $[L]_T$ is the molar concentration of the total POPC, then:

$$[C] = \frac{f_c}{1-f_c} [L]_T \quad (\text{A1.12})$$

The molar concentration of ‘free’ POPC, $[L]$, is $[L] = [L]_T - 2[C]$ (sterol-rich domains in bilayer matrixes involves a ~2:1 lipid:sterol proportion, with minimal variations among the phosphatidylcholine lipids family). Thus,

$$[L] = [L]_T \left(1 - 2 \frac{f_c}{1-f_c} \right) \quad (\text{A1.13})$$

$$[L_C] + [C] = 3 \frac{f_c}{1-f_c} [L]_T \quad (\text{A1.14})$$

Combining Eq. A1.9, A1.10, A1.13 and A1.14, a practical function is obtained, which can be used for non-linear regression analysis of experimental data (Figure A1.2). Data fitting with K_p previously calculated from pure POPC vesicles (5.1×10^{-3}) yielded $K_a = 3.1 \times 10^3$ and $K_a = 4.6 \times 10^3$, for 18 and 25% of cholesterol, respectively. It was considered for the fitting that $\gamma_{LC} \approx \gamma_L$. Although the strict statistical quality of the fit is not totally

satisfactory, probably due to the severe assumption of $I_{LC} = I_W$, the effect of adsorption on partition equilibrium in heterogeneous membranes is elucidative.

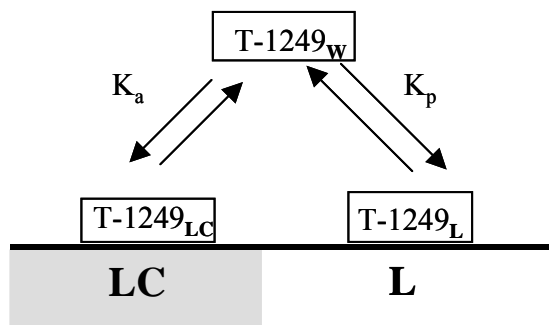


Figure A1.1. Diagram representing T-1249 distribution in 3 different locations: bulk aqueous media (W), ‘free’ POPC (L) and POPC/Cholesterol patches (LC).

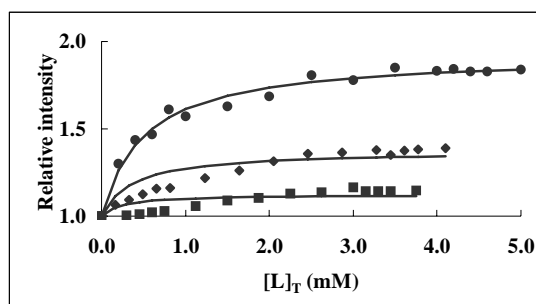


Figure A1.2. Partition plots of T-1249 to LUV of POPC/Cholesterol mixture. Fluorescence intensity dependence on the POPC concentration, $[Lipid]_{Total}$, for 0% (●), 18% (◆) and 25% (■) cholesterol. Eq. A1.11 was fitted to the experimental data for 18 and 25 % cholesterol (solid lines) using the previously calculated K_p for pure POPC vesicles (●; Figure 3 A) and both K_a and I_L as fitting parameters.

APPENDIX 2 – Fluorescence resonance energy transfer

The decay of donor fluorescence intensity in the absence of acceptor is:

$$I_D(t) = A_1 I_{D,B}(t) + (1 - A_1) I_{D,A}(t) \quad (\text{A2.1})$$

where A_1 (sole fitting parameter of the model) is the fraction of molecules in buffer. $I_{D,B}(t)$ and $I_{D,A}(t)$ are the fluorescence decays of the donor in buffer and adsorbed to POPC/cholesterol vesicles, respectively:

$$I_{D,B}(t) = \sum_i \alpha_{i,B} \exp\left(-\frac{t}{\tau_{i,B}}\right) \quad (\text{A2.2})$$

$$I_{D,A}(t) = \sum_i \alpha_{i,A} \exp\left(-\frac{t}{\tau_{i,A}}\right) \quad (\text{A2.3})$$

In the presence of a sterol (membrane-bound) acceptor, the fluorescence decay of the buffer sub-population is not affected, but the adsorbed donors fluorescence is extinct by acceptors localized in two parallel planes (Figure A2.1). The values of $W_1 = 10 \text{ \AA}$ and $W_2 = 30 \text{ \AA}$ were obtained on the basis of bilayer widths reported by others authors^{1,2} and molecular models. The donor fluorescence decay, in the presence of the acceptor is:

$$I_{D,A}(t) = A_1 I_{D,B}(t) + (1 - A_1) \cdot I_{D,A}(t) \cdot \rho_1(t) \cdot \rho_2(t) \quad (\text{A2.4})$$

The $\rho_i(t)$ functions denote the RET rates to acceptors located on the planes W_1 and W_2 away from the donor, respectively, and are given by ³:

$$\rho_i(t) = \exp \left\{ -2 \left(\frac{W_i}{R_0} \right)^2 n \pi R_0^2 \int_0^1 \frac{1 - \exp \left[\left(-\frac{t}{\langle \tau \rangle} \right) \left(\frac{R_0}{W_i} \right)^6 \alpha^6 \right]}{\alpha^3} d\alpha \right\} \quad (\text{A2.5})$$

where $\langle \tau \rangle$ is the mean fluorescence lifetime of the donor, R_0 is the Förster radius (Eq. 1) and n is the acceptor density (molecules/unit area), which was computed from:

$$n = \frac{[\text{DHE}]}{[\text{POPC}] \cdot \left(a_{\text{POPC}} + \frac{1}{2} a_{\text{chol}} - b \right)} \quad (\text{A2.6})$$

where $[\text{DHE}]$ and $[\text{POPC}]$ are the analytical concentrations of DHE and POPC, respectively; a_{POPC} and a_{chol} are the areas per POPC and cholesterol molecule, respectively, 66.4 \AA^2 ,⁴ and 37.7 \AA^2 ,⁵ on the bilayer plane; and b is the condensation effect of cholesterol on the bilayer area, for this composition, $7 \text{ \AA}^2/\text{POPC molecule}$.⁵

Finally, the FRET efficiency was calculated according to Eq. 2 where I_D and I_{DA} were obtained by numerical integration of the theoretical decay laws:

$$I_D = \int_0^{\infty} i_D(t) dt \quad (\text{A2.7})$$

$$I_{DA} = \int_0^{\infty} i_{DA}(t) dt \quad (\text{A2.8})$$

The sole fitting parameter, A_1 , was obtained from non-linear regression analysis of experimental data (Figure 5).

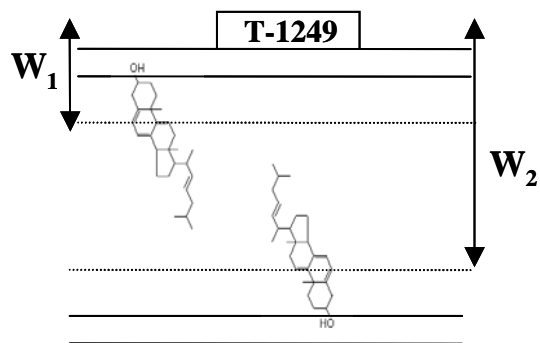


Figure A2.1. Diagram representing the donor-acceptor geometry in the lipidic bilayer: T-1249 adsorbed at the surface and sterols (DHE) in both leaflets of the membrane.

References

- 1 - de Almeida, R.F.M.; Loura, L.M.S.; Prieto, M.; Watts, A.; Federov, A.; Barrantes, F.J. *Biophys. J.* **2004**, *86*, 2261-2272.
- 2 - Nezil, F.A.; Bloom, M. *Biophys. J.* **492**, *61*, 1176-1183.
- 3 - Davenport, L.; Dale, R.E.; Bisby, R.B.; Cundall, R.B. *Biochemistry* **485**, *24*, 4097-4108.
- 4 - Chiu, S.W.; Jakobsson, E.; Subramaniam, S.; Scott, H.L. *Biophys. J.* **499**, *77*, 2462-2469.
- 5 - Smaby, J.M.; Momsen, M.M.; Brockman, H.L.; Brown, R.E. *Biophys. J.* **497**, *73*, 1492-1505.

Chapter III

PUTATIVE INHIBITION OF SARS-CoV BY THE HIV-1 FUSION INHIBITORS T20 AND T-1249

1. INTRODUCTION

Severe acute respiratory syndrome (SARS) is a new infectious disease that appeared in Guangdong Province (China) in November 2002 (WHO, http://www.who.int/csr/media/sars_wha.pdf). The disease had spread globally, about 8000 people were infected, resulting in more than 800 deaths (WHO, http://www.who.int/csr/sars/country/2003_08_15/en/). The etiological agent was identified as a novel coronavirus (CoV), the SARS-associated CoV or SARS-CoV (Drosten et al., 2003; Ksiazek et al., 2003; Marra et al., 2003; Peiris et al., 2003; Rota et al., 2003). The SARS-CoV (Figure III.1) is neither a mutant nor a recombinant of any known CoVs. Its genome sequence reveals that this novel agent does not belong to any of the known groups of CoVs, constituting a new group within the CoV family (Rota et al., 2003; Marra et al., 2003), although extensive genome and proteome analysis suggested that it is distantly related to group 2 CoVs (Snijder, 2003). CoVs are a family of enveloped, single-stranded-RNA viruses causing disease in humans and animals, but the other known CoVs that affect humans cause only the common cold. SARS-CoV possibly infected the human population from an animal reservoir by way of the wet markets in Guangdong Province (Guan et al., 2003). How the precursor animal CoV adapted to humans to achieve efficient human-to-human transmission is not known. The

virus was transmitted from person to person mainly via the respiratory route and close contact with patients (Stadler et al., 2003; Yu et al., 2004). SARS is an atypical pneumonia characterized by influenza-like symptoms including fever, cough and headache, non-treatable with conventional antibiotic therapy. Despite the lung is the most affected organ, the possibility of viral infection in multiple organs has been raised (Ding et al., 2004; Farcas et al., 2005). Although more than four years have passed since a large outbreak of SARS, SARS-CoV still represents a risk to humans. As SARS-CoV exists and can replicate in animal reservoirs, the possibility of its reintroduction in the human population and reemergence of its associate disease cannot be excluded (Webster, 2004; Lau et al., 2002; Li et al., 2005).

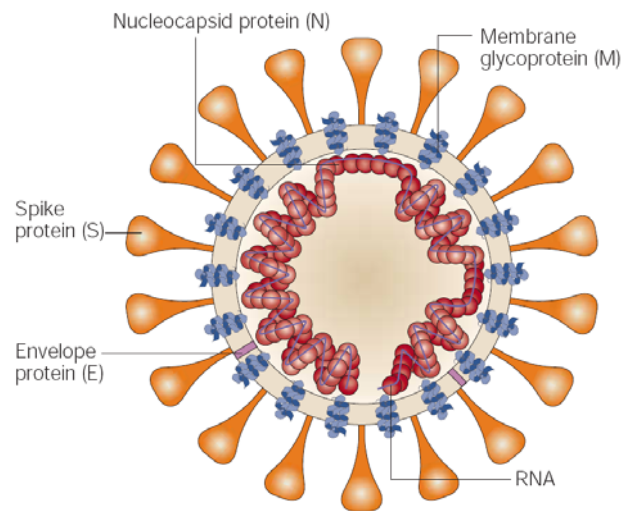


Figure III.1 – Schematic structure of the SARS-CoV virion. A lipid bilayer composes the viral envelope that surrounds the helical nucleocapsid, which is formed by the viral RNA genome and the viral nucleocapsid (N) protein. A corona of large and distinctive spikes is present in the envelope, as well the membrane (M) glycoprotein and the envelope (E) protein. The spikes are oligomers of the spike (S) glycoprotein, responsible for binding to receptors on host cells and fuse the viral envelope with target cell membranes (from Stadler et al., 2003).

The SARS-CoV genome encodes 28 proteins that include 16 non-structural proteins, 4 structural proteins and 8 accessory proteins (Bartlam et al., 2007). The structural proteins are the spike (S), the envelope (E), the membrane (M) and the nucleocapsid (N) proteins (Figure III.1). The S protein consists of three domains, the external N-terminal domain with the S1 and S2 subunits, a TM, and a short cytoplasmic domain at the C-terminal. This protein is a class I fusion protein that mediates the binding of the virus to

the host cell receptor and the subsequent fusion between the viral and host membranes (Gallagher and Buchmeier, 2001; Rota et al., 2003; Xiao and Dimitrov, 2004). However, unlike class I fusion proteins, cleavage between the S1 and S2 subunits of the S protein is not a requirement for fusion (Rota et al., 2003; Xiao et al., 2003; Xiao and Dimitrov, 2004). The S1 domain (N-terminal region) contains the sequence responsible for the binding to the SARS-CoV cell receptor, identified as the metallopeptidase angiotensin-converting enzyme 2 (ACE-2) (Li et al., 2003; Wong et al., 2004; Prabakaran et al., 2004). ACE-2 is present in lung alveolar epithelial cells, enterocytes of the small intestine, and the endothelial cells of arteries and veins and arterial smooth muscle in several organs (Hamming et al., 2004). ACE-2 localization may explain the tissue tropism of SARS-CoV for the lung and small intestine (Ding et al., 2004). Nevertheless, no virus infection is detected in endothelial cells, which express ACE-2 to a high level. The need of other cellular receptor(s) or coreceptor(s) may explain such behaviour (To and Lo, 2004). The S2 domain (membrane-anchored C-terminal region) that mediates membrane fusion, contains an internal FP and has two HR regions, NHR and CHR, forming coiled-coil structures (Bosch et al., 2004; Ingallinella et al., 2004; Liu et al., 2004; Tripet et al., 2004; Zhu et al., 2004). The putative FP has been identified upstream close to NHR (Sainz et al., 2005a). Similar to HIV-1, membrane-active regions probably with a role in the membrane fusion process were identified in the S2 sequence (Guillén et al., 2005; Sainz et al., 2005b). In SARS-CoV (Bosch et al., 2004; Ingallinella et al., 2004; Liu et al., 2004; Tripet et al., 2004; Zhu et al., 2004) as in several other viruses, HR regions have crucial importance for viral fusion. These regions form a 6HB structure, consisting of an inner trimeric coiled coil formed by NHR domains, with CHR domains surrounding the trimer, packed in antiparallel orientation (Supekar et al., 2004; Xu et al., 2004). This structure brings the viral and cellular membranes into close proximity, leading to membrane fusion. Synthetic peptides derived from the HR were shown to inhibit infection by either retroviruses (e.g., Lu et al., 1995; Kilby et al., 1998; Eckert and Kim, 2001a; Eckert and Kim, 2001b), paramyxoviruses (e.g., Joshi et al., 1998) or coronavirus (e.g., Bosch et al., 2003). Peptides derived from the CHR region can inhibit the viral infection by interfering with the 6HB formation. The possibility that CHR derived peptides act as SARS-CoV infection inhibitors was confirmed (Bosch et al., 2004; Liu et al., 2004; Zhu et al., 2004), albeit at much higher molar concentrations than similar inhibitors used to prevent HIV entry. Even though CHR peptides inhibitory properties may possibly be

affected by different factors, SARS-CoV 6HB lower stability, caused by a weaker interaction between the NHR and CHR regions, could be directly correlated with a lower potency of the CHR peptide in blocking the formation of this structure (Bosch et al., 2004; Liu et al., 2004; Supekar et al., 2004).

Considering that there are no specific and efficacious treatments available to prevent or treat SARS, the development of anti-SARS drugs to be active in future SARS outbreaks is crucial. The development of entry inhibitors, including inhibitor peptides derived from the CHR region as referred above, are a valuable option (Cinatl et al., 2005). However, the development and approval of novel antiviral drugs against SARS-CoV may take years. Several drugs already approved and in clinical use to other viral diseases had been tested as anti-SARS-CoV (Chen and Cao, 2004; Yamamoto et al., 2004; Chen et al., 2004; Zhang and Yap, 2004; Tan et al., 2004). Additionally and based on a structural analysis of HIV-1 gp41 and SARS-CoV S2 protein, Gallaher and Garry proposed that T20 could inhibit SARS-CoV infectivity, although with a limited activity (Gallaher and Garry, <http://www.virology.net/Articles/sars/s2model.html>). The study presented in this chapter helps to elucidate this theme.

2. WHY ARE HIV-1 FUSION INHIBITORS NOT EFFECTIVE AGAINST SARS-CoV? BIOPHYSICAL EVALUATION OF MOLECULAR INTERACTIONS

I, Ana Salomé Veiga, declare that the experimental design and work, data analysis and discussion were carried out by me under the advisor of Prof. Miguel Castanho. The peptide synthesis was done by Yunyun Yuan, Xuqin Li, and Dr. Gang Liu.

The manuscript was written by me and by my supervisor, Prof. Miguel Castanho. Theoretical deduction of simultaneous partition and interaction presented in Appendix 1 was performed by me and Prof. Miguel Castanho. Prof. Nuno Santos collaborated in the discussion and preparation of the manuscript.

I, Miguel Castanho, as Ana Salomé Veiga supervisor, hereby acknowledge and confirm the information above is correct.

Ana Salomé Veiga

Miguel Castanho

Why are HIV-1 fusion inhibitors not effective against SARS-CoV? Biophysical evaluation of molecular interactions

Salomé Veiga^a, Yunyun Yuan^b, Xuqin Li^b, Nuno C. Santos^c,
Gang Liu^{b,1}, Miguel A.R.B. Castanho^{a,*}

^a Centro de Química e Bioquímica, Faculdade de Ciências da Universidade de Lisboa, Campo Grande C8, 1749-016 Lisboa, Portugal

^b Chinese Academy of Medical Sciences and Peking Union Medical College, Institute of Materia Medica, 1 Xian Nong Tan St., Beijing 100050, P. R. China

^c Instituto de Biopatologia Química/Faculdade de Medicina de Lisboa and Unidade de Biopatologia Vascular/Instituto de Medicina Molecular, Av. Prof. Egas Moniz, 1649-028 Lisboa, Portugal

Received 12 July 2005; received in revised form 20 September 2005; accepted 6 October 2005

Available online 28 October 2005

Abstract

The envelope spike (S) glycoprotein of the severe acute respiratory syndrome associated coronavirus (SARS-CoV) mediates the entry of the virus into target cells. Recent studies point out to a cell entry mechanism of this virus similar to other enveloped viruses, such as HIV-1. As it happens with other viruses peptidic fusion inhibitors, SARS-CoV S protein HR2-derived peptides are potential therapeutic drugs against the virus. It is believed that HR2 peptides block the six-helix bundle formation, a key structure in the viral fusion, by interacting with the HR1 region. It is a matter of discussion if the HIV-1 gp41 HR2-derived peptide T20 (enfuvirtide) could be a possible SARS-CoV inhibitor given the similarities between the two viruses. We tested the possibility of interaction between both T20 (HIV-1 gp41 HR2-derived peptide) and T-1249 with S protein HR1- and HR2-derived peptides. Our biophysical data show a significant interaction between a SARS-CoV HR1-derived peptide and T20. However, the interaction is only moderate ($K_B = (1.1 \pm 0.3) \times 10^5 \text{ M}^{-1}$). This finding shows that the reasoning behind the hypothesis that T20, already approved for clinical application in AIDS treatment, could inhibit the fusion of SARS-CoV with target cells is correct but the effect may not be strong enough for application.

© 2005 Elsevier B.V. All rights reserved.

Keywords: T20; Enfuvirtide; T-1249; Fusion inhibitor; HIV-1; SARS-CoV

1. Introduction

The outbreak of severe acute respiratory syndrome (SARS) was caused by a novel coronavirus, the SARS-associated coronavirus (SARS-CoV) [1–5]. As SARS-CoV can replicate in an animal reservoir, it might be reintroduced in the human population (even as a more dangerous strain), originating a seasonal disease [6]. Considering that there is no specific treatment for this infection, it is necessary to develop antiviral agents to prevent possible future epidemics. Coronavirus are enveloped viruses and their entry into target cells is mediated by the spike (S) envelope glycoprotein [5,7]. Although SARS-

CoV S protein can be classified as a class I viral fusion protein, some features set it apart: for instance, cleavage between the S1 and S2 subunits of the S protein is not a requirement for fusion [5,7]. The S1 domain (N-terminal region) contains the sequence responsible for the binding to the SARS-CoV cell receptor ACE2 (angiotensin-converting enzyme 2) [8,9]. The S2 domain (membrane-anchored C-terminal region) mediates membrane fusion, and contains two heptad repeat regions, HR1 and HR2, forming coiled-coil structures [10–14]. In a number of viruses, including SARS-CoV [10–14], HR regions have determining importance for viral fusion: these regions form a six-helix bundle structure, consisting of an inner trimeric coiled coil formed by HR1 domains, with HR2 domains surrounding the trimer, packed in antiparallel orientation. This structure brings the viral and cellular membranes into close proximity, leading to membrane fusion. Synthetic peptides derived from the HR were shown to inhibit infection by either retroviruses

* Corresponding author. Fax: +351 21 7500088.

E-mail address: castanho@fc.ul.pt (M.A.R.B. Castanho).

¹ These authors contributed equally to the work.

(e.g., [15–18]), paramyxoviruses (e.g., [19]) or coronavirus (e.g., [20]). The peptides derived from the HR2 region can inhibit infection by interfering with the six-helix bundle formation. Thus, based on the behavior of other enveloped viruses like HIV-1, recent studies have suggested a cell entry mechanism of SARS-CoV similar to viruses with class I viral fusion proteins [10–13]. The potential of HR2-derived peptides as inhibitors of SARS-CoV infection was demonstrated [10,12,14]. In addition, based on a structural analysis of HIV-1 gp41 and SARS-CoV S protein, Gallaher and Garry proposed that T20 (enfuvirtide) could inhibit SARS-CoV infectivity, although with a limited activity [21]. T20 is a HIV-1 gp41 HR2-derived peptide that blocks entry of HIV-1 into the target cells, which is already in clinical use [22]. T-1249 is a second-generation HIV-1 fusion inhibitor with promising results [23]. In the present study, we have explored the potential of the HIV-1 HR2-derived peptide T20 and the related peptide T-1249 against SARS-CoV, using S protein HR1- and HR2-derived peptides (Table 1). The results obtained confirmed the occurrence of an interaction between the HIV-1 peptides and peptides derived from SARS-CoV HR1 as speculated [21]. However, the interaction does not seem to be strong enough to grant therapeutic efficiency, which justifies the limited activity foreseen by Gallaher and Garry [21] and recently confirmed in infectivity assays [24].

2. Experimental

2.1. Materials

T20 and T-1249 were a kind gift from Roche (Palo Alto, CA, USA). All the N α -L-Fmoc-protected amino acids, coupling reagents (DIC) and HOBt were obtained from GL Biochem (Shanghai, China). Fmoc rink MBHA resin (loading 0.44 mmol/g, 1% DVB, 100–200 mesh) was purchased from Hecheng, Co. (Tianjin, China). Other reagents used in peptide synthesis were obtained commercially and were of analytical grade. Unless otherwise stated, all solvents for synthesis were of analytical grade and used without further purification. DMF was redistilled under reduced pressure after dried over 4 Å molecular sieves overnight. 1,8-ANS (8-phenylamino-1-naphthalenesulfonic acid) and di-8-ANEPPS (4-[2-[6-(dioctylamino)-2-naphthalenyl]ethenyl]-1-(3-sulfopropyl)-pyridinium) were purchased from Molecular Probes (Eugene, OR, USA). POPC (1-palmitoyl-2-oleyl-*sn*-glycero-3-phosphocholine) was

from Avanti Polar-Lipids (Alabaster, AL, USA). HEPES and NaCl were from Merck (Darmstadt, Germany). 10 mM HEPES buffer pH 7.4, 150 mM NaCl, was used throughout the studies. T20 and T-1249 stock solutions in buffer were diluted to final desired concentrations. Stock solutions of SARS-CoV S protein-derived peptides were prepared in buffer with small amounts of DMSO and diluted to final concentrations. Through the experiments, DMSO concentration in the samples was at most 1.4% (v/v). All peptides solubilization required mild sonication, mainly HR1-derived peptides. The spectrofluorimeter used was a SLM Aminco 8100 with double monochromators and 450 W Xe lamp.

2.2. Methods

2.2.1. Peptide synthesis

The peptides were synthesized by a standard Fmoc/t-Bu protection strategy. After removal of Fmoc of Fmoc-rink MBHA resin by 20% Piperidine/DMF (v:v) treatment for 10 min twice, the resin was thoroughly washed by DMF, Methanol, DCM and DMF, three times each. Fmoc protective amino acid was then coupled onto the resin for 45 min at room temperature using 3-fold excess molar ratio of amino acid and 3-fold excess DIC and HOBt as coupling and additive reagents, respectively. Until Kaiser's test [25] showing to be negative, the Fmoc-deprotection and washing steps were performed again as described above. The next amino acid assembly was repeated. In case of Kaiser's test to be positive or weakly positive, a double coupling step was carried out until Kaiser's test to be negative. Otherwise, the remaining amino group after two-coupling steps was captured by 15% Ac₂O/DCM (v:v) for 30 min at room temperature. After all amino acids were successfully assembled onto resin, the last Fmoc group was removed and the resin was rinsed thoroughly with DMF, methanol and DCM. The resin must be completely dried under airflow at room temperature before the peptide was cleaved off resin.

Crude peptide attaching onto 100 mg resin was treated by TFA (4.0 mL), thioanisole (0.2 mL), phenol (0.3 g), deionized water (0.2 mL) and EDT (0.1 mL) for 2 h at room temperature. The 'peptide+resin' mixture was filtered and the tube was rinsed with 2–3 mL cleavage mixture. The combined solution was dried under a slow flow of nitrogen gas and then treated with ice-cooled methyl t-butyl ether-petroleum ether (3:1) to precipitate the peptide. The crude peptide was washed twice

Table 1
Sequences of HIV-1 fusion inhibitor peptides T20 and T-1249, and of the peptides derived from the HR1 and HR2 regions of SARS-CoV spike protein (Pep 1D, Pep 1E and Pep 2B, Pep HR2, respectively)

Peptide	Protein location	Sequence
T20	–	YTSLIHSLIEESQNQQEKNEQELLELDKWASLWNWF
T-1249	–	WQWEQKITALLEQAQIQEKNEYELQKLDKWASLWEIF
Pep 1D	900–921	ENQKQIANQFNKAISIQESLT
Pep 1E	931–951	QDVVNQNAQALNTLVKQLSSN
Pep 2B	1157–1178	SVVNIQKEIDRLNEVAKNLNES
Pep HR2	1150–1189	DISGINASVVNIQKEIDRLNEVAKNLNESLIDLQELGKYE

The corresponding amino acid residues in SARS-CoV S protein of the derived peptides used is in the table.

with ice-cooled methyl t-butyl ether-petroleum ether (3:1) and air dried naturally. The crude peptide was dissolved in 30–60% CH₃CN–H₂O (v:v) and purified by HPLC (Gilson 322 pump, Gilson UV/vis-152 detector, and Gilson 215 liquid handler) on a semi-preparative Vydac C18 column. The flow rate was 5 mL/min. The solvents were A: 5% CH₃CN in H₂O, B: 5% H₂O in CH₃CN. The pH was adjusted with TFA 0.05% (v/v). The detecting wavelength was 214 nm. Depending on the peptide sequences, the gradient was adjusted until the expected HPLC peak was separated very well. Collected fractions were analyzed by our HPLC-MS system on a Vydac C18 analytic column (4.6 μm × 25 cm). When both a purity of peptide over 95% and correct molecular weight were obtained, the peptide was lyophilized and used as a powder for subsequent studies.

2.2.2. SARS-CoV S protein-derived peptides influence on T20 and T-1249 fluorescence

S peptides are not intrinsically fluorescent, except for Pep HR2, which is weakly fluorescent in the operation conditions of our study, due to the Tyr residue. However, the presence of tryptophan residues in T20 and T-1249 enable the use of fluorescence techniques to study these molecules. To study the influence of S peptides on T20 (10 μM) or T-1249 (6.7 μM) fluorescence emission ($\lambda_{exc}=280$ nm; $\lambda_{em}=350$ nm) and conclude on mutual association, these peptides were titrated with successive additions of small amounts of S peptides (or just the solvent for controls). After each addition of peptide the sample was incubated for 10 min before measurement. Fluorescence intensity data was corrected for the dilution effect.

2.2.3. Hydrophobic interactions between T20 or T-1249 and S protein SARS-CoV-derived peptides

The existence of hydrophobic interactions between T20 or T-1249 and S peptides was studied by means of the ANS probe fluorescence ($\lambda_{exc}=372$ nm; $\lambda_{em}=480$ nm). ANS was added (final concentration 26 μM) to a sample of a selected peptide (6.7 μM for T-1249 and 10 μM for all the other peptides), and the other peptide was added in successive aliquots. The inverse situation (i.e., exchange of titrated and added peptide) was also carried out. To account for the possible self-aggregation of the added peptides, the same procedure was repeated in the absence of the titrated peptide, i.e., titration of an aqueous ANS solution only. After each peptide addition, the sample was incubated for 10 min before measurement. DMSO additions, in the same amounts present in peptide solutions, were used to control its effect on ANS fluorescence. Fluorescence intensity data were corrected for the dilution effect.

2.2.4. Membrane partition of SARS-CoV S protein-derived peptides

POPC (in chloroform) and di-8-ANEPPS (from a stock solution in ethanol) were mixed in a round bottom flask, and the solution was dried under a stream of nitrogen. Solvent removal was completed in vacuum, overnight. Large unilamellar vesicles (LUV) were prepared by extrusion techniques

[26]. Peptides were added afterwards. Di-8-ANEPPS excitation spectra were obtained with emission at 603 nm [27,28]. The final concentrations used were 200 μM for lipids, 10 μM for di-8-ANEPPS and 15 μM for all peptides.

2.2.5. Membrane partition of T20 and T-1249 in the presence of SARS-CoV S protein-derived peptides

POPC LUV were prepared by extrusion techniques [26] as before, except that the di-8-ANEPPS probe was not used. Membrane partition studies were performed by successive additions of small volumes of LUV (15 mM) to the peptide samples, with 10 min incubation in between. The peptide samples were composed of T20 or T-1249 alone or in mixtures with equimolar concentration of S peptides (T20 10 μM and T-1249 6.7 μM). The excitation wavelength used was 280 nm and the emission wavelength was 350 nm. Fluorescence intensity data were corrected for the dilution effect.

3. Results

3.1. Pep 1D presence lead to fluorescence variations in T20

S peptides (Table 1) influence on T20 and T-1249 fluorescence emission was used for the evaluation of peptides interactions. Titration of T20 with Pep 1D (Fig. 1A) or Pep 1E (results not shown) leads to a fluorescence emission intensity increase. A similar but not so pronounced result was obtained with T-1249 (Fig. 1B). Fluorescence variation was not detected for any of the others peptide pairs, e.g., T20 or T-1249 with Pep

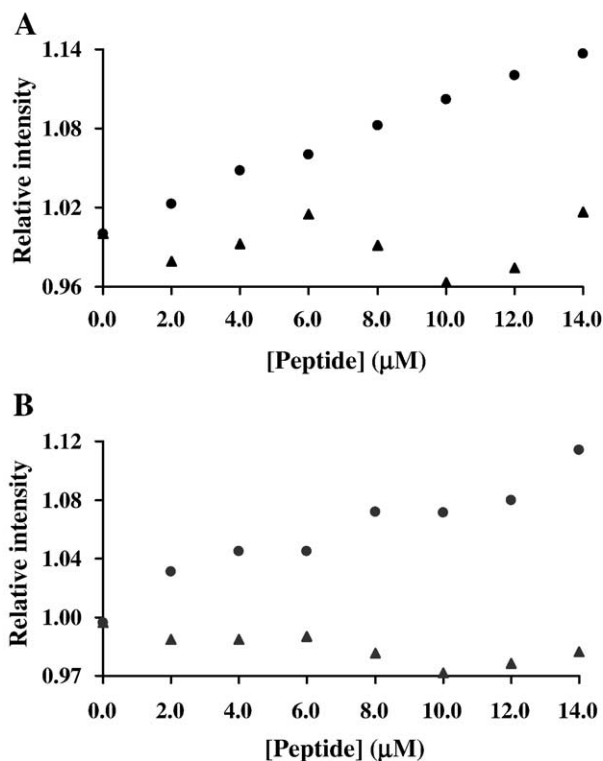


Fig. 1. T20 (A) and T-1249 (B) fluorescence intensity variation in the presence of Pep 1D (●) and Pep 2B (▲). Small amounts of S peptides were added to a sample of T20 (10 μM) or T-1249 (6.7 μM).

2B (Fig. 1A and B, respectively). DMSO presence has no effect on T20 and T-1249 fluorescence intensity.

3.2. Hydrophobic interactions occur between Pep 1D and T20

ANS (an environmentally sensitive probe) is essentially non fluorescent in water, becoming fluorescent in a less polar environment, e.g., when bound to hydrophobic sites in proteins [29,30]. It was shown before that this probe can be used to study peptide assemblies [30]. Therefore, we used the increase in ANS fluorescence intensity (increased quantum yield) to study the existence of hydrophobic binding between T20 or T-1249 and S peptides because this binding may lead to the formation of hydrophobic grooves where ANS can insert, with a concomitant increase in fluorescence intensity. To evaluate peptides interactions, pair-wise tests were carried out. Small amounts of one peptide were added to the other peptide/ANS sample. For each pair of studied peptides, reverse titration (i.e., titration of the first peptide with the second) was also carried out. To take into account eventual self-aggregation of the titrating peptide, all peptides were used to titrate ANS samples in buffer. The results show that Pep 1D (Fig. 2A), T-1249 (Fig. 2C) and Pep 1E (data not shown) self-aggregate. However, the ANS fluorescence increase observed with the addition of Pep 1D to T20 is larger than the observed with Pep 1D alone (self-aggregation), which is indicative of mutual binding between these peptides—Fig. 2A. The T20/Pep 1E mixture also indicates interaction (data not shown). Although similar, T-1249/Pep 1D results exhibit a larger variability (Fig. 2C). T-1249 does not interact with Pep 1E. Both T20 and T-1249 show no evidence of interaction when the other two S peptides are used (results for the T20/Pep 2B and T-1249/Pep 2B systems are shown in Fig. 2B and D, respectively, as an example). No DMSO effect on ANS fluorescence was detected. Peptides Pep 1D and Pep HR2 interact with each other (data not shown), in agreement with the results obtained by Liu et al. [12]. This result serves as a positive control of the method.

3.3. S protein-derived peptides do not interact with membranes

Due to the lack of intrinsic fluorescence in S peptides, the interaction studies with model membranes could not be done by a direct method. Thus, di-8-ANEPPS was used as a probe for peptide–membrane interaction. The magnitude of the membrane dipole potential is affected by membrane binding and by the insertion of molecules as such peptides. This change on the potential magnitude may be monitored by means of spectral shifts of the fluorescence indicator di-8-ANEPPS [27,28]. Fig. 3 shows the fluorescence difference spectra for all S peptides, as well as for T20 and T-1249. Fluorescence difference spectra were obtained by subtracting the excitation spectrum of di-8-ANEPPS-labeled POPC membranes in the absence and presence of the peptides. Before subtraction, the spectra were normalized to the integrated areas so that the difference spectra reflect only spectral shifts. Fluorescence intensity difference spectra for T20 and T-1249 (peptides known to interact with membranes [31,32]) and S peptides

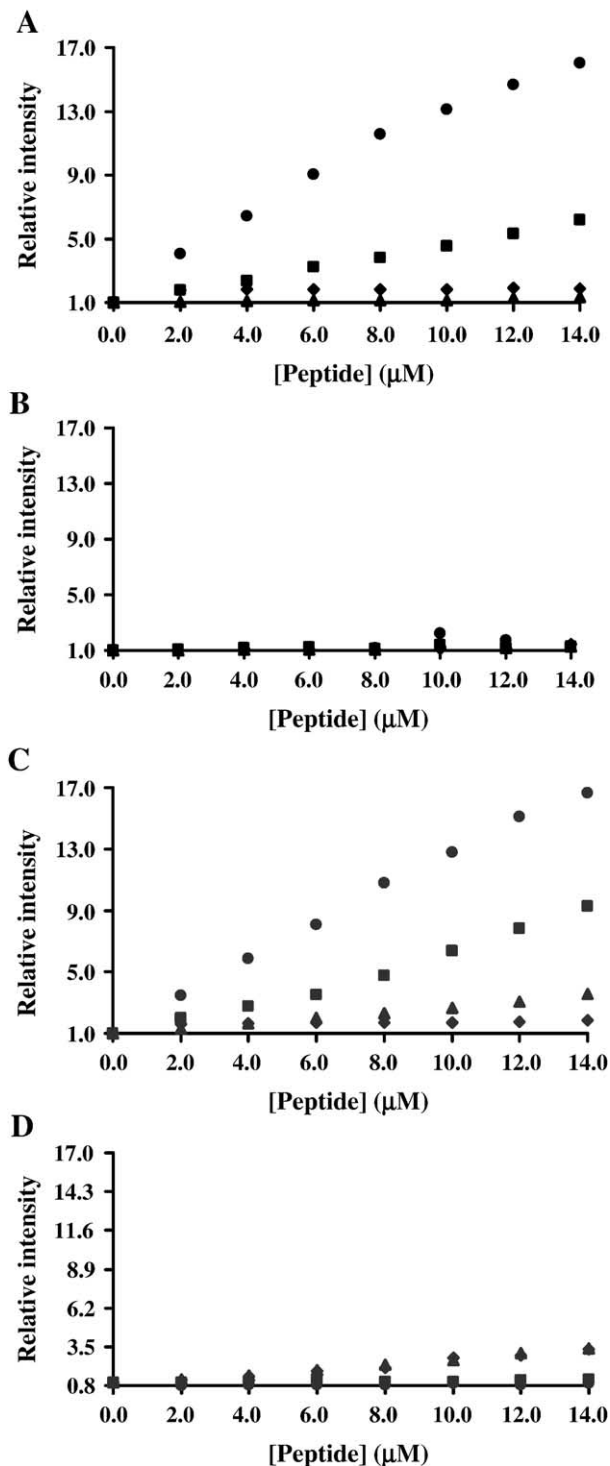


Fig. 2. ANS (26 μM) fluorescence intensity for the titration of (A) T20 with Pep 1D (and vice-versa), (B) T20 with Pep 2B (and vice-versa), (C) T-1249 with Pep 1 D (and vice-versa) and (D) T-1249 with Pep 2B (and vice-versa). Small amounts of Pep 1D or Pep 2B were added to a T20 or T-1249 sample containing ANS, and vice-versa. T20 or T-1249 added to S peptide (\blacklozenge) and S peptide added to T20 or T-1249 (\bullet) lead to different results. Small amounts of each peptide (\blacktriangle —T20 or T-1249; \blacksquare —S peptide, Pep 1D in panels A and C and Pep 2B in panels B and D) were added to a buffer/ANS sample to evaluate self-aggregation.

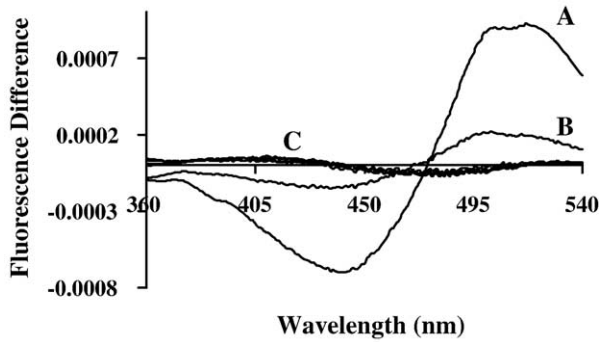


Fig. 3. Di-8-ANEPPS-labeled (10 μ M) membranes (POPC 200 μ M LUV) fluorescence difference spectra ($\lambda_{em}=603$ nm). The spectra were obtained by subtracting the excitation spectrum before the addition of peptides from the excitation spectra after the peptides addition (15 μ M). Before subtraction, the spectra were normalized to the integrated areas so that the difference spectra reflect only the spectral shifts. (A) T-1249, (B) T20 and (C) S peptides. The latter spectra have no meaningful difference among each other.

show no interaction of the latter with the membranes. The small DMSO amount present in the samples does not perturb membrane structure [33].

3.4. Pep 1D interferes with the membrane partition of T20

T20 and T-1249 membrane partition experiments were done in the presence and absence of S peptides as a tool to enable the calculation of peptide binding constants. A decrease in the partition occurs for T20 in the presence of Pep 1D (Fig. 4A). In the presence of Pep 1E the result is not so striking, although clear. T-1249 results were not conclusive. With Pep 2B and Pep HR2 no difference occurs in T20 and T-1249 partition (Fig. 4B). The small DMSO amounts used do not perturb membranes [33]. In agreement, DMSO had no significant effect on T20 and T-1249 partition to membranes.

4. Discussion

SARS-CoV membrane fusion mechanism is similar to that of class I viral fusion proteins, where HR regions have a very important role. The HR1 regions form a trimer where the HR2 regions pack onto the grooves in an antiparallel manner to form the six-helix bundle [12]. This structure leads to a close apposition of viral and target cell membranes, favoring the membrane fusion. The SARS-CoV S protein HR2-derived peptides are able to inhibit viral entry. HR2 peptides compete for binding to the HR1 region of the SARS-CoV S protein, blocking the six-helix bundle structure formation, and thus inhibiting fusion [10,12]. In our studies, we have explored the interaction between T20 (HIV-1 gp41 HR2-derived peptide) or T-1249 and SARS-CoV S protein HR1 (Pep 1D or Pep 1E)- or HR2 (Pep 2B or Pep HR2)-derived peptides, in order to explore a possible SARS-CoV fusion inhibition by the first ones.

T20 fluorescence increases in the presence of Pep 1D or Pep 1E (although with a better signal/noise ratio in the first case), but not in the presence of the other S peptides. The same occurs

for T-1249, although the results are not so evident. This increase in the fluorescence quantum yield probably indicates tryptophan residues exposure to a less polar environment, protected from the aqueous environment [34], revealing peptides interaction. Alternative explanations, such as a decrease in Trp fluorescence quenching by other peptide residues, cannot be ruled out. Nevertheless, the increase of ANS fluorescence intensity in the peptide/peptide titrations is an evidence for the formation of hydrophobic pockets. To assure that such increase is not due to the self-aggregation of the titrating peptide, instead of inter-association of different peptides, control experiments were performed in the absence of the titrated peptides. Although self-aggregation occurs for T-1249, Pep 1D and Pep 1E, a T20/Pep 1D inter-association of hydrophobic nature is evident. However, the titration of T20 with Pep 1D does not lead to precisely the same result as the opposite titration. The addition of Pep 1D to T20 lead to an ANS fluorescence increase larger than the increase caused by Pep 1D self-aggregation alone. The addition of T20 to Pep 1D does not result in a similar fluorescence increase. This occurs because T20 is not able to destroy Pep 1D aggregates, which prevent peptides interaction in a larger extent. The T20/Pep 1E and T-1249/Pep 1D systems lead to low signal/noise ratios, preventing straightforward conclusions. Yet, T-1249 and Pep 1E show no evidence for interaction. Both T20 and T-1249 show no interaction with HR2-derived peptides detectable by ANS fluorescence.

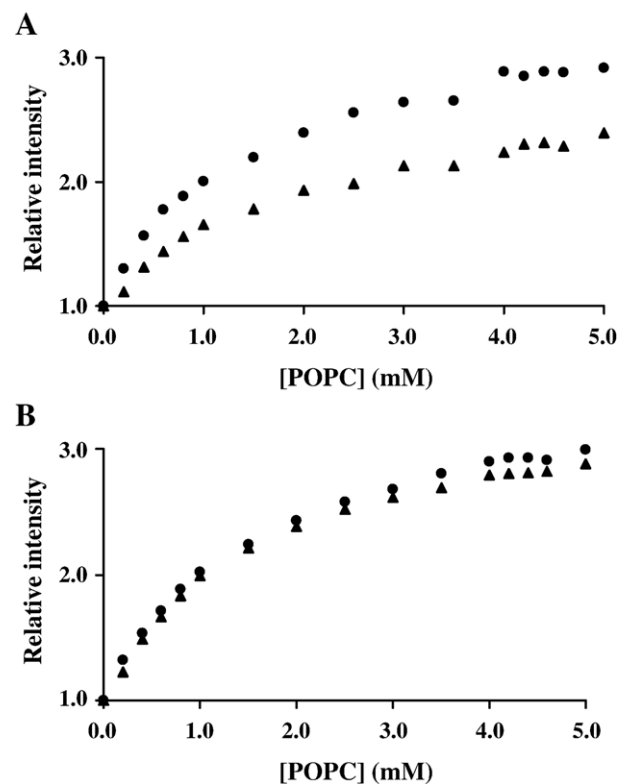


Fig. 4. Partition plots of T20 (10 μ M) to LUV of POPC. The experiments were done in the absence (●) and in the presence (▲) of equimolar S peptides Pep 1D (A) and Pep 2B (B).

Di-8-ANEPPS was used to probe the peptides interaction with membranes. It is known from other studies that both T20 and T-1249 interact with membranes to a reasonable extent [31,32]. In agreement with the previous results, T-1249 is the peptide that presents the most extensive interaction with membranes. From the comparison between all the fluorescence difference spectra intensity obtained (Fig. 3), it can be concluded that the S peptides have a very low or even null partition to membranes.

T20 and T-1249 membrane partition experiments were done in the absence and presence of S peptides (Fig. 4). T20 partition curves in the absence and in the presence of Pep 1D do not overlap. One possible explanation is that peptides interact in the aqueous medium and this additional equilibrium (interaction) competes with partition, decreasing the molar fraction of the molecules in the lipidic bilayers. The same occurs for T-1249/Pep 1D and for both peptides in the presence of Pep 1E. However, the statistical quality of the results worsens in these cases. In the presence of Pep 2B or Pep HR2, the partition of both T20 and T-1249 is not affected. It is possible to quantify the equilibria balance and rationalize the altered partition plots (Appendix A). This analysis takes into account the partition of T20 and T-1249 to LUV of POPC and the interaction in the aqueous medium with S peptides. Data fitting with Eq. (A1.7) (Appendix A) for T20 in the presence of Pep 1D (Appendix A; Fig. A1.2) leads to a binding coefficient of $K_B = (1.1 \pm 0.3) \times 10^5 \text{ M}^{-1}$ (means \pm standard deviation of four replicates). This value is in between the values obtained for very strong and specific binding, such as the binding of the S1 domain of SARS-CoV to ACE2 ($\sim 10^8 \text{ M}^{-1}$; Ref. [35]) and the values expected for moderately specific association pairs ($\sim 10^2 \text{ M}^{-1}$; Ref. [36]).

Taken together, the results obtained prove the occurrence of an interaction between T20 and Pep 1D. Taking into account that T20 is an HR2-derived peptide and Pep 1D is an HR1 peptide, our results seem to confirm at a first glance that SARS-CoV could be inhibited by T20, in agreement with the speculative reasoning by others [21]. Nevertheless, the interaction is too moderate to be able to provide therapeutic efficiency, even keeping in mind that SARS-CoV HR2 peptides are less potent fusion inhibitors than the corresponding HR2 peptides from other viruses [10,12]. For SARS-CoV, the inhibitory peptides concentrations were in the micromolar range, while T20, for instance, has activity in the nanomolar range against HIV-1 entry. Although the inhibitory properties of HR2 peptides could be affected by many different factors, SARS-CoV six-helix bundle lower stability, caused by a weaker interaction between the HR1 and HR2 regions, could be directly correlated with a lower potency of the HR2 peptide in blocking the formation of this structure [10,12,37].

In conclusion, our studies indicate a significant interaction between T20 and an S protein HR1-derived peptide (Pep 1D). This interaction could in principle be responsible for the inhibition of SARS-CoV membrane fusion by the most accepted mechanism involving HR2-derived peptides. However, the values found for K_B justify the absence of

strong anti-SARS activity in the most recent activity studies [24]. Lastly, it is worth mentioning that although a potential use of Pep 1D to block HIV-1 fusion becomes apparent from our work, it is known that HR1-derived peptides usually are less potent fusion inhibitors than HR2-derived peptides [16,38].

Acknowledgements

This project was partially funded by FCT-MCES (Portugal), including a grant (SFRH/BD/14336/2003) under the program POCTI to A.S.V., and by the Minister of Sciences and Technology, P. R. China (National Key Basic Research Program of China, No. 2003CB514109). T20 and T-1249 were kind gifts from Roche (Palo Alto, CA, USA).

Appendix A. Supplementary data

Supplementary data associated with this article can be found in the online version at doi:10.1016/j.bbagen.2005.10.001.

References

- [1] C. Drosten, S. Günther, W. Preiser, S. van der Werf, H. Brodt, S. Becker, H. Rabenau, M. Panning, L. Kolesnikova, R.A.M. Fouchier, A. Berger, A. Burguière, J. Cinatl, M. Eickmann, N. Escriou, K. Grywna, S. Kramme, J. Manuguerra, S. Müller, V. Rickerts, M. Stürmer, S. Vieth, H. Klenk, A.D.M.E. Osterhaus, H. Schmitz, H.W. Doerr, Identification of a novel coronavirus in patients with severe acute respiratory syndrome, *N. Engl. J. Med.* 348 (2003) 1967–1976.
- [2] T.G. Ksiazek, D. Erdman, C.S. Goldsmith, S.R. Zaki, T. Peret, S. Emery, S. Tong, C. Urbani, J.A. Comer, W. Lim, P.E. Rollin, S.F. Dowell, A. Ling, C.D. Humphrey, W. Shieh, J. Guarner, C.D. Paddock, P. Rota, B. Fields, J. DeRisi, J. Yang, N. Cox, J.M. Hughes, J.W. LeDuc, W.J. Bellini, L.J. Anderson, SARS Working Group, A novel coronavirus associated with severe acute respiratory syndrome, *N. Engl. J. Med.* 348 (2003) 1953–1966.
- [3] M.A. Marra, S.J.M. Jones, C.R. Astell, R.A. Holt, A. Brooks-Wilson, Y.S.N. Butterfield, J. Khattri, J.K. Asano, S.A. Barber, S.Y. Chan, A. Cloutier, S.M. Coughlin, D. Freeman, N. Gim, O.L. Griffith, S.R. Leach, M. Mayo, H. McDonald, S.B. Montgomery, P.K. Pandoh, A.S. Petrescu, A.G. Robertson, J.E. Schein, A. Siddiqui, D.E. Smailus, J.M. Stott, G.S. Yang, F. Plummer, A. Andonov, H. Artsob, N. Bastien, K. Bernard, T.F. Booth, D. Bowness, M. Czub, M. Drebot, L. Fernando, R. Flick, M. Garbutt, M. Gray, A. Grolla, S. Jones, H. Feldmann, A. Meyers, A. Kabani, Y. Li, S. Normand, U. Stroher, G.A. Tipples, S. Tyler, R. Vogrig, D. Ward, B. Watson, R.C. Brunham, M. Krajden, M. Petric, D.M. Skowronski, C. Upton, R.L. Roper, The genome sequence of the SARS-associated coronavirus, *Science* 300 (2003) 1399–1404.
- [4] J.S.M. Peiris, S.T. Lai, L.L.M. Poon, Y. Guan, L.Y.C. Yam, W. Lim, J. Nicholls, W.K.S. Yee, W.W. Yan, M.T. Cheung, V.C.C. Cheng, K.H. Chan, D.N.C. Tsang, R.W.H. Yung, T.K. Ng, K.Y. Yuen, members of the SARS study group, Coronavirus as a possible cause of severe acute respiratory syndrome, *Lancet* 361 (2003) 1319–1325.
- [5] P.A. Rota, M.S. Oberste, S.S. Monroe, W.A. Nix, R. Campagnoli, J.P. Icenogle, S. Peñaranda, B. Bankamp, K. Maher, M. Chen, S. Tong, A. Tamin, L. Lowe, M. Frace, J.L. DeRisi, Q. Chen, D. Wang, D.D. Erdman, T.C.T. Peret, C. Burns, T.G. Ksiazek, P.E. Rollin, A. Sanchez, S. Liffick, B. Holloway, J. Limor, K. McCaustland, M. Olsen-Rasmussen, R. Fouchier, S. Günther, A.D.M.E. Osterhaus, C. Drosten, M.A. Pallansch, L.J. Anderson, W.J. Bellini, Characterization of a novel coronavirus associated with severe acute respiratory syndrome, *Science* 300 (2003) 1394–1399.
- [6] H. Hofmann, K. Hattermann, A. Marzi, T. Gramberg, M. Geier, M.

- Krumbiegel, S. Kuate, K. Überla, M. Niedrig, S. Pöhlmann, S protein of severe acute respiratory syndrome-associated coronavirus mediates entry into hepatoma cell lines and is targeted by neutralizing antibodies in infected patients, *J. Virol.* 78 (2004) 6134–6142.
- [7] X. Xiao, D.S. Dimitrov, The SARS-CoV S glycoprotein, *Cell. Mol. Life Sci.* 61 (2004) 2428–2430.
- [8] W. Li, M.J. Moore, N. Vasilieva, J. Sui, S.K. Wong, M.A. Berne, M. Somasundaran, J.L. Sullivan, K. Luzuriaga, T.C. Greenough, H. Choe, M. Farzan, Angiotensin-converting enzyme 2 is a functional receptor for the SARS coronavirus, *Nature* 426 (2003) 450–454.
- [9] S.K. Wong, W. Li, M.J. Moore, H. Choe, M. Farzan, A 193-amino acid fragment of the SARS coronavirus S protein efficiently binds angiotensin-converting enzyme 2, *J. Biol. Chem.* 279 (2004) 3197–3201.
- [10] B.J. Bosch, B.E.E. Martina, R. van der Zee, J. Lepault, B.J. Hajjema, C. Versluis, A.J.R. Heck, R. de Groot, A.D.M.E. Osterhaus, P.J.M. Rottier, Severe acute respiratory coronavirus (SARS-CoV) infection inhibition using spike protein heptad repeat-derived peptides, *Proc. Natl. Acad. Sci. U. S. A.* 101 (2004) 8455–8460.
- [11] P. Ingallinella, E. Bianchi, M. Finotto, G. Cantoni, D.M. Eckert, V.M. Supekar, C. Bruckmann, A. Carfi, A. Pessi, Structural characterization of the fusion-active complex of severe acute respiratory syndrome (SARS) coronavirus, *Proc. Natl. Acad. Sci. U. S. A.* 101 (2004) 8709–8714.
- [12] S. Liu, G. Xiao, Y. Chen, Y. He, J. Niu, C.R. Escalante, H. Xiong, J. Farmer, A.K. Debnath, P. Tien, S. Jiang, Interaction between heptad repeat 1 and 2 regions in spike protein of SARS-associated coronavirus: implications for virus fusogenic mechanism and identification of fusion inhibitors, *Lancet* 363 (2004) 938–947.
- [13] B. Tripet, M.W. Howard, M. Jobling, R.K. Holmes, K.V. Holmes, R.S. Hodges, Structural characterization of the SARS-coronavirus spike S fusion protein core, *J. Biol. Chem.* 279 (2004) 20836–20849.
- [14] J. Zhu, G. Xiao, Y. Xu, F. Yuan, C. Zheng, Y. Liu, H. Yan, D.K. Cole, J.I. Bell, Z. Rao, P. Tien, G.F. Gao, Following the rule: formation of the 6-helix bundle of the fusion core from severe acute respiratory syndrome coronavirus spike protein and identification of potent peptide inhibitors, *Biochem. Biophys. Res. Commun.* 319 (2004) 283–288.
- [15] D.M. Eckert, P.S. Kim, Mechanisms of viral membrane fusion and its inhibition, *Annu. Rev. Biochem.* 70 (2001) 777–810.
- [16] D.M. Eckert, P.S. Kim, Design of potent inhibitors of HIV-1 entry from the gp41 N-peptide region, *Proc. Natl. Acad. Sci. U. S. A.* 98 (2001) 11187–11192.
- [17] J.M. Kilby, S. Hopkins, T.M. Venetta, B. DiMassimo, G.A. Cloud, J.Y. Lee, L. Alldredge, E. Hunter, D. Lambert, D. Bolognesi, T. Matthews, M.R. Johnson, M.A. Nowak, G.M. Shaw, M.S. Saag, Potent suppression of HIV-1 replication in humans by T-20, a peptide inhibitor of gp41-mediated virus entry, *Nat. Med.* 4 (1998) 1302–1307.
- [18] M. Lu, S.C. Blacklow, P.S. Kim, A trimeric structural domain of the HIV-1 transmembrane glycoprotein, *Nat. Struct. Biol.* 2 (1995) 1075–1082.
- [19] S.B. Joshi, R.E. Dutch, R.A. Lamb, A core trimer of the paramyxovirus fusion protein: parallels to influenza virus hemagglutinin and HIV-1 gp41, *Virology* 248 (1998) 20–34.
- [20] B.J. Bosch, R. van der Zee, C.A.M. de Haan, P.J.M. Rottier, The coronavirus spike protein is a class I virus fusion protein: structural and functional characterization of the fusion core complex, *J. Virol.* 77 (2003) 8801–8811.
- [21] W.R. Gallaher, R.F. Garry, Model of the pre-insertion region of the spike (S2) fusion glycoprotein of the human SARS coronavirus: implications for antiviral therapeutics, <http://www.virology.net/Articles/sars/s2model.html>. (Accessed 13 May 2003).
- [22] J.M. Kilby, J.J. Eron, Novel therapies based on mechanisms of HIV-1 cell entry, *N. Engl. J. Med.* 348 (2003) 2228–2238.
- [23] J.J. Eron, R.M. Gulick, J.A. Bartlett, T. Merigan, R. Arduino, J.M. Kilby, B. Yangco, A. Diers, C. Drobnos, R. DeMasi, M. Greenberg, T. Melby, C. Raskino, P. Rusnak, Y. Zhang, R. Spence, G.D. Miralles, Short-term safety and antiretroviral activity of T-1249, a second-generation fusion inhibitor of HIV, *J. Infect. Dis.* 189 (2004) 1075–1083.
- [24] N. Yamamoto, R. Yang, Y. Yoshinaka, S. Amari, T. Nakano, J. Cinatl, H. Rabenau, H.W. Doerr, G. Hunsmann, A. Otaka, H. Tamamura, N. Fujii, N. Yamamoto, HIV protease inhibitor nelfinavir inhibits replication of SARS-associated coronavirus, *Biochem. Biophys. Res. Commun.* 318 (2004) 719–725.
- [25] G. Liu, K.S. Lam, One-bead one compound combinatorial library method, in: H. Fenniri (Ed.), *Combinatorial Chemistry: Practical Approach*, Oxford Univ. Press, Oxford, 2000, pp. 33–49.
- [26] L.D. Mayer, M.J. Hopes, P.R. Cullis, Vesicles of variable sizes produced by a rapid extrusion procedure, *Biochim. Biophys. Acta* 858 (1986) 161–168.
- [27] J. Cladera, I. Martin, P. O'Shea, The fusion domain of HIV gp41 interacts specifically with heparan sulfate on the T-lymphocyte cell surface, *EMBO J.* 20 (2001) 19–26.
- [28] J. Cladera, P. O'Shea, Intramembrane molecular dipoles affect the membrane insertion and folding of a model amphiphilic peptide, *Biophys. J.* 74 (1998) 2434–2442.
- [29] M. Bertsch, A.L. Mayburd, R.J. Kassner, The identification of hydrophobic sites on the surface of proteins using absorption difference spectroscopy of bromophenol blue, *Anal. Biochem.* 313 (2003) 187–195.
- [30] S. Ganesh, R. Jayakumar, Circular dichroism and Fourier transform infrared spectroscopic studies on self-assembly of tetrapeptide derivative in solution and solvated film, *J. Pept. Res.* 61 (2003) 122–128.
- [31] S. Veiga, S. Henriques, N.C. Santos, M. Castanho, Putative role of membranes in the HIV fusion inhibitor enfuvirtide mode of action at the molecular level, *Biochem. J.* 377 (2004) 107–110.
- [32] A.S. Veiga, N.C. Santos, L.M.S. Loura, A. Fedorov, M.A.R.B. Castanho, HIV fusion inhibitor peptide T-1249 is able to insert or adsorb to lipidic bilayers. Putative correlation with improved efficiency, *J. Am. Chem. Soc.* 126 (2004) 14758–14763.
- [33] Y.N. Abdiche, D.G. Myszkka, Probing the mechanism of drug/lipid membrane interactions using Biacore, *Anal. Biochem.* 328 (2004) 233–243.
- [34] N.C. Santos, M. Castanho, Fluorescence spectroscopy methodologies on the study of proteins and peptides. On the 150th anniversary of protein fluorescence, *Trends Appl. Spectrosc.* 4 (2002) 113–125.
- [35] J. Sui, W. Li, A. Murakami, A. Tamin, L.J. Matthews, S.K. Wong, M.J. Moore, A.St.C. Tallarico, M. Olurinde, H. Choe, L.J. Anderson, W.J. Bellini, M. Farzan, W.A. Marasco, Potent neutralization of severe acute respiratory syndrome (SARS) coronavirus by a human mAb to S1 protein that blocks receptor association, *Proc. Natl. Acad. Sci. U. S. A.* 101 (2004) 2536–2541.
- [36] Y. Kubota, Y. Motoda, Y. Shigemune, Y. Fujisak, Fluorescence quenching of 10-methylacridinium chloride by nucleotides, *Photochem. Photobiol.* 29 (1979) 1099–1106.
- [37] V.M. Supekar, C. Bruckmann, P. Ingallinella, E. Bianchi, A. Pessi, A. Carfi, Structure of a proteolytically resistant core from the severe acute respiratory syndrome coronavirus S2 fusion protein, *Proc. Natl. Acad. Sci. U. S. A.* 101 (2004) 17958–17963.
- [38] C.E. Baldwin, R.W. Sanders, B. Berkhout, Inhibiting HIV-1 entry with fusion inhibitors, *Curr. Med. Chem.* 10 (2003) 1633–1642.

Supplementary data (Veiga, S. et al)

APPENDIX 1 - Simultaneous partition and interaction

Multiple equilibria are involved when T20 or T-1249 (generally referred to as T_X hereafter) in solution are in the presence of S protein derived peptides (generally, P_S) and membranes (Figure A1.1). T_X may be free in the bulk aqueous media (FW), associated with P_S in the bulk aqueous media (IW) or bound to POPC membranes (L). The total T20 or T-1249 fluorescence intensity is given by $I = I_{FW} \cdot X_{FW} + I_{IW} \cdot X_{IW} + I_L \cdot X_L$, where I_i and X_i are the fluorescence intensities that would be obtained if all the peptides were located in the environment i ($i = FW, IW$ or L) and the molar fractions of the peptide in that environment, respectively. In this simple model we assume both the interaction between T_X and P_S to be in a 1:1 proportion and no membrane partition of T_X/P_S . It is known from our experiments with the di-8-ANEPPS probe that P_S partition into membranes does not occur at all. Considering that the quantum yield of the free T_X peptide in bulk aqueous media does not differ much from the quantum yield of the associated peptide in water (see Figure 1 in the text – a moderate increase is expected), then I_{FW} can be considered equal to I_{IW} with reasonable approximation and:

$$I = I_{FW}(1 - X_L) + I_L X_L \quad (A1.1)$$

Considering the equilibria in Figure A1.1 (interaction between T_X and P_S peptides in solution and insertion of T_X in POPC membrane):

$$\frac{n_L}{n_{FW} + n_L} = \frac{K_p \gamma_L [L]}{1 + K_p \gamma_L [L]} \quad (A1.2)$$

$$[P_S]K_B = \frac{n_{IW}}{n_{FW}} \quad (A1.3)$$

where n_i are the moles of the peptide in the environment i ; K_p and K_B are the partition and binding coefficients, respectively, of the peptides, as defined in Eq. A1.4 and A1.5; $[P_S]$ and $[L]$ are the S peptide and lipid molar concentrations, respectively; and, γ_L is the average lipid molar volume. Combining Eq. A1.2 and A1.3, it is possible to calculate the molar fraction of peptides inserted in the POPC membrane (X_L ; equation A1.6):

$$K_p = \frac{[T_X]_L}{[T_X]_W} \quad (A1.4)$$

$$K_B = \frac{[T_X P_S]_W}{[T_X]_W [P_S]_W} \quad (A1.5)$$

$$X_L = \frac{K_p \gamma_L [L]}{1 + K_p \gamma_L [L] + K_B [P_S]} \quad (A1.6)$$

Thus, Eq. A1.1 can be rewritten as:

$$\frac{I}{I_{FW}} = 1 - \frac{K_p \gamma_L [L]}{1 + K_p \gamma_L [L] + K_B [P_S]} + \frac{I_L}{I_{FW}} \left(\frac{K_p \gamma_L [L]}{1 + K_p \gamma_L [L] + K_B [P_S]} \right) \quad (A1.7)$$

which describes the fluorescence intensity dependence on lipid concentration.

Eq. A1.7 was fitted to the experimental data using the K_p and I_L/I_{FW} values calculated in the absence of S peptide (Figure A1.2). For the T20/Pep 1D pair $K_B = (1.1 \pm 0.3) \times 10^5 \text{ M}^{-1}$ (means \pm standard deviation of four replicates).

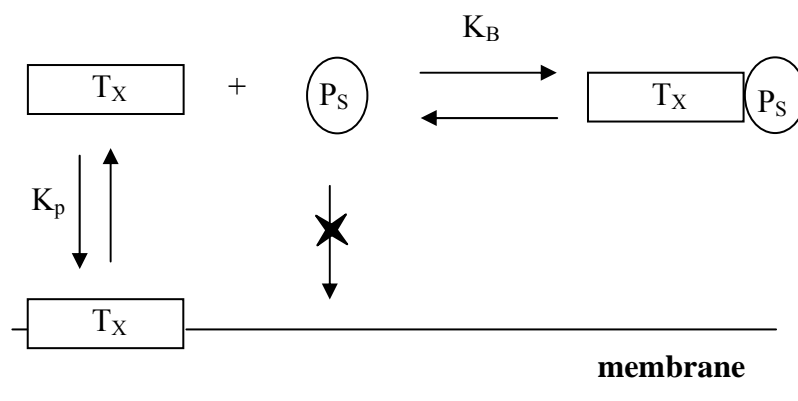


Figure A1.1. T_X distribution: free in the bulk aqueous media (FW), interacting with P_S in the bulk aqueous media (IW) and bound to POPC membranes (L).

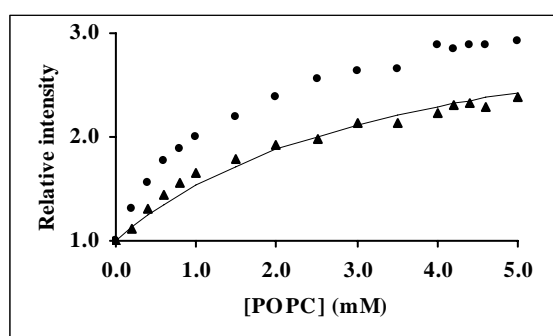


Figure A1.2. Partition plots of T20 to LUV of POPC in the absence (●) and presence (▲) of Pep 1D. Eq. A1.7 was fitted to the experimental data for T20 in the presence of Pep 1D (solid line) using the calculated K_p for T20 alone. K_B is a fitting parameter.

Chapter IV

THE gp41 *MEMBRANE PROXIMAL REGION* ROLE ON HIV-1 FUSION PROCESS

1. INTRODUCTION

HIV-1 entry into target cells occurs through a mechanism mediated by the gp120/gp41 envelope glycoprotein complex. gp120 binding to cellular receptors induces conformational changes in the gp120/gp41 complex that allows membrane fusion and viral entry to occur. Several gp41 regions have been involved in the membrane destabilization and fusion process: the FP is essential for the fusion process by inserting into the target cell membrane and causing membrane perturbations (e.g., Tamm and Han, 2000; Epanand, 2003); the two HR sequences, NHR and CHR, tightly associate in order to form the 6HB structure that brings the viral and cell membrane into close proximity for fusion to occur (e.g., Chan and Kim, 1998; Wyatt and Sodroski, 1998; Eckert and Kim, 2001a). It has been also proposed, based on their behaviour in the presence of membranes, that these regions have a role in membrane fusion (Rabenstein and Shin, 1995; Peisajovich et al., 2000; Kliger et al., 2000; Sackett and Shai, 2002; Sackett and Shai, 2003; Shnaper et al., 2004; Pascual et al., 2005a; Korazim et al., 2006); due to its action on membranes an essential role for the LR in the fusion process was suggested (Santos et al., 1998; Contreras et al., 2001; Pascual et al., 2005b).

The MPR, on the gp41 ectodomain C-terminal, is located between the CHR and the TM and is unusually rich in Trp residues (Figure IV.1). Mutational and functional

analyses on the gp41 ectodomain within the MPR showed a crucial role for this region in gp41-mediated membrane fusion (Salzwedel et al., 1999; Muñoz-Barroso et al., 1999), being dispensable for the gp41/gp120 normal maturation, transport and CD4-binding ability (Salzwedel, 1999). Studies with a synthetic peptide corresponding to the MPR sequence revealed its ability to interact with membranes, and induce membrane fusion and destabilization (Suárez et al., 2000a,b). Therefore this region could destabilize membranes, which is thought to be a crucial step in the membrane fusion process. This peptide adopts a α -helical conformation in membrane mimetic environment and inserts near the membrane interface, parallel to the membrane plane (Schibli et al., 2001). Some data also support a role for the MPR in gp41 aggregation at the fusion site (Sáez-Cirion et al., 2002; Sáez-Ciri3n et al., 2003), important to the fusion process since it seems that several trimers are needed to form a fusion pore.

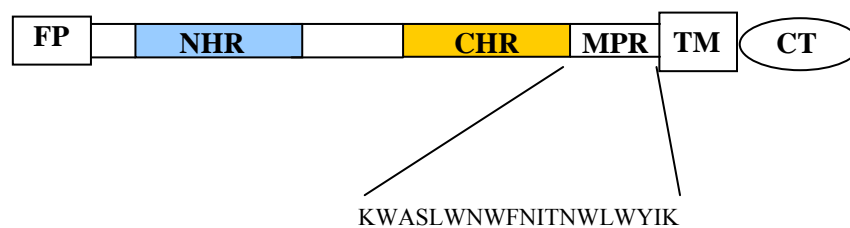


Figure IV.1 – gp41 *membrane proximal region* (MPR) location and sequence (residues 665-683).

The importance of the MPR for the membrane fusion process was confirmed in studies with the intact gp41, although it was suggested that the MPR is not required for membrane destabilization (Dimitrov et al., 2003). Given the proximity of the MPR to the viral membrane, it is conceivable that similarly to the FP effect on the target cell membrane, this gp41 region act primarily by perturbing the viral envelope. In fact, the presence of Chol and SM, major components of the viral membrane, have an important role on the membrane perturbing actions of a MPR derived peptide (Sáez-Cirion et al., 2002; Shnaper et al., 2004). Leakage experiments revealed that SM presence activated the permeabilization induced by the peptide by increasing its surface aggregation in membranes. The presence of Chol stimulates the MPR membrane destabilization action (Sáez-Cirion et al., 2002). It was suggested that a C-terminal domain including both CHR and MPR is specific in its mode of action in perturbing Chol-rich membranes,

while an N-terminal domain composed of both FP and NHR is potent toward membranes devoid of Chol (Shnaper et al., 2004).

There is a growing interest in peptides and proteins that specifically bind to or are believed to be able to induce the formation of Chol-rich membrane domains. Peptides and proteins are supposed to promote the formation of Chol-rich domains by preferentially interacting with Chol, or alternatively as a result of being excluded from these domains while promoting their clustering (Epanand, 2004; Epanand, 2006). It was proposed that a small amino acid sequence within the MPR – LWYIK – is a Chol binding domain (Vincent et al., 2002), in agreement with a previously defined Chol recognition/interaction amino acid consensus pattern (-L/V-(X)₁₋₅-Y-(X)₁₋₅-R/K-), in which (X)₁₋₅ represents between one and five residues of any amino acid (Li and Papadopoulos, 1998). The virus membrane is rich in Chol and SM (Aloia et al., 1993; Brügger et al., 2006), which is related to the preferential budding of the virions through lipid rafts domains (Nguyen and Hildreth, 2000; Ono and Freed, 2001; Pickl et al., 2001). Studies with a small synthetic peptide corresponding to the putative gp41 MPR Chol binding sequence suggested that Chol can promote the insertion of the peptide into a membrane and the peptide will sequester Chol in order to produce Chol-enriched domains (Epanand et al., 2003; Epanand et al., 2005; Epanand et al., 2006). This Chol binding activity was related to the ability of the gp41 to partition into Chol rich lipid raft domains. The following paper sheds light on this issue.

2. THE INFLUENCE OF CHOLESTEROL ON THE INTERACTION OF HIV GP41 MEMBRANE PROXIMAL REGION-DERIVED PEPTIDES WITH LIPID BILAYERS

I, Ana Salomé Veiga, declare that the experimental design and work, data analysis and discussion were carried out by me under the advisor of Prof. Miguel Castanho.

The manuscript was written by me and by my supervisor Prof. Miguel Castanho.

I, Miguel Castanho, as Ana Salomé Veiga supervisor, hereby acknowledge and confirm the information above is correct.

Ana Salomé Veiga

Miguel Castanho

The influence of cholesterol on the interaction of HIV gp41 membrane proximal region-derived peptides with lipid bilayers

Ana S. Veiga and Miguel A. R. B. Castanho

Centro de Química e Bioquímica, Faculdade de Ciências da Universidade de Lisboa, Portugal

Keywords

cholesterol; gp41; HIV-1; membrane proximal region; membranes

Correspondence

A. S. Veiga, Centro de Química e Bioquímica, Fac. Ciências da Universidade Lisboa, Campo Grande C8, P 1749-016 Lisbon, Portugal
Fax: +351 21 7500088
Tel: +351 21 7500000
E-mail: asveiga@fc.ul.pt

(Received 16 July 2007, revised 1 August 2007, accepted 3 August 2007)

doi:10.1111/j.1742-4658.2007.06029.x

A small amino acid sequence (LWYIK) inside the HIV-1 gp41 ectodomain membrane proximal region (MPR) is commonly referred to as a cholesterol-binding domain. To further study this unique and peculiar property we have used fluorescence spectroscopy techniques to unravel the membrane interaction properties of three MPR-derived synthetic peptides: the membrane proximal region peptide-complete (MPRP-C) which corresponds to the complete MPR; the membrane proximal region peptide-short (MPRP-S), which corresponds to the last five MPR amino acid residues (the putative cholesterol-binding domain) and the membrane proximal region peptide-intermediate (MPRP-I), which corresponds to the MPRP-C peptide without the MPRP-S sequence. MPRP-C and MPRP-I membrane interaction is largely independent of the membrane phase. Membrane interaction of MPRP-S occurs for fluid phase membranes but not in gel phase membranes or cholesterol-containing bilayers. The gp41 ectodomain MPR may have a very specific function in viral fusion through the concerted and combined action of cholesterol-binding and non-cholesterol-binding domains (i.e. domains corresponding to MPRP-S and MPRP-I, respectively).

HIV-1 entry into target cells occurs through a mechanism mediated by the envelope glycoprotein. Expressed on the surface of the viral membrane as an oligomeric protein (trimer), this glycoprotein is composed of two subunits that are noncovalently associated: gp120, the surface glycoprotein, and gp41, the transmembrane glycoprotein [e.g. 1–3]. gp120 binding to CD4 and chemokine receptors in the surface of the target cells induces a series of conformational changes in the gp120/gp41 complex that allows membrane fusion and viral entry to occur [e.g. 1–4].

The virus membrane is rich in cholesterol and sphingomyelin [5]; this composition is related to the prefer-

ential budding of the virions through lipid rafts domains [6,7]. Enriched in cholesterol and sphingolipid, lipid rafts are plasma membrane domains organized in a tightly packed, liquid-ordered manner and are involved in several cellular processes besides viral entry, such as membrane trafficking or signal transduction [8,9].

The fusion peptide (on the amino-terminal region of the gp41 ectodomain) serves an essential role for the fusion process by inserting into the target cell membrane and causing its destabilization [10,11]. The two heptad repeat sequences (HR1, adjacent to the fusion peptide and HR2, preceding the transmembrane

Abbreviations

Ac, acetyl; FP, fusion peptide; HR1 and HR2, heptad repeat sequences; K_p , partition coefficient; LUV, large unilamellar vesicles; MPR, membrane proximal region; MPRP-C, (membrane proximal region peptide-complete); MPRP-I, (membrane proximal region peptide-intermediate); MPRP-S, (membrane proximal region peptide-short); POPC, 1-palmitoyl-2-oleoyl-*sn*-glycero-3-phosphocholine; DPPC, 1,2-dipalmitoyl-*sn*-glycero-3-phosphocholine; POPG, 1-palmitoyl-2-oleoyl-*sn*-glycero-3-[phospho-rac-(1-glycerol)]; di-8-ANEPPS, (4-[2-[6-(diethylamino)-2-naphthalenyl]ethenyl]-1-(3-sulfopropyl)-pyridinium); TM, transmembrane sequence; λ , wavelength; λ_{exc} , excitation wavelength; λ_{em} , emission wavelength.



Fig. 1. gp41 structure schematic representation. FP, fusion peptide; HR1 and HR2, heptad repeat sequences; TM, transmembrane sequence and MPR, membrane proximal region.

domain) tightly associate to form the six-helix bundle structure that brings the viral and cell membrane into close proximity for viral entry [1,3,4]. There is also a membrane proximal region (MPR; unusually rich in tryptophan residues) located between the HR2 and the transmembrane domains (Fig. 1) that is essential in gp41-mediated fusion [12–14]. The synthetic peptide corresponding to this region has the capacity of partition into membranes, destabilizing them [15,16] and the presence of cholesterol and sphingomyelin (major components of the viral membrane) have an important role for the membrane perturbing actions of the peptide [17,18].

There is a growing interest in proteins and peptides that specifically bind to or are able to induce the formation of cholesterol-rich membrane domains. It was proposed that a small amino acid sequence (LWYIK) within the MPR is a cholesterol-binding domain [19], in agreement with a previously defined cholesterol recognition/interaction amino acid consensus [20]. This small peptide was also suggested as a promoter for cholesterol-rich domains [21–23].

In the present work we studied three synthetic peptides, differing in length, derived from the gp41 ecto-domain MPR (Table 1): membrane proximal region peptide-complete (MPRP-C), which corresponds to the complete region (19 amino acid residues); membrane proximal region peptide-short (MPRP-S), which corresponds to the last five amino acid residues (corresponding to the domain considered to be cholesterol binding); and membrane proximal region peptide-intermediate (MPRP-I) which corresponds to the MPRP-C peptide without the MPRP-S peptide sequence (14 amino acid residues). Our aim was to study the interaction of the peptide MPRP-S [acetyl (Ac)-LWYIK-NH₂]

Table 1. Sequences of HIV-1 gp41 membrane proximal region derived peptides MPRP-C, MPRP-S and MPRP-I used in the study. The corresponding amino acid residues in gp41 protein of the derived peptides used is in the table.

Peptide	Protein location	Sequence
MPRP-C	665–683	Ac-KWASLWNWFNITNWLWYIK-NH ₂
MPRP-S	679–683	Ac-LWYIK-NH ₂
MPRP-I	665–678	Ac-KWASLWNWFNITNW-NH ₂

with biological membrane models of different composition. A comparative study with the other two peptides (MPRP-C and MPRP-I) was carried out to unravel the role of the MPR domains in gp41-membrane interaction, mainly with cholesterol-rich domains.

Results

Photophysical characterization

The maxima emission wavelengths (λ_{em}) measured (on the corrected spectra) were 338, 346 and 339 nm for MPRP-C, MPRP-S and MPRP-I, respectively (353, 360 and 356 nm, respectively, the noncorrected spectra), as shown in Fig. 2A. There is a slightly nonlinear dependence of the peptide fluorescence intensity with its concentration for MPRP-C and MPRP-I, whereas a linear dependence is detected for MPRP-S (Fig. 2B). Fluorescence quenching by acrylamide leads to nonlinear Stern–Volmer plots for MPRP-C and MPRP-I and a linear plot for MPRP-S (Fig. 2C).

Membrane partition studies

A theoretical hydrophobicity analysis of the MPR sequence was performed to estimate the regions of the sequence with a tendency to the membrane–water interface ($\Delta G_{wif} < 0$) and with a higher tendency toward insertion in membranes ($\Delta G_{oct} < 0$) [24]. The results are shown in Fig. 3 and the tendency toward insertion in membranes is evenly spread over the sequence. However, one cannot completely exclude the possibility that some accumulation of negative-free energy for partition into membranes is present in the short segment at the end of the sequence, corresponding to the cholesterol-binding domain (MPRP-S).

The peptides used in this work are intrinsically fluorescent and both fluorescence intensity and anisotropy data were collected to draw conclusions about the interaction of peptides with large unilamellar vesicles (LUV). The fluorescence quantum yield is dependent on the polarity of the microenvironment of the Trp residues, as well as on the peptide conformation. Both are affected upon insertion of the peptides in membranes. Additionally, the membranes are viscous media, which dictate a potential increase in fluorescence anisotropy upon insertion of the peptides in membranes.

Fluorescence intensity measurements

In the presence of 1-palmitoyl-2-oleyl-*sn*-glycero-3-phosphocholine (POPC) LUV, a liquid-crystalline lipid with packing density and fluidity properties similar to

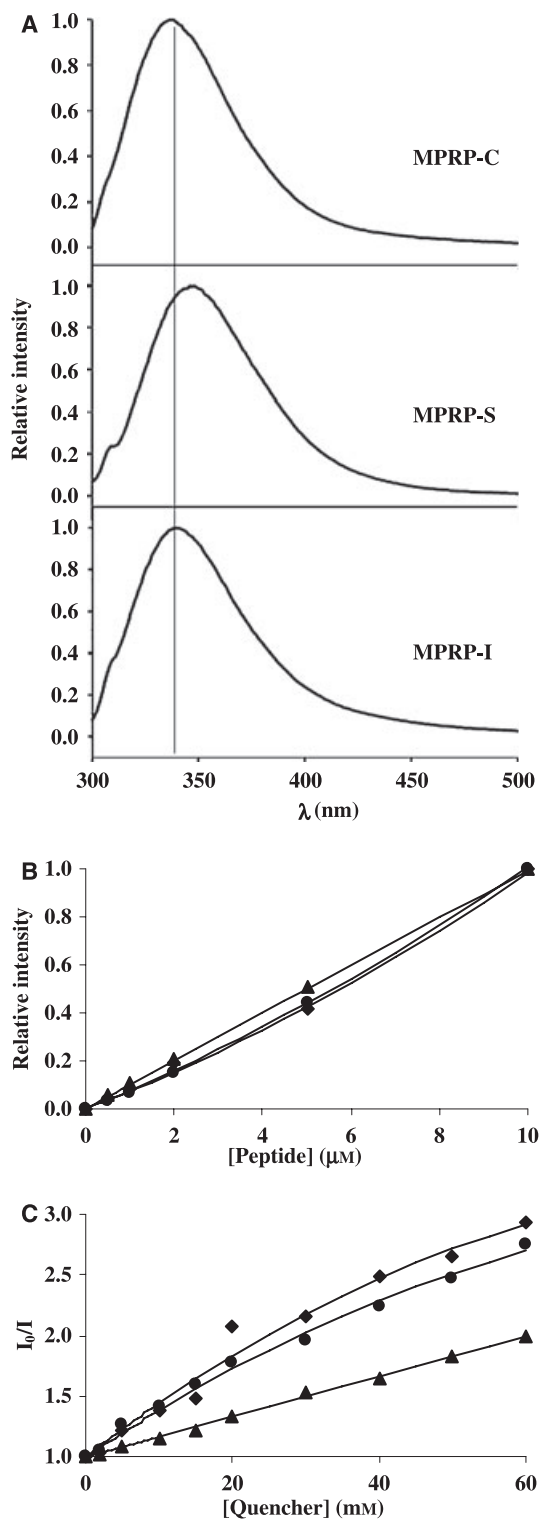


Fig. 2. (A) MPRP-C, MPRP-S and MPRP-I (10 μM for all peptides) emission spectra ($\lambda_{\text{exc}} = 280$ nm) in aqueous solution; (B) Peptide fluorescence intensity dependence on concentration for MPRP-C (●), MPRP-S (▲) and MPRP-I (◆). $\lambda_{\text{exc}} = 280$ nm and $\lambda_{\text{em}} = 353$, 360 and 356 nm for MPRP-C, MPRP-S and MPRP-I, respectively; (C) Stern-Volmer plots for MPRP-C (●), MPRP-S (▲) and MPRP-I (◆) fluorescence quenching by acrylamide. Small amounts of quencher were added (in a range of 0–60 mM) to peptide samples (10 μM for all peptides) with 10 min incubation in between. $\lambda_{\text{exc}} = 290$ nm and $\lambda_{\text{em}} = 353$, 360 and 356 nm for MPRP-C, MPRP-S and MPRP-I, respectively. The data were corrected with the correction factor C [34] accounting for both inner filter effect and light absorption by the quencher.

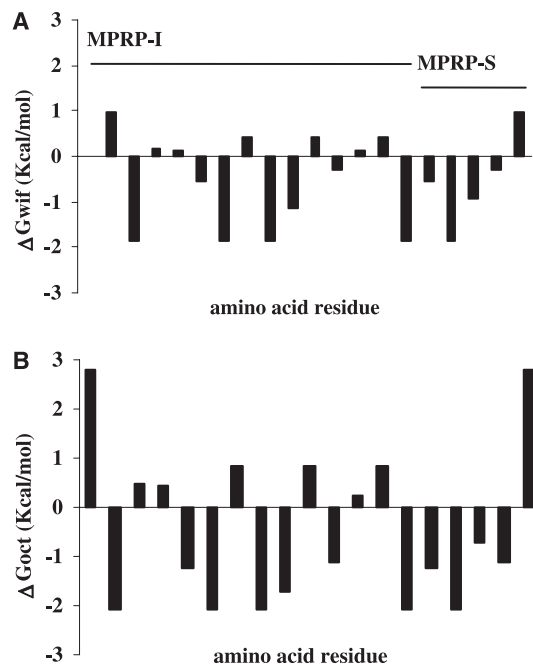


Fig. 3. Theoretical analysis of partition into membranes of membrane proximal region sequence. (A) Values of $\Delta G_{\text{wif}} < 0$ indicate the sequence residues with tendency to the membrane-water interface. (B) Values of $\Delta G_{\text{oct}} < 0$ indicate the residues with a higher tendency towards insertion in membranes.

biological membranes, an increase in the peptides fluorescence intensity occurs, which is more pronounced for MPRP-C and MPRP-I. Figure 4A–C shows the results obtained for MPRP-C, MPRP-S and MPRP-I,

respectively. The fluorescence intensity increase is coincident with a fluorescence emission spectra blue-shift of 5, 3 and 11 nm for MPRP-C, MPRP-S and MPRP-I, respectively, when [POPC] = 3 mM. The spectral shift is due to the incorporation of the peptides in a more hydrophobic environment, the lipid. The partition coefficient between the aqueous and lipid phases, $K_p = [\text{peptide}]_L / [\text{peptide}]_W$, can be determined to quantify the extent of the peptide incorporation in LUV bilayers. $[\text{peptide}]_L$ and $[\text{peptide}]_W$ are the peptide concentrations in the lipidic and aqueous

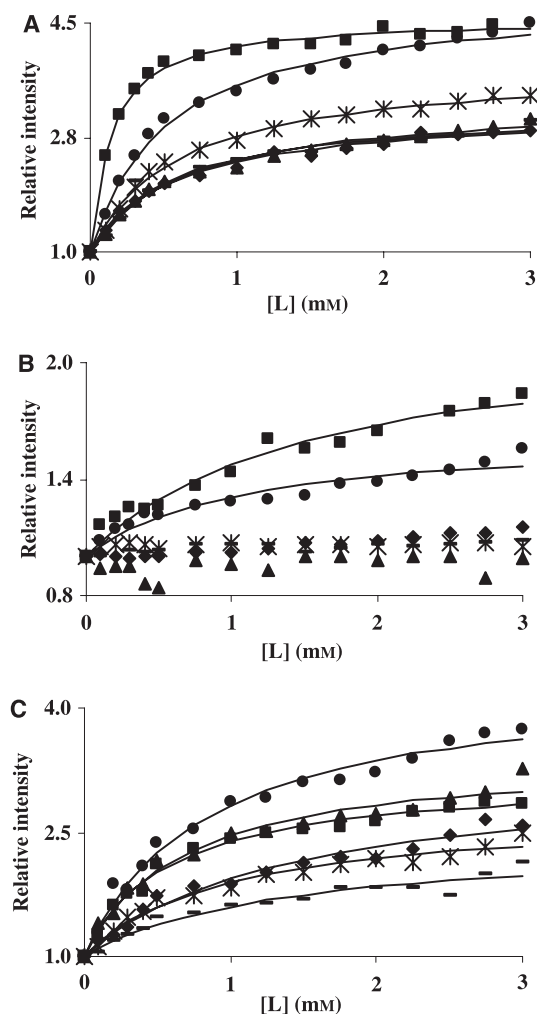


Fig. 4. Partition plots (obtained with fluorescence intensity data) of MPRP-C (A), MPRP-S (B) and MPRP-I (C) to LUV of POPC (●), DPPC (◆), negatively charged POPG (20% POPG in POPC; ■), and POPC/cholesterol mixtures [18% (▲), 25% (*) and 33% mol cholesterol (-)]. The solid lines are fittings of eqn (1) to the experimental data. [L] is the concentration of the lipid available in the outer leaflet. $\lambda_{exc} = 280$ nm and $\lambda_{em} = 353$, 360 and 356 nm for MPRP-C, MPRP-S and MPRP-I, respectively. All peptides were used at a concentration of 10 μ M.

environment, respectively. K_p is calculated from the fluorescence intensity data (I) using Eqn (1) [25]:

$$\frac{I}{I_W} = \frac{1 + K_p \gamma_L \frac{I_L}{I_W} [L]}{1 + K_p \gamma_L [L]} \quad (1)$$

where I_W and I_L are the limit fluorescence intensities when all the peptide is in the water or lipidic phase, respectively; γ_L is the lipidic molar volume [26] and [L] is the concentration of the lipid accessible to the peptide (the outer leaflet of the bilayer). In the presence of POPC LUV, for MPRP-C,

MPRP-S and MPRP-I the obtained K_p values were $(2.5 \pm 0.3) \times 10^3$, $(1.2 \pm 0.4) \times 10^3$ and $(1.5 \pm 0.3) \times 10^3$, respectively.

The results of fluorescence intensity dependence on other lipid compositions are also shown in Fig. 4A–C. DPPC LUV allows the study of the partition of the peptides into rigid membranes because 1,2-dipalmitoyl-*sn*-glycero-3-phosphocholine (DPPC) bilayers are in gel phase at 25 °C. K_p values of $(2.6 \pm 0.3) \times 10^3$ and $(1.1 \pm 0.3) \times 10^3$ were obtained for MPRP-C and MPRP-I, respectively. MPRP-S partition is insignificant and is not possible to calculate the exact K_p value using Eqn (1).

Although POPC is a good model for the outer leaflet of mammal cell membranes, POPG 20 mol% in POPC/POPG LUV mimics the environment of the inner leaflet of mammal biomembranes and it offers an opportunity to study the influence of electrostatic interaction in the partition of MPR peptides. MPRP-C, MPRP-S and MPRP-I have positive net formal charges of +2, +1 and +1, respectively. K_p values of $(9.5 \pm 0.7) \times 10^3$ for MPRP-C, $(0.9 \pm 0.3) \times 10^3$ for MPRP-S and $(2.3 \pm 0.3) \times 10^3$ for MPRP-I were obtained.

To study the effect of cholesterol on peptide–membrane interactions, POPC/cholesterol LUV with an increasing cholesterol content of 18, 25 and 33 mol% were used. For MPRP-C the obtained K_p values are, respectively, $(2.0 \pm 0.3) \times 10^3$, $(2.2 \pm 0.2) \times 10^3$ and $(2.5 \pm 0.5) \times 10^3$ for 18, 25 and 33 mol% cholesterol. With MPRP-I, K_p slightly decreases with increasing cholesterol content: $(1.9 \pm 0.4) \times 10^3$, $(1.4 \pm 0.3) \times 10^3$ and $(1.0 \pm 0.4) \times 10^3$, respectively. MPRP-S partition to POPC/cholesterol LUV is not detectable for any of the different cholesterol contents and it is not possible to calculate a K_p . Studies of MPRP-S with POPC and POPC/cholesterol LUV have applied different peptide concentrations and incubation times, and have found similar results (not shown). Table 2

Table 2. Partition coefficients (K_p) for peptides MPRP-C, MPRP-S and MPRP-I in the presence of different LUV compositions.

K_p ($\times 10^3$)	MPRP-C	MPRP-S	MPRP-I
POPC	2.5 ± 0.3	1.2 ± 0.4	1.5 ± 0.3
DPPC	2.6 ± 0.3	–	1.1 ± 0.3
POPC/POPG	9.5 ± 0.7	0.9 ± 0.3	2.3 ± 0.3
POPG 20 mol%			
POPC/cholesterol	2.0 ± 0.3	–	1.9 ± 0.4
cholesterol 18 mol%			
POPC/cholesterol	2.2 ± 0.2	–	1.4 ± 0.3
cholesterol 25 mol%			
POPC/cholesterol	2.5 ± 0.5	–	1.0 ± 0.4
cholesterol 33 mol%			

summarizes the partition coefficients determined for the peptides in the different lipid compositions studied.

Fluorescence anisotropy measurements

When only one Trp residue is present in a peptide sequence, as is the case with MPRP-S, the application of anisotropy-based methodologies is possible. At variance to this, when more than one Trp residue is present (as in the case of MPRP-C and MPRP-I, where five and four Trp residues are present, respectively) anisotropy-based methodologies are not possible because intramolecular energy migration (homo-transfer) mechanisms are operative. Energy migration leads to an anisotropy value close to zero regardless of the rotational freedom of the fluorophores or their excited state life-time. In this way steady-state fluorescence anisotropy studies were carried out to obtain additional information about MPRP-S interaction with POPC and POPC/cholesterol LUV. Equation (1) can also be applied to calculate K_p values with fluorescence anisotropy data [25]. Results obtained with 30 μM MPRP-S samples and 10 min incubation time, in the presence of POPC and POPC/cholesterol (33 mol% cholesterol) LUV are shown in Fig. 5. In agreement with the results obtained with other peptide concentrations and incubation time conditions (not shown), there is evidence of peptide interaction with POPC LUV, but not when cholesterol is present (for any of the POPC/cholesterol LUV mixtures).

4-[2-[6-(Diocetyl-amino)-2-naphthalenyl]ethenyl]-1-(3-sulfopropyl)-pyridinium (Di-8-ANEPPS) fluorescence

Di-8-ANEPPS, a dye sensitive to changes in the membrane dipole potential, was used as a probe for additional studies on peptide-membrane interaction. The

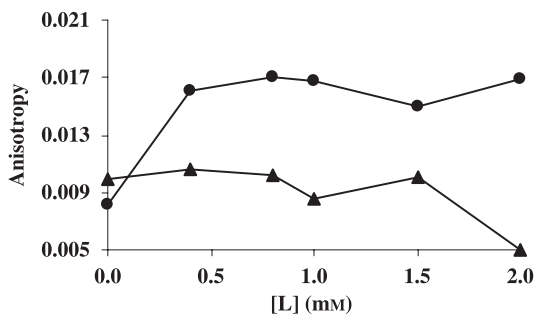


Fig. 5. Partition plots (obtained with fluorescence anisotropy data) of MPRP-S (30 μM) to LUV of POPC (●) and POPC/cholesterol mixture, 33 mol% cholesterol (▲). [L] is the total lipid concentration. $\lambda_{\text{exc}} = 290 \text{ nm}$ and $\lambda_{\text{em}} = 360 \text{ nm}$.

magnitude of the membrane dipole potential is affected by membrane binding and by the insertion of molecules (including peptides). The change of the potential magnitude may be monitored through the spectral shifts of the fluorescence indicator di-8-ANEPPS [27,28]. Di-8-ANEPPS excitation spectra were obtained setting λ_{em} as the peak of the emission spectra, which depends on the lipids used. Fluorescence difference spectra of di-8-ANEPPS-labeled POPC or POPC/cholesterol membranes were obtained by subtracting the excitation spectrum before the addition of peptides from the excitation spectrum in the presence of peptides. Before subtraction, the spectra were normalized to the integrated areas so that the difference spectra would reflect only spectral shifts [27,28]. Figure 6A and B shows the obtained fluorescence difference spectra of di-8-ANEPPS-labeled POPC and POPC/cholesterol (33 mol% cholesterol), respectively, in the presence of MPRP-C [30 μM (a)], MPRP-I [30 μM (b)] and MPRP-S (50 μM (c)). MPRP-C has the most significant membrane interaction, followed by MPRP-I and MPRP-S

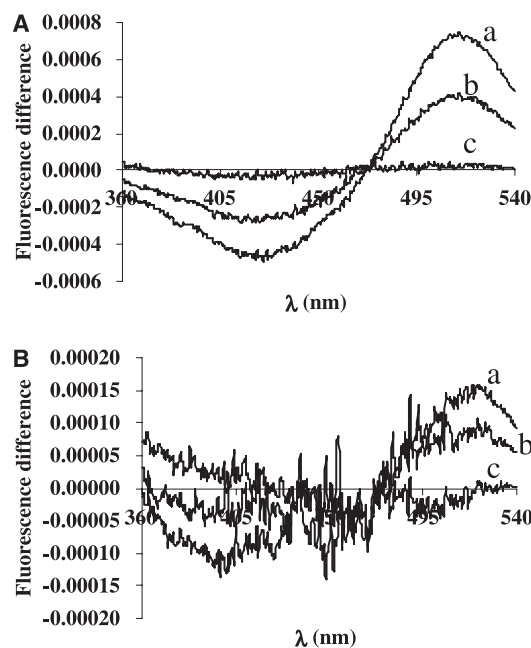


Fig. 6. Di-8-ANEPPS-labeled POPC (A) and POPC/cholesterol, 33 mol% (B) LUV fluorescence difference spectra, in the presence of (a) MPRP-C, (b) MPRP-I and (c) MPRP-S. The spectra were obtained by subtracting the excitation spectrum before the addition of peptides from the excitation spectra after addition of the peptides (30 μM for MPRP-C and MPRP-I and 50 μM for MPRP-S), with $\lambda_{\text{em}} = 578 \text{ nm}$ and 568 nm for POPC and POPC/cholesterol LUV, respectively. Before subtraction, the spectra were normalized to the integrated areas to reflect only the spectral shifts. The dye and lipid concentrations used were 10 μM and 200 μM , respectively.

(for which the membrane interaction is undetectable) for both LUV systems used. The results show that this methodology is not sensitive enough to detect the binding of small peptides to lipid bilayers. The MPRP-S partition cannot be detected with ANEPPS as it was with partition studies. The results obtained in the presence of POPC/cholesterol LUV of 18 and 25 mol% cholesterol (not shown) are in agreement with what is shown in Fig. 6, as well as the results obtained with other peptide concentrations (15 μM for MPRP-C and MPRP-I and 30 μM for MPRP-S).

Discussion

The HIV-1 gp41 ectodomain comprises, in addition to the fusion peptide and the two heptad repeat sequences (HR1 and HR2), an MPR (rich in Trp residues) localized between the HR2 and transmembrane domains (Fig. 1). Several studies show the importance of the MPR for membrane perturbing actions and the fusion process mediated by gp41. The small sequence LWYIK within the MPR is taken as a cholesterol-binding domain. Peptides that specifically bind to or are able to induce the formation of cholesterol-rich domains are quite rare and peculiar, and therefore attract a lot of attention. In our studies we have explored the membrane interaction properties of three gp41 MPR-derived synthetic peptides (Table 1), including the cholesterol presence effect.

Because Trp residue emission is sensitive to the local microenvironment of the residues [29], maxima λ_{em} obtained for MPRP-C and MPRP-I in bulk-aqueous phase are consistent with Trp residues in an apolar environment, at variance with MPRP-S (350 nm is the maximum λ_{em} of free Trp in bulk aqueous environment). Accordingly, nonlinear concentration effect and solution fluorescence quenching Stern–Volmer plots revealed that hydrophobic pockets are present in MPRP-C and MPRP-I, indicating that aggregation or clustering may occur.

In the presence of POPC LUV, a lipid in fluid liquid–crystalline phase, MPRP-C has the more extensive partition into the bilayer, followed by the other two peptides with similar K_p values. For DPPC LUV the MPRP-C partition constant is similar to the one obtained with POPC. For MPRP-I the partition constant slightly decreases, whereas for MPRP-S the partition constant becomes insignificant, probably due to the rigidity of the bilayers, which are in gel phase. For the POPC/POPG mixture a remarkable increase in the MPRP-C partition constant occurs, when compared with the partition obtained with POPC. This result can be related to electrostatic interactions between the

peptide, which has a +2 net formal charge, and the negatively charged lipid. For MPRP-I, the partition constant increase was not as high and in the case of MPRP-S the partition constant remained unchanged relative to POPC. The peptide charge has a more pronounced effect in MPRP-C because it has +2 net charge. The other peptides, MPRP-S and MPRP-I, with a +1 net charge do not respond and respond only weakly, respectively, to the electrostatic effect.

Depending on its molar fraction, the presence of cholesterol on POPC LUV may lead to the formation of a liquid-ordered phase. A moderate cholesterol content on the POPC/cholesterol LUV enables the coexistence of cholesterol-rich (in a liquid-ordered phase) and cholesterol-poor areas (in a liquid-disordered phase). With an increase in cholesterol content, the liquid-ordered membrane fraction increases and may reach the point where all of the membrane is homogeneous. The MPRP-C is insensitive to the cholesterol content in the membrane, which is in agreement with the insensitivity of the peptide to the membrane phase (K_p in DPPC and POPC remains constant). Therefore, MPRP-C interacts with all membrane regions regardless of its rigidity and no specific interaction with cholesterol is detected. For MPRP-I the same trend applies, although a slight decrease in K_p with cholesterol content cannot be discarded. In the case of MPRP-S no membrane interaction can be detected in the presence of cholesterol, which is in agreement with $K_p \sim 0$ in DPPC. As for MPRP-C, it is the membrane phase that regulates K_p , not specific interactions with cholesterol. The partition curves obtained with anisotropy data further confirmed the partition data for MPRP-S. Membrane interaction does not occur when cholesterol is present in the LUV composition.

To investigate whether the interaction of peptides with membranes could consist of superficial adsorption only, which could remain undetected in fluorescence intensity and anisotropy experiments due to the unrestricted exposition of the indole Trp moiety to bulk aqueous phase, the di-8-ANEPPS dye was placed in the lipid bilayers to detect any changes in the membrane dipole potential due to peptide adsorption. In the presence of POPC and POPC/cholesterol (33 mol%) LUV the fluorescence difference spectra obtained confirm the trend previously discussed for Trp fluorescence data: a decrease on membrane interaction in the direction MPRP-C > MPRP-I > MPRP-S (Fig. 6). The results exclude extensive adsorption of MPRP-S to membranes. Moreover, Fig. 6A shows that the MPRP-S peptide does not perturb the membranes very much as ANEPPS fluorescence is not affected by the presence of peptide in spite of $K_p = (1.2 \pm 0.4) \times 10^3$.

The membrane interaction behaviour of MPRP-C and MPRP-I is independent of the membrane phase but not of the presence of charged lipids. Cholesterol does not reduce the extent of or potentiate membrane interaction. The similarity of K_p values for MPRP-C in the presence of membrane with or without cholesterol is in agreement with other studies [17]. For MPRP-S, peptide–membrane interaction occurs for fluid phase LUV (POPC and POPC/POPG). However, no interaction is detected in the presence of gel phase membranes and cholesterol. The membrane phase governs the peptide–membrane interactions and no specific interaction with cholesterol needs to be invoked.

MPRP-S interacts with: (a) exposed cholesteryl residues [19]; (b) cholesterol molecules cosolubilized with lipid and peptide prior to preparation of the bilayers [21]; and (c) cholesterol molecules in sonicated (unstable) vesicles challenged with high peptide/lipid molar ratios (1:1 [22] and 1:10 [23]), where peptide-induced perturbation of the bilayer may be extreme and bring the peptide in contact with cholesterol. This interaction is related to the presence of a cholesterol recognition amino acid consensus pattern [20]. Although the Trp residue may contribute to this recognition/interaction [23], the main role belongs to Tyr [20,22,23], in agreement with the ability of Tyr side chains to be modulated by cholesterol in bilayers [30–33].

This study shows that in unperturbed bilayers the consensus region (MPRP-S) of the ectodomain membrane proximal region (MPRP-C) does not interact with gel and liquid-ordered bilayers (i.e. cholesterol-rich bilayers), where cholesterol is buried in the membrane palisades. It is the MPRP-I sequence that probably confers the main membrane interaction properties to the membrane proximal region. The most peculiar property of MPRP-I (and MPRP-C) is the insensitivity of K_p to lipid phase; this may be the key to the pretransmembrane biological function because it potentially interacts both with the HIV-1 envelope and the host cell plasma membrane. However, one must remember that membrane interactions of peptides can be enhanced by a concerted action of several membrane-binding motifs or by the particular disposition of key residues in the context of long peptides or even in the context of the full protein. Bearing this in mind, a MPRP-S role in the interaction of the MPR with membranes cannot be excluded.

The gp41 ectodomain MPR may therefore have a very specific function in viral fusion through the concerted and combined action of cholesterol-binding and non-cholesterol-binding domains (i.e. domains corresponding to MPRP-S and MPRP-I, respectively, in the fusion process).

Experimental procedures

The peptides Ac-KWASLWNWFNITNWLWYIK-NH₂ (MPRP-C), Ac-LWYIK-NH₂ (MPRP-S) and Ac-KWASLWNWFNITNWNH₂ (MPRP-I) were purchased > 90% pure from AnaSpec, Inc. (San Jose, CA). POPC, DPPC and POPG were purchased from Avanti Polar-Lipids (Alabaster, AL), and cholesterol was purchased from Sigma (St. Louis, MO). Di-8-ANEPPS was purchased from Molecular Probes (Eugene, OR). Hepes and NaCl were from Merck (Darmstadt, Germany). Hepes buffer 10 mM, pH 7.4, 150 mM NaCl, was used throughout the studies. MPRP-C, MPRP-S and MPRP-I stock solutions in buffer were diluted to final desired concentrations. MPRP-I stock solutions were prepared in buffer with small amounts of dimethylsulfoxide. The final concentration of dimethylsulfoxide in the samples through the experiments was at most 1.4% (v/v). The solubilization of all peptides was improved with mild bath sonication. The spectrofluorimeter used was a Jobin Ivon Fluorolog 3 (Edison, NJ, USA) (double monochromators; 450 W Xe lamp).

Photophysical characterization of peptides

The studied peptides contain tryptophan residues (Table 1), which makes fluorescence techniques suitable tools. To study the peptide concentration effect on the fluorescence emission of the peptide, fluorescence emission spectra (excitation wavelength, $\lambda_{exc} = 280$ nm) were determined for each peptide concentration (0.1–10 μ M). In quenching studies with acrylamide in solution, small amounts of quencher were added (in a range of 0–60 mM) to peptide samples (10 μ M) with 10 min incubation in between; $\lambda_{exc} = 290$ nm and $\lambda_{em} = 353$, 360 and 356 nm for MPRP-C, MPRP-S and MPRP-I, respectively. The data were corrected with the correction factor C [34] accounting for both inner filter effect and light absorption by the quencher.

Membrane partition studies

MPRP-C, MPRP-S and MPRP-I membrane interaction studies were carried out with large unilamellar vesicles as membrane model systems. LUV of pure POPC and DPPC and mixtures of POPC/POPG 80 : 20 (mol%) and POPC/cholesterol 67 : 33, 75 : 25 and 82 : 18 (mol%) were used. DPPC or POPC and POPG or cholesterol (when required), were mixed in chloroform, in a round-bottom flask and the solution was dried under a gentle stream of nitrogen. Solvent removal was completed in vacuum for 8–10 h. LUV were prepared by extrusion techniques [35] using 100 nm pore size filters.

Membrane partition studies were performed by adding small volumes of concentrated LUV stock solutions to the peptide samples (10 μ M), followed by incubation for

10 min before measurements. MPRP-S studies with POPC and POPC/cholesterol mixtures were also carried out using additional peptide samples of 5, 30 or 150 μM , followed by immediate measurements or 10 min of incubation time.

Fluorescence intensity measurements

Fluorescence intensity data was measured at $\lambda_{\text{exc}} = 280$ nm and $\lambda_{\text{em}} = 353, 360$ and 356 nm for MPRP-C, MPRP-S and MPRP-I, respectively. All the data were corrected for background intensities (by subtracting a blank vesicle sample), progressive peptide dilution and for light scattering effects associated with LUV [36].

Fluorescence anisotropy measurements

Fluorescence anisotropies (r) were determined according to Eqn (2):

$$r = \frac{(I_{\text{VV}} - GI_{\text{VH}})}{(I_{\text{VV}} + 2GI_{\text{VH}})} \quad (2)$$

where I_{VV} and I_{VH} are the fluorescence intensities from polarized emission and $G = I_{\text{HV}}/I_{\text{HH}}$ is the instrumental factor. The subscripts indicate the vertical (V) or horizontal (H) orientations of the excitation and emission polarizers. The fluorescence intensities were measured at $\lambda_{\text{exc}} = 290$ nm and $\lambda_{\text{em}} = 360$ nm and corrected for background intensities (by subtracting a blank vesicle sample) and light scattering effects associated with LUV.

di-8-ANEPPS fluorescence measurements

POPC and cholesterol (when required), in chloroform, and di-8-ANEPPS (from a stock solution in ethanol) were mixed in a round-bottom flask. LUV were prepared as described previously. Peptides MPRP-C, MPRP-I (at 15 μM or 30 μM) and MPRP-S (at 30 μM or 50 μM) were added afterwards. Di-8-ANEPPS excitation spectra were obtained setting λ_{em} at 578 nm when in POPC membranes, and at 568 nm when in POPC/cholesterol membranes. The final concentrations used were 200 μM of lipid and 10 μM of di-8-ANEPPS.

Acknowledgements

This work was partially funded by FCT-Mes (Portugal), including a grant (SFRH/BD/14336/2003) under the program POCTI to ASV.

References

1 Chan DC & Kim PS (1998) HIV entry and its inhibition. *Cell* **93**, 681–684.

- 2 Wyatt R & Sodroski J (1998) The HIV-1 envelope glycoproteins: fusogens, antigens, and immunogens. *Science* **280**, 1884–1888.
- 3 Eckert DM & Kim PS (2001) Mechanisms of viral membrane fusion and its inhibition. *Annu Rev Biochem* **70**, 777–810.
- 4 LaBranche CC, Galasso G, Moore JP, Bolognesi DP, Hirsch MS & Hammer SM (2001) HIV fusion and its inhibition. *Antiviral Res* **50**, 95–115.
- 5 Aloia RC, Tian H & Jensen FC (1993) Lipid composition and fluidity of the human immunodeficiency virus envelope and host cell plasma membranes. *Proc Natl Acad Sci USA* **90**, 5181–5185.
- 6 Nguyen DH & Hildreth JEK (2000) Evidence for budding of human immunodeficiency virus type 1 selectively from glycolipid-enriched membrane lipid rafts. *J Virol* **74**, 3264–3272.
- 7 Ono A & Freed EO (2001) Plasma membrane rafts play a critical role in HIV-1 assembly and release. *Proc Natl Acad Sci USA* **98**, 13925–13930.
- 8 Simons K & Ikonen E (1997) Functional rafts in cell membranes. *Nature* **387**, 569–572.
- 9 Silvius JR (2003) Role of cholesterol in lipid raft formation: lessons from lipid model systems. *Biochim Biophys Acta* **1610**, 174–183.
- 10 Tamm LK & Han X (2000) Viral fusion peptides: a tool set to disrupt and connect biological membranes. *Biosci Rep* **20**, 501–518.
- 11 Epand RM (2003) Fusion peptides and the mechanism of viral fusion. *Biochim Biophys Acta* **1614**, 116–121.
- 12 Salzwedel K, West JT & Hunter E (1999) A conserved tryptophan-rich motif in the membrane-proximal region of the human immunodeficiency virus type 1 gp41 ectodomain is important for env-mediated fusion and viral infectivity. *J Virol* **73**, 2469–2480.
- 13 Muñoz-Barroso I, Salzwedel K, Hunter E & Blumenthal R (1999) Role of the membrane-proximal domain in the initial stages of human immunodeficiency virus type 1 envelope glycoprotein-mediated membrane fusion. *J Virol* **73**, 6089–6092.
- 14 Dimitrov AS, Rawat SS, Jiang S & Blumenthal R (2003) Role of the fusion peptide and membrane-proximal domain in HIV-1 envelope glycoprotein-mediated membrane fusion. *Biochemistry* **42**, 14150–14158.
- 15 Suárez T, Gallaher WR, Agirre A, Goñi FM & Nieva JL (2000) Membrane interface-interacting sequences within the ectodomain of the human immunodeficiency virus type 1 envelope glycoprotein: putative role during viral fusion. *J Virol* **74**, 8038–8047.
- 16 Suárez T, Nir S, Goñi FM, Saéz-Cirión A & Nieva JL (2000) The pre-transmembrane region of the human immunodeficiency virus type-1 glycoprotein: a novel fusogenic sequence. *FEBS Lett* **477**, 145–149.
- 17 Sáez-Cirion A, Nir S, Lorizate M, Agirre A, Cruz A, Pérez-Gil J & Nieva JL (2002) Sphingomyelin and

- cholesterol promote HIV-1 gp41 pretransmembrane sequence surface aggregation and membrane restructuring. *J Biol Chem* **277**, 21776–21785.
- 18 Shnaper S, Sackett K, Gallo SA, Blumenthal R & Shai Y (2004) The C- and the N-terminal regions of glycoprotein 41 ectodomain fuse membranes enriched and not enriched with cholesterol, respectively. *J Biol Chem* **279**, 18526–18534.
 - 19 Vincent N, Genin C & Malvoisin E (2002) Identification of a conserved domain of the HIV-1 transmembrane protein gp41 which interacts with cholesterol groups. *Biochim Biophys Acta* **1567**, 157–164.
 - 20 Li H & Papadopoulos V (1998) Peripheral-type benzodiazepine receptor function in cholesterol transport. Identification of a putative cholesterol recognition/interaction amino acid sequence and consensus pattern. *Endocrinology* **139**, 4991–4997.
 - 21 Epand RM, Sayer BG & Epand RF (2003) Peptide-induced formation of cholesterol-rich domains. *Biochemistry* **42**, 14677–14689.
 - 22 Epand RF, Sayer BG & Epand RM (2005) The tryptophan-rich region of HIV gp41 and the promotion of cholesterol-rich domains. *Biochemistry* **44**, 5525–5531.
 - 23 Epand RF, Thomas A, Brasseur R, Vishwanathan SA, Hunter E & Epand RM (2006) Juxtamembrane protein segments that contribute to recruitment of cholesterol into domains. *Biochemistry* **45**, 6105–6114.
 - 24 White SH & Wimley WC (1998) Hydrophobic interactions of peptides with membrane interfaces. *Biochim Biophys Acta* **1376**, 339–352.
 - 25 Santos NC, Prieto M & Castanho MARB (2003) Quantifying molecular partition into model systems of biomembranes: an emphasis on optical spectroscopic methods. *Biochim Biophys Acta* **1612**, 123–135.
 - 26 Chiu SW, Jakobsson E, Subramaniam S & Scott HL (1999) Combined Monte Carlo and molecular dynamics simulation of fully hydrated dioleoyl and palmitoyl-oleoyl phosphatidylcholine lipid bilayers. *Biophys J* **77**, 2462–2469.
 - 27 Cladera J & O'Shea P (1998) Intramembrane molecular dipoles affect the membrane insertion and folding of a model amphiphilic peptide. *Biophys J* **74**, 2434–2442.
 - 28 Cladera J, Martin I & O'Shea P (2001) The fusion domain of HIV gp41 interacts specifically with heparin sulphate on the T-lymphocyte cell surface. *EMBO J* **20**, 19–26.
 - 29 Lakowicz JR (1999) *Principles of Fluorescence Spectroscopy*, 2nd edn. Kluwer Academic/Plenum Publishers, New York.
 - 30 Lopes SCDN, Fedorov A & Castanho MARB (2004) Cholesterol modulates maculosin's orientation in model systems of biological membranes. Relevance towards putative molecular recognition. *Steroids* **69**, 825–830.
 - 31 Lopes SCDN, Fedorov A & Castanho MARB (2005) Lipidic membranes are potential 'catalysts' in the ligand activity of the multifunctional pentapeptide neokytorphin. *Chembiochem* **6**, 697–702.
 - 32 Lopes SCDN, Fedorov A & Castanho MARB (2006) Chiral recognition of D-kytorphin by lipidic membranes: relevance toward improved analgesic efficiency. *ChemMedChem* **1**, 723–728.
 - 33 Lopes SCDN, Soares CM, Baptista AM, Goormaghtigh E, Costa Cabral BJ & Castanho MARB (2006) Conformational and orientational guidance of the analgesic dipeptide kytorphin induced by lipidic membranes: putative correlation toward receptor docking. *J Phys Chem B* **110**, 3385–3394.
 - 34 Coutinho A & Prieto M (1993) Ribonuclease T1 and alcohol dehydrogenase fluorescence quenching by acrylamide. *J Chem Educ* **70**, 425–428.
 - 35 Mayer LD, Hopes MJ & Cullis PR (1986) Vesicles of variable sizes produced by a rapid extrusion procedure. *Biochim Biophys Acta* **858**, 161–198.
 - 36 Ladokhin AS, Jayasinghe S & White SH (2000) How to measure and analyze tryptophan fluorescence in membranes properly, and why bother? *Anal Biochem* **285**, 235–245.

Chapter V

THE ROLE OF MEMBRANES IN THE HIV-1 ANTIBODIES 2F5 AND 4E10 MODE OF ACTION

1. INTRODUCTION

Only few human potent and broadly neutralizing MAbs against HIV-1 primary isolates, targeting different envelope glycoprotein complex epitopes, have been identified (Trkola et al., 1995; D'Souza et al., 1997; Zwick et al., 2001). 2F5 and 4E10 are two of these (Conley et al., 1994; Trkola et al., 1995; Stiegler et al., 2001; Zwick et al., 2001) and recognize epitopes whose core sequences are ELDKWA and NWF(D/N)IT, respectively, both localized on the MPR gp41 ectodomain (Figure V.1). Nevertheless, the 2F5 epitope extends toward outside the MPR N-terminal (Muster et al., 1993; Parker et al., 2001; Stiegler et al., 2001; Zwick et al., 2001; Zwick et al., 2005; Brunel et al., 2006). It is not well established the gp41 state at which 2F5 binds to its epitope since there were suggestions that 2F5 binds both to its epitope in the fusion intermediate prehairpin structure (Gorny and Zolla-Pazner, 2000; Follis et al., 2002; de Rosny et al., 2004) and in the native form of gp41 (Gorny and Zolla-Pazner, 2000; Barbato et al., 2003; de Rosny et al., 2004). For 4E10 it was also proposed that additionally to the MPR, it recognizes the N-terminal sequences of gp120 and gp41 on the native protein (Hager-Braun et al., 2006).

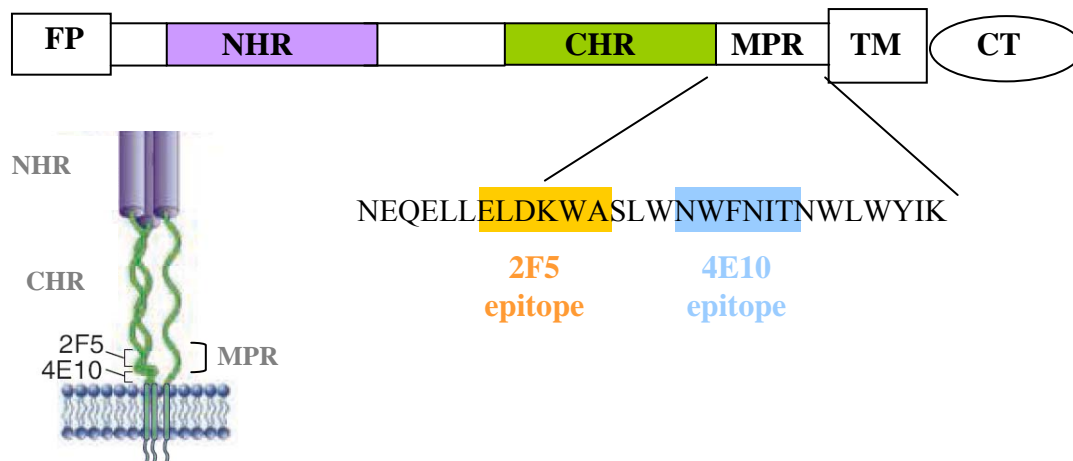


Figure V.1 – 2F5 and 4E10 binding sites on the gp41. 4E10 epitope is entirely within the MPR, while 2F5 epitope extends toward outside the MPR N-terminal end. Both MAbs epitopes are very close to the membrane (Adapted from Nabel, 2005).

It was suggested based on the crystal structures of 2F5 (Ofek et al., 2004) and 4E10 (Cardoso et al., 2005), that these MAbs can interact with the viral membrane (Figure V.2) through a hydrophobic surface present on the long third complementarity-determining region of the heavy chain (CDR H3). Both 2F5 and 4E10 have an unusually long and hydrophobic CDR H3. This interaction possibly facilitates the binding to the MAbs epitopes, known to be localized very close to the viral membrane. For 2F5, the interactions between its CDR H3 and the epitope occur predominantly with residues at the CDR H3 base, the CDR H3 apex residues remaining unbound to gp41. Ofek and co-workers suggested the existence at the apex of a hydrophobic surface composed by the hydrophobic amino acids Leu, Phe, Val, and Ile, that may be responsible for 2F5 binding to the membrane, facilitating the epitope binding. The 4E10 CDR H3 presents, similarly to 2F5, a large surface that is not implicated in the contact with the epitope, raising the possibility of further viral membrane contacts. The CDR H3 tip contains a hydrophobic surface, similar to the one described for the 2F5 CDR H3, in which two Trp residues could facilitate interactions with the viral membrane. Additionally, Gly residues present on the same surface may confer conformational flexibility that allows 4E10 to access the viral membrane when bound to the MPR gp41 epitope (Cardoso et al., 2005).

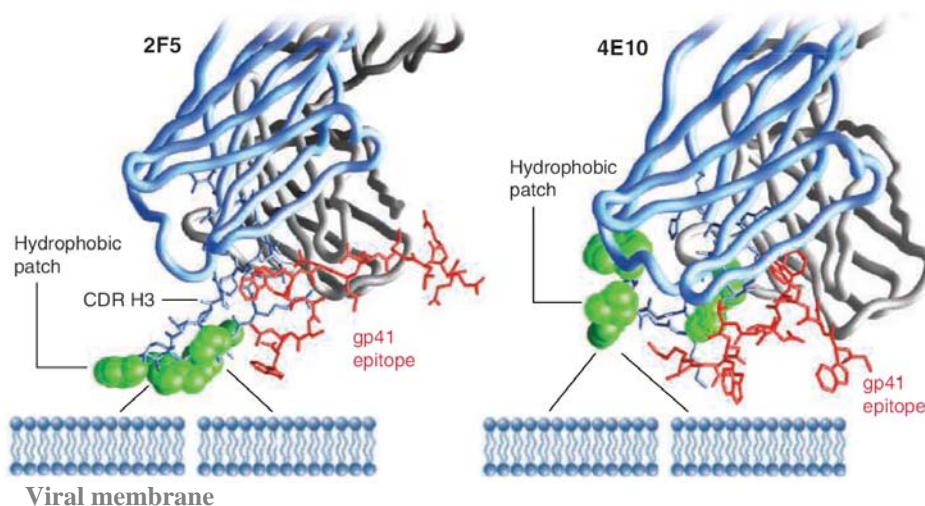


Figure V.2 – Possible interaction of the MAbs 2F5 and 4E10 with the viral membrane through a hydrophobic patch present on the CDR H3 (Adapted from Nabel, 2005).

Actually, some studies indicate a correlation between these MAbs binding to the gp41 with the presence of membranes. Both MAbs recognize their epitopes when the gp41 is inserted in a membrane (Lenz et al., 2005). 2F5 and 4E10 binding affinity for the epitope is enhanced when gp41 is membrane-bound relative to gp41 in the absence of lipids. This result suggests a possible dependence of the epitope conformation on the presence or absence of lipid (Grundner et al., 2002; Ofek et al., 2004).

Further studies showed that a direct binding of both 2F5 and 4E10 to some membranes or membrane lipids can occur. Haynes et al. (Haynes et al., 2005) demonstrated that the MAbs 2F5 and 4E10 interact with cardiolipin (CL), a phospholipid to which Abs are formed in lupus, and others auto-antigens, in a similar way to those of Abs associated with autoimmune diseases (auto-antibodies). However, CL is usually present only on the inner membrane of mitochondria and has not been reported to be present on plasma membrane or HIV-1 envelope (Alving et al., 2006). Additionally these authors found that 4E10 react also with PS, PC, PE and SM (Haynes et al., 2005). Studies with membrane model systems reported 2F5 and 4E10 binding to PC, PG and CL liposomes (Sánchez-Martínez et al., 2006a; Sánchez-Martínez et al., 2006b). Very recently, our study as well as other contemporary study showed that 2F5 membrane interactions are weak when compared with those of 4E10, but binding of 2F5 to CL seems to be specific (Sánchez-Martínez et al., 2006b). It was also shown that gp41-derived epitope sequences recognition by the MAbs can occur in a membrane context (Sánchez-Martínez et al., 2006b; Alam et al., 2007). 4E10 can also bind to

phosphatidylinositol-4-phosphate (PIP), specifically through a phosphate-binding subsite (Brown et al., 2007; Beck et al., 2007), resembling anti-PIP Abs (Brown et al., 2007). MAbs specific to PIP also resemble 4E10 in that they neutralize HIV-1 (Brown et al., 2007). Since lipids like PS, PE or PIP might be exposed at the HIV surface (Alving et al., 2006), both 2F5 and 4E10 could in theory be used as Abs to lipids to neutralize HIV.

The major challenge in the development of an AIDS vaccine that elicits broadly neutralizing Abs, is the design of immunogens that present the epitopes in a way that mimics their structure on the native HIV-1 envelope glycoprotein complex. Despite 2F5 and 4E10 epitopes being particularly promising, eliciting these neutralizing MAbs has been revealed a not easy task (Coëffier et al., 2001; Joyce et al., 2002). The fusion inhibitor T20, whose sequence contains the 2F5 epitope, was proposed as a vaccine candidate. However, even with the use of T20 analogs with increased α -helix content that bind to 2F5 as well as or better than the native T20, conjugate vaccines prepared from the peptides fail to elicit neutralizing responses in vitro (Joyce et al., 2002). This general lack of success is probably a result of failure of the synthetic epitopes to adopt a conformation similar to the native epitope in the viral context, and in this way, Abs can be generated but cannot recognize the functional trimeric viral proteins. The studies presented in this chapter help to elucidate the membranes' involvement on these MAbs action.

2. THE MEMBRANES' ROLE IN THE HIV-1 NEUTRALIZING MONOCLONAL ANTIBODY 2F5 MODE OF ACTION NEEDS RE-EVALUATION

I, Ana Salomé Veiga, declare that the experimental design and work, data analysis and discussion were carried out by me under the advisor of Prof. Miguel Castanho.

The manuscript was written by me and by my supervisor Prof. Miguel Castanho.

I, Miguel Castanho, as Ana Salomé Veiga supervisor, hereby acknowledge and confirm the information above is correct.

Ana Salomé Veiga

Miguel Castanho

Short communication

The membranes' role in the HIV-1 neutralizing monoclonal antibody 2F5 mode of action needs re-evaluation

Ana Salomé Veiga, Miguel A.R.B. Castanho*

*Centro de Química e Bioquímica, Faculdade de Ciências da Universidade de Lisboa, Campo Grande Ed. C8,
1749-016 Lisboa, Portugal*

Received 16 November 2005; accepted 3 February 2006

Abstract

2F5, a monoclonal antibody that neutralizes HIV-1 primary isolates, recognizes an epitope in the membrane proximal region of the glycoprotein gp41 ectodomain. It is believed that binding to the viral membrane is a step in the antibody mode of action, as usual in ligand membrane receptor interactions. We investigated the interaction of 2F5 with membrane model systems, namely large unilamellar vesicles, by means of fluorescence techniques. There were no significant interactions of 2F5 with model viral membranes or with model target cell membranes. Thus, the usual three-step 'membrane catalysis' method is not followed by 2F5 in its mode of action.

© 2006 Elsevier B.V. All rights reserved.

Keywords: MAb 2F5; HIV-1; Membrane; Fluorescence

Human immunodeficiency virus type 1 (HIV-1) entry into target cells occurs through a mechanism mediated by the envelope glycoprotein. Expressed on the viral membrane surface as trimer, this glycoprotein is composed of two noncovalently associated subunits, gp120 (surface glycoprotein) and gp41 (transmembrane glycoprotein) (Chan and Kim, 1998; Wyatt and Sodroski, 1998; Eckert and Kim, 2001). The gp120 binding to CD4 and chemokine receptors at the target cell surface induces conformational changes in the glycoprotein complex. Subsequent changes within the gp41 ectodomain involve the formation of a six-helix bundle structure (hairpin structure) allowing membrane fusion and viral entry (Chan and Kim, 1998; Wyatt and Sodroski, 1998; Eckert and Kim, 2001; LaBranche et al., 2001; Cooley and Lewin, 2003).

A few human monoclonal antibodies (mAbs) that neutralize a broad range of HIV-1 primary isolates, targeting different envelope glycoprotein epitopes, have been identified (Trkola et al., 1995; D'Souza et al., 1997; Zwick et al., 2001). The mAb 2F5 is one of these and recognizes an epitope, containing the sequence ELDKWA, in the membrane proximal region of the gp41 ectodomain (Muster et al., 1993; Parker et al., 2001). It has been proposed that 2F5 can bind its epi-

tope in the prehairpin structure, a fusion intermediate (Gorny and Zolla-Pazner, 2000; Follis et al., 2002; de Rosny et al., 2004), although there are also indications that binding can occur with the native form of gp41 (Gorny and Zolla-Pazner, 2000; Barbato et al., 2003; de Rosny et al., 2004). Additionally, 2F5 binding affinity for the epitope is enhanced when gp41 is in a lipidic environment (Grundner et al., 2002; Ofek et al., 2004). The interactions between the 2F5 third complementarity-determining region of the heavy chain (CDR H3) and the epitope in gp41 occur predominantly with residues at the CDR H3 base. Thus, there are CDR H3 residues that remain unbound to gp41, including at the apex (Ofek et al., 2004). Ofek et al. (2004) suggested the existence at the apex of a hydrophobic surface composed by the hydrophobic amino acids Leu, Phe, Val, and Ile. Given the viral membrane proximity to the 2F5 epitope, this hydrophobic surface may be responsible for 2F5 binding to the membrane facilitating the epitope binding (Ofek et al., 2004).

We investigated mAb 2F5 membrane interactions using membrane model systems (large unilamellar vesicles, LUV) of pure POPC (1-palmitoyl-2-oleyl-sn-glycero-3-phosphocholine; Avanti Polar-Lipids, Alabaster, AL) and POPC/Cholesterol 67:33 (mol%). Cholesterol was purchased from Sigma (St. Louis, MO). POPC is a lipid with packing density and fluidity properties similar to biological membranes and the mixture POPC/Cholesterol mimic the viral membrane, which is rich in

* Corresponding author. Tel.: +351 21 7500931; fax: +351 21 7500088.
E-mail address: castanho@fc.ul.pt (M.A.R.B. Castanho).

cholesterol (Aloia et al., 1993; Campbell et al., 2002; Raulin, 2002).

2F5 is intrinsically fluorescent due to the presence of aromatic amino acids (tryptophan, tyrosine and phenylalanine), which enable the study of this molecule using fluorescence techniques. A spectrofluorimeter SLM Aminco 8100 with double monochromators and 450 W Xe lamp was used. Human HIV-1 gp41 monoclonal antibody 2F5 (IgG1 isotype, kappa chain) was provided by the EU Programme EVA Centralised Facility for AIDS Reagents, National Institute for Biological Standards and Control, UK, and from Dr. Hermann Katinger. 2F5 stock solutions (100 μg of purified antibody in 2 mM acetic acid (pH 4.0) + 10% maltose) were diluted with buffer (10 mM Hepes buffer pH 7.4, 150 mM NaCl) to the final desired concentrations.

Initially, an evaluation of the Fab 2F5 3D structure (PDB entry 2F5B) revealed that some of the aromatic residues are exposed at the mAb surface. As Trp and Tyr residues have propensity to insert into membranes and a tendency to locate at the membrane–water interface (White and Wimley, 1998; Killian and von Heijne, 2000), they may potentially help the interaction of the 2F5 with the viral membrane, in addition to the hydrophobic surface proposed by others (Ofek et al., 2004).

As the Trp residues' emission is sensitive to their local environment (Lakowicz, 1999), the measured emission maximum wavelength of ~ 330 nm (320 nm in the corrected spectrum compared to 350 nm of free Trp in aqueous environment) of 2F5 1.5 μM (Fig. 1A) reveals that most Trp residues are buried inside the protein in the absence of membranes. This result was confirmed with a solution quenching study with acrylamide (Fig. 1B). The very small quenching efficiency shows that the aqueous quencher does not contact the Trp residues.

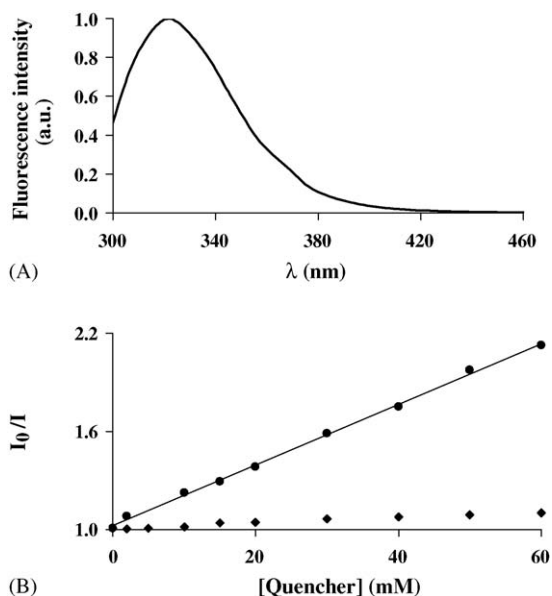


Fig. 1. (A) 2F5 (1.5 μM) emission spectra in aqueous solution. (B) Stern–Volmer plot for 2F5 (\blacklozenge) and free Trp in solution (\bullet) fluorescence quenching by acrylamide. Small amounts of quencher were added (in a range of 0–60 mM) to a 2F5 sample (1.5 μM) with 10 min incubation interval. The excitation and emission wavelengths used were 290 and 330 nm, respectively. The data were corrected with the correction factor C (Coutinho and Prieto, 1993) accounting for both inner filter effect and light absorption by the quencher.

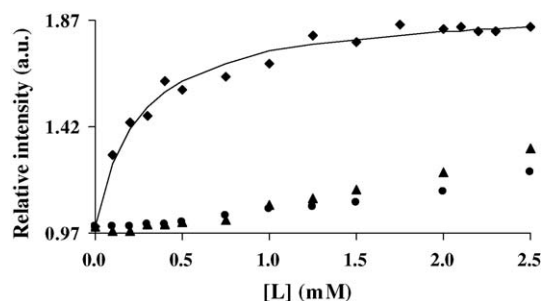


Fig. 2. Partition plots of 2F5 (1.5 μM) to LUV of POPC (\bullet) and POPC/Chol (\blacktriangle). For the sake of comparison, the partition plot of T-1249 (a molecule that interacts moderately with membranes (Veiga et al., 2004)) to LUV of POPC is presented (\blacklozenge). [L] is the concentration of the lipid available to 2F5 or T-1249 (i.e., the outer hemilayer of the vesicles).

Large unilamellar vesicles (~ 100 nm diameter) were used to study the interaction of 2F5 with membranes. POPC alone or mixed with cholesterol (in chloroform) were placed in a round bottom flask, and the solution was dried under a stream of nitrogen. Solvent removal was completed in vacuum, overnight. Finally, the LUV were prepared by extrusion techniques (Mayer et al., 1986). Membrane partition studies were achieved by successive additions of small aliquots of LUV (15 mM) to the mAb samples (1.5 μM) with 10 min incubation intervals. The excitation and emission wavelengths used were 280 and 330 nm, respectively. Fluorescence intensity data was corrected for the dilution effect. The results obtained show no occurrence of shifts of the emission spectra upon addition of POPC or POPC/Chol vesicles (the spectra are similar to those in aqueous solution—data not shown). No concomitant increase in 2F5 fluorescence intensity was observed (Fig. 2). These findings suggest that 2F5 does not partition to the membranes through an extensive anchoring of a significant number of Trp residues.

However, the hydrophobic surface proposed to interact with membranes does not contain Trp residues and it could be argued that a mild interaction with the membrane could take place strictly involving this restricted surface. One Phe residue is present but Phe fluorescence is less sensitive to environment polarity than Trp fluorescence and the interaction with the lipids could thus remain undetected. To test this hypothesis we performed studies with di-8-ANEPPS (4-[2-[6-(dioctylamino)-2-naphthalenyl]ethenyl]-1-(3-sulfopropyl)-pyridinium; Molecular Probes, Eugene, OR), a dye sensitive to changes in the membrane dipole potential, which has been shown to detect protein membrane interaction (O'Shea, 2003) and can thus be used to probe the 2F5 interaction with membranes. Changes on the membrane dipole potential magnitude, incited by membrane binding and insertion of molecules, may be monitored by means of spectral shifts of the fluorescence indicator di-8-ANEPPS (Cladera and O'Shea, 1998; Cladera et al., 2001). POPC, and cholesterol when required, and di-8-ANEPPS (from a stock solution in ethanol) were used to prepare LUV by extrusion techniques as mentioned before. Di-8-ANEPPS excitation spectra were obtained with emissions set at 600 nm (for POPC membranes) or 578 nm (for POPC/Chol membranes). The concentrations used were 200 μM for lipids, 10 μM for di-8-ANEPPS and

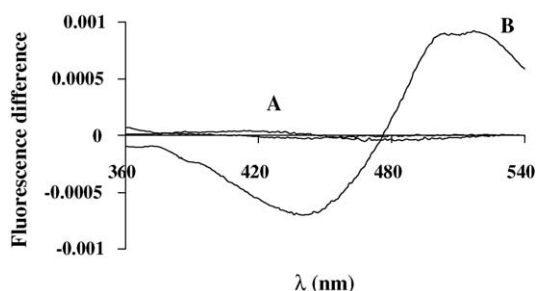


Fig. 3. Fluorescence difference spectra of di-8-ANEPPS-labeled POPC and POPC/Chol membranes in the presence of 2F5 (A). Both spectra overlap and were obtained by subtracting the excitation spectrum before the addition of 2F5 from the excitation spectrum after 2F5 (2 μ M) addition, with $\lambda_{em} = 600$ nm and $\lambda_{em} = 578$ nm for POPC and POPC/Chol membranes, respectively. Before subtraction, the spectra were normalized to the integrated areas to reflect only the spectral shifts. Dye and lipid concentrations used were 10 μ M and 200 μ M, respectively. The difference spectrum obtained with di-8-ANEPPS-labeled POPC membranes in the presence of T-1249 (a molecule that interacts moderately with membranes (Veiga et al., 2004)) is depicted for comparison (B).

2 μ M for 2F5. Fig. 3 shows the fluorescence difference spectra of di-8-ANEPPS-labeled POPC or POPC/Chol membranes, which were obtained by subtracting the excitation spectrum before the addition of 2F5 from the excitation spectrum in the presence of 2F5. Before subtraction the spectra were normalized to the integrated areas to reflect only spectral shifts (Cladera and O'Shea, 1998; Cladera et al., 2001). Difference spectra intensity obtained for both studied cases indicates that there are no interactions of 2F5 with the membranes, which is reinforced by comparing with the fluorescence difference spectrum of T-1249 (Fig. 3), a molecule known to interact moderately with membranes (Veiga et al., 2004, 2006).

In conclusion, no interaction occurs between the mAb 2F5 and both the cell and viral model membranes. Thus 2F5 does not use membrane interaction prior to gp41 docking, i.e., does not follow the classical 'membrane catalysis' scheme (Sargent and Schwyzer, 1986; Castanho and Fernandes, 2006). In the classical 'membrane catalysis' scheme the local concentrating effect of the membrane is expected to increase the occupied-to-unoccupied binding sites in the membrane by a factor that equals the molar ratio partition coefficient (Castanho and Fernandes, 2006). Probably, membranes play a role simply by inducing the best epitope conformation for binding (Grundner et al., 2002; Ofek et al., 2004), but not through a preparation of 2F5 for better docking. Taking together the results in this study with the others on the molecular level action of 2F5 (Ofek et al., 2004), it seems reasonable to speculate that 2F5 binds to the protein epitope, which in turn causes the CDR H3 region to bind to the membrane and stabilize docking.

Acknowledgments

This project was partially funded by FCT-MCIES (Portugal), including a grant (SFRH/BD/14336/2003) under the program POCTI to A.S.V. Monoclonal antibody 2F5 was provided by Dr. Hermann Katinger through the NIBSC Centralised Facility for AIDS Reagents supported by EU Programme EVA and the UK Medical Research Council.

References

- Aloia, R.C., Tian, H., Jensen, F.C., 1993. Lipid composition and fluidity of the human immunodeficiency virus envelope and host cell plasma membranes. *Proc. Natl. Acad. Sci. USA* 90, 5181–5185.
- Barbato, G., Bianchi, E., Ingallinella, P., Hurni, W.H., Miller, M.D., Ciliberto, G., Cortese, R., Bazzo, R., Shiver, J.W., Pessi, A., 2003. Structural analysis of the epitope of the anti-HIV antibody 2F5 sheds light into its mechanism of neutralization and HIV fusion. *J. Mol. Biol.* 330, 1101–1115.
- Campbell, S.M., Crowe, S.M., Mak, J., 2002. Virion-associated cholesterol is critical for the maintenance of HIV-1 structure and infectivity. *AIDS* 16, 2253–2261.
- Castanho, M.A.R.B., Fernandes, M.X., 2006. Lipid membrane-induced optimization for ligand-receptor docking: recent tools and insights for the 'membrane catalysis' model. *Eur. Biophys. J.* 35, 92–103.
- Chan, D.C., Kim, P.S., 1998. HIV entry and its inhibition. *Cell* 93, 681–684.
- Cladera, J., Martin, I., O'Shea, P., 2001. The fusion domain of HIV gp41 interacts specifically with heparan sulfate on the T-lymphocyte cell surface. *EMBO J.* 20, 19–26.
- Cladera, J., O'Shea, P., 1998. Intramembrane molecular dipoles affect the membrane insertion and folding of a model amphiphilic peptide. *Biophys. J.* 74, 2434–2442.
- Cooley, L.A., Lewin, S.R., 2003. HIV-1 cell entry and advances in viral entry inhibitor therapy. *J. Clin. Virol.* 26, 121–132.
- Coutinho, A., Prieto, M., 1993. Ribonuclease T₁ and alcohol dehydrogenase fluorescence quenching by acrylamide. *J. Chem. Educ.* 70, 425–428.
- de Rosny, E., Vassell, R., Jiang, S., Kunert, R., Weiss, C.D., 2004. Binding of the 2F5 monoclonal antibody to native and fusion-intermediate forms of human immunodeficiency virus type 1 gp41: implications for fusion-inducing conformational changes. *J. Virol.* 78, 2627–2631.
- D'Souza, M.P., Livnat, D., Bradac, J.A., Bridges, S.H., the AIDS clinical trials group antibody selection working group, and collaborating investigators, 1997. Evaluation of monoclonal antibodies to human immunodeficiency virus type 1 primary isolates by neutralization assays: performance criteria for selecting candidate antibodies for clinical trials. *J. Infect. Dis.* 175, 1056–1062.
- Eckert, D.M., Kim, P.S., 2001. Mechanisms of viral membrane fusion and its inhibition. *Annu. Rev. Biochem.* 70, 777–810.
- Follis, K.E., Larson, S.J., Lu, M., Nunberg, J.H., 2002. Genetic evidence that interhelical packing interactions in the gp41 core are critical for transition of the human immunodeficiency virus type 1 envelope glycoprotein to the fusion-active state. *J. Virol.* 76, 7356–7362.
- Gorny, M.K., Zolla-Pazner, S., 2000. Recognition by human monoclonal antibodies of free and complexed peptides representing the prefusogenic and fusogenic forms of human immunodeficiency virus type 1 gp41. *J. Virol.* 74, 6186–6192.
- Grundner, C., Mirzabekov, T., Sodroski, J., Wyatt, R., 2002. Solid-phase proteoliposomes containing human immunodeficiency virus envelope glycoproteins. *J. Virol.* 76, 3511–3521.
- Killian, J.A., von Heijne, G., 2000. How proteins adapt to a membrane–water interface. *Trends Biochem. Sci.* 25, 429–434.
- LaBranche, C.C., Galasso, G., Moore, J.P., Bolognesi, D.P., Hirsch, M.S., Hammer, S.M., 2001. HIV fusion and its inhibition. *Antiviral Res.* 50, 95–115.
- Lakowicz, J.R., 1999. *Principles of Fluorescence Spectroscopy*, 2nd ed. Kluwer Academic/Plenum Publishers, New York.
- Mayer, L.D., Hopes, M.J., Cullis, P.R., 1986. Vesicles of variable sizes produced by a rapid extrusion procedure. *Biochim. Biophys. Acta* 858, 161–168.
- Muster, T., Steindl, F., Purtscher, M., Trkola, A., Klima, A., Himmler, G., Rucker, F., Katinger, H., 1993. A conserved neutralizing epitope on gp41 of human immunodeficiency virus type 1. *J. Virol.* 67, 6642–6647.
- Ofek, G., Tang, M., Sambor, A., Katinger, H., Mascola, J.R., Wyatt, R., Kwong, P.D., 2004. Structure and mechanistic analysis of the anti-human immunodeficiency virus type 1 antibody 2F5 in complex with its gp41 epitope. *J. Virol.* 78, 10724–10737.

- O'Shea, P., 2003. Intermolecular interactions with/within cell membranes and the trinity of membrane potentials: kinetics and imaging. *Biochem. Soc. Trans.* 31, 990–996.
- Parker, C.E., Deterding, L.J., Hager-Braun, C., Binley, J.M., Schülke, N., Katinger, H., Moore, J.P., Tomer, K.B., 2001. Fine definition of the epitope on the gp41 glycoprotein of human immunodeficiency virus type 1 for the neutralizing monoclonal antibody 2F5. *J. Virol.* 75, 10906–10911.
- Raulin, J., 2002. Human immunodeficiency virus and host cell lipids. Interesting pathways in research for a new HIV therapy. *Prog. Lipid Res.* 41, 27–65.
- Sargent, D.F., Schwyzer, R., 1986. Membrane lipid phase as catalyst for peptide–receptor interactions. *Proc. Natl. Acad. Sci. USA* 83, 5774–5778.
- Trkola, A., Pomales, A.B., Yuan, H., Korber, B., Maddon, P.J., Allaway, G.P., Katinger, H., Barbas III, C.F., Burton, D.R., Ho, D.D., Moore, J.P., 1995. Cross-clade neutralization of primary isolates of human immunodeficiency virus type 1 by human monoclonal antibodies and tetrameric CD4-IgG. *J. Virol.* 69, 6609–6617.
- Veiga, A.S., Santos, N.C., Loura, L.M.S., Fedorov, A., Castanho, M.A.R.B., 2004. HIV fusion inhibitor peptide T-1249 is able to insert or adsorb to lipidic bilayers. Putative correlation with improved efficiency. *J. Am. Chem. Soc.* 126, 14758–14763.
- Veiga, S., Yuan, Y., Li, X., Santos, N.C., Liu, G., Castanho, M.A.R.B., 2006. Why are HIV-1 fusion inhibitors not effective against SARS-CoV? Biophysical evaluation of molecular interactions. *Biochim. Biophys. Acta* 1760, 55–61.
- White, S.H., Wimley, W.C., 1998. Hydrophobic interactions of peptides with membrane interfaces. *Biochim. Biophys. Acta* 1376, 339–352.
- Wyatt, R., Sodroski, J., 1998. The HIV-1 envelope glycoproteins: fusogens, antigens, and immunogens. *Science* 280, 1884–1888.
- Zwick, M.B., Labrijn, A.F., Wang, M., Spenlehauer, C., Saphire, E.O., Binley, J.M., Moore, J.P., Stiegler, G., Katinger, H., Burton, D.R., Parren, P.W.H.I., 2001. Broadly neutralizing antibodies targeted to the membrane-proximal external region of human immunodeficiency virus type 1 glycoprotein gp41. *J. Virol.* 75, 10892–10905.

3. REAL-TIME BIOSENSOR INTERACTIONS OF HIV-1 ANTIBODIES 2F5 AND 4E10 WITH A GP41 EPITOPE PREBOUND TO HOST CELL AND VIRAL MEMBRANE MIMETICS

I, Ana Salomé Veiga, declare that the experimental design and work, data analysis and discussion were carried out by me under the advisor of Prof. Miguel Castanho and Prof. Marie Isabel Aguilar. Experimental design and data analysis were also helped by Dr. Leonard Pattenden. Peptide synthesis was done by me with the help and supervision of Dr. Jordan Fletcher.

The manuscript was written by me, my supervisor Prof. Miguel Castanho, Prof. Marie Isabel Aguilar and Dr. Leonard Pattenden.

I, Miguel Castanho, as Ana Salomé Veiga supervisor, hereby acknowledge and confirm the information above is correct.

Ana Salomé Veiga

Miguel Castanho

**REAL-TIME BIOSENSOR INTERACTIONS OF HIV-1
ANTIBODIES 2F5 AND 4E10 WITH A GP41 EPITOPE PREBOUND
TO HOST CELL AND VIRAL MEMBRANE MIMETICS**

Ana Salomé Veiga¹, Leonard Keith Pattenden², Jordan M. Fletcher², Miguel Castanho¹
and Marie-Isabel Aguilar^{2,*}

1 – Centro de Química e Bioquímica, Faculdade de Ciências da Universidade de Lisboa, Campo Grande
Ed. C8, 1749-016 Lisboa, Portugal

2 – Department of Biochemistry and Molecular Biology, Monash University, Clayton, Victoria 3800,
Australia

* Corresponding author: Marie-Isabel Aguilar, Department of Biochemistry and
Molecular Biology, Monash University, Clayton, Victoria 3800, Australia. Phone: +61-
3-9905-3723. Fax: +61-3-9905-3726. E-mail: mibel.aguilar@med.monash.edu.au

Abstract

Two HIV-1 recognition domains to human monoclonal antibodies 2F5 (ELDKWA) and 4E10 (NWFNIT) serve as promising models for immunogens in vaccine development against HIV-1. However, the failure of these recognition domains to generate broadly reactive neutralizing antibodies, and known membrane-binding properties of the antibodies raised to these recognition domains suggests that additional features or recognition motifs are required to form an efficient immunogen, which could possibly include membrane components. In this study we use an extended peptide-epitope sequence derived from the gp41 native sequence (H-NEQELLELDKWASLWNWFNITNWLWYIK-NH) that contains the two recognition domains to 2F5 and 4E10, to examine the role of model cell (POPC) and viral (POPC/Cholesterol/sphingomyelin) membranes, to determine the role of membranes in the recognition of these two antibodies. Using a surface plasmon resonance biosensor, the binding of 2F5 and 4E10 is compared and contrasted to membranes in the presence and absence of prebound peptide-epitope showing the recognition of gp41-derived epitope sequences by 2F5 and 4E10 occurs in a membrane context. The recognition of the peptide-epitope is found to be distinctly different; in the case of 2F5 the membrane appears to directly participate in epitope recognition with greatly reduced binding of 2F5 seen to membranes alone, but in contrast 4E10 can bind strongly to membranes in the presence or absence of the peptide-epitope with more favourable dissociation rates demonstrated in the presence of the peptide-epitope.

Introduction

The viral envelope glycoprotein responsible for the human immunodeficiency virus type 1 (HIV-1) entry into target cells is composed of the surface glycoprotein gp120 and the transmembrane glycoprotein gp41 (10, 11, 31). The binding of gp120 to cellular receptors and subsequent changes within the gp41 ectodomain involve the formation of a six-helix bundle structure and leads to both membrane fusion and viral entry (e.g., 10, 11, 17, 31).

The human monoclonal antibodies (MAbs) 2F5 and 4E10 are two rare, broadly neutralizing antibodies against HIV-1 (27, 29, 34) that interact with epitopes in the membrane proximal region (MPR) of HIV-1 gp41. Specifically, these MAbs recognize epitopes in gp41 with core sequences ELDKWA, for 2F5 (extending a little over the MPR N-terminal limit), and NWF(D/N)IT, for 4E10 (8, 20, 22, 27, 34, 35). These peptidic epitopes have attracted increasing attention as promising models for immunogens in vaccine development (33).

In designing a more efficient gp41-based immunogen, it is known that the binding affinity of 2F5 and 4E10 for the epitopes is enhanced when gp41 is in a lipidic or membrane environment (15, 18, 21). Indeed, based on the crystal structures of 2F5 and 4E10, it has been proposed that these MAbs can interact with the viral membrane through a hydrophobic surface present on the third complementarity-determining region of the heavy chain (CDR H3), possibly facilitating binding to gp41 epitopes that lie close to the membrane (9, 21). Additional studies have shown diverse lipid species can be important to 2F5 and 4E10 recognition comprising both neutral and anionic phospholipids (23, 24), including specialised anionic lipids such phosphatidylinositol-4-phosphate (PIP) (5, 6) and cardiolipin (CL) (16) which has recently been studied using Surface Plasmon Resonance (SPR) (2).

An overall conclusion that has been drawn is the recognition of gp41-derived epitope sequences by 2F5 and 4E10 occurs in a membrane context (2, 24). However, the questions the field is still addressing is the relevance of a lipid environment; whether the membrane participates or is tolerated in binding to 2F5 and 4E10 as inferred by structural biologists, or whether a lipid environment allows small gp41 epitopes to adopt a more structured (immunogenic) conformation which is then recognised by the MAbs or whether it is a combination of membranes enhancing epitope structure as well as directly forming part of a combined lipid-peptide antigen? The implication of understanding how 2F5 and 4E10 MAbs recognise their gp41 epitopes could lead to the development of more successful immunogens which either utilise lipids to improve structure and foreignness or perhaps have designed gp41-like epitopes constrained in pre-ordered immunogenic conformations.

In the present work we examine the role of both cell and viral membranes in the mechanism of action of these two MAbs. Specifically, the interactions of 2F5 and 4E10 were investigated in the presence and absence of a gp41 peptide that encompasses both 2F5 and 4E10 recognised epitopes, that were prebound to model cell and viral membranes. We employed an SPR optical biosensor, which are increasingly used to directly study membrane-mediated interactions, as opposed to the majority of membrane-binding studies that use liposome-based ELISA assays or fluorescent binding experiments that indirectly measure binding events. This study provides new insight into the molecular properties important to the recognition of gp41 epitopes by these two important MAbs.

Materials and Methods

2-(1H-7-Azabenzotriazol-1-yl)-1,1,3,3-tetramethyl uronium hexafluorophosphate (HATU), N-methyl pyrrolidone (NMP), dimethylformamide (DMF), diisopropylethylamine (DIPEA), piperidine, triisopropylsilane (TIPS) and trifluoroacetic acid (TFA) were of peptide synthesis grade and obtained from Auspep (Melbourne, Australia). POPC (1-palmitoyl-2-oleyl-*sn*-glycero-3-phosphocholine) was purchased from Avanti Polar-Lipids (Alabaster, AL, USA). Sphingomyelin (SM; chicken egg yolk), Cholesterol (Chol), (3-[3-Cholamidpropyl)-dimethyl-ammonio]-1-propanesulfonate (CHAPS) and Sodium Dodecyl Sulfate (SDS)) were obtained from Sigma (St. Louis, MO, USA). HEPES was obtained from Sigma (Castle Hill, NSW, Australia) and NaCl was from Amresco (Solon, OH, USA). 10mM HEPES buffer pH 7.4, 150mM NaCl, was used throughout the studies by dilution from a 10x stock. The SPR system used was a BIACORE T100 analytical system (Biacore, Uppsala, Sweden) using L1 sensor chip (Series S; Biacore) for liposome attachment. The regeneration solutions were SDS 0.5% (w/v), 20mM CHAPS, 10mM NaOH (20% methanol) and 10mM NaOH. All the solutions used in the T100 were freshly prepared and filtered through a 0.22 μ m filter.

Antibodies

Human HIV-1 gp41 monoclonal antibodies 2F5 and 4E10 from Dr. H. Katinger and Polymun Scientific were provided by the EU Programme EVA Centralised Facility for AIDS Reagents, National Institute for Biological Standards and Control, UK and were also purchased from Polymun Scientific (Vienna, Austria). In order to avoid signal response variations during the SPR experiments because of the differences between the MAb solutions and the running buffer, 2F5 and 4E10 (up to 100 μ L) were dialysed in

HEPES buffer (500mL) for >16h using a 10kDa SnakeSkin™ Pleated Dialysis Tubing (Pierce, Rockford, IL, USA). The MAbs were quantified with the modified Lowry, *DC* protein assay (Bio-Rad, Gladesville, NSW, Australia). The dialysis buffer was subsequently used as running buffer in SPR experiments, thereby removing refractive index changes between solutions. Refractive index differences between different MAB preparations was <2RU.

Peptide synthesis

Rink amide resin was obtained from Novabiochem (San Diego, CA, USA) and Fmoc-L-amino acids were obtained from GL Biochem (Shanghai, China). The peptide H-NEQELLELDKWASLWNWFNITNWLWYIK-NH (hereafter referred to as peptide-epitope) was synthesised on a 0.1mmol scale on Rink amide resin using a Liberty™ microwave peptide synthesiser (CEM™; NC, USA) employing Fmoc solid-phase techniques (for review see 12). The peptide-epitope was assembled by systemically repeated steps of “double” coupling and “double” deprotection. “Double” coupling: Fmoc-amino acid (5 eq.), HATU (4.5 eq.), DIPEA (10 eq.), in NMP for 2 × 5min, with 20W microwave irradiation at 75°C. “Double” deprotection: 20% piperidine in NMP (1 × 30s, with 40W irradiation at 38°C; followed by 1 × 3min, with 40W irradiation at 75°C). Following linear assembly, the peptide was cleaved from the resin with simultaneous removal of side-chain protecting groups by treatment with a cleavage cocktail (2mL) consisting of TFA (95%), TIPS (2.5%) and H₂O (2.5%) for 3h at room temperature. Suspended resin was removed by filtration and the peptide precipitated in ice-cold diethyl ether. Solid material was then collected in a sintered glass funnel (pore-size 4), washed with diethyl ether, dissolved with 1:1 MeCN/H₂O, and lyophilised. An initial analysis of the crude material by RP-HPLC and mass spectrometry suggested the

presence of multiple N-carboxy groups presumably resulting from the incomplete removal of *t*-butoxycarbonyl sidechain protection from the indol nitrogen of the five tryptophan residues present (13). Decarboxylation of these carbamic acid intermediates was achieved by dissolving the crude material in 9:9:2 MeCN/H₂O/CH₃COOH and stirring at room temperature overnight. The peptide was then purified by preparative RP-HPLC using an Agilent HP1100 system fitted with a Vydac™ C₁₈ (250mm × 22mm) reverse-phase column. The eluents used were 0.1% TFA in H₂O (A) and 0.1% TFA in MeCN (B); the peptide was eluted by applying a linear gradient (at 6mL/min) of 0% to 60 % B over 60min. Fractions collected were examined by analytical RP-HPLC and those found to contain exclusively the desired product were pooled and lyophilised. Analysis of the purified final product by RP-HPLC indicated a purity of >90%. Successful synthesis was confirmed by electrospray-ionisation mass spectrometry (MW_{observed}: 3652.8; MW_{theoretical}: 3650.8).

Peptide stock solutions were prepared in dimethyl sulfoxide (DMSO) and diluted to desired concentrations with HEPES buffer. The total DMSO concentration was maintained at 0.14% (v/v) in the peptide samples through the experiments to aid peptide solubility, as low DMSO concentrations are reported not to perturb particular liposomal compositions (1). This value is well below the chemical compatibility of the L1 chips (10%), and was confirmed not to cause observed baseline changes in this study using buffer-only injections over membrane surfaces. Peptide concentrations were quantified with the modified Lowry, *DC* protein assay (Bio-Rad, Gladesville, NSW, Australia).

Liposome preparation and lipid bilayers formation

Small unilamellar vesicles (SUV) of POPC and a mixture of POPC/Chol/SM (1:1:1) were used through the studies. POPC (dissolved in chloroform) alone or mixed with

Chol (in chloroform) and SM (in chloroform/methanol mixture 2:1 (v/v)) was dried under a gentle stream of nitrogen. Solvent removal was completed *in vacuo*, overnight. The lipid was suspended in HEPES buffer to a final concentration of 1mM, and sized by subjection to seven repeated freeze/thaw cycles and extrusion (19 times) through polycarbonate filters (50nm pore diameter).

All biosensor experiments were conducted at 25°C, with sample injections using instrument high-performance parameters and collection rates at 10Hz. The L1 sensor chip surface was washed as part of a start-up cycle by the sequential injection of 20mM CHAPS (5µL/min flow rate, 60s contact time), 10mM NaOH in 20% methanol (50µL/min, 36s) and 10mM NaOH (50µL/min, 36s). SUVs were captured onto the L1 surface at a flow rate of 2µL/min (2,400s). A 10mM NaOH pulse was used to remove loosely bound liposomes from the surface (50µL/min, 36s) resulting in a stable baseline. Typical capture levels were 10,000 – 12,000RU throughout the experiments.

MAbs binding to the bilayer membranes

Solutions of 2F5 (0.06µM-0.3µM) and 4E10 (0.06µM-0.5µM) in HEPES buffer were studied in the presence of peptide-epitope concentrations of 0.3, 0.5 and 1µM prebound to membrane surfaces. The MAb binding was also studied in the presence of a blank control of DMSO 0.14% (v/v) in buffer. Pre-binding of the peptide-epitope (or blank control treatment) was achieved by injection of solutions over the membrane surfaces (5µL/min, 180s). Upon completion of the injection, the flow was continued at 5µL/min for a dissociation time of 60s before the MAb solutions were injected over the lipid surface containing the peptide (or blank). The MAb solutions were injected using different contact times at a constant flow of 5µL/min (2F5 contact time 90s, 4E10 contact time 60s), followed by a uniform dissociation time of 600s. After each MAb

binding assay, the sensor surface was regenerated with 0.5% (w/v) SDS (5 μ L/min, 60s), followed by the sequential injection of 20mM CHAPS (5 μ L/min, 60s), 10mM NaOH in 20% methanol (50 μ L/min, 36s) and 10mM NaOH (50 μ L/min, 36s).

Results

We investigated the interaction of the HIV-1 MAbs 2F5 and 4E10 with model membranes using an SPR biosensor, which detects changes in the refractive index at the sensor surface caused by mass changes. Throughout the studies we used model membrane systems that mimic the conditions present on both the target cell and viral membranes. Liposomes of POPC were used to mimic the target cell membrane as POPC is a neutral lipid (at the pH conditions used) with fluidity properties similar to biological membranes (14). Liposomes composed of POPC/Chol/SM (1:1:1) were used to mimic the viral membrane, which is rich in Chol and SM (3, 7). Liposomes were reproducibly immobilized on the surface of the sensor chip to $\sim 10,000$ RU for POPC and $\sim 12,000$ RU for POPC/Chol/SM vesicles. The interaction of the MAbs with each membrane was investigated in the presence and absence of the peptide-epitope. The peptide-epitope was prebound at either 0.3, 0.5 or $1\mu\text{M}$ to concentration-dependent levels ranging from 350 – 500 RU for POPC and for POPC/Chol/SM. Immediately following pre-binding (60s), injections of the MAbs were subsequently made to determine the binding of the MAbs to the different peptide-epitope membranes. When the MAbs were injected across the immobilized liposomes over a range of concentrations (0.06 - $0.3\mu\text{M}$ for 2F5 and 0.06 - $0.5\mu\text{M}$ for 4E10), the surface response, reporting protein bounded to the membrane, was found to increase with higher protein concentrations. A fresh liposome surface was generated for each MAb binding test to prevent carry-over of bound material influencing subsequent measurements. It was found a more rigorous regeneration protocol was necessary to completely restore baseline conditions; requiring two detergent washes, a Methanol:sodium hydroxide pulse and sodium hydroxide pulse to ensure the regeneration detergents did not carry-

over to impede subsequent liposomal capture or form mixed micelles with captured liposomes.

2F5 membrane interactions

Figures 1A and B show the sensorgrams obtained for the binding of 2F5 to POPC and POPC/Chol/SM liposomes in the absence of the peptide-epitope. The results obtained were very similar for both membranes, with a general increase in binding concomitant to increasing concentrations of 2F5.

In general the shapes of the sensorgrams for 2F5 interactions in the absence of the peptide-epitope with both POPC and POPC/Chol/SM are non-ideal, showing a dispersion-like effect at the end of the association phase, which is more pronounced in Figure 1B (POPC/Chol/SM). Such dispersion effects are typically caused by collapsing of the separating “bubbles” that partition the sample plug from running buffer as part of high-performance injections, causing the injected sample to be diluted by running buffer during the course of injections. In this manner, dispersion only influences the final parts of the association phase during the course of the injection which can be seen on the POPC surfaces (Figure 1A). We do not conclude DMSO carryover between injections has caused the effect as it is not seen in analogous 4E10 experiments with the blank control or subsequent 2F5 experiments in the presence of the peptide-epitope, furthermore the effect of DMSO is to cause a significant increase in the response due to the higher refractive index of DMSO than the buffer solution, as opposed to reduced responses observed here. Similarly we do not conclude the dialysis was incomplete as dialysis conditions were exhaustive (16h) and do not show the same effects in other 2F5 experiments using the same batch of buffer-exchanged MAb. The POPC/Chol/SM surfaces (Figure 1B) suggests an explanation as there are more pronounced effects

which continue after the association phase, before rising after 200s on the sensorgrams, resulting in a net higher response than baseline or expected from the initial dissociation levels prior to 200s. Because the dispersion-like effect continues beyond the association phase it suggests remodelling of the surface may occur in the presence of the 2F5 MAb – possibly enhanced by the DMSO on the surface prior to 2F5 being injected. Despite the dispersion-like effect, it is notable the binding of 2F5 to both of the membranes appears to be reversible; in general there is significant dissociation of 2F5, though the signal often did not return to baseline, reflecting the presence of a small proportion of strongly bound 2F5 to the membranes in the absence of the peptide-epitope.

To study the 2F5 membrane interactions in the presence of the membrane bound peptide-epitope, the binding of 2F5 at each concentration was measured with a range of peptide-epitope concentrations pre-bound to the membrane. Figure 2 shows the sensorgrams for 0.1 and 0.2 μ M 2F5 using a range of peptide-epitope concentrations (0.3-1 μ M) and it is evident that; binding is so tight that very little 2F5 comes off the surface during the dissociation phase, indicating an almost irreversible association of 2F5 in the presence of the peptide-epitope over the course of the assay for both membranes studied and for all 2F5 concentrations (Figures 2 and 3) as opposed to membranes alone (Figure 1). Thus, the binding of the MAb in the presence of the peptide-epitope is much stronger than the binding to the membrane alone. However, for the 2F5 0.06-0.1 μ M concentration range in the presence of POPC and 0.06-0.08 μ M in the presence of POPC/Chol/SM, there was no simple correlation between the 2F5 binding and the concentration of peptide-epitope present. Figures 2A and C show that for 2F5 0.1 μ M in POPC and for 2F5 0.08 μ M in POPC/Chol/SM, for instance, the presence of a lower peptide-epitope concentration leads to higher 2F5 response increases. Analysis of the other 2F5 concentrations (0.2-0.3 μ M in POPC and 0.1-0.3 μ M

in POPC/Chol/SM) revealed the opposite trend, an increase in MAb binding with epitope concentration bound. As shown in Figures 2B and D for 2F5 0.2 μ M in POPC and POPC/Chol/SM, respectively, the higher MAb response increase occurs in the presence of higher peptide-epitope concentrations.

Additionally, the variation of the 2F5 concentrations with a fixed peptide-epitope concentration leads to a binding increase proportional to the MAb concentration, as is shown in Figures 3A and B for peptide-epitope 1 μ M (as an example) in POPC and POPC/Chol/SM, respectively.

4E10 membrane interactions

The sensorgrams associated with the membrane binding properties of 4E10 in the presence of POPC and POPC/Chol/SM liposomes, respectively, are shown in Figures 4A and B. In both cases the response observed at the end of the association phase increased with increases in 4E10 concentration, with two exceptions: 0.5 μ M on POPC liposomes (not shown) and 0.2 and 0.3 μ M 4E10 on POPC/Chol/SM liposomes. Nevertheless, globally the 4E10 membrane binding is reversible displaying a distinct dissociation phase following the clear and regularly shaped association phase.

The interaction of 4E10 with each membrane in the presence of the membrane bound peptide-epitope was performed at 4E10 concentrations of 0.06-0.5 μ M with a range of peptide-epitope concentrations of 0.3-1 μ M. For POPC liposomes at the lower 4E10 concentrations (0.06-0.3 μ M), there is a general decrease in the MAb response with increasing peptide-epitope concentration, as shown in Figure 5A. At higher 4E10 concentrations (0.5 μ M) (Figure 5B) there was an increase in the MAb response in the presence of two different peptide-epitope concentrations. However, for all peptide-epitope concentrations the dissociation phase shows less 4E10 dissociation when

compared with the blank indicating that the presence of the peptide epitope increases the affinity of the 4E10 for the membrane.

In POPC/Chol/SM liposomes, the sensorgrams obtained for lower 4E10 concentrations show less relative MAb response increase when the peptide-epitope is present. For higher 4E10 concentrations the response is similar, regardless of the presence of peptide-epitope. Nevertheless the observed 4E10 dissociation rate is less, with less 4E10 leaving the surface when the peptide-epitope is present (Figure 5C and D, for 4E10 0.3 and 0.5 μ M, respectively), as observed before for POPC liposomes.

Overall it can be concluded from the sensorgrams in Figures 6A and B obtained for a range of 4E10 concentrations, that at a particular peptide-epitope concentration the MAb response increase is proportional to the MAb concentration, with 1 μ M peptide-epitope in POPC and POPC/Chol/SM, respectively.

Discussion

2F5 and 4E10 are two MAbs against HIV-1 whose epitopes are closely localized in the gp41 MPR (2F5 epitope extends slightly outside the MPR N-terminus), in the vicinity of the viral membrane. In the native state the MPR is believed to lie parallel to the surface of the viral membrane external layer (32). However, previous experimental studies show that the MPR has tendency to partition into membranes (26, 28) and it is possible that this region is membrane-associated during the virus-cell fusion event. In a membrane mimetic environment an MPR synthetic peptide has been shown to adopt a helical conformation parallel to the membrane, near the lipid interfacial region (25). The x-ray crystal structure of 2F5 and 4E10 complexed to its synthetic epitopes revealed that the epitopes adopt a β -turn and α -helical conformation, respectively (9, 21). However the crystallographic evidence lacks a membrane context there is no general consensus about the MPR structure in the context of the native gp120-gp41 or during the fusion process. It has been proposed that the 2F5 and 4E10 MAbs interact with the viral membrane through a CDR H3 hydrophobic surface (9, 21) and other studies with liposomes have shown that the binding of 2F5 and 4E10 to the epitopes increases when gp41 is presented in a lipid environment (15, 21). The goal of this present study was to examine the membrane interactions of 2F5 and 4E10 using POPC and POPC/Chol/SM liposomes as membrane models to mimic the host cell and viral membranes, respectively. The study was performed in the presence and absence of a peptide-epitope (H-NEQELLELDKWASLWNWFNITNWLWYIK-NH), which has membrane binding properties and contains both 2F5 (ELDKWA) and 4E10 (NWFNIT) epitopes flanked by native gp41 sequences. The use of this peptide-epitope, rather than each MAb core epitope sequence separately, allows the binding properties of each MAb to be studied with the inclusion of the flanking residues, which are naturally included in the whole

gp41 envelope, can facilitate secondary structure and provide a more substantive context to the epitopes and thereby stabilize a better mimetic of the natural epitope conformation.

The results obtained allow a number of conclusions to be made about the membrane binding characteristics of the MAbs. In addition, it was not possible to calculate the detailed kinetics and affinity parameters associated with the binding because most of the experimental sensorgrams are more complex than can be analysed by the currently available kinetic models preventing any curve fitting to be performed.

The analysis of the sensorgrams obtained for 2F5 demonstrate that the membrane binding behaviour of the MAb is similar in both POPC and POPC/Chol/SM model membranes. Specifically, 2F5 binds reversibly to the membrane in the absence of the peptide-epitope. Although weak compared to binding with membrane peptide-epitopes, 2F5 membrane binding was detectable, at variance with fluorescence techniques (30). This can be related to the difference in the methods and experimental conditions used. Namely, the detection of membrane binding by Trp fluorescence is only detectable if there is a significant change in Trp fluorescence upon membrane binding. In contrast, the sensitive SPR technique allows the membrane binding to be followed in real-time during the entire binding process.

The binding of 2F5 was increased significantly in the presence of the membrane-bound peptide-epitope complex and exhibited irreversible binding over the course of the assay, i.e. there was no desorption during the dissociation phase. At low 2F5 concentrations there was no correlation between the level of bound MAb and the concentration of peptide-epitope bound to the membrane. However, at high 2F5 concentrations increases in the peptide-epitope concentration enhanced the MAb binding.

In contrast, 4E10 bound strongly to both POPC and POPC/Chol/SM membranes even when the peptide-epitope was absent, and clearly bound more strongly to each membrane studied than 2F5, which is in agreement with other studies (24). When the membrane bound peptide-epitope is present the results obtained are also different from those observed with 2F5. Interestingly, in the presence of the peptide-epitope, a decrease in the response is obtained for low 4E10 concentrations. For high MAb concentrations similar responses to the blank (membrane only) were obtained. However, in all situations the 4E10 dissociation is decreased in the presence of the peptide-epitope when compared with the membrane alone. Thus, 4E10 binds to the membrane equally well in the presence or absence of peptide-epitope but the presence of the peptide significantly stabilizes the binding resulting in very little dissociation in both POPC and POPC/Chol/SM membranes.

Given the proximity of 2F5 and 4E10 epitopes to the viral membrane, it may be anticipated that the MAbs may bind more strongly to the model viral membrane (POPC/Chol/SM) than to the model mammalian membrane (POPC). However, the binding of each MAbs was similar with both lipid mixtures, both in the presence and absence of the peptide epitope.

These results agree in part with other studies that show that 2F5 and 4E10 bind non-specifically to neutral and anionic phospholipids (Phosphatidylcholine and Phosphatidylglycerol for 2F5 and Phosphatidylcholine, Sphingomyelin, Phosphatidylethanolamine, Phosphatidylglycerol and Phosphatidylserine for 4E10), and bind more strongly to CL (16, 23, 24). Nevertheless, Chol seems to be important to the 4E10 epitope recognition (19).

The results obtained also show that 2F5 binding to the membrane increases significantly in the presence of the peptide-epitope while 4E10 binding to either

membrane is not solely dependent on the presence of the epitope. These results are not in agreement with previous studies (24), where the binding to membrane alone of both MAbs was decreased when compared to the membrane loaded with the epitope. The differences obtained could be related to the different techniques used in both studies, liposome-based ELISA vs. SPR. Additionally, both 2F5 and 4E10 could probably be used as MAbs to lipids to neutralize HIV but 4E10 is a better candidate given its stronger membrane binding properties. It has been reported that 4E10 may bind specifically to a PIP through a phosphate-binding subsite (5, 6). Lipids like PS or PIP might be exposed at the HIV surface (4).

In conclusion the results suggest that both 2F5 and 4E10 have the capacity to bind to membranes (although weakly for 2F5) and membrane-bound epitopes. This shows that 4E10 has a greater capacity to access the epitope located close to the membrane surface. This association is quite extensive by itself and not enhanced by the presence of the epitope, though the dissociation from the complex is notably reduced in the presence of the peptide-epitope. Although this membrane binding property of 4E10 can reduce the global concentration of free MAbs, it is at the same time a unique property that allows recognition of an epitope which is so close to the membrane. 2F5 has lower affinity for the membranes but binds strongly to its epitope in a membrane context. Our results confirm that this high affinity for the epitope in the presence of a membrane is a result of the induction of a membrane-dependent epitope conformation optimal for the binding (15, 21). However, a small contribution of the lipids to stabilize epitope binding, given the membrane proximity, cannot be discarded. This contribution probably involves the hydrophobic surface of the 2F5 CDR H3 region. For the MAb 4E10 the binding to the membrane is strong and does not depend of the peptide-epitope presence. However the binding seems to be stabilized in the presence of the epitope. Probably the 4E10 innate

capacity to binds membranes allows a stable binding with the epitope in a membrane context. These differences in the MAbs behaviour could be related to different epitope gp41 positions or the way they recognize and/or bind to the epitope.

Acknowledgments

This project was partially funded by FCT-MCTES (Portugal), including a grant (SFRH/BD/14336/2003) under the program POCTI to A.S.V. Bifonds travel allowance is also acknowledged. Monoclonal antibodies 2F5 and 4E10 were provided by Dr. Hermann Katinger and Polymun Scientific through the NIBSC Centralised Facility for AIDS Reagents supported by EU Programme EVA and the UK Medical Research Council. The support of the Australian Research Council is also acknowledged.

References

1. Abdiche, Y. N., and D. G. Myszka. 2004. Probing the mechanism of drug/lipid membrane interactions using Biacore. *Anal. Biochem.* **328**:233-243.
2. Alam, S. M., M. McAdams, D. Boren, M. Rack, R.M. Scearce, F. Gao, Z.T. Camacho, D. Gewirth, G. Kelsoe, P. Chen, and B.F. Haynes. 2007. The role of antibody polyspecificity and lipid reactivity in binding of broadly neutralizing anti-HIV-1 envelope human monoclonal antibodies 2F5 and 4E10 to glycoprotein 41 membrane proximal envelope epitopes. *J. Immunol.* **187**:4424-4435.
3. Aloia, R. C., H. Tian, and F. C. Jensen. 1993. Lipid composition and fluidity of the human immunodeficiency virus envelope and host cell plasma membranes. *Proc. Natl. Acad. Sci. USA* **90**:5181-5185.
4. Alving, C. R., Z. Beck, N. Karasavva, G. R. Matyas, and M. Rao. 2006. HIV-1, lipid rafts, and antibodies to liposomes: implications for anti-viral-neutralizing antibodies. *Mol. Membr. Biol.* **23**:453-465.
5. Beck, Z., N. Karasavvas, J. Tong, G. R. Matyas, R. Mangala, and C. R. Alving. 2007. Calcium modulation of monoclonal antibody binding to phosphatidylinositol phosphate. *Biochem. Biophys. Res. Commun.* **354**:747-751.
6. Brown, B. K., N. Karasavvas, Z. Beck, G. R. Matyas, D. L. Birx, V. R. Polonis, and C. R. Alving. 2007. Monoclonal antibodies to phosphatidylinositol phosphate neutralize human immunodeficiency virus type 1: role of phosphate-binding subsites. *J. Virol.* **81**:2087-2091.
7. Brügger, B., B. Glass, P. Haberkant, I. Leibrecht, F. T. Wieland, and H.-G. Kräusslich. 2007. The HIV lipidome: a raft with an unusual composition. *Proc. Natl. Acad. Sci.* **103**:2641-2646.

8. Brunel, F. M., M. B. Zwick, R. M. F. Cardoso, J. D. Nelson, I. A. Wilson, D. N. Burton, and P. E. Dawson. 2006. Structure-function analysis of the epitope for 4E10, a broadly neutralizing human immunodeficiency virus type 1 antibody. *J. Virol.* **80**:1680-1687.
9. Cardoso, R. M. F., M. B. Zwick, R. L. Stanfield, R. Kunert, J. M. Binley, H. Katinger, D. R. Burton, and I. A. Wilson. 2005. Broadly neutralizing anti-HIV antibody 4E10 recognizes a helical conformation of a highly conserved fusion-associated motif in gp41. *Immunity* **22**:163-173.
10. Chan, D. C., and P. S. Kim. 1998. HIV entry and its inhibition. *Cell* **93**:681-684.
11. Eckert, D. M., and P. S. Kim. 2001. Mechanisms of viral membrane fusion and its inhibition. *Annu. Rev. Biochem.* **70**:777-810.
12. Fields, G. B., and R. L. Noble. 1990. Solid phase peptide synthesis utilizing 9-fluorenylmethoxycarbonyl amino acids. *Int. J. Pept. Protein Res.* **35**:161-214.
13. Franzén, H., L. Grehn, and U. Ragnarsson. 1984. Synthesis, properties, and use of Nⁱⁿ-Boc-tryptophan derivatives. *J. Chem. Soc., Chem. Commun.* **24**:1699-1770.
14. Gennis, R. B., 1989. *Biomembranes - molecular structure and function*, Springer-Verlay, New York.
15. Grundner, C., T. Mirzabekov, J. Sodroski, and R. Wyatt. 2002. Solid-phase proteoliposomes containing human immunodeficiency virus envelope glycoproteins. *J. Virol.* **76**:3511-3521.
16. Haynes, B. F., J. Fleming, E. W. St. Clair, H. Katinger, G. Stiegler, R. Kunert, J. Robinson, R. M. Scarce, K. Plonk, H. F. Staats, T. L. Ortel, H. Liao, and S. M. Alam. 2005. Cardiolipin polyspecific autoreactivity in two broadly neutralizing HIV-1 antibodies. *Science* **308**:1906-1908.

17. LaBranche, C. C., G. Galasso, J. P. Moore, D. P. Bolognesi, M. S. Hirsch, and S. M. Hammer. 2001. HIV fusion and its inhibition. *Antiviral Res.* **50**:95-115.
18. Lenz, O., M. T. Dittmar, A. Wagner, B. Ferko, K. Vorauer-Uhl, G. Stiegler, and W. Weissenhorn. 2005. Trimeric membrane-anchored gp41 inhibits HIV membrane fusion. *J. Biol. Chem.* **280**:4095-4101.
19. Lorizate, M., A. Cruz, N. Huarte, R. Kunert, J. Pérez-Gil, and J. L. Nieva. 2006. Recognition and blocking of HIV-1 gp41 pre-transmembrane sequence by monoclonal 4E10 antibody in a raft-like membrane environment. *J. Biol. Chem.* **281**:39598-39606.
20. Muster, T., F. Steindl, M. Purtscher, A. Trkola, A. Klima, G. Himmler, F. Ruker, and H. Katinger. 1993. A conserved neutralizing epitope on gp41 of human immunodeficiency virus type 1. *J. Virol.* **67**:6642-6647.
21. Ofek, G., M. Tang, A. Sambor, H. Katinger, J. R. Mascola, R. Wyatt, and P. D. Kwong. 2004. Structure and mechanistic analysis of the anti-human immunodeficiency virus type 1 antibody 2F5 in complex with its gp41 epitope. *J. Virol.* **78**:10724-10737.
22. Parker, C. E., L. J. Deterding, C. Hager-Braun, J. M. Binley, N. Schülke, H. Katinger, J. P. Moore, and K. B. Tomer. 2001. Fine definition of the epitope on the gp41 glycoprotein of human immunodeficiency virus type 1 for the neutralizing monoclonal antibody 2F5. *J. Virol.* **75**:10906-10911.
23. Sánchez-Martínez, S., M. Lorizate, H. Katinger, R. Kunert, G. Basañez, and J. L. Nieva. 2006a. Specific phospholipid recognition by human immunodeficiency virus type-1 neutralizing anti-gp41 2F5 antibody. *FEBS Lett.* **580**:2395-2399.

24. Sánchez-Martínez, S., M. Lorizate, H. Katinger, R. Kunert, and J. L. Nieva. 2006b. Membrane association and epitope recognition by HIV-1 neutralizing anti-gp41 2F5 and 4E10 antibodies. *AIDS Res. Hum. Retroviruses* **22**:998-1006.
25. Schibli, D. J., R. C. Montelaro, and H. J. Vogel. 2001. The membrane-proximal tryptophan-rich region of the HIV glycoprotein, gp41, forms a well-defined helix in dodecylphosphocholine micelles. *Biochemistry* **40**:9570-9578.
26. Shnaper, S., K. Sackett, S. A. Gallo, R. Blumenthal, and Y. Shai. 2004. The C- and the N-terminal regions of glycoprotein 41 ectodomain fuse membranes enriched and not enriched with cholesterol, respectively. *J. Biol. Chem.* **279**:18526-18534.
27. Stiegler, G., R. Kunert, M. Purtscher, S. Wolbank, R. Voglauer, F. Steindl, and H. Katinger. 2001. A potent cross-clade neutralizing human monoclonal antibody against a novel epitope on gp41 of human immunodeficiency virus type 1. *AIDS Res. Hum. Retroviruses* **17**:1757-1765.
28. Suárez T., W. R. Gallaher, A. Agirre, F. M. Goñi, and J. L. Nieva. 2000. Membrane interface-interacting sequences within the ectodomain of the human immunodeficiency virus type 1 envelope glycoprotein: putative role during viral fusion. *J. Virol.* **74**:8038-8047.
29. Trkola, A., A. B. Pomales, H. Yuan, B. Korber, P. J. Maddon, G. P. Allaway, H. Katinger, C. F. Barbas III, D. R. Burton, D. D. Ho, and J. P. Moore. 1995. Cross-clade neutralization of primary isolates of human immunodeficiency virus type 1 by human monoclonal antibodies and tetrameric CD4-IgG. *J. Virol.* **69**:6609-6617.
30. Veiga, A. S., and M. A. R. B. Castanho. 2006. The membranes' role in the HIV-1 neutralizing monoclonal antibody 2F5 mode of action needs re-evaluation. *Antiviral Res.* **71**:69-72.

31. Wyatt, R., and J. Sodroski. 1998. The HIV-1 envelope glycoproteins: fusogens, antigens, and immunogens. *Science* **280**:1884-1888.
32. Zhu, P., J. Liu, J. Bess Jr, E. Chertova, J. D. Lifson, H. Grisé, G. A Ofek, K. A. Taylor, and K. H. Roux. 2006. Distribution and three-dimensional structure of AIDS virus envelope spikes. *Nature* **441**:847-852.
33. Zwick, M. B. 2005. The membrane-proximal external region of HIV-1 gp41: a vaccine target worth exploring. *Aids* **19**:1725-1737.
34. Zwick, M. B., A. F. Labrijn, M. Wang, C. Spenlehauer, E. O. Saphire, J. M. Binley, J. P. Moore, G. Stiegler, H. Katinger, D. R. Burton, and P. W. H. I. Parren. 2001. Broadly neutralizing antibodies targeted to the membrane-proximal external region of human immunodeficiency virus type 1 glycoprotein gp41. *J. Virol.* **75**:10892-10905.
35. Zwick, M. B., R. Jensen, S. Church, M. Wang, G. Stiegler, R. Kunert, H. Katinger, and D. R. Burton. 2005. Anti-Human immunodeficiency virus type 1 (HIV-1) antibodies 2F5 and 4E10 require surprisingly few crucial residues in the membrane-proximal external region of glycoprotein gp41 to neutralize HIV-1. *J. Virol* **79**:1252-1261.

Figure Legends

Figure 1 – Sensorgrams obtained for 2F5 binding to immobilized POPC (A) and POPC/Chol/SM (1:1:1) (B) lipid membrane surface (L1 chip). 2F5 was injected over a freshly prepared lipid surface, and the subsequent association and dissociation were monitored. 2F5 0.06 μ M, 0.08 μ M and 0.1 μ M (a), 0.2 μ M (b) and 0.3 μ M (c) in (A); 2F5 0.06 μ M (a), 0.08 μ M (b), 0.1 μ M (c), 0.2 μ M (d) and 0.3 μ M (e) in (B).

Figure 2 – Sensorgrams obtained for 2F5 binding to immobilized POPC (A and B) and POPC/Chol/SM (1:1:1) (C and D) lipid membrane surface (L1 chip) in the presence of peptide-epitope range of concentrations (0 μ M (a), 0.3 μ M (d), 0.5 μ M (c) and 1 μ M (b) in (A); 0 μ M (a), 0.3 μ M (b), 0.5 μ M (c) and 1 μ M (d) in (B); 0 μ M (a), 0.3 μ M (d), 0.5 μ M (b) and 1 μ M (c) in (C); 0 μ M (a), 0.3 μ M (b), 0.5 μ M (c) and 1 μ M (d) in (D)). 2F5 concentrations of 0.1 μ M (A), 0.2 μ M (B), 0.08 μ M (C) and 0.2 μ M (D) were injected over a freshly prepared lipid surface, and the subsequent association and dissociation were monitored.

Figure 3 – Sensorgrams obtained for 2F5 binding to immobilized POPC (A) and POPC/Chol/SM (1:1:1) (B) lipid membrane surface (L1 chip) in the presence of 1 μ M of peptide-epitope. 2F5 of varying concentrations (0.06 μ M (a), 0.08 μ M (b), 0.1 μ M (c), 0.2 μ M (d), and 0.3 μ M (e) in (A); 0.06 μ M (a), 0.08 μ M and 0.1 μ M (b), 0.2 μ M (c), and 0.3 μ M (d) in (B)) was injected over a freshly prepared lipid surface, and the subsequent association and dissociation were monitored.

Figure 4 – Sensorgrams obtained for 4E10 binding to immobilized POPC (A) and POPC/Chol/SM (1:1:1) (B) lipid membrane surface (L1 chip). 4E10 of varying concentrations was injected over a freshly prepared lipid surface, and the subsequent association and dissociation were monitored. 4E10 0.06 μ M (a), 0.08 μ M (b), 0.1 μ M (c), 0.2 μ M (d), and 0.3 μ M (e) in (A); 4E10 0.06 μ M (a), 0.08 μ M (b), 0.1 μ M (c), 0.2 μ M (e), 0.3 μ M (d), and 0.5 μ M (f) in (B).

Figure 5 – Sensorgrams obtained for 4E10 binding to immobilized POPC (A and B) and POPC/Chol/SM (1:1:1) (C and D) lipid membrane surface (L1 chip) in the presence of peptide-epitope range of concentrations (0 μ M (b), 0.3 μ M (c), 0.5 μ M (a) and 1 μ M (d) in (A); 0 μ M (a), 0.3 μ M (c), 0.5 μ M (b) and 1 μ M (d) in (B); 0 μ M (a), 0.3 μ M (d), 0.5 μ M (c) and 1 μ M (b) in (C); 0 μ M (a), 0.3 μ M (c), 0.5 μ M (b) and 1 μ M (d) in (D)). 4E10 concentrations of 0.3 μ M (A), 0.5 μ M (B), 0.2 μ M (C) and 0.5 μ M (D) were injected over a freshly prepared lipid surface, and the subsequent association and dissociation were monitored.

Figure 6 – Sensorgrams obtained for 4E10 binding to immobilized POPC (A) and POPC/Chol/SM (1:1:1) (B) lipid membrane surface (L1 chip) in the presence of 1 μ M of peptide-epitope. 4E10 of varying concentrations (0.06 μ M (a), 0.08 μ M (b), 0.1 μ M (c), 0.2 μ M (d), 0.3 μ M (f), and 0.5 μ M (e) in (A); 0.06 μ M (a), 0.08 μ M (b), 0.1 μ M (c), 0.2 μ M (d), 0.3 μ M (e), and 0.5 μ M (f) in (B)) was injected over a freshly prepared lipid surface, and the subsequent association and dissociation were monitored.

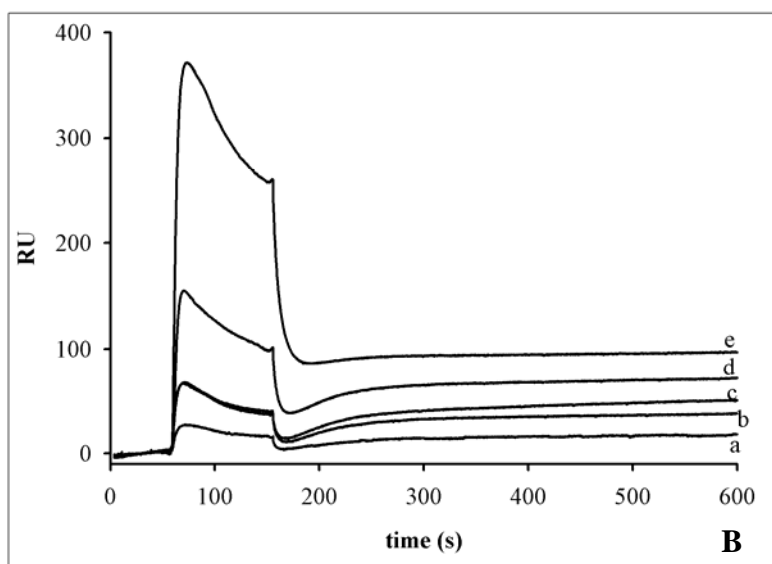
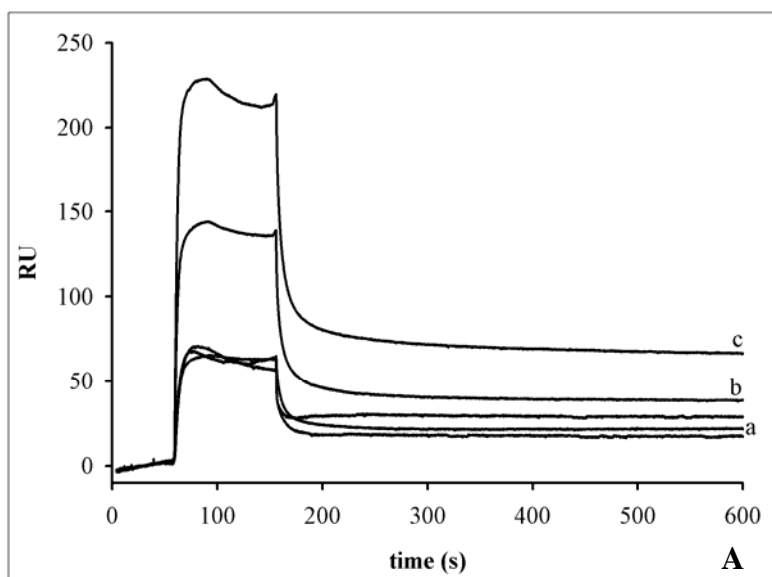


Figure 1

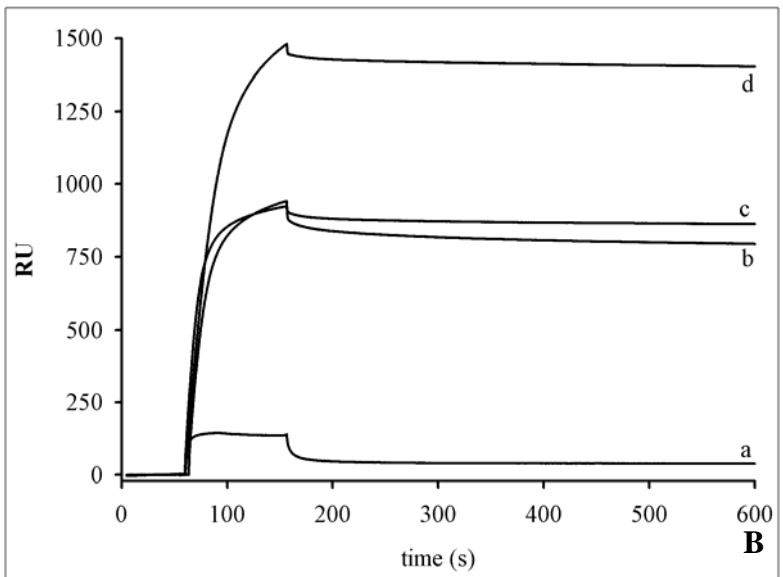
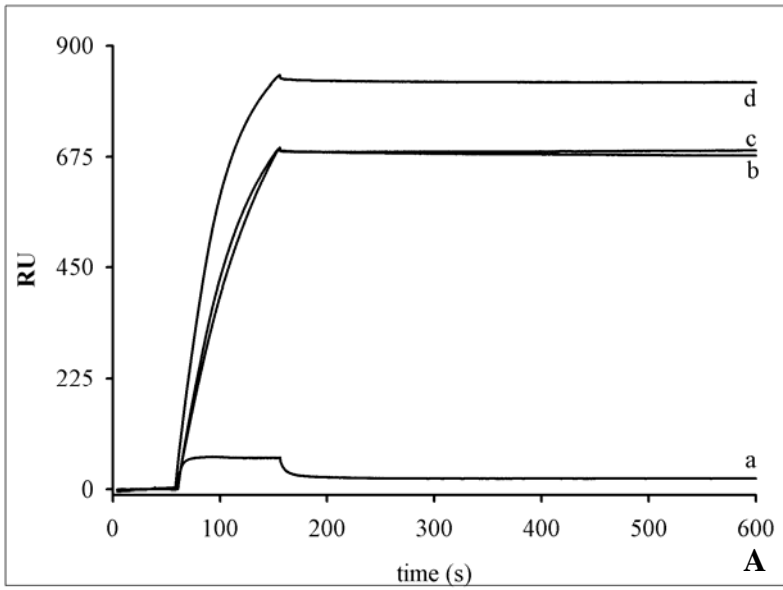


Figure 2

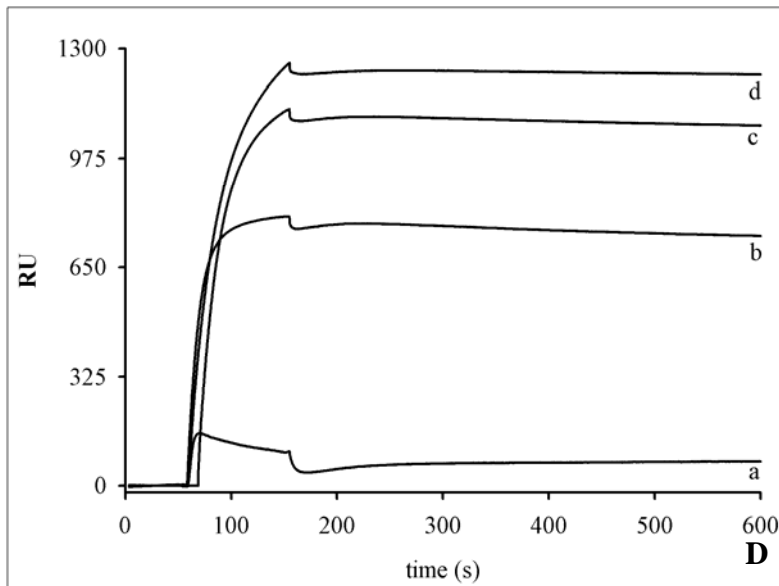
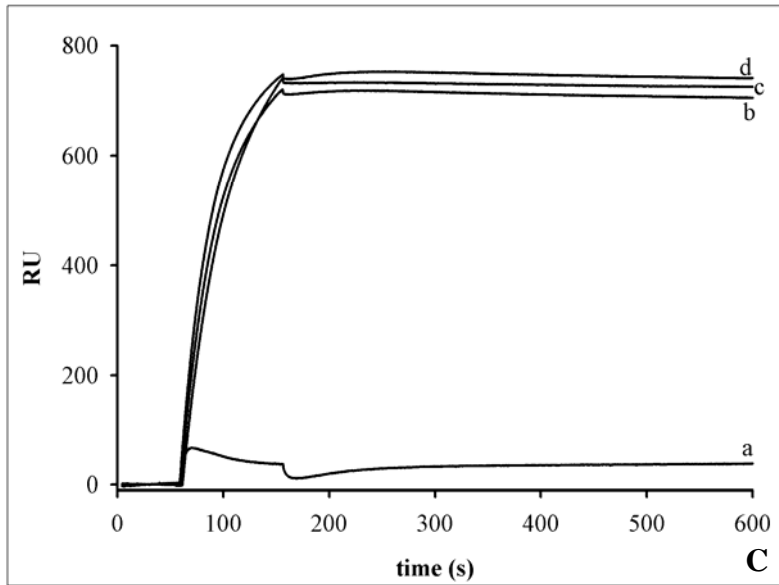


Figure 2

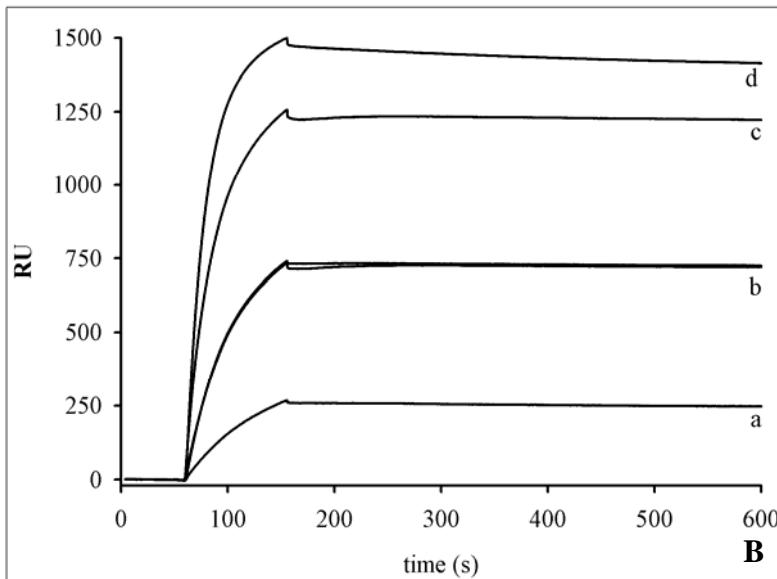
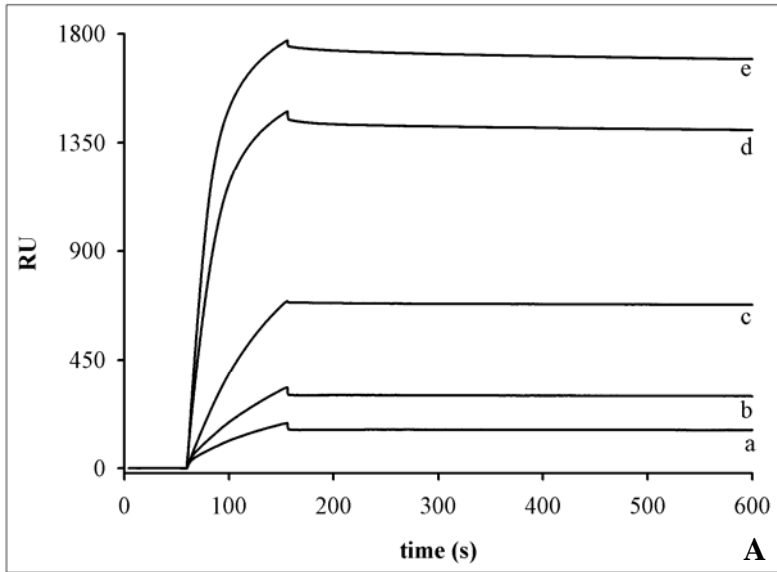


Figure 3

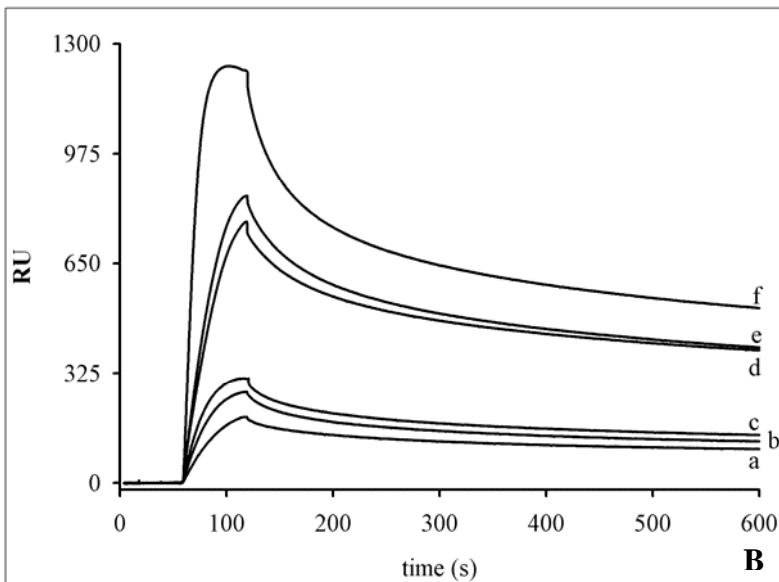
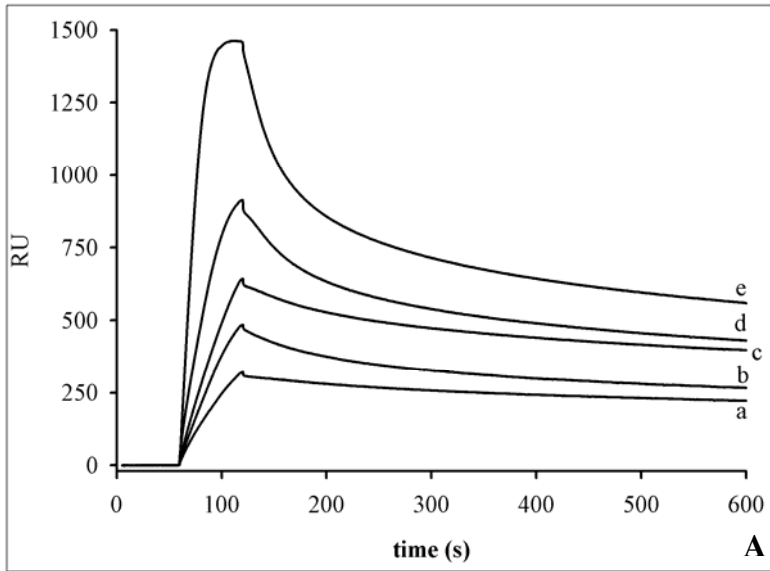


Figure 4

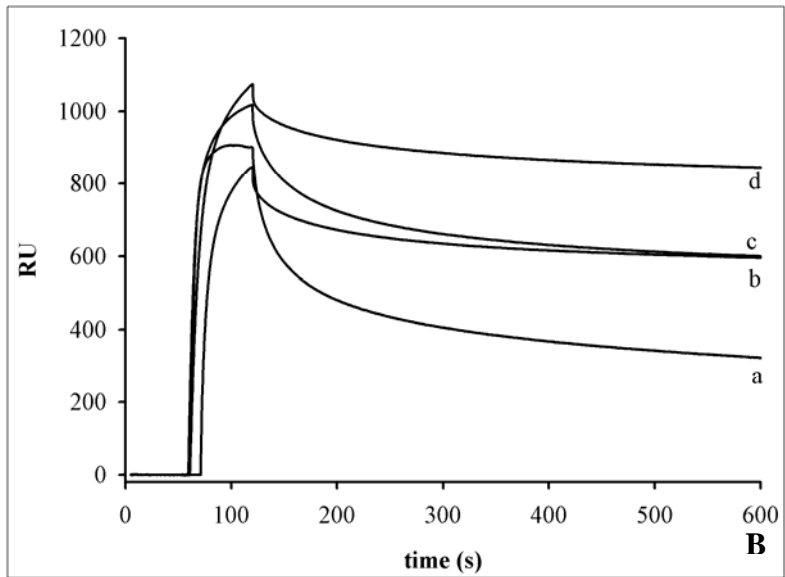
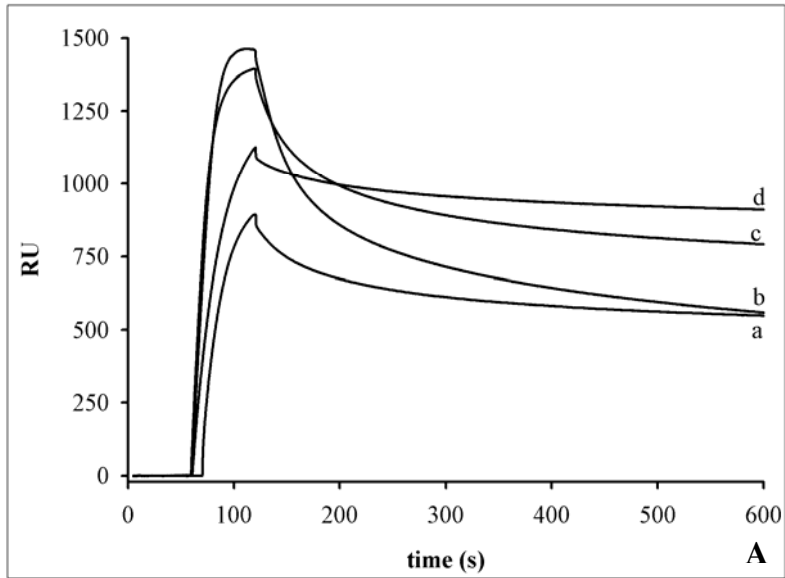


Figure 5

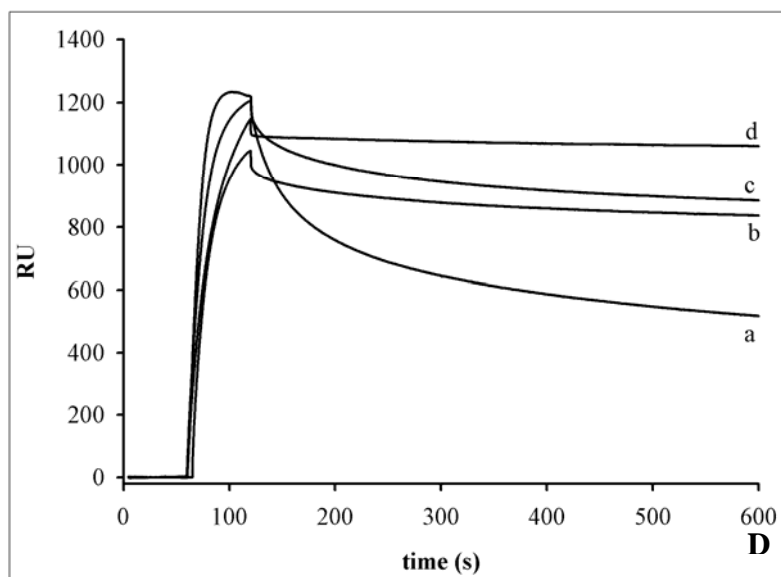
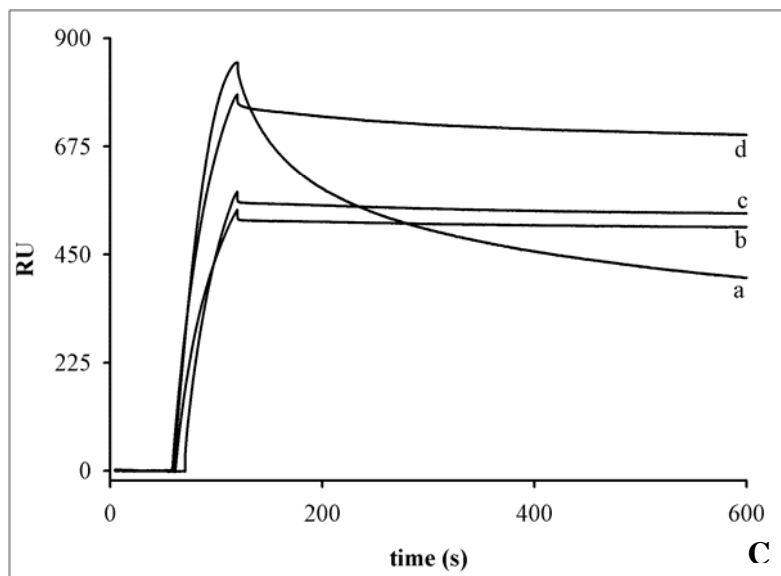


Figure 5

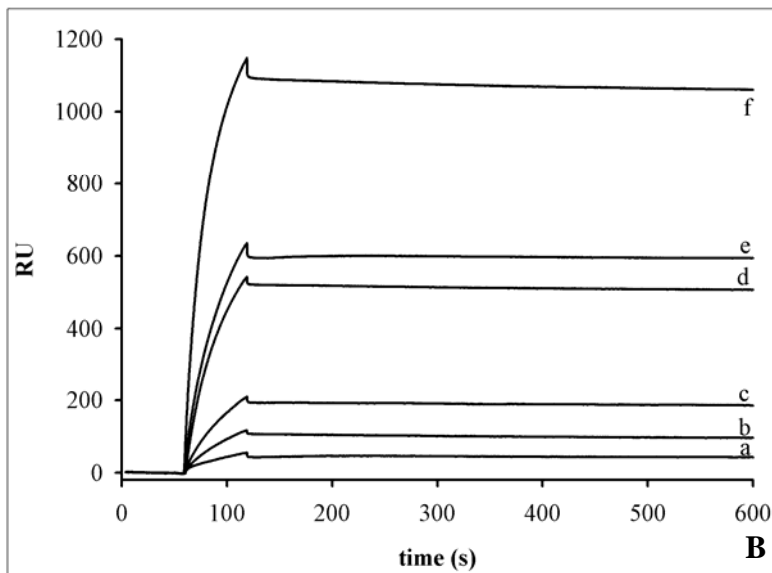
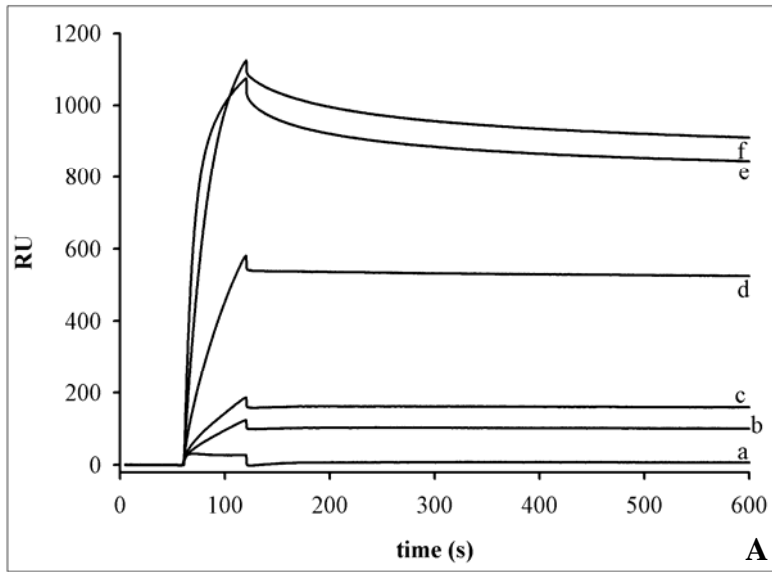


Figure 6

Chapter VI

FINAL CONCLUSIONS

With an estimated 39.5 (34.1-47.1) million individuals infected HIV-1 worldwide, there is an urgent need to identify new anti-viral approaches and develop neutralizing vaccines to combat this virus. The HIV-1 envelope glycoprotein complex is an attractive therapeutic target because it mediates the viral entry. Inhibitors that target these proteins act at the viral entry level, thus preventing infection. Despite the substantial scientific effort on the HIV-1 entry mechanism investigation and the huge progress that has been made in the last years, several aspects of the molecular mechanism remain unclear. Additionally, structural and functional studies of the envelope proteins have led to the development of viral entry inhibitors, but no complete clarification of the structure adopted by the proteins during the entry process exist. All these uncertainties limit the improvement of existent antivirals and also the development of new and more efficient ones, and ultimately the development of a vaccine.

The studies presented in this work were essentially biophysical, particularly fluorescence spectroscopy studies, in the characterization of the biomembranes role on a number of HIV-1 gp41 related processes. These studies are also a demonstration of the potential of biophysical applications to this kind of studies. Membrane model systems were used in this work to obtain a quantitative basis for the studies, controlling the variables in the experiments, essential in the studies performed, while maintaining the main properties of the biomembranes. The questions studied here are still object of an open debate, namely, the biomembranes role on the mode of action of the HIV-1 fusion inhibitors T20 and T-1249, the importance of biomembranes for the MAbs 2F5 and 4E10 neutralizing action, and the role of the gp41 MPR on the membranes fusion

process in the viral entry. To understand the interactions between viral peptides in the entry process, as the precise mechanism of viral inhibitors action, is essential to the improvement of the existing antiviral strategies and to the development of new ones with a more effective action.

T20, a HIV-1 fusion inhibitor, was the first of a new class, the entry inhibitors, to be approved for clinical use. Despite its proven clinical efficacy and being already in clinical use, its mode of inhibition is not yet clearly understood. The most accepted mechanism of action is the one proposed to C-peptides in general, which involve the binding to the NHR region blocking the 6HB structure formation. In this study, a theoretical analysis of the hydrophobicity and interface affinity of T20 amino acids sequence clearly suggests that it may interact with biological membranes, which was confirmed experimentally. The results obtained allow to propose an alternative or additional model for the T20 action at the molecular level. T20 attaches to membranes in an interfacial position reaching local high concentrations. When the virus approaches the cell surface, its outer membrane will not compete for T20 uptake due to its high content in Chol. Therefore, the cell membrane can function as a reservoir of T20, increasing local concentration at the fusion site. However, local concentration of aqueous T20 is kept high to allow interaction with the NHR region in the aqueous solution. Moreover, high local concentration at the cell membrane surface enable direct contact of the peptide with gp41 C-terminal region, when T20 homologous sequence comes in contact with the lipidic matrix to form the fusion pore. The possible binding of T20 to its gp41 homologous sequence in a membrane context, inhibiting pore formation, has been reported by other authors (Muñoz-Barroso et al., 1998; Kliger et al., 2001). T20 interactions with lipid bilayers was also reported in recent studies as having importance on its membrane fusion inhibitory activity (Liu et al., 2007b).

In fact the binding of T20 to the NHR region to create a stable 6HB structure has never been demonstrated, and some recent studies re-open this question (Liu et al., 2005; Liu et al., 2007b). They showed that, unlike C34, T20 cannot interact with NHR region derived peptides to form a stable 6HB. Thus, although T20 can bind to the gp41 NHR, this binding may not be strong enough to justify its strong inhibitory activity. It was suggested that T20 can have multiple sites of action in gp41 and gp120, and its inhibitory activity may be a combinatory effect of different action mechanisms (Liu et al., 2005). T20 can exert its effect by interacting with gp41 NHR region, inhibiting the

6HB formation. Additionally, T20 can inhibit viral fusion by interfering with the FP (Mobley et al., 2001). T20 can interact with the gp41 C-terminal region, acting at a later step of membrane fusion to prevent fusion pore formation, as also proposed by other authors (Muñoz-Barroso et al., 1998; Kligler et al., 2001). The coreceptor binding site on gp120 may be another target site for T20, blocking the interaction with coreceptors. These findings are in agreement with other studies that showed that T20 can bind to CXCR4 (Xu et al., 2000) and/or can interact with the gp120 coreceptor binding site (Yuan et al., 2004; Alam et al., 2004). All of these interactions can cause inhibition of viral fusion by T20.

Gene therapy based approaches are being developed to achieve an alternative administration of these inhibitory peptides. It was shown that membrane-anchored T20, expressed on target cells surface, inhibit viral replication at the level of HIV-1 entry (Hildinger et al., 2001). This expression at the target cells surface leads to high local concentration of the peptide at the action site. Other study has shown that liposome-reconstituted trimeric gp41 fragments, containing C-terminal gp41 regions that include T20 sequence, also have HIV-1 inhibitory activity (Lenz et al., 2005). Melikyan et al. compared the mechanism of action of membrane-anchored peptides expressed by target cells with the ones coexpressed with the envelope glycoprotein on effector cells. While peptides at the target cell surface block inhibition by the binding to the NHR and prevent 6HB formation, peptides expressed by effector cells bind to a new found intermediate, between the prehairpin and the 6HB, preventing pore formation (Melikyan et al., 2006).

Based on the knowledge on T20 properties, other C-peptides have been designed in order to obtain inhibitors with improved efficiency, including against the viruses that are resistant to T20 (Dwyer et al., 2007; Deng et al., 2007).

T-1249, a second generation fusion inhibitor, is more potent than T20 and also retains activity against most T20-resistant HIV-1 strains. Although its mechanism of action is not well known, it is believed that T-1249 acts like most C-peptides. Its propensity to interact with biomembranes was studied. At variance with T20, T-1249 adsorbs to raft like platforms in lipid membranes. It was suggested that T-1249 ability to bind both to the target cell and virus membranes may play an important role in T-1249 mode of action and provide a peptide reservoir at the site of action. The differences relative to T20 in membrane interaction properties, help to explain its improved activity.

In spite of the promising results, T-1249 clinical development was put on indefinite hold. The decision was made not because safety, efficacy and tolerability reasons, but because the current formulation of T-1249 would not be suitable for use in large-scale clinical trials (Martín-Carbonero, 2004).

SARS-CoV is the viral agent responsible for SARS. Identified as a novel CoV, there is no specific treatment for this disease. Due to the need to identify antiviral agents with efficacy against this virus, several drugs already approved and in clinical use were tested. A structural analysis of the SARS-CoV glycoprotein S2 showed a number of similarities with the HIV-1 gp41, like the presence of a NHR, a CHR and a MPR rich in aromatic amino acid residues (Gallaher and Garry, <http://www.virology.net/Articles/sars/s2model.html>). At the CHR there is a sequence, ELDKY, very similar to the HIV-1 gp41 sequence ELDKW. In HIV-1 the peptide ELDKWA is a neutralization epitope recognized by the MAb 2F5. Based on a possible cross-reactivity with the ELDKY region, this MAb can have some neutralizing activity against SARS-CoV (Gallaher and Garry, <http://www.virology.net/Articles/sars/s2model.html>). However, to the best of my knowledge, this possibility was never tested. The HIV-1 gp41 ELDKWA motif is also present on T20. It was proposed that T20 may have some activity against SARS-CoV (Gallaher and Garry, <http://www.virology.net/Articles/sars/s2model.html>). As in HIV-1, SARS-CoV HR regions form a 6HB structure that brings the viral and cellular membranes into close proximity, leading to membrane fusion. Synthetic peptides derived from the CHR were able to inhibit viral infection by interfering with the 6HB formation (Bosch et al., 2004; Liu et al., 2004; Zhu et al., 2004). Based on the most commonly accepted mechanism of action, T20 can bind to the NHR region blocking 6HB formation. The study presented here focus on the interaction of T20 and T-1249 with SARS-CoV S2 protein NHR and CHR derived peptides. It was shown that there is interaction between T20 and a SARS-CoV S2 protein NHR derived peptide, but this interaction could be too weak to inhibit infection. On the other hand and based on the recent proposals for T20 action, it could be speculated that it can inhibit SARS-CoV targeting different regions, as it targets gp41 and gp120 on HIV-1. However, Yamamoto et al. that performed a study to identify anti-SARS drugs available for clinical use, including T20 and found no viral inhibition with this peptide (Yamamoto et al., 2004). Nevertheless, this result is questionable since the results obtained for other drugs tested

are contradictory with the results obtained by other similar studies. While Yamamoto et al. reported the inhibition of SARS-CoV replication by nelfinavir, a widely used HIV-1 protease inhibitor, other study by Tan et al. showed that this inhibition does not occur (Tan et al., 2004). In the same way, Zhang and Yap (Zhang and Yap, 2004) proposed that two others HIV-1 PIs, lopinavir and ritonavir, could inhibit SARS-CoV, at variance with the results reported by reported by Yamamoto et al..

The results showed in chapter IV confirm that the HIV-1 gp41 MPR has a key role in the viral fusion process. It has been shown that this region has the capacity to interact with and destabilize membranes, in a similar way to the FP action in the target cell membrane. Due to the Chol-rich viral membrane proximity, the MPR effect could be exerted at this level. Besides, this region contains at its C-terminal a small sequence defined as a Chol binding domain. The influence of Chol in the membrane interactions of MPR-derived peptides was investigated. In this study the peptides used correspond to the whole MPR, to the Chol binding sequence and to the peptide corresponding to the MPR without the Chol binding sequence. The results obtained are not in agreement with a direct interaction of the small sequence with Chol. However, one needs to stress that in the studies where the specific interaction was proposed, the small Chol binding sequence interactions with Chol were tested in extreme conditions (Vincent et al., 2002; Epand et al., 2003; Epand et al., 2005; Epand et al., 2006). The results presented in this study show that the Chol binding sequence does not interact with gel and liquid-ordered membranes (i.e. Chol-rich membranes). It is the remaining part of the complete MPR sequence that confers the main membrane-interaction properties. Both this sequence and the complete MPR are insensitive to the lipid phase, which may be the key for the MPR biological function. By interacting equally well with the HIV-1 envelope and target cell membrane, the MPR promotes their contact, viral fusion evolving from the physical contact of these bilayers. MPR ability to bind to viral and host cell membranes simultaneously leads to the merging of the two membranes (fusion). This is in agreement with findings that show that the MPR is essential for fusion. Upon virus-cell membrane contact, the two bilayers will perturb each other and the lamellar phases will be locally disrupted. In this step, the Chol binding domain may come in contact with Chol released by the perturbed viral membrane and sequester it. A Chol-depleted membrane is easier to merge with the more fluid cell membrane, thus facilitating the fusion process. Therefore, the gp41 ectodomain MPR may have a very specific function in viral fusion through the concerted and combined action of Chol-binding and non-

Chol binding domains (i.e. domains corresponding to the Chol binding sequence and the peptide corresponding to the MPR without the Chol binding sequence, respectively, in the fusion process). However, one needs to recall that membrane interactions of peptides can be enhanced by a concerted action of several membrane-binding motifs or by the particular disposition of key residues in the context of long peptides or even in the context of the whole protein. In this way, one cannot exclude a role for the small Chol binding sequence in the interaction of the MPR with membranes.

2F5 and 4E10 are two potent and broadly neutralizing MAbs against HIV-1, whose epitopes are localized in the gp41 MPR. It was proposed separately, based on crystallography studies, its interaction with membranes through a hydrophobic surface present on the CDR H3 (Ofek et al., 2004; Cardoso et al., 2005). In this study both MAbs membrane interactions were studied by the use of target cell and viral membranes models. In the initial study here presented, no relevant membrane interactions were detected for 2F5. However, studies by other authors suggest that 2F5 binds to membranes of selected compositions, but the simultaneous study of 4E10 showed that, in comparative terms, 2F5 binding is weak (Haynes et al., 2005; Sánchez-Martínez et al., 2006 a,b; Brown et al., 2007). In the second study presented here, 2F5 and 4E10 membrane interactions were studied in the presence and absence of a peptide that contains both MAbs epitope. Both 2F5 and 4E10 have the capacity to bind to both target cell and viral model membranes, being 2F5 interactions very weak, especially when compared to 4E10. Both MAbs bind irreversibly to membranes when its epitope is present, showing a high degree of recognition of the epitope presented in membranes. This capacity of interactions with biomembranes can be a MAbs adaptation to bind to an epitope that is so close to the membrane and/or, there exist an epitope optimal conformation that is membrane-dependent.

As a whole this thesis contributed to the state-of-the-art in the understanding of lipid membranes role in viral inhibition during pre-infective stages by showing that:

- 1) Fusion inhibitor peptides T20 and T-1249 have the ability to interact with membranes and this might have a role on their action mechanism
- 2) Membrane lipid phase modulate the fusion inhibitors membrane interactions and this might be related with their differential efficiency
- 3) Both MAbs 2F5 and 4E10 have the capacity to interact with membranes in the absence and presence of their epitopes and membrane might be implicated on these MAbs mode of action

- 4) The membrane catalyst principle (Castanho and Fernandes, 2006) can be applied to the mechanism of action of fusion inhibitor peptides and MAbs, although peptides don't have a specific membrane receptor
- 5) Protein-lipid interaction in HIV fusion is not limited to the action of the FP

Chapter VII

ANNEX I

An insight on the leading HIV entry inhibitors

An Insight on the Leading HIV Entry Inhibitors

Ana Salomé Veiga¹, Nuno C. Santos² and Miguel A. R. B. Castanho*¹

¹*Centro de Química e Bioquímica, Faculdade de Ciências da Universidade de Lisboa, Campo Grande Ed. C8, 1749-016 Lisboa, Portugal;* ²*Instituto de Biopatologia Química / Faculdade de Medicina de Lisboa and Unidade de Biopatologia Vascular / Instituto de Medicina Molecular, Av. Prof. Egas Moniz, 1649-028 Lisboa, Portugal*

Received: July 03, 2005; Accepted: August 17, 2005; Revised: September 14, 2005

Abstract: The main strategies nowadays to fight AIDS rely on chemical therapy to inhibit the reverse transcriptase or protease of HIV. However, a synthetic 36 amino-acids peptide that blocks the entry of the virus in the target cells (enfuvirtide) has recently reached approval for clinical application. This molecule may probably be just the leader of a new generation of drugs that is about to emerge to interrupt the first step in the HIV life cycle, i.e. preventing the virus from actually entering cells. This paper reviews the enfuvirtide path from clinical trials to the attempts to detail its molecular-level mode of action. It is commonly accepted that this peptide would block the fusion between viral and cell plasma membrane through binding to the N-terminal heptad repeat (NHR) region of the viral protein gp41. However, there has been growing evidence that this model of action may be unrealistic, the action of enfuvirtide being more complex and diverse than initially thought. Membrane-assisted local concentration increase and interference with gp120/co-receptor docking may also contribute for the inhibitory action of the peptide. Selected HIV-entry inhibitors on clinical trials are presented to characterize the future drugs in the market in this class.

Keywords: Entry, attachment, fusion, binding, entrance inhibitor, HIV, AIDS, virus, chemokine, peptide, receptor, co-receptor, synergism, clinical trial, enfuvirtide.

1. INTRODUCTION

Combination therapy with reverse transcriptase and protease inhibitors is the most common current treatment of HIV-1 infection [1,2]. Despite the success of this therapy, namely reducing morbidity and mortality of HIV-1 infected patients [3-6], it has adverse effects and drug resistant HIV-1 strains emerged [7-11]. A new class of antiviral agents is in development, the entry inhibitors. These molecules target the first step in the HIV-1 replication cycle, the viral entry [12-15]. Unlike reverse transcriptase and protease inhibitors, which target post-entry steps, entry or fusion inhibitors act extracellularly preventing viral entry into target cells. The most advanced and already approved by the Food and Drug Administration fusion inhibitor is enfuvirtide (T20; DP-178) from Trimeris/Roche [16].

HIV-1 Entry

The HIV-1 envelope glycoproteins complex is expressed on the surface of the viral membrane as an oligomeric protein (trimer) and mediates the viral entry. The complex is composed of two subunits noncovalently associated: gp120, the surface glycoprotein, which interacts with cellular receptors, and gp41, the transmembrane glycoprotein, responsible for fusion of the viral and cellular membranes [e.g. 12,17,18]. HIV-1 entry into target cells is a multi-step process that is initiated by gp120 binding to the CD4 receptor, present in the target cells surface. This contact

induces a conformational change in gp120 enabling it to bind to a cellular co-receptor, usually CCR5 or CXCR4. gp120 binding to CD4 and co-receptor induces conformational changes in gp41 exposing the N-terminal fusion peptide and allowing its insertion into target cell membrane, thereby connecting both membranes. Subsequent changes within the gp41 ectodomain involve the interaction of two heptad repeat sequences (HR1, next the fusion peptide and HR2, preceding the transmembrane domain) and a six-helix bundle structure (also called hairpin structure) is formed. The hairpin formation brings the viral and cell membrane into closed proximity, allowing fusion of the membranes and then entry of the virus [12,13,17-19].

Each of the main steps in the HIV-1 entry process can be a target for entry inhibitors. The ones currently under development fall into three categories: gp120-CD4 binding inhibitors, gp120-co-receptors binding inhibitors, and membrane fusion inhibitors, which interfere with gp41 conformational changes [2,14,16,20]. Fusion inhibitors are the leading compounds, one of them, enfuvirtide, being already approved for clinical applications.

2. ENFUVIRTIDE CLINICAL TRIALS

The publication in 1998 of the results of the TRI-001 clinical trial [21] is considered as the proof-of-concept that the entrance of the virus in the cell of the host can be blocked *in vivo* by enfuvirtide. This study evaluated the use of enfuvirtide subcutaneous infusion, as monotherapy, during 14 days. The TRI-001 allowed concluding that the administration, during a reduced period, is safe and induces a significant (1.14 log₁₀) viral charge decrease in the group that received a 90 mg deliverable dose of enfuvirtide (100 mg nominal dose) twice daily.

*Address correspondence to this author at the Centro de Química e Bioquímica, Faculdade de Ciências, Universidade de Lisboa, Campo Grande C8, 1749-016 Lisboa, Portugal; Tel: + 351 21 7500931; Fax: +351 21 7500088; E-mail: castanho@fc.ul.pt

The TRI-003 phase II trial [22], conducted during 28 days with 78 patients, lead to the adoption of subcutaneous injection as the preferential route of administration of enfuvirtide, and evaluated the pharmacokinetics of this and other forms of administration. This study results showed that subcutaneous injection presents significant advantages when compared with subcutaneous infusion, in terms of administration simplicity, tolerability, plasma pharmacokinetics and antiviral response predictability.

The phase II multicenter trial T20-205 [23] tested the administration of 45 mg of enfuvirtide twice daily by subcutaneous injection, in association with conventional optimized therapy, to 71 patients, during 48 weeks, for tests of genotype resistance. 56% of the patients who had kept the treatment presented significant improvements, with a decrease for less than 400 copies of HIV-1 RNA/mL.

The T20-206 assay had the purpose of comparing different enfuvirtide therapeutic doses in addition to conventional antiretroviral therapies [24]. The results of this random study indicated the dose of 90 mg twice daily as the one that, combined with other antiretrovirals, reduces the viral load more efficiently.

The T20-208 phase II trial [25] had the purpose of studying the pharmacokinetics and tolerability of the administration of enfuvirtide in different doses and in formulations of different strengths. This study enabled the optimization of the formulation and dosage to be used in the subsequent phase III trials: twice daily administration of 90 mg enfuvirtide in a single injection of a high-strength formulation in carbonate (instead of the administration of the same 90 mg in two 45 mg injections of a lower-strength formulation, used in most of the previous clinical trials).

A study carried out with 12 HIV-infected patients previously enrolled on the phase II T20-205, T20-206 or T20-208 trials evaluated the pharmacokinetics and relative bioavailability of enfuvirtide following subcutaneous injection at three separate anatomical sites: abdomen, thigh and arm [26]. The relative bioavailabilities of enfuvirtide, taking abdomen as a reference site, were 101% for thigh and 117% for arm. Independently of the slightly higher bioavailability observed for the arm injection, and of some differences on the injection site reactions, the authors considered that the comparability among the three injection sites allows to the infected patients the freedom to choose (and to rotate, if necessary) among these three possible sites of injection.

The publication in 2001 of a study involving the follow-up of 39 patients during 3 years demonstrated that the primary resistance to enfuvirtide treatment is a rare event [27]. However, the authors warned that the emergence of future variants of the virus resistant to this therapy cannot be ruled out. More recently, another study [28] also indicated that primary genotypic enfuvirtide resistance seems to be rare, regardless of subtype or prior antiretroviral therapy. The emergence of enfuvirtide resistant virus in patients receiving enfuvirtide monotherapy was identified by the first time by Wei *et al.* [29], in patients enrolled in the TRI-001 clinical trial [21], receiving an antiretroviral dosage

considerably lower than the later approved for clinical use, during only 14 days.

The enfuvirtide absorption and disposition pharmacokinetics after both intravenous and subcutaneous administration were evaluated in the controlled clinical pharmacokinetic study T20-501 [30]. The same work evaluated the dose proportionality of enfuvirtide pharmacokinetic parameters at higher subcutaneous doses. The 12 patients received randomly four different single doses of enfuvirtide (90 mg intravenous and 45, 90, and 180 mg subcutaneous) separated by a one week washout. Based on the results, a structural pharmacokinetic model was developed, allowing the description of the absorption and disposition kinetics of enfuvirtide plasma concentration after subcutaneous administration. The study also indicated that enfuvirtide is almost completely absorbed from subcutaneous depot, and that the pharmacokinetic parameters were linear up to a dose of 180 mg.

Based on the findings of the previous phases I and II clinical trials, it were the two TORO (T-20 vs. Optimized Regimen Only) phase III clinical trials that set the conditions for the approval of enfuvirtide for clinical use. The TORO 1 trial [31] was conducted with patients from North-America and Brazil, while TORO 2 [32] enrolled patients from Europe and Australia. Both TORO studies compared the efficacy and safety of 24 weeks of combined treatment with enfuvirtide (90 mg twice daily) and an optimized background antiretroviral regimen with the efficacy and safety of the optimized background regimen alone. The patients (491 in TORO 1 and 504 in TORO 2) had at least six months of previous treatment with agents in three classes of antiretroviral drugs, resistance to drugs in these classes, or both, and at least 5000 viral copies/mL. At the end of the 24 weeks, the groups taking enfuvirtide had a least-squares mean decrease from baseline in the viral load of 1.696 and 1.429 \log_{10} copies/mL in TORO 1 and TORO 2, respectively, compared with a decrease of 0.764 and 0.648 \log_{10} copies/mL in the TORO 1 and TORO 2 control groups ($P < 0.001$ for both pairs). The mean increases in CD4⁺ cell counts were 76 and 65.5 mm^{-3} (TORO 1 and TORO 2 enfuvirtide groups, respectively), compared with 32 and 38.0 mm^{-3} for their control groups ($P < 0.001$ for both pairs). These studies demonstrated the significance of the antiretroviral and immunologic benefits of the addition of enfuvirtide to optimized antiretroviral regimens in patients with HIV-1 infections resistant to previously established therapies, and in patients who had previously received multiple antiretroviral drugs.

The most common adverse events associated with enfuvirtide administration are injection-site reactions. The TORO studies reported injection-site reactions in 98% of the patients, including pain, discomfort, erythema, induration, nodules, cysts, pruritus and ecchymosis associated with the injection-site [31,32]. Despite this extremely high incidence, only 4.4% of the patients abandoned the treatment due to injection-site reactions [e.g. 33]. The biopsies carried out in a study of injection-site reactions in 7 patients receiving enfuvirtide revealed inflammatory responses consistent with a localized hypersensitivity reaction, regardless of the type of clinical lesion and even in its absence [34].

The incidences of most of the other adverse events reported in the TORO study for the group of patients treated with enfuvirtide combined with background antiviral therapy were not significantly different from those observed for the control group, treated with the background antiretroviral therapy only [31,32]. However, the incidences of pneumonia (mainly bacterial) and lymphadenopathy were significantly higher in the group using enfuvirtide, as indicated by the combined analysis of the TORO studies after 48 weeks of treatment [e.g. 33]. The statically significant increase on pneumonia incidence in the group of patients taking enfuvirtide combined with optimized background therapy may be related with enfuvirtide administration, or it can also result of an unexplained abnormally low incidence of pneumonia in the control group. Studies carried out with HIV-infected patients on highly active antiretroviral therapy (HAART) indicate pneumonia incidences considerably higher than those reported for the control groups of the TORO studies, and comparable with the observed for the groups taking enfuvirtide combined with optimized background therapy [e.g., 35,36]. The results of the TORO studies, at the 24th week of the treatment, also indicated a higher incidence of some laboratory parameters outside the upper limit of normal in the group taking enfuvirtide; namely, eosinophilia, increased triglycerides, creatine phosphokinase, amylase, lipase, alanine aminotransferase, aspartate aminotransferase and γ -glutamyl transferase levels, and decreased hemoglobin concentration. However, at the 48th week of treatment the incidences of these laboratory abnormalities were similar in the enfuvirtide and control groups, or even lower in the enfuvirtide group.

The safety, tolerability, antiretroviral activity, dosage and pharmacokinetics of the pediatric use of enfuvirtide were evaluated in some phase I/II clinical trials [37-40], which will not be described here.

3. RECENT HIGHLIGHTS IN THE MOLECULAR-LEVEL ACTION OF THE FUSION INHIBITORS ENFUVIRTIDE AND T-1249: A PLETHORA OF SITES OF ACTION

Enfuvirtide is a synthetic 36 amino-acids peptide derived from a C-terminal sequence of HIV-1 gp41 [41,42]. There are several proposals for the enfuvirtide inhibitory action mechanism involving target sites in gp41 and gp120. In the most accepted mechanism of action model, enfuvirtide binds to the HR1 region of gp41 preventing the formation of the six-helix bundle structure and thereby fusion is blocked [16,41,43-45]. Viral resistance to enfuvirtide is associated with mutations in the GIV sequence of the HR1 region [45]. However, enfuvirtide lacks some amino-terminal residues present in other gp41 HR2 sequence based peptides (C-peptides) thought as essential for the binding to the HR1 region and HIV-1 entry inhibition [41,46]. Also it was suggested that enfuvirtide binding affinity to the HR1 region cannot justify its strong inhibitory activity [47], and most recently Liu *et al.* showed that enfuvirtide cannot interact with HR1 region derived peptides to form a stable six-helix bundle [48]. The existence of a second binding site for enfuvirtide on gp41 was proposed by Muñoz-Barroso *et al.* [49], involving the contact site of gp41 oligomers cluster to form a fusion pore, which is required for the occurrence of

the complete fusion process [18,50]. Kliger *et al.* showed that enfuvirtide can bind membranes and oligomerize, but unlike in aqueous solution, it cannot interact with the HR1 region in the membrane environment [51]. Thus, in agreement with these ideas, there are two enfuvirtide binding sites in gp41, contributing to fusion inhibition. By interacting with the HR1 region in aqueous solution enfuvirtide inhibits the formation of the six-helix bundle structure and by interacting with the gp41 C-terminal region in the membrane environment fusion pore formation is prevented [47,49,51]. Other studies suggest that membranes play a role in enfuvirtide action, namely in increasing concentration in its site of action [52,53]. A theoretical analysis of the hydrophobicity and interface affinity of enfuvirtide amino acids sequence clearly suggests that it may interact with biological membranes, which is confirmed experimentally. Enfuvirtide interaction with membranes has peculiar features [53]: i) incorporation into neutral liquid-crystal lipid membranes is extensive ($K_p = (1.6 \pm 0.1) \times 10^3$; $G = -6.6 \text{ kcal mol}^{-1}$); ii) cholesterol and/or physiological concentrations of negatively charged lipids modulate the incorporation in lipid membranes; iii) a shallow position in the lipid membrane makes it readily available for interaction with gp41; and iv) it has similar secondary structure (random coil) whether in aqueous or lipid environment, therefore no conformational energetic barrier can prevent enfuvirtide from being active both in aqueous solution and lipid membranes. An alternative or additional model for the enfuvirtide action at the molecular level was proposed (Fig. 1). It was also proposed that enfuvirtide may bind to the gp41 fusion peptide in aqueous medium preventing its insertion into the target cell membrane. Thus, concomitant to the HR1 binding, association with the fusion peptide may contribute to block viral entry [54,55]. It appears that sensitivity to enfuvirtide can be also modulated by co-receptor specificity, determined by the V3 loop region of gp120. X4 viruses, that utilize CXCR4 co-receptor for entry, are much more sensitive to enfuvirtide than R5 viruses, which utilize CCR5 [56]. Reeves *et al.* showed that co-receptor binding affinity and co-receptor expression levels are related with enfuvirtide sensitivity [57]. More recently, it was proposed that enfuvirtide can interact with the gp120 co-receptor binding site, blocking gp120 binding to the co-receptor and thus inhibiting viral infection [48,58,59]. This interaction occurs in a CD4-induced manner [58,59] with the gp120 of X4 viruses, which could explain the increased sensitivity of these viruses to enfuvirtide [58]. In this way gp120 can be another target site contributing to enfuvirtide inhibitory activity. However, different studies carried out with isolates from different clinical trials have not identified significant differences in enfuvirtide susceptibility for patients harbouring CCR5, CXCR4 or dual tropic viruses, indicating that viral tropism has no clinically relevant effect on the enfuvirtide therapy efficiency [e.g. 60,61]. New studies are needed to further clarify this matter of debate.

T-1249, a second generation fusion inhibitor that follows enfuvirtide, is a 39 amino-acids peptide composed of sequences derived from HIV-1, HIV-2 and simian immunodeficiency virus (SIV) [62]. More potent than enfuvirtide, this fusion inhibitor also retains activity against most enfuvirtide-resistant HIV-1 strains [2,19,63,64].

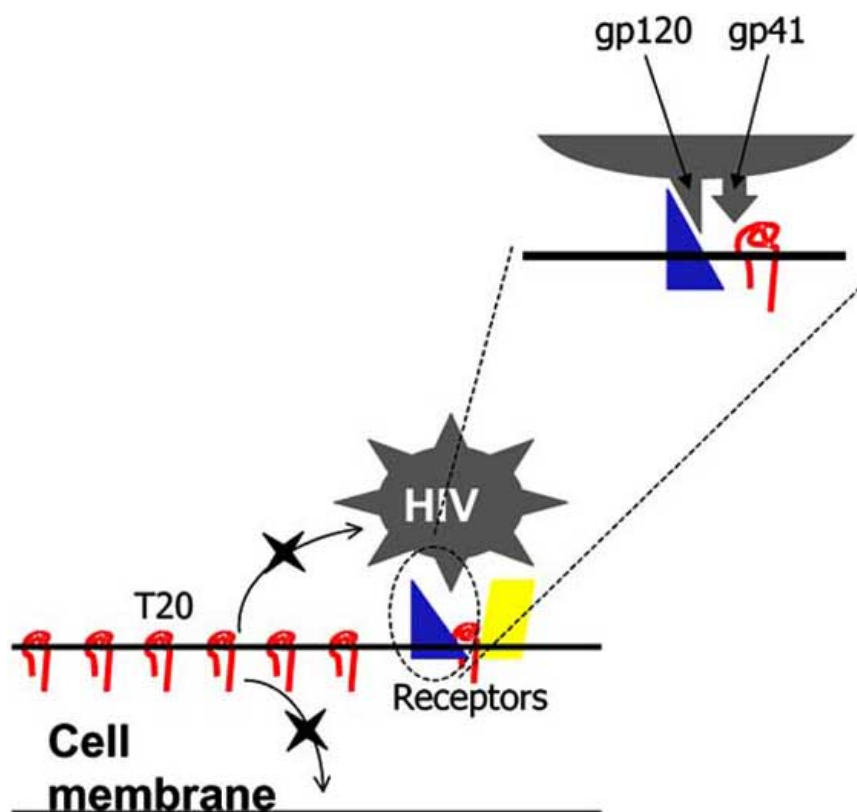


Fig. (1). A model for the enfuvirtide action at the molecular level. Enfuvirtide (T20) attaches to membranes in an interfacial position, reaching high local concentrations. Translocation is prevented by phospholipid charge effects (among others). When the virus approaches the cell surface, its outer membrane will not compete for enfuvirtide uptake due to its higher cholesterol content. Upon binding, gp41 is exposed near the membrane interface, where enfuvirtide is present in high local concentrations (adapted from [53]).

Although its mechanism of action is not well known, it is believed that T-1249 acts like most C-peptides, interacting with HR1 region preventing hairpin structure formation [16,60]. It was suggested that T-1249 ability to bind both the target cell and virus membranes may play an important role in T-1249 mode of action and provide a peptide reservoir at the action site [65]. At variance with enfuvirtide, T-1249 adsorbs to rafts and gel-like platforms in lipid membranes, this difference being one possible explanation for its improved activity.

In spite of the optimistic results *in vitro*, T-1249 clinical trials were put on hold (Table 1).

4. TOWARDS THE FIRST GENERATION OF A NEW CLASS OF DRUGS

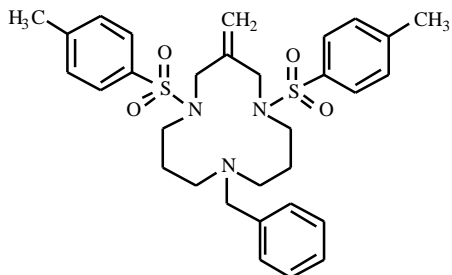
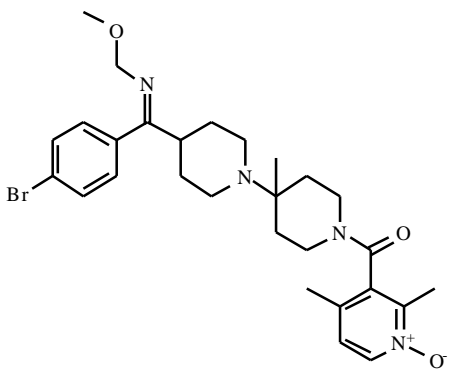
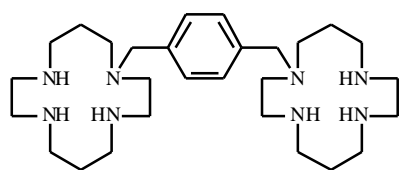
While gp41/gp120-related inhibitors, mainly enfuvirtide, are undoubtedly in the front line of clinical applications of HIV-entry inhibitors, an overview of the recent patents in this field reveals an additional trend for the future. Chemokine receptors are clearly the focus of attention [66-80]. Table 1 lists some of the CCR5 and CXCR4 antagonists currently under clinical trials. Altogether with CD4-targeted strategies and enfuvirtide related peptides, these molecules form a promising pool of candidate drugs to keep the pace in the fight against HIV. A detailed analysis of their action can be found in references 81-83. AMD3100 is a very specific

antagonist for CXCR4 and is a potent inhibitor of X4 HIV-1 replication. AMD070 is an orally bioavailable derivative of AMD3100 as potent as its parent molecule. SCH-C can also be administered orally and preliminary clinical data proved its ability to significantly reduce R5 HIV-1 viral load. Several related molecules allowed equal or better affinity for the CCR5 receptor.

An obvious approach to HIV entry inhibition would be to prevent gp120 to dock CD4 receptors. Soluble CD4 for competitive inhibition of attachment would be the simplest strategy. However, soluble CD4 performs poorly in AIDS patients. CD4-immunoglobulins fusion proteins have better pharmacokinetics, affinity for gp120 and minimal immunogenic effects. PRO542 is CD4-IgG2, a tetrameric CD4-based fusion protein comprising human IgG2 in which the HIV-binding region of CD4 has replaced the Fv portions of both heavy and light chains. In phase I clinical trials, PRO542 showed antiviral activity as well as a favourable safety and pharmacological profile. Enfuvirtide acts synergistically with PRO542 [84].

A more indirect approach is to down-modulate the CD4 receptor. CADA (Table 1) inhibits HIV infection by the specific down-modulation of CD4, probably by means of down-regulation of CD4 expression at the (post)translational level [81]. CADA also exhibits a synergistic action with enfuvirtide, as well as AMD3100.

Table 1. Short Survey of Some Molecules for their Action Preventing the Entry of HIV into Target Cells. Most Information Regarding Clinical Trials Status can be Found at www.clinicaltrials.gov and <http://hiv.net> (Accessed June 2005)

Name	Molecule	Site of action	Company	Clinical trials
T20 = Enfuvirtide	36 amino-acids peptide [53]	gp41, gp120	Roche / Trimeris	As Fuzeon on the market
T-1249	39 amino-acids peptide [65]	gp41 (only?)	Roche / Trimeris	Stopped; Clinical development on hold ¹
CADA		CD4 (down-modulator)	-----	-----
PRO542	CD4-IgG ₂	CD4/gp120 binding	Progenics	Phase II
SCH-C		CCR5 antagonist	Schering-Plough	Stopped ²
SCH-D	SCH-C derivative	CCR5 antagonist	Schering-Plough	Phase II ³
UK427,857	-----	CCR5 antagonist	Pfizer	Phase II ⁴
AMD3100		CXCR4 antagonist	AnorMED	Stopped ⁵
AMD070 = AMD 11070	AMD3100 derivative	CXCR4 antagonist	AnorMED	Phase I/II

1- <http://trimeris.com/pipeline/t-1249.html> (accessed June 2005): «In January 2004, the clinical development of T-1249 was put on hold due to challenges in achieving the desired technical profile of the current formulation. The compound's safety, efficacy and tolerability were no way related to the decision».

2- Heart rhythm disturbance was reported.

3- No serious side effects yet known.

4- No side effects occurred during Phase I.

5- Cardiotoxic.

5. CURRENT & FUTURE DEVELOPMENTS

The synergism among efficient HIV-entry inhibitors is probably the main reason to be optimistic in having powerful

tools to interrupt the HIV life cycle in the first step. Interruption of the entry step in the HIV life cycle may be of comparable importance in the future to reverse transcriptase or protease inhibition. This new front against HIV will

further help controlling AIDS for the sake of the comfort and longevity of the patients.

ACKNOWLEDGMENTS

ASV thanks Fundação para a Ciência e A Tecnologia (Portugal) for grant SFRH/BD/14336/2003. Mr. Hansjörg Möst is acknowledged for his collaboration.

REFERENCES

- [1] De Clercq E. New developments in anti-HIV chemotherapy. *Biochim Biophys Acta* 2002; 1587: 258-75.
- [2] Gulick RM. New antiretroviral drugs. *Clin Microbiol Infect* 2003; 9: 186-93.
- [3] Palella FJ, Delaney KM, Moorman AC, *et al.* Declining morbidity and mortality among patients with advanced human immunodeficiency virus infection. *N Eng J Med* 1998; 338: 853-60.
- [4] Mocroft A, Katlama C, Johnson AM, *et al.* AIDS across Europe, 1994-98: the EuroSIDA study. *Lancet* 2000; 356: 291-6.
- [5] Li Y, McDonald AM, Dore GJ and Kaldor JM. Improving survival following AIDS in Australia, 1991-1996. *AIDS* 2000; 14: 2349-54.
- [6] Louie M and Markowitz M. Goals and milestones during treatment of HIV-1 infection with antiretroviral therapy: a pathogenesis-based perspective. *Antiviral Res* 2002; 55: 15-25.
- [7] Brinkman K, ter Hofstede HJM, Burger DM, Smeitink JAM and Koopmans PP. Adverse effects of reverse transcriptase inhibitors: mitochondrial toxicity as common pathway. *AIDS* 1998; 12: 1735-44.
- [8] Carr A, Samaras K, Thorisdottir A, Kaufmann GR, Chisholm DJ and Cooper DA. Diagnosis, prediction, and natural course of HIV-1 protease-inhibitor-associated lipodystrophy, hyperlipidaemia, and diabetes mellitus: a cohort study. *Lancet* 1999; 353: 2093-9.
- [9] Yerly S, Kaiser L, Race E, Bru J-P, Clavel F and Perrin L. Transmission of antiretroviral-drug-resistant HIV-1 strains. *Lancet* 1999; 354: 729-33.
- [10] Hirsch MS, Conway B, D'Aquila RT, *et al.* Antiretroviral drug resistance testing in adults with HIV infection: implications for clinical management. *JAMA* 1998; 279: 1984-91.
- [11] Carr A. Toxicity of antiretroviral therapy and implications for drug development. *Nature* 2003; 2: 624-34.
- [12] Eckert DM and Kim PS. Mechanisms of viral membrane fusion and its inhibition. *Annu Rev Biochem* 2001; 70: 777-810.
- [13] LaBranche CC, Galasso G, Moore JP, Bolognesi DP, Hirsch MS and Hammer SM. HIV fusion and its inhibition. *Antiviral Res* 2001; 50: 95-115.
- [14] O'Hara BM and Olson WC. HIV entry inhibitors in clinical development. *Curr Opin Pharm* 2002; 2: 523-8.
- [15] Moore JP and Doms RW. The entry of entry inhibitors: a fusion of science and medicine. *Proc Natl Acad Sci USA* 2003; 100: 10598-602.
- [16] Kilby JM and Eron JJ. Novel therapies based on mechanisms of HIV-1 cell entry. *N Engl J Med* 2003; 348: 2228-38.
- [17] Wyatt R and Sodroski J. The HIV-1 envelope glycoproteins: fusogens, antigens, and immunogens. *Science* 1998; 280: 1884-8.
- [18] Chan DC and Kim PS. HIV entry and its inhibition. *Cell* 1998; 93: 681-4.
- [19] Cooley LA and Lewin SR. HIV-1 cell entry and advances in viral entry inhibitor therapy. *J Clin Virol* 2003; 26: 121-32.
- [20] Markovic I and Clouse KA. Recent advances in understanding the molecular mechanisms of HIV-1 entry and fusion: revisiting current targets and considering new options for therapeutic intervention. *Curr HIV Res* 2004 2: 223-34.
- [21] Kilby JM, Hopkins S, Venetta TM, *et al.* Potent suppression of HIV-1 replication in humans by T-20, a peptide inhibitor of gp41-mediated virus entry. *Nat Med* 1998; 4: 1302-7.
- [22] Kilby JM, Lalezari JP, Eron JJ, *et al.* The safety, plasma pharmacokinetics, and antiviral activity of subcutaneous enfuvirtide (T-20), a peptide inhibitor of gp41-mediated virus fusion, in HIV-infected adults. *AIDS Res Hum Retroviruses* 2002; 18: 685-93.
- [23] Lalezari JP, Eron JJ, Carlson M, *et al.* A phase II clinical study of the long-term safety and antiviral activity of enfuvirtide-based antiretroviral therapy. *AIDS* 2003; 17: 691-8.
- [24] Lalezari JP, DeJesus E, Northfelt DW, *et al.* A controlled Phase II trial assessing three doses of enfuvirtide (T-20) in combination with abacavir, amprenavir, ritonavir and efavirenz in non-nucleoside reverse transcriptase inhibitor-naive HIV-infected adults. *Antivir Ther* 2003; 8: 279-87.
- [25] Wheeler DA, Lalezari JP, Kilby JM, *et al.* Safety, tolerability, and plasma pharmacokinetics of high-strength formulations of enfuvirtide (T-20) in treatment-experienced HIV-1-infected patients. *J Clin Virol* 2004; 30: 183-90.
- [26] Lalezari JP, Patel IH, Zhang X, *et al.* Influence of subcutaneous injection site on the steady-state pharmacokinetics of enfuvirtide (T-20) in HIV-1-infected patients. *J Clin Virol* 2003c; 28: 217-22.
- [27] Zöllner B, Feuchat H-H, Schröter M, *et al.* Primary genotypic resistance of HIV-1 to the fusion inhibitor T-20 in long-term infected patients. *AIDS* 2001; 15: 935-6.
- [28] Roman F, Gonzalez D, Lambert C, *et al.* Uncommon mutations at residue positions critical for enfuvirtide (T-20) resistance in enfuvirtide-naive patients infected with subtype B and non-B HIV-1 strains. *J Acquir Immune Defic Syndr* 2003; 33: 134-9.
- [29] Wei X, Decker JM, Liu H, *et al.* Emergence of resistant human immunodeficiency virus type 1 in patients receiving fusion inhibitor (T-20) monotherapy. *Antimicrob Agents Chemother* 2002; 46: 1896-905.
- [30] Zhang X, Nieforth K, Lang JM, *et al.* Pharmacokinetics of plasma enfuvirtide after subcutaneous administration to patients with human immunodeficiency virus: Inverse gaussian density absorption and 2-compartment disposition. *Clin Pharmacol Ther* 2002; 72: 10-9.
- [31] Lalezari JP, Henry K, O'Hearn M, *et al.* TORO 1 Study Group. Enfuvirtide, an HIV-1 fusion inhibitor, for drug-resistant HIV infection in North and South America. *N Engl J Med* 2003; 348: 2175-85.
- [32] Lazzarin A, Clotet B, Cooper D, *et al.* TORO 2 Study Group. Efficacy of enfuvirtide in patients infected with drug-resistant HIV-1 in Europe and Australia. *N Engl J Med* 2003; 348: 2186-95.
- [33] Fung HB, Guo Y. Enfuvirtide: a fusion inhibitor for the treatment of HIV infection. *Clin Ther* 2004; 26: 352-78.
- [34] Ball RA, Kinchelov T, ISR Substudy Group. Injection site reactions with the HIV-1 fusion inhibitor enfuvirtide. *J Am Acad Dermatol* 2003; 49: 826-31.
- [35] Tumbarello M, Tacconelli E, de Gaetano Donati K, Cauda R. HIV-associated bacterial pneumonia in the era of highly active antiretroviral therapy. *J Acquir Immune Defic Syndr Hum Retrovirol* 1999; 20: 208-9.
- [36] de Gaetano Donati K, Bertagnolio S, Tumbarello M, *et al.* Effect of highly active antiretroviral therapy on the incidence of bacterial pneumonia in HIV-infected subjects. *Int J Antimicrob Agents* 2000; 16: 357-60.
- [37] Church JA, Cunningham C, Hughes M, *et al.* Safety and antiretroviral activity of chronic subcutaneous administration of T-20 in human immunodeficiency virus 1-infected children. *Pediatr Infect Dis J* 2002; 21: 653-9.
- [38] Church JA, Hughes M, Chen J, *et al.* Long term tolerability and safety of enfuvirtide for human immunodeficiency virus 1-infected children. *Pediatr Infect Dis J* 2004; 23: 713-8.
- [39] Soy D, Aweeka FT, Church JA, *et al.* Population pharmacokinetics of enfuvirtide in pediatric patients with human immunodeficiency virus: searching for exposure-response relationships. *Clin Pharmacol Ther* 2003; 74: 569-80.
- [40] Bellibas SE, Siddique Z, Dorr A, *et al.* Pharmacokinetics of enfuvirtide in pediatric human immunodeficiency virus 1-infected patients receiving combination therapy. *Pediatr Infect Dis J* 2004; 23: 1137-41.
- [41] Wild CT, Shugars DC, Greenwell TK, McDanal CB, Matthews TJ. Peptides corresponding to a predictive α -helical domain of human immunodeficiency virus type 1 gp41 are potent inhibitors of virus infection. *Proc Natl Acad Sci USA* 1994; 91: 9770-4.
- [42] Wild C, Greenwell T, Shugars D, Rimsky-Clarke L, Matthews T. The inhibitory activity of an HIV type 1 peptide correlates with its ability to interact with a leucine zipper structure. *AIDS Res Hum Retroviruses* 1995; 11: 323-5.

- [43] Chen C, Matthews TJ, McDanal CB, Bolognesi DP, Greenberg ML. A molecular clasp in the human immunodeficiency virus (HIV) type 1 TM protein determines the anti-HIV activity of gp41 derivatives: implication for viral fusion. *J Virol* 1995; 69: 3771-7.
- [44] Lawless MK, Barney S, Guthrie KI, Bucy TB, Petteway SR, Merutka G. HIV-1 membrane fusion mechanism: structural studies of the interactions between biologically-active peptides from gp41. *Biochemistry* 1996; 35: 13697-708.
- [45] Rimsky LT, Shugars DC, Matthews TJ. Determinants of human immunodeficiency virus type 1 resistance to gp41-derived inhibitory peptides. *J Virol* 1998; 72: 986-93.
- [46] Chan DC, Chutkowski CT, Kim PS. Evidence that a prominent cavity in the coiled coil of HIV type 1 gp41 is an attractive drug target. *Proc Natl Acad Sci USA* 1998; 95: 15613-7.
- [47] Ryu J-R, Jin B-S, Suh M-J, *et al.* Two interaction modes of the gp41-derived peptides with gp41 and their correlation with antimembrane fusion activity. *Biochem Biophys Res Commun* 1999; 265: 625-9.
- [48] Liu S, Lu H, Niu J, Xu Y, Wu S, Jiang S. Different from the HIV fusion inhibitor C34, the anti-HIV drug fuzeon (T-20) inhibits HIV-1 entry by targeting multiple sites in gp41 and gp120. *J Biol Chem* 2005; 280: 11259-73.
- [49] Muñoz-Barroso I, Durell S, Sakaguchi K, Appella E, Blumenthal R. Dilatation of the human immunodeficiency virus-1 envelope glycoprotein fusion pore revealed by the inhibitory action of a synthetic peptide from gp41. *J Cell Biol* 1998; 140: 315-23.
- [50] Blumenthal R, Sarkar DP, Durell S, Howard DE, Morris SJ. Dilatation of the influenza hemagglutinin fusion pore revealed by the kinetics of individual cell-cell fusion events. *J Cell Biol* 1996; 135: 63-71.
- [51] Klinger Y, Gallo SA, Peisajovich SG, *et al.* Mode of action of an antiviral peptide from HIV-1. Inhibition at a post-lipid mixing stage. *J Biol Chem* 2001; 276: 1391-7.
- [52] Hildinger M, Dittmar MT, Schult-Dietrich P, *et al.* Membrane-anchored peptide inhibits human immunodeficiency virus entry. *J Virol* 2001; 75: 3038-42.
- [53] Veiga S, Henriques S, Santos NC, Castanho M. Putative role of membranes in the HIV fusion inhibitor enfuvirtide mode of action at the molecular level. *Biochem J* 2004; 377: 107-10.
- [54] Mobley PW, Pilpa R, Brown C, Waring AJ, Gordon LM. Membrane-perturbing domains of HIV type 1 glycoprotein 41. *AIDS Res Hum Retroviruses* 2001; 17: 311-27.
- [55] Jiang S, Zhao Q, Debnath AK. Peptide and non-peptide HIV fusion inhibitors. *Curr Pharm Design* 2002; 8: 563-80.
- [56] Derdeyn CA, Decker JM, Sfakianos JN, *et al.* Sensitivity of human immunodeficiency virus type 1 to the fusion inhibitor T-20 is modulated by coreceptor specificity defined by the V3 loop of gp120. *J Virol* 2000; 74: 8358-67.
- [57] Reeves JD, Gallo SA, Ahmad N, *et al.* Sensitivity of HIV-1 to entry inhibitors correlates with envelope/coreceptor affinity, receptor density, and fusion kinetics. *Proc Natl Acad Sci USA* 2002; 99: 16249-54.
- [58] Yuan W, Craig S, Si Z, Farzan M, Sodroski J. CD4-induced T20 binding to human immunodeficiency virus type 1 gp120 blocks interaction with the CXCR4 coreceptor. *J Virol* 2004; 78: 5448-57.
- [59] Alam SM, Paleos CA, Liao H-X, Searce R, Robinson J, Haynes BF. An inducible HIV type 1 gp41 HR-2 peptide-binding site on HIV type 1 envelope gp120. *AIDS Res Hum Retroviruses* 2004; 20: 836-45.
- [60] Greenberg ML, Cammack N. Resistance to enfuvirtide, the first HIV fusion inhibitor. *J Antimicrob Chemother* 2004; 54: 333-40.
- [61] Matthews T, Salgo M, Greenberg M, Chung J, DeMasi R, Bolognesi D. Enfuvirtide: the first therapy to inhibit the entry of HIV-1 into host CD4 lymphocytes. *Nat Rev Drug Discov* 2004; 3: 215-25.
- [62] Eron JJ, Gulick RM, Bartlett JA, *et al.* Short-term safety and antiretroviral activity of T-1249, a second-generation fusion inhibitor of HIV. *J Infect Dis* 2004; 189: 1075-83.
- [63] Root MJ, Steger HK. HIV-1 gp41 as a target for viral entry inhibition. *Curr Pharm Design* 2004; 10: 1805-25.
- [64] Lalezari JP, Bellos NC, Sathasivam K, *et al.* T-1249 retains potent antiretroviral activity in patients who had experienced virological failure while on an enfuvirtide-containing treatment regimen. *J Infect Dis* 2005; 191: 1155-63.
- [65] Veiga AS, Santos NC, Loura LMS, Fedorov A, Castanho MARB. HIV fusion inhibitor peptide T-1249 is able to insert or adsorb to lipidic bilayers. Putative correlation with improved efficiency. *J Am Chem Soc* 2004; 126: 14758-63.
- [66] Kim, R.M., Chang, J., Chapman, K.T., Mills, S.G.: US2002193407A1 (2002).
- [67] Willoughby C.A., Rosauber, K., Chapman, K.T., Mills, S.G., Shen, D.-M., Shu M.: US2002198178A1 (2002).
- [68] Kim, R.M., Chang, J., Chapman, K.T., Mills, S.G.: WO03030898A1 (2003).
- [69] Bridger, G.J., Skerlj, R.T., Kaller, A.L. *et al.*: WO03055876A1 (2003).
- *[70] Olson, W.C., Maddon, P.J.: WO03072766A1 (2003).
- *[71] Olson, W.C., Maddon, P.J., Tsurushita, N., Hinton, P.R., Vasquez, M.: US2003228306A1 (2003).
- [72] Duan M., Kazmierski, W.M., Aquino, C.J.: WO04054581A2 (2004).
- [73] Kazmierski, W.M., Aquino, C.J., Bifulco, N. *et al.*: WO04054974A2 (2004).
- [74] Peckham, J.P., Aquino, C.J., Kazmierski, W.M.: WO04055010A2 (2004).
- [75] Aquino, C.J., Chong, P.Y., Duan M., Kazmierski, W.M.: WO04055011A1 (2004).
- [76] Youngman, M., Kazmierski, W.M., Yang, H., Aquino, C.J.: WO04055012A1 (2004).
- [77] Bridger, G., McEachern, E. J., Skerlj, R. *et al.*: WO04091518A2 (2004).
- [78] Bridger, G.J., McEachern, E. J., Skerlj, R., Schols, D.: WO04093817A2 (2004).
- [79] Bridger, G.J., Kaller, A., Harwig, C. *et al.*: WO04106493A2 (2004).
- [80] Perros, M., Price, D.A., Stammen, B.L.C., Wood, A.: EP1526134A2 (2005).
- [81] De Clercq E. HIV-chemotherapy and -prophylaxis: new drugs, leads and approaches. *Int J Biochemistry Cell Biology* 2004; 36: 1800-22.
- [82] Vermeire K, Schols D, Bell TW. CD4 down-modulating compounds with potent anti-HIV activity. *Curr Pharm Design* 2004; 10: 1795-803.
- [83] Menéndez-Arias L, Esté JA. HIV-resistance to viral entry inhibitors. *Curr Pharm Design* 2004; 10: 1845-60.
- [84] Nagashima KA, Thompson DA, Rosenfield SI, Maddon PJ, Dragic T and Olson WC. Human Immunodeficiency Virus Type 1 entry inhibitors PRO 542 and T-20 Are Potently Synergistic in Blocking Virus-Cell and Cell-Cell fusion. *J Infect Dis* 2001; 183: 1121-5.

Chapter VIII

ANNEX II

Hepatitis C virus core protein binding to lipid membranes: the role of domains 1 and 2.

Hepatitis C virus core protein binding to lipid membranes: the role of domains 1 and 2

A. J. Pérez-Berná,¹ A. S. Veiga,² M. A. R. B. Castanho² and J. Villalaín¹

¹Instituto de Biología Molecular y Celular, Universidad "Miguel Hernández", Elche-Alicante, Spain; and ²Centro de Química e Bioquímica, Faculdade de Ciências da Universidade de Lisboa, Campo Grande, Lisboa, Portugal

Received July 2007; accepted for publication October 2007

SUMMARY. We have analysed and identified different membrane-active regions of the Hepatitis C virus (HCV) core protein by observing the effect of 18-mer core-derived peptide libraries from two HCV strains on the integrity of different membrane model systems. In addition, we have studied the secondary structure of specific membrane-interacting peptides from the HCV core protein, both in aqueous solution and in the presence of model membrane systems. Our results show that the HCV core protein region comprising the C-terminus of domain 1 and the N-terminus of domain 2 seems to be the most active in membrane interaction, although a role in protein-protein interaction cannot

be excluded. Significantly, the secondary structure of nearly all the assayed peptides changes in the presence of model membranes. These sequences most probably play a relevant part in the biological action of HCV in lipid interaction. Furthermore, these membranotropic regions could be envisaged as new possible targets, as inhibition of its interaction with the membrane could potentially lead to new vaccine strategies.

Keywords: assembly, capsid, core protein, HCV, hepatitis, lipid.

INTRODUCTION

Hepatitis C virus (HCV) is an enveloped positive single-stranded RNA virus that belongs to the genus *Hepacivirus* in the family *Flaviviridae*, and is the leading cause of acute and chronic liver disease in humans, including chronic hepatitis, cirrhosis, and hepatocellular carcinoma [1–3]. There exists no vaccine to prevent HCV infection and current therapeutic agents have limited success against HCV [4]. The HCV genome consists of one translational open reading frame encoding a polyprotein precursor, including structural and non-structural proteins, that is cleaved by host and viral proteases (Fig. 1a). The structural proteins consist of the core protein, which forms the viral nucleocapsid, and the envelope glycoproteins E1 and E2, both of them transmem-

brane proteins. The HCV cell entry is achieved by the fusion of viral and cellular membranes, and the morphogenesis and virion budding has been suggested to take place in the endoplasmic reticulum [5]. HCV proteins are very sensitive to folding, assembly, mutations or deletions. Besides, the HCV genome is widely heterogeneous; the errors during its replication cause a high rate of mutations. Therefore, the region implicated in fusion and/or budding must interact with the membranes and should be a conservative sequence. Finding protein-membrane and protein-protein interaction inhibitors could be a good strategy against HCV infection as they might prove to be potential therapeutic agents.

The HCV core protein is highly basic and shows homology with the nucleocapsid protein of other flaviviruses. This protein is well conserved among the different HCV strains [6] and is important for HCV infection diagnosis by the detection of either specific anti-HCV core protein antibodies or circulatory viral antigens. The core protein has regulatory roles on cell functions like immune presentation, apoptosis, lipid metabolism and transcription [7–9]. Additionally, this protein has oncogenic potential playing an important role in the regulation of HCV-infected cell growth, transformation to a tumorigenic phenotype and development of hepatocellular carcinoma [10]. Recombinant cDNA expression studies of this protein have identified two major protein core species, p23 and p21 [8]. The later is the predominant species and is

Abbreviations: CF, 5-Carboxyfluorescein; Chol, cholesterol; EPC, egg 1-phosphatidylcholine; HCV, hepatitis C virus; LUV, large unilamellar vesicles; MLV, multilamellar vesicles; NBD-PE, N-(7-nitrobenz-2-oxa-1,3-diazol-4-yl)-1,2-dihexadecanoyl-sn-glycero-3-phosphoethanolamine; N-RhB-PE, lissamineTM rhodamine B 1,2-dihexadecanoyl-sn-glycero-3-phosphoethanolamine; SM, egg sphingomyelin; T_m, temperature of the gel-liquid crystalline phase transition.

Correspondence: Dr. José Villalaín, Instituto de Biología Molecular y Celular, Campus de Elche, Universidad "Miguel Hernández", E-03202 Elche-Alicante (España-Spain). E-mail: jvillalain@umh.es.

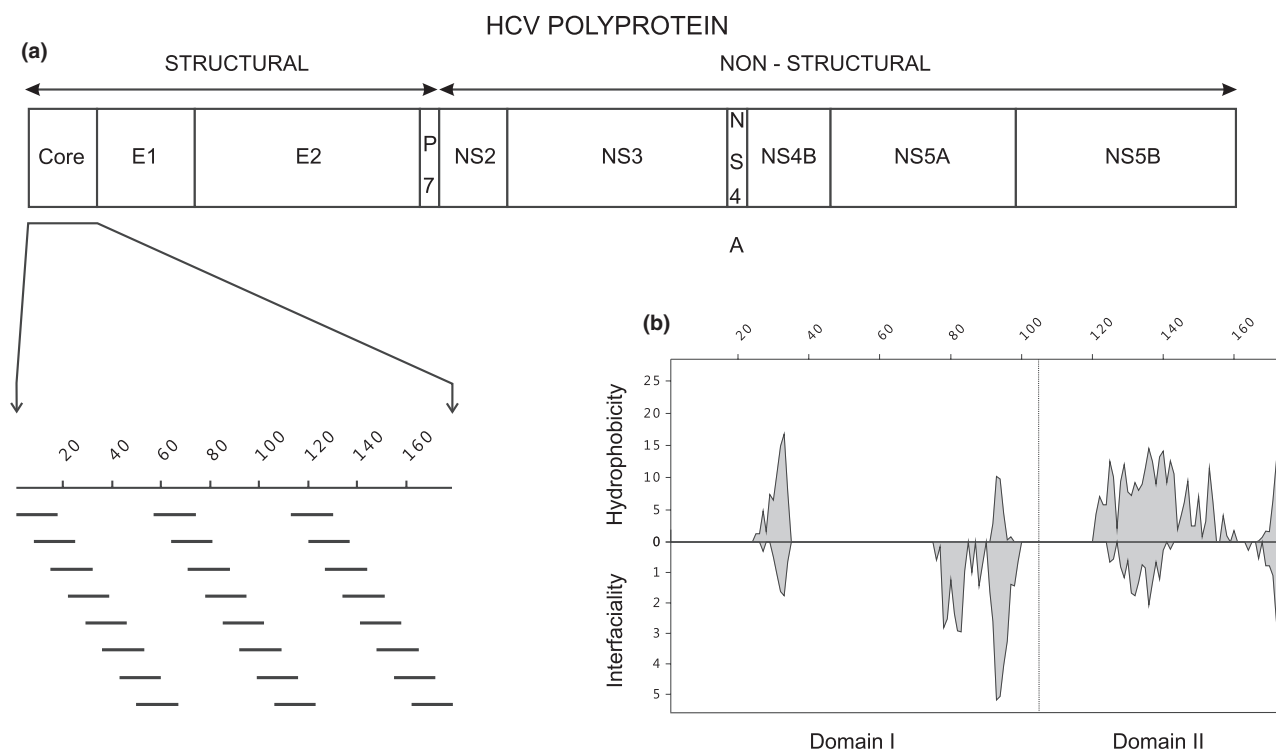


Fig. 1 (a) Scheme of the hepatitis C virus (HCV) structural and non-structural proteins according to literature consensus. The sequence and relative location of the twenty-seven 18-mer peptides derived from the HCV core protein are shown with respect to the sequence of the protein. Maximum overlap between adjacent peptides is 11 amino acids. (b) Analysis of the hydrophobicity and interfaciality distribution according to the scales of Wimley and White [22,23] using a window of 11 amino acids along the HCV core sequence without any assumption about secondary structure.

found in viral particles from infected sera, probably being the mature form of the protein. Although the three dimensional structure of this protein is unknown three distinct domains can be considered in the full-length immature protein [11,12], i.e. domain 1, comprising amino acids 1–117 and having several positive charges involved in RNA binding and including the immunodominant antigenic site, domain 2, comprising amino acids 117–171 and putatively responsible of its association with lipid droplets, and domain 3, comprising amino acids 171–191, a signal peptide upstream of the E1 glycoprotein. Significantly, the mature core protein is a dimeric helical protein exhibiting membrane protein features [11].

Recently, we have identified the membrane-active regions 2,3 of the HIV gp41, SARS-CoV spike and HCV E1 and E2 glycoproteins by observing the effect of glycoprotein-derived peptide libraries on model membrane integrity [13–15]. These results have permitted us to suggest the possible location of different segments in these proteins which might be implicated in protein–lipid and protein–protein interactions, helping us to understand the processes which give rise to the interaction between the protein and the membrane. Additionally, HCV membrane assembly and budding is an attractive target for anti-HCV therapy, as it has been

proposed that the core protein has an important role in viral assembly. To investigate the structural basis of the protein core interaction with the membrane and identify new targets for searching viral assembly inhibitors, we have analysed and identified different membrane-active regions of the HCV core protein by observing the effect of 18-mer core-derived peptide libraries from two HCV strains, namely, HCV 1AH77 and HCV 1B4J, on the integrity of different membrane model systems. Furthermore, we have studied the secondary structure of specific membrane-interacting peptides, both in aqueous solution and in the presence of model membrane systems, to understand the molecular mechanism of viral budding as well as making possible the future development of HCV assembly inhibitors which may lead to new vaccine strategies.

MATERIALS AND METHODS

Materials and reagents

Egg L-phosphatidylcholine (EPC), egg sphingomyelin (SM), liver lipid extract (a 2:1 chloroform:methanol extract of liver tissue) and cholesterol (Chol) were obtained from Avanti Polar Lipids (Alabaster, AL, USA). 5-Carboxyfluorescein (CF)

(>95% by high performance liquid chromatography), and sodium dithionite were from Sigma-Aldrich (Madrid, Spain). Lissamine rhodamine B 1,2-dihexadecanoyl-sn-glycero-3-phosphoethanolamine (N-RhB-PE) and N-(7-nitrobenz-2-oxa-1,3-diazol-4-yl)-1,2-dihexadecanoyl-sn-glycero-3-phosphoethanolamine (NBD-PE) were obtained from Molecular Probes Inc. (Eugene, OR, USA). Three sets of 18-mer peptides derived from the core protein (Fig. 1a) of hepatitis C virus strains 1B4J and 1AH77 having 11-amino acid overlap between sequential peptides were obtained through the NIH AIDS Research and Reference Reagent Program (Division of AIDS, NIAID, NIH, Bethesda, MD, USA). All other reagents used were of analytical grade from Sigma-Aldrich. Water was deionized, twice-distilled and passed through a Milli-Q equipment (Millipore Ibérica, Madrid, Spain) to a resistivity better than 18 M Ω cm.

Sample preparation

For infrared spectroscopy, aliquots containing the appropriate amount of lipid in chloroform/methanol (2:1, v/v) were placed in a test tube containing 100 μ g of dried lyophilized peptide to obtain a final lipid/peptide mole ratio of 50:1. After vortexing, the solvents were removed by evaporation under a stream of O₂-free nitrogen, and finally, traces of solvents were eliminated under vacuum in the dark for more than 3 h. The samples were hydrated in 100 μ L of D₂O buffer containing 20 HEPES, 50 NaCl, 0.1 mM EDTA, pH 7.4 and incubated at 10 °C above the phase transition temperature (T_m) of the phospholipid mixture with intermittent vortexing for 45 min to hydrate the samples and obtain multilamellar vesicles (MLV). The samples were frozen and thawed five times to ensure complete homogenization and maximization of peptide/lipid contacts with occasional vortexing. Finally the suspensions were centrifuged at 15 000 rpm at 25 °C for 15 min to remove the peptide possibly unbound to the membranes. The pellet was resuspended in 30 μ L of D₂O buffer. The phospholipid and peptide concentrations were measured by methods described previously [16,17].

Membrane-leakage measurement

Aliquots containing the appropriate amount of lipid in chloroform/methanol (2:1 v/v) were placed in a test tube, the solvents were removed by evaporation under a stream of O₂-free nitrogen, and finally traces of solvents were eliminated under vacuum in the dark for more than 3 h. For assays of vesicle leakage at pH 7.4, buffer containing 10 Tris-HCl, 20 NaCl, 40 CF, and 0.1 mM EDTA, pH 7.4, was used [13]. To obtain MLV, 1 mL of buffer was added to the dry phospholipid mixture and vortexed at room temperature until a clear suspension was obtained. Large unilamellar vesicles (LUV) with a mean diameter of 90 nm were prepared from MLV by the extrusion method [14] using polycarbonate filters with a pore size of 0.1 μ m (Nuclepore Corp., Cambridge,

CA, USA). Breakdown of the vesicle membrane leads to content leakage. Non-encapsulated CF was separated from the vesicle suspension through a Sephadex G-75 filtration column (Pharmacia, Uppsala, Sweden) eluted with buffer containing either 10 Tris-HCl, 100 NaCl and 0.1 mM EDTA, pH 7.4. Membrane rupture (leakage) of intraliposomal CF was assayed by treating the probe-loaded liposomes (final lipid concentration, 0.125 mM) with the appropriate amounts of peptide on microtitre plates using a microplate reader (FLUOstar; BMG Labtech, Offenburg, Germany), stabilized at 25 °C with the appropriate amounts of peptide, each well containing a final volume of 170 μ L. The medium in the microtitre plates was continuously stirred to allow the rapid mixing of peptide and vesicles. Leakage was assayed until no more change in fluorescence was obtained. Changes in fluorescence intensity were recorded with excitation and emission wavelengths set at 492 and 517 nm, respectively. Excitation and emission slits were set at 5 nm. One hundred per cent release was achieved by adding Triton X-100 to the microtiter plate to a final concentration of 0.5% (wt/wt). Fluorescence measurements were made initially with probe-loaded liposomes, afterwards by adding peptide solution and finally by adding Triton X-100 to obtain 100% leakage. Leakage was quantified on a percentage basis according to the equation,

$$\%L = \frac{(F_t - F_0) \times 100}{F_{100} - F_0}$$

where F_t is the equilibrium value of fluorescence after peptide addition, F_0 is the initial fluorescence of the vesicle suspension, and F_{100} is the fluorescence value after the addition of Triton X-100.

Phospholipid-mixing measurement

Peptide-induced vesicle lipid mixing (hemifusion) was measured by resonance energy transfer [18]. This assay is based on the decrease in resonance energy transfer between two probes (NBD-PE and RhB-PE) when the lipids of the probe-containing vesicles are allowed to mix with lipids from vesicles lacking the probes. The concentration of each of the fluorescent probes within the liposome membrane was 0.6 mol%. For assays of lipid mixing, 1 mL of buffer (10 HEPES, 100 mM NaCl, pH 7.4) was added to the dry phospholipid mixture (containing either 0.6 mol % NBD-PE and N-RhBPE or 0.12 mol% NBD-PE and N-RhB-PE, or no probes), and MLV were obtained by vortexing at room temperature. LUV were prepared from MLV by the extrusion method as above, using polycarbonate filters with a pore size of 0.2 μ m (Nuclepore Corp). The use of 0.2 μ m pore-size filters gives place to larger liposomes and henceforth greater fluorescence intensity per surface unit. Labelled and unlabelled vesicles in a proportion 1:4 were placed in a 5 mm \times 5mm fluorescence cuvette at a final lipid

concentration of 100 μM in a final volume of 400 μL , stabilized at 25 $^{\circ}\text{C}$ under constant stirring. The fluorescence was measured using a Varian Cary Eclipse fluorescence spectrometer using 467 nm and 530 nm for excitation and emission, respectively. Excitation and emission slits were set at 10 nm. As labelled and unlabelled vesicles were mixed in a proportion of 1 to 4 respectively, 100% phospholipid mixing was estimated with a liposome preparation in which the membrane concentration of each probe was 0.12%. Phospholipid mixing was quantified on a percentage basis according to the equation,

$$\% PM = \frac{(F_f - F_0) \times 100}{F_{100} - F_0},$$

F_f being the equilibrium value of fluorescence after peptide addition to a liposome mixture containing liposomes having 0.6% of each probe plus liposomes without any fluorescent probe, F_0 the initial fluorescence of the vesicles and F_{100} is the fluorescence value of the liposomes containing 0.12% of each probe.

Inner-monolayer phospholipid-mixing measurement

Peptide-induced phospholipid-mixing (fusion) of the inner monolayer was measured by a modification of the phospholipid-mixing measurement stated above [19]. LUVs were treated with sodium dithionite to completely reduce the NBD-labelled phospholipid located at the outer monolayer of the membrane. Final concentration of sodium dithionite was 100 mM (from a stock solution of 1 M dithionite in 1 M TRIS, pH 10.0) and incubated for approximately 1 h on ice in the dark. Sodium dithionite was then removed by size exclusion chromatography through a Sephadex G-75 filtration column (Pharmacia, Uppsala, Sweden) eluted with buffer containing 10 TRIS, 100 NaCl, 1 mM EDTA, pH 7.4. The proportion of labelled and unlabelled vesicles, lipid concentration and other experimental and measurement conditions were the same as indicated above for the phospholipid mixing assay.

Infrared spectroscopy

Approximately 30 μL of a pelleted sample in D_2O were placed between two CaF_2 windows separated by 56- μm thick Teflon spacers in a liquid demountable cell (Harrick, Ossining, NY, USA). The spectra were obtained in a Bruker IFS55 spectrometer using a deuterated triglycine sulphate detector. Each spectrum was obtained by collecting 200 interferograms with a nominal resolution of 2/cm, transformed using triangular apodization and, to average background spectra between sample spectra over the same time, a sample shuttle accessory was used to obtain sample and background spectra. The spectrometer was continuously purged with dry air at a dew point of -40°C to remove atmospheric water vapour from the bands of interest. All samples were

equilibrated at the lowest temperature for 20 min before acquisition. An external bath circulator connected to the infrared spectrometer controlled the sample temperature. For temperature studies, samples were scanned using 20 $^{\circ}\text{C}$ intervals and a 15-min delay between each consecutive scan. Subtraction of buffer spectra taken at the same temperature as the samples was performed interactively using either GRAMS32 or Spectra-Calc (Galactic Industries, Salem, MA, USA) as described previously [20,21]. Frequencies at the centre of gravity, when necessary were measured by taking the top 10 points of each specific band and fitted to a Gaussian band. The criterion used for buffer subtraction in the C=O and amide regions was the removal of the band near 1210/cm, and a flat baseline between 1800 and 2100/cm.

RESULTS

The peptide libraries used in this study and their correlation with the HCV core protein sequence are depicted in Fig. 1a, where it can be observed that the 18-mer peptide libraries include the whole HCV core protein sequence. Second and third consecutive peptides in the library have an overlap of 811 and 4 amino acids, respectively. The analysis of the hydrophobicity and interfaciality distribution along the core sequence of HCV 1B4J strain (the data obtained for the HCV 1AH77 strain is nearly identical) without any assumption about secondary structure is shown in Fig. 1b [13,22,23]. Although the three dimensional structure of the core protein is not known, these data give us a depiction of the potential surface zones that could be possibly implicated in either the modulation of membrane binding or protein-protein interaction or both. As it is observed in Fig. 1b, it is evident about the existence of different regions with large hydrophobic and interfacial values along the core sequence; these surfaces should be biologically functional in their roles as these patches of positive hydrophobicity and interfaciality along the surface of the core protein could favour the interaction with other similar patches along other core proteins, different proteins or with the surface of the membrane.

Membrane rupture, hemifusion and fusion

We have studied the effect of the 18-mer peptide libraries derived from the HCV core protein 1AH77 and 1B4J strains on membrane rupture, i.e. leakage, for different liposome compositions (Fig. 2); the lipidic composition of the model membranes have been EPC/Chol at a phospholipid molar ratio of 5:1, EPCSM at a phospholipid molar ratio of 5:1, EPCSM/Chol at a phospholipid molar ratio of 5:1:1, and a lipid extract of liver membranes (containing 42% EPC, 22% PE, 7% Chol, 8% PI, 1% LPC, and 21% neutral lipids). The presence of both SM and Chol has been related to the occurrence of laterally segregated membrane microdomains

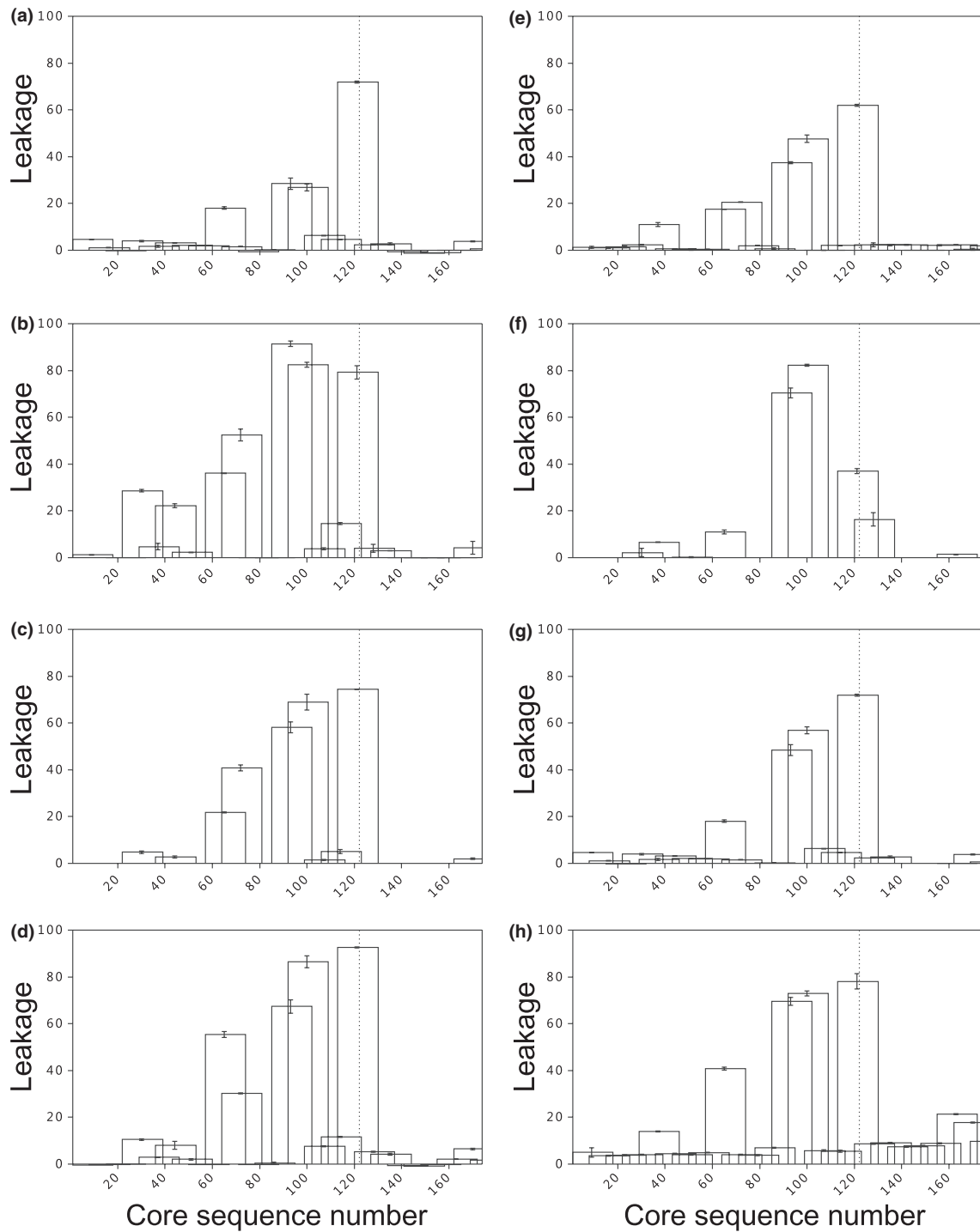


Fig. 2 Effect of the 18-mer peptides derived from the hepatitis C virus (HCV) core protein of HCV 1AH77 (a–d) and HCV 1B4J (e–h) strains on the release (membrane rupture) of large unilamellar vesicles (LUV) contents for different lipid compositions. Leakage data for LUVs composed of (a,e) egg α -phosphatidylcholine/cholesterol (EPC/Chol) at a phospholipid molar ratio of 5:1, (b,f) EPC/egg sphingomyelin (SM) at a phospholipid molar ratio of 5:1, (c,g) EPC/SM/Chol at a phospholipid molar ratio of 5:1:1, and (d,h) lipid extract of liver membranes. Vertical bars indicate SDs of the mean of triplicate samples. The dotted line divides regions corresponding to core domains I and II.

or 'lipid rafts', and it has been found that there is an important relationship between membrane interaction and Chol and SM membrane content for several viruses [24].

When the 18-mer peptides were assayed on EPC/Chol liposomes, some peptides exerted a significant leakage effect (Figs 2a,f). The most remarkable effects were induced

by peptide comprising residues 113–130. Other peptides which elicited important leakage values were peptides comprising residues 57–74, 85–102 and 92–109 for strain 1AH77 and 29–46, 57–74, 64–81, 85–102 and 92–109 for strain 1B4J. The leakage pattern was slightly different when liposomes composed of EPC/SM were tested (Figs 2b,f), as the most significant effect appeared now for peptides comprising residues 85–102 and 92–109. Peptide 113–130 also showed a significant leakage effect. Other significant leakage values were found for peptides 22–39, 36–53, 57–74 and 64–81 for strain 1AH77 and 64–81 and 120–137 for strain 1B4J. When liposomes composed of EPC/SM/Chol at a molar ratio of 5:1:1 were assayed (Figs 2c,g), a similar pattern to liposomes containing EPC/Chol was found. The most notable effect was induced by peptide comprising residues 113–130, whereas peptides 57–74, 64–81, 85–102 and 92–109 for strain 1AH77 and peptides 57–74, 85–102, and 92–109 for strain 1B4J elicited also significant leakage values. For liposomes composed of a lipid extract of liver membranes, the same peptide sequences displayed significant leakage values (Figs 2d,h). As it was found above, the most significant values were found for the peptide comprising residues 113–130, but peptides 85–102 and 92–109 showed also significant leakage. Peptides 57–74 and 64–81 for strain 1AH77 and peptide 57–74 for strain 1B4J displayed significant leakage values.

When the 18-mer core derived peptides from strain 1AH77 were assayed for hemifusion on both EPC/SM/Chol and liver extract liposomes, peptide comprising residues 29–46 displayed significant values (Figs 3a,b). Other peptides which elicited important hemifusion values (10%) defined a region comprising amino acids 85–130, with hemifusion values ranging from 10 to 25%. Slightly lower hemifusion values were found for core-derived peptides from strain 1B4J than for strain 1AH77 using both types of liposomes, EPC/SM/Chol and liver extract (Figs 3e,f). When the 18-mer core-derived peptides from strains 1AH77 and 1B4J were assayed for fusion on both EPC/SM/Chol and liver extract liposomes, peptide comprising residues 29–46 was the one which displayed significant fusion values (Figs 3c,d,g,h). The region comprising amino acids 85–130 (five peptides in total) was also found to have relatively high hemifusion and fusion values for both strains.

The summary of membrane leakage, membrane hemifusion and membrane fusion results obtained for both 1AH77 and 1B4J strains is presented in Fig. 4a, whereas the global average result is displayed in Fig. 4b. It is possible to detect various segments with large leakage values, which coincide with segments displaying significant hemifusion and fusion values. However, it is also possible to detect segments displaying high hemifusion and fusion values but low leakage values. These results have permitted us to study specific peptides comprising different zones by infrared spectroscopy as shown below.

Fourier-transformed infrared spectroscopy structural assays

Peptides which displayed significant leakage, hemifusion and fusion effects (Fig. 4b), i.e. peptides corresponding to sequences 29–46, 57–74, 85–102, 106–123, and 155–172 were chosen for structural infrared assays both in aqueous solution (aqueous solutions of peptides 85–102 and 153–172 additionally contained 10% TFE) and in the presence of membrane model systems composed of either EPC/SM/Chol at a 5:1:1 molar ratio or a liver lipid extract (Fig. 5). Spectra were obtained at five different temperatures (5, 25, 45, 65 and 85 °C) and no any significant differences was found between them, indicating a high degree of conformational stability of the peptides. For simplicity, we will describe spectra obtained at 25 °C. The assignment of the Amide I' component bands to specific structural features has been described previously [25]. As observed in Fig. 5, there were significant changes in the Amide I' envelope band depending on the peptide and the specific lipid composition used.

The Amide I' band of the peptide derived from the core 29–46 region in aqueous solution (Fig. 5a) displays a narrow band at 1672/cm and a shoulder with at least two broad bands at about 1645 and 1628/cm. The band envelope of the Amide I' band of the peptide bound to raft model membranes was significantly different to that found for the peptide in aqueous solution, as maximum of the band appeared at about 1628/cm with small bands at about 1672 and 1644/cm (Fig. 5a). In the presence of liver lipid extract membranes, the Amide I' band was similar to the one found in the presence of raft-containing membranes, but a more intense band at about 1671/cm. These differences in band intensities for the 29–46 peptide would imply that β -turn should be the most significant secondary structure in aqueous solution, whereas in the presence of both raft and liver extract model membranes the most significant one should be β -sheet.

The Amide I' band of the peptide derived from the core 57–74 sequence in aqueous solution displayed a broad band with a maximum at about 1672/cm and a shoulder at about 1648/cm (Fig. 5b). The band envelope of the Amide I' band of this peptide bound to raft model membranes was significantly different to that found for the peptide in aqueous solution, as the maximum of the band appeared at about 1637/cm with a small shoulder at about 1648/cm. In the presence of model membranes composed of liver lipid extract, the Amide I' band of the peptide displayed a maximum at about 1648/cm. The intensity maxima for the core 57–74 sequence would imply that the most significant structure in aqueous solution and in the presence of liposomes composed of a liver extract should be random, but β -sheet in the presence of PC/SM/Chol at a molar ratio of 2:1:1.

The peptides derived from the core 85–102 sequence of strains 1AH77 and 1B4J have similar sequences: the cysteine present in the 91 position of the strain 1AH77 is replaced

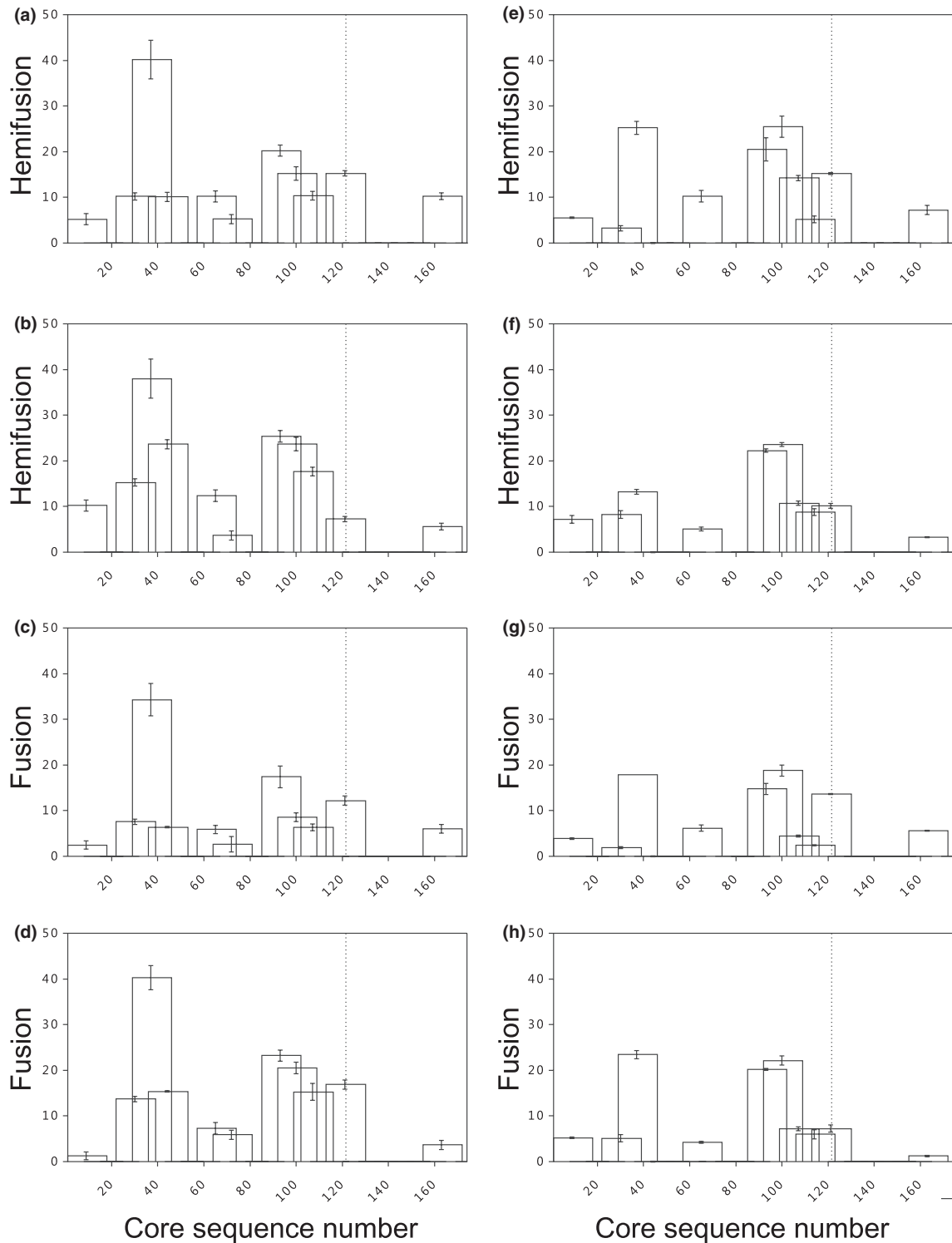


Fig. 3 Effect of the 18-mer peptides derived from the hepatitis C virus (HCV) core protein of HCV 1AH77 (a–d) and HCV 1B4J (e–h) strains on hemifusion (a,b,e,f) and fusion (c,d,g,h) for large unilamellar vesicles composed of (a,c,e,g) egg 1-phosphatidylcholine/egg sphingomyelin/cholesterol at a phospholipid molar ratio of 5:1:1, and (b,d,f,h) lipid extract of liver membranes. Vertical bars indicate SDs of the mean of triplicate samples. The dotted line divides regions corresponding to core domains I and II.

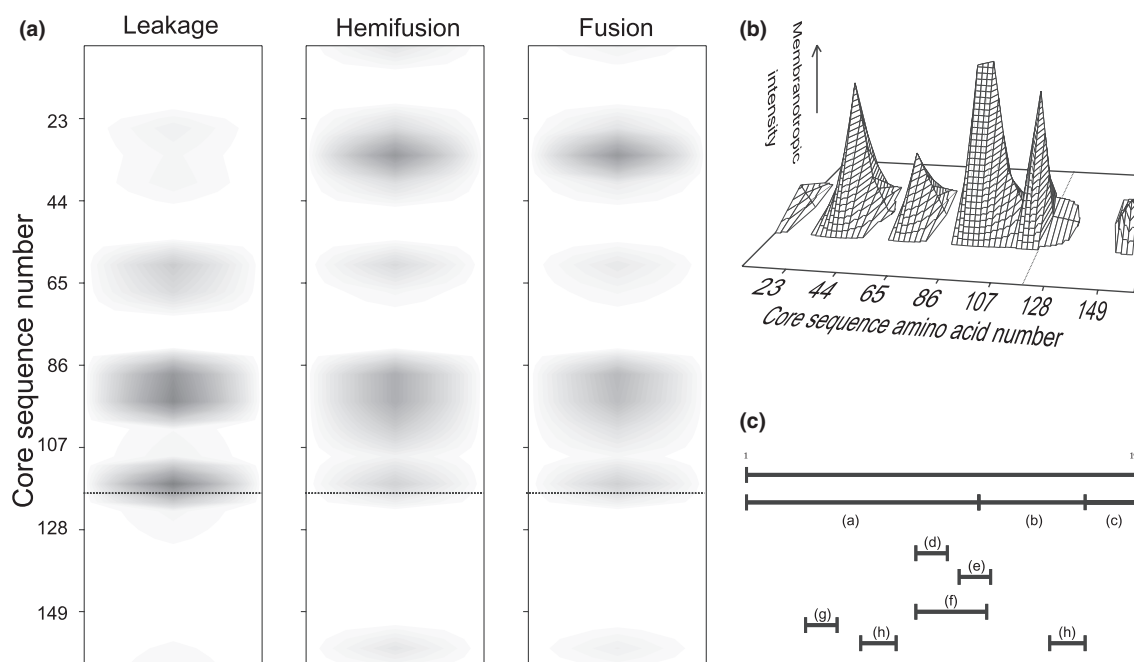


Fig. 4 (a) Summary of all experimental membrane leakage, hemifusion and fusion data presented in this work corresponding to the core-derived 18-mer peptides for both 1AH77 and 1B4J strains representing the full core sequence and for all liposome compositions studied (the darker, the greater membrane-active effect). (b) Summary of all the experimental data along the consensus scheme of the core protein highlighting the experimentally determined membrane-active regions. The dotted line divides regions corresponding to core domains I and II. (c) Pictorial survey of the most important membrane-active regions of hepatitis C virus (HCV) core protein. Membrane-active sequences found in this study (d,e,g,h) are depicted along sequences reported in the literature (a,b,c,f). (a) Domain 1: this sequence is regarded as the RNA-binding region with immunodominant antigenic properties [11,36]. (b) Domain 2: putatively responsible for the association with lipids [11,36]. (c) Domain 3: signal peptide [11,36]. (d) Membrane-leakage, hemifusion, and fusion activities with high interfacial values (see text). (e) Membrane-leakage activity (see text). (f) Homotypic interactions [27] and association to ER and mitochondrial membranes [35]. (g) Maximal hemifusion and fusion activities (see text); part of the HCV major antigenic domain sequence; exposed region for protein-membrane interaction. (h) Both sequences have low but constant rupture, hemifusion and fusion properties (see text).

by a leucine in the 1B4J strain. In aqueous solution, both peptides show a relatively broad Amide I' band with a maximum at approximately 1647/cm and a shoulder at about 1672/cm, much more intense for the peptide derived from the 1B4J strain than for the 1AH77 one (Figs 5c,d). In the presence of raft model membranes, the maximum of the Amide I' band in both cases is shifted to lower wavenumbers, displaying an Amide I' maxima at about 1638/cm with a shoulder at about 1671/cm. In the presence of liver lipid extract membranes, the Amide I' band of both peptides display a broad band with a maximum at about 1650/cm. These differences in band intensities would imply that disordered structure should be the most significant secondary structure in aqueous solution for the 1AH77 derived peptide, but random and β -turn for the 1B4J peptide; however, in the presence of both raft and liver extract model membranes, the most significant one should be either disordered structure and/or β -sheet.

The Amide I' band of the peptide derived from the core 106–123 and 155–172 sequences in aqueous solution display a narrow band at about 1672/cm and a shoulder at

about 1647/cm (Figs 5e,f). The band envelope of the Amide I' band of both peptides bound to raft model membranes was significantly different to that found for the peptides in aqueous solution, as the maximum of the band appeared at about 1638/cm with shoulders at about 1667/cm. In the presence of model membranes composed of liver lipid extract, the Amide I' band of both peptides were rather similar to the ones found in the presence of raft membranes, but the band at 1665/cm presented a higher intensity. These differences in band intensities for the core 106–123 and 155–172 sequences would imply that β -turn should be the most significant secondary structure in aqueous solution, together with random structure, whereas in the presence of both raft and liver extract model membranes, the most predominant secondary structure should be β -helix followed by β -turn.

DISCUSSION

Viral morphogenesis is one of the most important steps in the viral cycle involving lipid membranes and is not as well characterized as the fusion event. For enveloped viruses, the

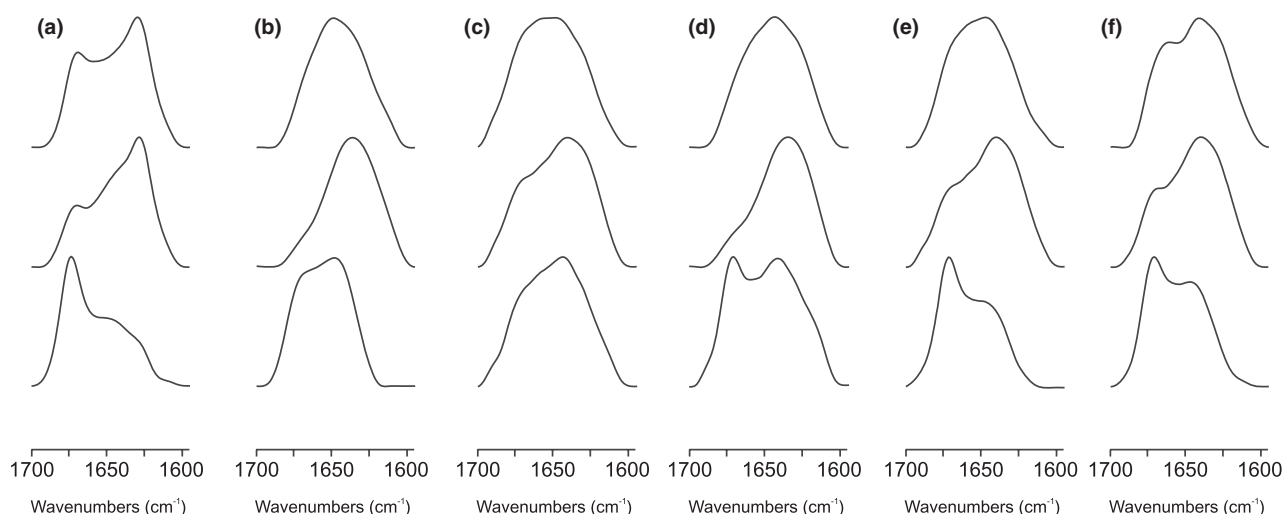


Fig. 5 Amide I' band spectra of peptides at 25 °C corresponding to core sequences (a) 29–46, (b) 57–74, (c) 85–102 (1AH77 strain), (d) 85–102 (1B4J strain), (e) 106–123 and (f) 155–172 in aqueous solution (lower spectra), in the presence of liposomes composed of egg L-phosphatidylcholine/egg sphingomyelin/cholesterol at a 5:1:1 molar ratio (middle spectra) and in the presence of liposomes composed of a liver lipid extract (upper spectra).

assembly of the virions takes place in the host cell membrane and in the case of HCV it has been suggested that the virus particles assembly occurs in the endoplasmic reticulum membranes [26] where the core protein might play a central role in viral particle formation as well as it might drive the budding process [27]. Significantly, the HCV core protein is very well conserved among different HCV strains [6] and has important regulatory roles on different cell functions. Interestingly, the HCV core protein has been reported to be associated with raft sub-domains in the absence of other viral non-structural proteins [28]. Rafts, rigid membrane sub-domains located predominantly in the plasma membrane are described to be important in the HCV replication cycle, assembly of virions and budding from the host cell. For this reason, we have chosen membrane model systems composed not only of a liver lipid extract but also of EPC, SM and Chol [29,30], as mimetic of model membranes containing raft domains. As the biological roles of the HCV core protein can be modulated by membranes, we have identified the membrane-active regions of the HCV core protein by studying the effect of two core-derived peptide libraries from HCV on the integrity of membrane model systems. Furthermore, to obtain information on the structural basis of the interaction of the protein with model membranes, we have studied the secondary structure of specific membrane-interacting peptides both in aqueous solution and in the presence of model membrane systems. In this way, it would be possible to identify important regions which might be implicated in the budding molecular mechanism, and therefore could be used as new targets for searching viral assembly inhibitors as well as making possible the future development of HCV assembly inhibitors which may lead to new vaccine strategies.

As it can be observed in Figs 4a,b, we have been able to discern different zones along the core sequence displaying different membranotropic properties. When leakage was assayed, and all the values were taken into account for all membrane compositions assayed, two zones displayed significant membrane rupture activity, i.e. regions defined by amino acids 85–102 and 106–123. The first region displayed a high interfacial value along its sequence; however, the second one did not show significant hydrophobic and interfacial values. In this context, it is interesting to note that the region comprising residues 85–123 has been described to be important in homotypic interactions which might be a prerequisite for assembly and budding of HCV-like viral particles [27,31]. Significantly, mutant core proteins without the 80–118 amino acid residues reduced, but did not abolish the association with lipid droplets [32,33]. Interestingly, the interaction of a region composed of amino acids 72–91 with the E1 glycoprotein [34] has been described; this region might be also important for association with the endoplasmic reticulum and the mitochondrial outer membranes [35]. Notably, region 85–102 coincides with a hydrophobic cluster located in domain 1 of the core protein and region 106–123 partially overlaps with another one located in domain 2 [36]. By infrared spectroscopy, it was possible to observe that the 85–102 region displayed different types of secondary structure, as random structure was the major one in aqueous solution but an increase in β -sheet in the presence of model membranes was observed. Although these regions present high levels of membrane rupture, hemifusion and fusion in the whole protein context, this region might be implicated in protein homodimerization but not in protein-membrane interactions.

Sequences 85–102 and 106–123, apart from being the ones which elicited the most leakage effect, displayed also significant hemifusion and fusion activities but region 29–46 displayed the highest hemifusion and fusion values together with low-leakage values (Fig. 4). As observed in Fig. 1b, this region displays high hydrophobicity and interfaciality values along its sequence. By infrared spectroscopy, it was determined that in aqueous solution, the predominant secondary structure was β -turn but β -sheet in the presence of model membranes composed of either raft or liver extract lipids. This region has two sequential glycines which might confer a high flexibility to the peptide and might act as a hinge around which the conformation could change. Moreover, this region is part of the HCV major antigenic domain sequence [37], being probably exposed and implicated in protein-membrane interactions. On the other hand, it has been demonstrated that uniformly packed virus particles are generated only by segment composed by amino acid residues 1–82, whereas region 29–46 is the only one in the N-terminal half of the core protein found to interact with lipids [38]. For this reason, this region might be an important one for the HCV assembly. Another interesting core sequences pertain to the 57–74 and 155–172 regions, as they displayed low but constant membrane rupture, hemifusion and fusion activities (Fig. 4a). It has been described that the ability of the core protein to associate with lipid droplets is lost when the 153–172 region containing the YATG motif is deleted [27]. These regions, having low but significant membrane-active activities, might be implicated in the interaction with membranes.

Additionally to its role in the viral morphogenesis and budding, the core protein is also important in the disassembly event during the viral uncoating that occurs at the target cell in a post-fusion stage. For this reason, this protein is very flexible [5]. The predicted structure of the whole 14 protein using CD indicated that the protein has 16% of β -helix structure, 29% β -sheet structure and β -turns and 55% of random coil, whereas the C-terminal truncated protein was largely unordered [9]. As shown in this work, nearly all the peptides we have assayed display a major random coil or turn structure in solution; however, their structure changes in the presence of model membranes. This information could suggest that the membranotropic regions which we have detected along the core sequence might be involved in the interaction, not only with membranes, but also with proteins, even other core proteins and therefore responsible of their oligomerization.

Altogether, our results show that most of the HCV core protein membrane-active regions we have presented in this work are located in domain 1 (Fig. 4c), whatever interaction parameter is considered. However, the prevalent idea is that domain 1 might be the RNA-binding region whereas domain 2 of the HCV core protein would be responsible for membrane-binding (domain 3 is a signal peptide) [11,12].

Gathering related results in the literature, it is clear that a domain 1 vs domain 2 reasoning is not appropriate to unravel the foundations of HCV core-protein interaction with lipids. The region comprising the C-terminus of domain 1 and N-terminus of domain 2 seems to be the most active in membrane interaction, although a role in protein-protein interaction cannot be excluded. There is a sequence in domain 1 of maximal fusion and hemifusion (sequence f in Fig. 4c) that belongs to the major antigenic sequence of HCV. This sequence most probably plays a part in the biological action of HCV in lipid interaction whether during assembly, or fusion, or both. A more exhaustive study of these lipid-peptide interactions might help in the understanding of the HCV budding molecular mechanism as well as making possible the future development of anti-HCV drugs targeted to budding. These membranotropic regions could be envisaged as new possible targets, as inhibition of its interaction with the membrane could potentially lead to new vaccine strategies.

ACKNOWLEDGEMENTS

A. J. Pérez-Berná is a recipient of pre-doctoral fellowship from the Autonomous Government of the Valencian Community, Spain. A. S. Veiga acknowledges a grant (SFRH/BD/14336/2003) under the program POCTI to FCT-MCIES (Portugal). This study was funded in full by Ministerio de Ciencia y Tecnología, Spain, grant number BFU2005-00186-BMC (J. Villalaín). We are especially grateful to the National Institutes of Health AIDS Research and Reference Reagent Program, Division of AIDS, NIAID, NIH, for the peptides used in this work, as well as to Ana I. Gómez for expert technical assistance.

REFERENCES

- 1 Chen SL, Morgan TR. The natural history of hepatitis C virus (HCV) infection. *Int J Med Sci* 2006; 3(2): 47–52.
- 2 Penin F, Dubuisson J, Rey FA, Moradpour D, Pawlotsky JM. Structural biology of hepatitis C virus. *Hepatology* 2004; 39(1): 5–19.
- 3 Tan SL, Pause A, Shi Y, Sonenberg N. Hepatitis C therapeutics: current status and emerging strategies. *Nat Rev Drug Discov* 2002; 1(11): 867–881.
- 4 Qureshi SA. Hepatitis C virus-biology, host evasion strategies, and promising new therapies on the horizon. *Med Res Rev* 2007; 27(3): 353–373.
- 5 Vauloup-Fellous C, Pene V, Garaud-Aunis J *et al.* Signal peptide peptidase-catalyzed cleavage of hepatitis C virus core protein is dispensable for virus budding but destabilizes the viral capsid. *J Biol Chem* 2006; 281(38): 27679–27692.
- 6 Cha TA, Beall E, Irvine B *et al.* At least five related, but distinct, hepatitis C viral genotypes exist. *Proc Natl Acad Sci USA* 1992; 89(15): 7144–7148.
- 7 Lee SK, Park SO, Joe CO, Kim YS. Interaction of HCV core protein with 14-3-3epsilon protein releases Bax to activate

- apoptosis. *Biochem Biophys Res Commun* 2007; 352(3): 756–762.
- 8 Irshad M, Dhar I. Hepatitis C virus core protein: an update on its molecular biology, cellular functions and clinical implications. *Med Princ Pract* 2006; 15(6): 405–416.
 - 9 Kunkel M, Watowich SJ. Biophysical characterization of hepatitis C virus core protein: implications for interactions within the virus and host. *FEBS Lett* 2004; 3: 174–180.
 - 10 Kato N. Molecular virology of hepatitis C virus. *Acta Med Okayama* 2001; 55(3): 133–159.
 - 11 Boulant S, Vanbelle C, Ebel C, Penin F, Lavergne JP. Hepatitis C virus core protein is a dimeric alpha-helical protein exhibiting membrane protein features. *J Virol* 2005; 79(17): 11353–11365.
 - 12 McLauchlan J. Properties of the hepatitis C virus core protein: a structural protein that modulates cellular processes. *J Viral Hepat* 2000; 7(1): 2–14.
 - 13 Guillen J, Perez-Berna AJ, Moreno MR, Villalain J. Identification of the membrane-active regions of the severe acute respiratory syndrome coronavirus spike membrane glycoprotein using a 1618-mer peptide scan: implications for the viral fusion mechanism. *J Virol* 2005; 79(3): 1743–1752.
 - 14 Perez-Berna AJ, Moreno MR, Guillen J, Bernabeu A, Villalain J. The membrane-active regions of the hepatitis C virus E1 and E2 envelope glycoproteins. *Biochemistry* 2006; 45(11): 3755–3768.
 - 15 Moreno MR, Giudici M, Villalain J. The membranotropic regions of the endo and ecto domains of HIV gp41 envelope glycoprotein. *Biochim Biophys Acta* 2006; 1758(1): 111–123.
 - 16 Böttcher CSF, Van Gent CM, Fries C. A rapid and sensitive sub-micro phosphorus determination. *Anal Chim Acta* 1961; 1061: 203–204.
 - 17 Edelhoch H. Spectroscopic determination of tryptophan and tyrosine in proteins. *Biochemistry* 1967; 6(7): 1948–1954.
 - 18 Struck DK, Hoekstra D, Pagano RE. Use of resonance energy transfer to monitor membrane fusion. *Biochemistry* 1981; 20(14): 4093–4099.
 - 19 Meers P, Ali S, Erukulla R, Janoff AS. Novel inner monolayer fusion assays reveal differential monolayer mixing associated with cation-dependent membrane fusion. *Biochim Biophys Acta* 2000; 1467(1): 227–243.
 - 20 Contreras LM, Aranda FJ, Gavilanes F, Gonzalez-Ros JM, Villalain J. Structure and interaction with membrane model systems of a peptide derived from the major epitope region of HIV protein gp41: implications on viral fusion mechanism. *Biochemistry* 2001; 40(10): 3196–3207.
 - 21 Pascual R, Moreno MR, Villalain J. A peptide pertaining to the loop segment of human immunodeficiency virus gp41 binds and interacts with model biomembranes: implications for the fusion mechanism. *J Virol* 2005; 79(8): 5142–5152.
 - 22 Wimley WC, White SH. Experimentally determined hydrophobicity scale for proteins at membrane interfaces. *Nat Struct Biol* 1996; 3(10): 842–848.
 - 23 White SH, Wimley WC. Membrane protein folding and stability: physical principles. *Annu Rev Biophys Biomol Struct* 1999; 28: 319–365.
 - 24 Ahn A, Gibbons DL, Kielian M. The fusion peptide of Semliki Forest virus associates with sterol-rich membrane domains. *J Virol* 2002; 76(7): 3267–3275.
 - 25 Pascual R, Contreras M, Fedorov A, Prieto M, Villalain J. Interaction of a peptide derived from the N-heptad repeat region of gp41 Env ectodomain with model membranes. Modulation of phospholipid phase behavior. *Biochemistry* 2005; 44(43): 14275–14288.
 - 26 Ait-Goughoulte M, Hourieux C, Patient R, Trassard S, Brand D, Roingeard P. Core protein cleavage by signal peptide peptidase is required for hepatitis C virus-like particle assembly. *J Gen Virol* 2006; 4: 855–860.
 - 27 Hourieux C, Ait-Goughoulte M, Patient R *et al.* Core protein domains involved in hepatitis C virus-like particle assembly and budding at the endoplasmic reticulum membrane. *Cell Microbiol* 2007; 9(4): 1014–1027.
 - 28 Matto M, Rice CM, Aroeti B, Glenn JS. Hepatitis C virus core protein associates with detergent-resistant membranes distinct from classical plasma membrane rafts. *J Virol* 2004; 78(21): 12047–12053.
 - 29 de Almeida RF, Fedorov A, Prieto M. Sphingomyelin/phosphatidylcholine/cholesterol phase diagram: boundaries and composition of lipid rafts. *Biophys J* 2003; 85(4): 2406–2416.
 - 30 de Almeida RF, Loura LM, Fedorov A, Prieto M. Lipid rafts have different sizes depending on membrane composition: a time-resolved fluorescence resonance energy transfer study. *J Mol Biol* 2005; 346(4): 1109–1120.
 - 31 Nolandt O, Kern V, Muller H *et al.* Analysis of hepatitis C virus core protein interaction domains. *J Gen Virol* 1997; 6: 1331–1340.
 - 32 Hope RG, McLauchlan J. Sequence motifs required for lipid droplet association and protein stability are unique to the hepatitis C virus core protein. *J Gen Virol* 2000; 8: 1913–1925.
 - 33 Hope RG, Murphy DJ, McLauchlan J. The domains required to direct core proteins of hepatitis C virus and GB virus-B to lipid droplets share common features with plant oleosin proteins. *J Biol Chem* 2002; 277(6): 4261–4270.
 - 34 Nakai K, Okamoto T, Kimura-Someya T *et al.* Oligomerization of hepatitis C virus core protein is crucial for interaction with the cytoplasmic domain of E1 envelope protein. *J Virol* 2006; 80(22): 11265–11273.
 - 35 Suzuki R, Sakamoto S, Tsutsumi T *et al.* Molecular determinants for subcellular localization of hepatitis C virus core protein. *J Virol* 2005; 79(2): 1271–1281.
 - 36 Boulant S, Montserret R, Hope RG *et al.* Structural determinants that target the hepatitis C virus core protein to lipid droplets. *J Biol Chem* 2006; 281(31): 22236–22247.
 - 37 Jolivet-Reynaud C, Dalbon P, Viola F *et al.* HCV core immunodominant region analysis using mouse monoclonal antibodies and human sera: characterization of major epitopes useful for antigen detection. *J Med Virol* 1998; 56(4): 300–309.
 - 38 Majeau N, Gagne V, Boivin A *et al.* The N-terminal half of the core protein of hepatitis C virus is sufficient for nucleocapsid formation. *J Gen Virol* 2004; 4: 971–81.

Chapter IX

BIBLIOGRAPHY

Aasa-Chapman MMI, Hayman A, Newton P, Cornforth D, Williams I, Borrow P, Balfe P, and McKnight A (2004) Development of the antibody response in acute HIV-1 infection. *Aids* 18, 371-381.

Alam SM, Paleos CA, Liao H-X, Scarce R, Robinson J, and Haynes BF (2004) An inducible HIV type 1 gp41 HR-2 peptide-binding site on HIV type 1 envelope gp120. *Aids Res. Hum. Retrovir.* 20, 836-845.

Alam SM, McAdams M, Boren D, Rak M, Scarce RM, Gao F, Camacho ZT, Gewirth D, Kelsoe G, Chen P, and Haynes BF (2007) The role of antibody polyspecificity and lipid reactivity in binding of broadly neutralizing anti-HIV-1 envelope human monoclonal antibodies 2F5 and 4E10 to glycoprotein 41 membrane proximal envelope epitopes. *J. Immunol.* 178, 4424-4435.

Allaway GP, Davis-Bruno KL, Beaudry GA, Garcia EB, Wong EL, Ryder AM, Hasel KW, Gauduin MC, Koup RA, McDougal JS, et al. (1995) Expression and characterization of CD4-IgG2, a novel heterotetramer that neutralizes primary HIV type 1 isolates. *Aids Res. Hum. Retrovir.* 11, 533-539.

Aloia RC, Tian H, and Jensen FC (1993) Lipid composition and fluidity of the human immunodeficiency virus envelope and host cell plasma membranes. *Proc. Natl. Acad. Sci. USA* 90, 5181-5185.

Alving CR, Beck Z, Karasavva N, Matyas GR, and Rao M (2006) HIV-1, lipid rafts, and antibodies to liposomes: implications for anti-viral-neutralizing antibodies. *Mol. Membr. Biol.* 23, 453-465.

Bacia K, Scherfeld D, Kahya N, and Schwille P (2004) Fluorescence correlation spectroscopy relates rafts in model and native membranes. *Biophys. J.* 87, 1034-1043.

Barbato G, Bianchi E, Ingallinella P, Hurni WH, Miller MD, Ciliberto G, Cortese R, Bazzo R, Shiver JW, and Pessi A (2003) Structural analysis of the epitope of the anti-HIV antibody 2F5 sheds light into its mechanism of neutralization and HIV fusion. *J. Mol. Biol.* 330, 1101-1115.

Bartlam M, Xu Y, and Rao Z (2007) Structural proteomics of the SARS coronavirus: a model response to emerging infectious diseases. *J. Struct. Funct. Genomics. In press*, DOI 10.1007/s10969-007-9024-5.

Beck Z, Karasavvas N, Tong J, Matyas GR, Mangala R, and Alving CR (2007) Calcium modulation of monoclonal antibody binding to phosphatidylinositol phosphate. *Biochem. Biophys. Res. Commun.* 354, 747-751.

Berger EA, Murphy PM, and Farber JM (1999) Chemokine receptors as HIV-1 coreceptors: roles in viral entry, tropism, and disease. *Annu. Rev. Immunol.* 17, 657-700.

Blumenthal R, Sarkar DP, Durell S, Howard DE, and Morris SJ (1996) Dilation of the influenza hemagglutinin fusion pore revealed by the kinetics of individual cell-cell fusion events. *J. Cell Biol.* 135, 63-71.

Bosch BJ, van der Zee R, de Haan CAM, and Rottier PJM (2003) The coronavirus spike protein is a class I virus fusion protein: structural and functional characterization of the fusion core complex. *J. Virol.* 77, 8801-8811.

Bosch BJ, Martina BEE, van der Zee R, Lepault J, Haijema BJ, Versluis C, Heck AJR, de Groot R, Osterhaus ADME, and Rottier PJM (2004) Severe acute respiratory coronavirus (SARS-CoV) infection inhibition using spike protein heptad repeat-derived peptides. *Proc. Natl. Acad. Sci. USA* 101, 8455-8460.

Bratton DL, Fadok VA, Richter DA, Kailey JM, Guthrie LA, and Henson PM (1997) Appearance of phosphatidylserine and apoptotic cells requires calcium-mediated nonspecific flip-flop and is enhanced by loss of the aminophospholipid translocase. *J. Biol. Chem.* 272, 26159-26165.

Brinkman K, ter Hofstede HJM, Burger DM, Smeitink JAM, and Koopmans PP (1998) Adverse effects of reverse transcriptase inhibitors: mitochondrial toxicity as common pathway. *Aids* 12, 1735-44.

Briz V, Poveda E, and Soriano V (2006) HIV entry inhibitors: mechanisms of action and resistance pathways. *J. Antimicrob. Chemother.* 57, 619-627.

Brown BK, Karasavvas N, Beck Z, Matyas GR, Birx DL, Polonis VR, and Alving CR (2007) Monoclonal antibodies to phosphatidylinositol phosphate neutralize human immunodeficiency virus type 1: role of phosphate-binding subsites. *J. Virol.* 81, 2087-2091.

Brügger B, Glass B, Haberkant P, Leibrecht I, Wieland FT, and Kräusslich H-G (2006) The HIV lipidome: a raft with an unusual composition. *Proc. Natl. Acad. Sci. USA* 103, 2641-2646.

Brunel FM, Zwick MB, Cardoso RMF, Nelson JD, Wilson IA, Burton DN, and Dawson PE (2006) Structure-function analysis of the epitope for 4E10, a broadly neutralizing human immunodeficiency virus type 1 antibody. *J. Virol.* 80, 1680-1687.

Burkly LC, Olson D, Shapiro R, Winkler G, Rosa JJ, Thomas DW, Williams C, and Chisholm P (1992) Inhibition of HIV infection by a novel CD4 domain 2-specific monoclonal antibody. Dissecting the basis for its inhibitory effect on HIV-induced cell fusion. *J. Immunol.* 149, 1779-1787.

Campbell SM, Crowe SM, and Mak J (2001) Lipid rafts and HIV-1: from viral entry to assembly of progeny virions. *J. Clin. Virol.* 22, 217-227.

Campbell SM, Crowe SM, and Mak J (2002) Virion-associated cholesterol is critical for the maintenance of HIV-1 structure and infectivity. *Aids* 16, 2253-2261.

Campbell S, Gaus K, Bittman R, Jessup W, Crowe S, and Mak J (2004) The raft-promoting property of virion-associated cholesterol, but not the presence of virion-associated Brij 98 rafts, is a determinant of human immunodeficiency virus type 1 infectivity. *J. Virol.* 78, 10556-10565.

Cardoso RMF, Zwick MB, Stanfield RL, Kunert R, Binley JM, Katinger H, Burton DR, and Wilson IA (2005) Broadly neutralizing anti-HIV antibody 4E10 recognizes a helical conformation of a highly conserved fusion-associated motif in gp41. *Immunity* 22, 163-173.

Carr A, Samaras K, Thorisdottir A, Kaufmann GR, Chisholm DJ, and Cooper DA (1999) Diagnosis, prediction, and natural course of HIV-1 protease-inhibitor-associated lipodystrophy, hyperlipidaemia, and diabetes mellitus: a cohort study. *Lancet* 353, 2093-2099.

Carr A (2003) Toxicity of antiretroviral therapy and implications for drug development. *Nature* 2, 624-634.

Castanho MARB and Fernandes MX (2006) Lipid membrane-induced optimization for ligand-receptor docking: recent tools and insights for the “membrane catalysis” model. *Eur. Biophys. J.* 35, 92-103.

Center RJ, Leapman RD, Lebowitz J, Arthur LO, Earl PL, and Moss B (2002) Oligomeric structure of the human immunodeficiency virus type 1 envelope protein on the virion surface. *J. Virol.* 76, 7863-7867.

Chambers P, Pringle CR, and Easton AJ (1990) Heptad repeat sequences are located adjacent to hydrophobic regions in several types of virus fusion glycoproteins. *J. Gen. Virol.* 71, 3075-3080.

Chan DC, Fass D, Berger JM, and Kim PS (1997) Core structure of gp41 from the HIV envelope glycoprotein. *Cell* 89, 263-273.

Chan DC and Kim PS (1998) HIV entry and its inhibition. *Cell* 93, 681-684.

Chan DC, Chutkowski CT, and Kim PS (1998) Evidence that a prominent cavity in the coiled coil of HIV type 1 gp41 is an attractive drug target. *Proc. Natl. Acad. Sci. USA* 95, 15613-15617.

Chen C-H, Matthews TJ, McDanal CB, Bolognesi DP, and Greenberg ML (1995) A molecular clasp in the human immunodeficiency virus (HIV) type 1 TM protein determines the anti-HIV activity of gp41 derivatives: implication for viral fusion. *J. Virol.* 69, 3771-3777.

Chen F, Chan KH, Jiang Y, Kao RYT, Lu HT, Fan KW, Cheng VCC, Tsui WHW, Hung IFN, Lee TSW, et al. (2004) In vitro susceptibility of 10 clinical isolates of SARS coronavirus to selected antiviral compounds. *J. Clin. Virol.* 31, 69-75.

Chen XP and Cao Y (2004) Consideration of highly active antiretroviral therapy in the prevention and treatment of severe acute respiratory syndrome. *Clin. Infect. Dis.* 38, 1030-1032.

Chesebro B, Buller R, Portis J, and Wehrly K (1990) Failure of human immunodeficiency virus entry and infection in CD4-positive human brain and skin cells. *J. Virol.* 64, 215-221.

Cinatl J, Jr, Michaelis M, Hoever G, Preiser W, and Doerr HW (2005) Development of antiviral therapy for severe acute respiratory syndrome. *Antiviral Res.* 66, 81-97.

Clapham PR, Blanc D, and Weiss RA (1991) Specific cell surface requirements for the infection of CD4-positive cells by human immunodeficiency virus types 1 and 2 and by simian immunodeficiency virus. *Virology* 181, 703-715.

Clapham PR and McKnight A (2002) Cell surface receptors, virus entry and tropism of primate lentiviruses. *J. Gen. Virol.* 83, 1809-1829.

Coëffier E, Clément J-M, Cussac V, Khodaei-Boorane N, Jehanno M, Rojas M, Dridi A, Latour M, El Habib R, Barré-Sinoussi F, et al. (2001) Antigenicity and immunogenicity of the HIV-1 gp41 epitope ELDKWA inserted into permissive sites of the MalE protein. *Vaccine* 19, 684-693.

Conley AJ, Kessler II JA, Boots LJ, Tung J-S, Arnold BA, Keller PM, Shaw AR, and Emini EA (1994) Neutralization of divergent human immunodeficiency virus type 1 variants and primary isolates by IAM-41-2F5, an anti-gp41 human monoclonal antibody. *Proc. Natl. Acad. Sci. USA* 91, 3348-3352.

Contreras LM, Aranda FJ, Gavilanes F, González-Ros JM, and Villalaín J (2001) Structure and interaction with membrane model systems of a peptide derived from the major epitope region of HIV protein gp41: implications on viral fusion mechanism. *Biochemistry* 40, 3196-3207.

Dando TM and Perry CM (2003) Enfuvirtide. *Drugs* 63, 2755-2766.

de Almeida RFM, Fedorov A, and Prieto M (2003) Sphingomyelin/Phosphatidylcholine/Cholesterol phase diagram: boundaries and composition of lipid rafts. *Biophys. J.* 85, 2406-2416.

de Almeida RFM, Loura LMS, Fedorov A, and Prieto M (2005) Lipid rafts have different sizes depending on membrane composition: a time-resolved fluorescence resonance energy transfer study. *J. Mol. Biol.* 346, 1109-1120.

De Clercq E (2004) HIV-chemotherapy and –prophylaxis: new drugs, leads and approaches. *Int. J. Biochem. Cell Biol.* 36, 1800-1822.

Deng Y, Zheng Q, Ketas TJ, Moore JP, and Lu M (2007) Protein design of a bacterially expressed HIV-1 gp41 fusion inhibitor. *Biochemistry* 46, 4360-4369.

De Planque MRR, Bonev BB, Demmers JAA, Greathouse DV, Koeppe II RE, Separovic F, Watts A, and Killian JA (2003) Interfacial anchor properties of tryptophan residues in transmembrane peptides can dominate over hydrophobic matching effects in peptide-lipid interactions. *Biochemistry* 42, 5341-5348.

Derdeyn CA, Decker JM, Sfakianos JN, Wu X, O'Brien WA, Ratner L, Kappes JC, Shaw GM, and Hunter E (2000) Sensitivity of human immunodeficiency virus type 1 to the fusion inhibitor T-20 is modulated by coreceptor specificity defined by the V3 loop of gp120. *J. Virol.* 74, 8358-8367.

Derdeyn CA, Decker JM, Sfakianos JN, Zhang Z, O'Brien WA, Ratner L, Shaw GM, and Hunter E (2001) Sensitivity of human immunodeficiency virus type 1 to fusion inhibitors targeted to the gp41 first heptad repeat involves distinct regions of gp41 and is consistently modulated by gp120 interactions with the coreceptor. *J. Virol.* 75, 8605-8614.

De Rosny E, Vassel R, Jiang S, Kunert R, and Weiss C (2004) Binding of the 2F5 monoclonal antibody to native and fusion-intermediate forms of human immunodeficiency virus type 1 gp41: implications for fusion-inducing conformational changes. *J. Virol.* 78, 2627-2631.

Derossi D, Chassaing G, and Prochiantz A (1998) Trojan peptides: the penetratin system for intracellular delivery. *Trends Cell Biol.* 8, 84-87.

Di Bello C, Pasquato A, and Dettin M (2004) Synthetic peptides for AIDS research. *Curr. Protein Pept. Sci.* 5, 225-234.

Dietrich C, Yang B, Fujiwara T, Kusumi A, and Jacobson K (2002) Relationship of lipid rafts to transient confinement zones detected by single particle tracking. *Biophys. J.* 82, 274-284.

Dimitrov AS, Rawat SS, Jiang S, and Blumenthal R (2003) Role of the fusion peptide and membrane-proximal domain in HIV-1 envelope glycoprotein-mediated membrane fusion. *Biochemistry* 42, 14150-14158.

Ding Y, He L, Zhang Q, Huang Z, Che X, Hou J, Wang H, Shen H, Qiu L, Li Z, et al. (2004) Organ distribution of severe acute respiratory syndrome (SARS) associated coronavirus (SARS-CoV) in SARS patients: implications for pathogenesis and virus transmission pathways. *J. Pathol.* 203, 622-630.

Douek DC, Picker LJ, and Koup RA (2003) T cell dynamics in HIV-1 infection. *Annu. Rev. Immunol.* 21, 265-304.

Drosten C, Günther S, Preiser W, van der Werf S, Brodt H, Becker S, Rabenau H, Panning M, Kolesnikova L, Fouchier RAM, et al. (2003) Identification of a novel coronavirus in patients with severe acute respiratory syndrome. *N. Engl. J. Med.* 348, 1967-1976.

D'Souza MP, Livnat D, Bradac JA, Bridges SH, the AIDS clinical trials group, Antibody selection working group, and collaborating investigators (1997) Evaluation of monoclonal antibodies to human immunodeficiency virus type 1 primary isolates by neutralization assays: performance criteria for selecting candidate antibodies for clinical trials. *J. Infect. Dis.* 175, 1056-1062.

Dwyer JJ, Wilson KL, Davison DK, Freel SA, Seedorff JE, Wring SA, Tvermoes NA, Matthews TJ, Greenberg ML, and Delmedico MK (2007) Design of helical, oligomeric HIV-1 fusion inhibitor peptides with potent activity against enfuvirtide-resistant virus. *Proc. Natl. Acad. Sci. USA* 104, 12772-12777.

Eckert DM and Kim PS (2001a) Mechanisms of viral membrane fusion and its inhibition. *Annu. Rev. Biochem.* 70, 777-810.

Eckert DM and Kim PS (2001b) Design of potent inhibitors of HIV-1 entry from the gp41 N-peptide region. *Proc. Natl. Acad. Sci. USA* 98, 11187-11192.

Eddidin M (2003a) Lipids on the frontier: a century of cell-membrane bilayers. *Nature* 4, 414-418.

Eddidin M (2003b) The state of lipid rafts: from model membranes to cells. *Annu. Rev. Biophys. Biomolec. Struct.* 32, 257-283.

Epanand RM and Vogel HJ (1999) Diversity of antimicrobial peptides and their mechanisms of action. *Biochim. Biophys. Acta* 1462, 11-28.

Epanand RM (2003) Fusion peptides and the mechanism of viral fusion. *Biochim. Biophys. Acta* 1614, 116-121.

Epanand RM, Sayer BG, and Epanand RF (2003) Peptide-induced formation of cholesterol-rich domains. *Biochemistry* 42, 14677-14689.

Epanand RM (2004) Do proteins facilitate the formation of cholesterol-rich domains? *Biochim. Biophys. Acta* 1666, 227-238

Epanand RF, Sayer BG, and Epanand RM (2005) The tryptophan-rich region of HIV gp41 and the promotion of cholesterol-rich domains. *Biochemistry* 44, 5525-5531.

Epanand RM (2006) Cholesterol and the interaction of proteins with membrane domains. *Prog. Lipid Res.* 45, 279-294.

Epanand RF, Thomas A, Brasseur R, Vishwanathan SA, Hunter E, and Epanand RM (2006) Juxtamembrane protein segments that contribute to recruitment of cholesterol into domains. *Biochemistry* 45, 6105-6114.

Eron JJ, Gulick RM, Bartlett JA, Merigan T, Arduino R, Kilby JM, Yangco B, Diers A, Drobnes C, DeMasi R, et al. (2004) Short-term safety and antiretroviral activity of T-1249, a second-generation fusion inhibitor of HIV. *J. Infect. Dis.* 189, 1075-1083.

Fadok VA, Voelker DR, Campbell PA, Cohen JJ, Bratton DL, and Henson PM (1992) Exposure of phosphatidylserine on the surface of apoptotic lymphocytes triggers specific recognition and removal by macrophages. *J. Immunol.* 148, 2207-2216.

Farcas GA, Poutanen SM, Mazzulli T, Willey BM, Butany J, Asa SL, Faure P, Akhavan P, Low DE, and Kain KC (2005) Fatal severe acute respiratory syndrome is associated with multiorgan involvement by coronavirus. *J. Infect. Dis.* 191, 193-197.

Feigenson GW and Buboltz JT (2001) Ternary phase diagram of dipalmitoyl-PC/dilauroyl-PC/cholesterol: nanoscopic domain formation driven by cholesterol. *Biophys. J.* 80, 2775-2788.

Ferrantelli F and Ruprecht RM (2002) Neutralizing antibodies against HIV – back in the major leagues? *Curr. Opin. Immunol.* 14, 495-502.

Follis KE, Larson SJ, Lu M, and Nunberg JH (2002) Genetic evidence that interhelical packing interactions in the gp41 core are critical for transition of the human immunodeficiency virus type 1 envelope glycoprotein to the fusion-active state. *J. Virol.* 76, 7356-7362.

Fragoso R, Ren D, Zhang X, Su MW-C, Burakoff SJ, and Jin Y-J (2003) Lipid raft distribution of CD4 depends on its palmitoylation and association with Lck, and evidence for CD4-induced lipid raft aggregation as an additional mechanism to enhance CD3 Signalling. *J. Immunol.* 170, 913-921.

Furuta RA, Wild CT, Weng Y, and Weiss CD (1998) Capture of an early fusion-active conformation of HIV-1 gp41. *Nat. Struct. Biol.* 5, 276-279.

Gallagher TM and Buchmeier MJ (2001) Coronavirus spike proteins in viral entry and pathogenesis. *Virology* 279, 371-374.

Gallaher WR and Garry RF. Model of the pre-insertion region of the spike (S2) fusion glycoprotein of the human SARS coronavirus: implications for antiviral therapeutics. *Virology*. <http://www.virology.net/Articles/sars/s2model.html>. (Accessed 13 May 2003).

Gallo SA, Puri A, and Blumenthal R (2001) HIV-1 gp41 six-helix bundle formation occurs rapidly after the engagement of gp120 by CXCR4 in the HVI-1 env-mediated fusion process. *Biochemistry* 40, 12231-12236.

Gallo SA, Clore GM, Louis JM, Bewley CA, and Blumenthal R (2004) Temperature-dependent intermediates in HIV-1 envelope glycoprotein-mediated fusion revealed by inhibitors that target N- and C-terminal helical regions of HIV-1 gp41. *Biochemistry* 43, 8230-8233.

Gennis RB (1989) *Biomembranes - molecular structure and function*, Springer-Verlag, New York, NJ, USA.

Gorny MK and Zolla-Pazner S (2000) Recognition by human monoclonal antibodies of free and complexed peptides representing the prefusogenic and fusogenic forms of human immunodeficiency virus type 1 gp41. *J. Virol.* 74, 6186-6192.

Graham DRM, Chertova E, Hilburn JM, Arthur LO, and Hildreth JEK (2003) Cholesterol depletion of human immunodeficiency virus type 1 and simian immunodeficiency virus with β -cyclodextrin inactivates and permeabilizes the virions: evidence for virion-associated lipid rafts. *J. Virol.* 77, 8237-8248.

Greenberg ML, Davison D, Jin L, Mosier S, Melby T, Sista P, Demasi R, Miralles D, Cammack N, and Matthews TJ (2002) In vitro antiviral activity of T-1249 a second generation fusion inhibitor. *Antivir. Ther.* 7, S10.

Greenberg ML and Cammack N (2004) Resistance to enfuvirtide, the first HIV fusion inhibitor. *J. Antimicrob. Chemother.* 54, 333-340.

Grundner C, Mirzabekov T, Sodroski J, and Wyatt R (2002) Solid-phase proteoliposomes containing human immunodeficiency virus envelope glycoproteins. *J. Virol.* 76, 3511-3521.

Guan Y, Zheng BJ, He YQ, Liu XL, Zhuang ZX, Cheung CL, Luo SW, Li PH, Zhang LJ, Guan YJ et al (2003) Isolation and characterization of viruses related to the SARS coronavirus from animals in southern china. *Science* 302, 276-278.

Guillén J, Pérez-Berná AJ, Moreno MR, and Villalaín J (2005) Identification of the membrane-active regions of the severe-acute respiratory syndrome coronavirus spike membrane glycoprotein using a 16/18-mer peptide scan: implications for the viral fusion mechanism. *J. Virol.* 79, 1743-1752.

Gulick RM (2003) New antiretroviral drugs. *Clin. Microbiol. Infect.* 9, 186-193.

Guo Q, Ho H-T, Dicker I, Fan L, Zhou N, Friborg J, Wang T, McAuliffe BV, Wang HH, Rose RE, et al. (2003) Biochemical and genetic characterizations of a novel human immunodeficiency virus type 1 inhibitor that blocks gp120-CD4 interactions. *J. Virol.* 77, 10528-10536.

Guyader M, Kiyokawa E, Abrami L, Turelli P, and Trono D (2002) Role for human immunodeficiency virus type 1 membrane cholesterol in viral internalization. *J. Virol.* 76, 10356-10364.

Hager-Braun C, Katinger H, and Tomer KB (2006) The HIV-neutralizing monoclonal antibody 4E10 recognizes N-terminal sequences on the native antigen. *J. Immunol.* 176, 7471-7481.

Hamming I, Timens W, Bulthuis MLC, Lely AT, Navis GJ, and van Goor H (2004) Tissue distribution of ACE2 protein, the functional receptor for SARS coronavirus. A first step in understanding SARS pathogenesis. *J. Pathol.* 203, 631-637.

Hancock REW and Diamond G (2000) The role of cationic antimicrobial peptides in innate host defences. *Trends Microbiol.* 8, 402-410.

Hancock JF (2007) Lipid rafts: contentious only from simplistic standpoints. *Nat. Rev. Mol. Cell Biol.* 7, 456-462.

Haynes BF, Fleming J, St. Clair EW, Katinger H, Stiegler G, Kunert R, Robinson J, Scarce RM, Plonk K, Staats HF, Ortel TL, Liao H-X, and Alam SM (2005) Cardiolipin polyspecific autoreactivity in two broadly neutralizing HIV-1 antibodies. *Science* 308, 1906-1908.

Hildinger M, Dittmar MT, Schult-Dietrich P, Fehse B, Schnierle BS, Thaler S, Stiegler G, Welker R, and von Laer D (2001) Membrane-anchored peptide inhibits human immunodeficiency virus entry. *J. Virol.* 75, 3038-3042.

Hirsch MS, Conway B, D'Aquila RT, Johnson VA, Brun-Vezinet F, Clotet B, Demeter LM, Hammer SM, Jacobsen DM, Kuritzkes DR, et al. (1998) Antiretroviral drug resistance testing in adults with HIV infection: implications for clinical management. *Jama* 279, 1984-1991.

Ichiyama K, Yokoyama-Kumakura S, Tanaka Y, Tanaka R, Hirose K, Bannai K, Edamatsu T, Yanaka M, Niitani Y, Miyano-Kurosaki N, et al. (2003) A duodenally absorbable CXC chemokine receptor 4 antagonist, KRH-1636, exhibits a potent and selective anti-HIV-1 activity. *Proc. Natl. Acad. Sci. USA* 100, 4185-4190.

Ingallinella P, Bianchi E, Finotto M, Cantoni G, Eckert DM, Supekar VM, Bruckmann C, Carfi A, and Pessi A (2004) Structural characterization of the fusion-active complex of severe acute respiratory syndrome (SARS) coronavirus. *Proc. Natl. Acad. Sci. USA* 101, 8709-8714.

Ipsen JH, Mouritsen OG, and Bloom M (1990) Relationships between lipid membrane area, hydrophobic thickness, and acyl-chain orientational order. The effects of cholesterol. *Biophys. J.* 57, 405-412.

Jacobson K, Mouritsen OG, and Anderson RGW (2007) Lipid rafts: at a crossroad between cell biology and physics. *Nat. Cell Biol.* 9, 7-14.

Janeway CA, Travers P, Walport M, Shlomchik M (2001) *Immunobiology, The immune system in health and disease*, fifth edition, Garland Publishing, New York.

Jiang S, Zhao Q, and Debnath AK (2002) Peptide and non-peptide HIV fusion inhibitors. *Curr. Pharm. Design* 8, 563-580.

Joshi SB, Dutch RE, and Lamb RA (1998) A core trimer of the paramyxovirus fusion protein: parallels to influenza virus hemagglutinin and HIV-1 gp41. *Virology* 248, 20-34.

Joyce JG, Hurni WM, Bogusky MJ, Garsky VM, Liang X, Citron MP, Danzeisen RC, Miller MD, Shiver JW, and Keller PM (2002) Enhancement of α -helicity in the HIV-1 inhibitory peptide DP178 leads to an increased affinity for human monoclonal antibody 2F5 but does not elicit neutralizing responses *in vitro*. *J. Biol. Chem.* 277, 45811-45820.

Kilby JM, Hopkins S, Venetta TM, DiMassimo B, Cloud GA, Lee JY, Alldredge L, Hunter E, Lambert D, Bolognesi D, et al. (1998) Potent suppression of HIV-1 replication in humans by T-20, a peptide inhibitor of gp41-mediated virus entry. *Nat. Med.* 4, 1302-1307.

Kilby JM and Eron JJ (2003) Novel therapies based on mechanisms of HIV-1 cell entry. *N. Engl. J. Med.* 348, 2228-2238.

Kilgore NR, Salzwedel K, Reddick M, Allaway GP, and Wild CT (2003) Direct evidence that C-peptide inhibitors of human immunodeficiency virus type 1 entry bind to the gp41 N-helical domain in receptor-activated viral envelope. *J. Virol.* 77, 7669-7672.

Killian JA and von Heijne G (2000) How proteins adapt to a membrane-water interface. *Trends Biochem. Sci.* 25, 429-434.

Kliger Y and Shai Y (1997) A leucine zipper-like sequence from the cytoplasmic tail of the HIV-1 envelope glycoprotein binds and perturbs lipid bilayers. *Biochemistry* 36, 5157-5169.

Kliger Y and Shai Y (2000) Inhibition of HIV-1 entry before gp41 folds into its fusion-active conformation. *J. Mol. Biol.* 295, 163-168.

Kliger Y, Peisajovich SG, Blumenthal R, and Shai Y (2000) Membrane-induced conformational change during the activation of HIV-1 gp41. *J. Mol. Biol.* 301, 905-914.

Kliger Y, Gallo SA, Peisajovich SG, Muñoz-Barroso I, Avkin S, Blumenthal R, and Shai Y (2001) Mode of action of an antiviral peptide from HIV-1. Inhibition at a post-lipid mixing stage. *J. Biol. Chem.* 276, 1391-1397.

Korazim O, Sackett K, and Shai Y (2006) Functional and structural characterization of HIV-1 gp41 ectodomain regions in phospholipid membranes suggests that the fusion-active conformation is extended. *J. Mol. Biol.* 364, 1103-1117.

Kozak SL, Heard JM, and Kabat D (2002) Segregation of CD4 and CXCR4 into distinct lipid microdomains in T lymphocytes suggests a mechanism for membrane destabilization by human immunodeficiency virus. *J. Virol.* 76, 1802-1815.

Kranenburg M and Smit B (2005) Phase behaviour of model lipid bilayers. *J. Phys. Chem. B* 109, 6653-6663.

Ksiazek TG, Erdman D, Goldsmith CS, Zaki SR, Peret T, Emery S, Tong S, Urbani C, Comer JA, Lim W, Rollin PE, Dowell SF, Ling A-E, et al. (2003) A novel coronavirus associated with severe acute respiratory syndrome. *N. Engl. J. Med.* 348, 1953-1966.

Kwong PD, Wyatt R, Robinson J, Sweet RW, Sodroski J, and Hendrickson WA (1998) Structure of an HIV gp120 envelope glycoprotein in complex with the CD4 receptor and a neutralizing human antibody. *Nature* 393, 648-659.

LaBranche CC, Galasso G, Moore JP, Bolognesi DP, Hirsch MS and Hammer SM (2001) HIV fusion and its inhibition. *Antiviral Res.* 50, 95-115.

Ladokhin AS and White SH (1999) Folding of amphipathic α -helices on membranes: energetics of helix formation by melittin. *J. Mol. Biol.* 285, 1363-1369.

Lazzarin A, Clotet B, Cooper D, Reynes J, Arastéh K, Nelson M, Katlama C, Stellbrink H-J, Delfraissy J-F, Lange J, et al. (2003) Efficacy of enfuvirtide in patients infected with drug-resistant HIV-1 in Europe and Australia. *N. Engl. J. Med.* 348, 2186-2195.

Lalezari JP, Henry K, O'Hearn M, Montaner JSG, Piliero PJ, Trottier B, Walmsley S, Cohen C, Kuritzkes DR, Eron JJ, et al. (2003) Enfuvirtide, and HIV-1 fusion inhibitor, for drug-resistant HIV infection in north and south America. *N. Engl. J. Med.* 348, 2175-2185.

Lalezari JP, Bellos NC, Sathasivam K, Richmond GJ, Cohen CJ, Myers RA, Henry DH, Raskino C, Melby T, Murchison H, et al. (2005) T-1249 retains potent antiretroviral activity in patients who had experienced virological failure while on an enfuvirtide-containing treatment regimen. *J. Infect. Dis.* 191, 1155-1163.

Lau SKP, Woo PCY, Li KSM, Huang Y, Tsoi H-W, Wong BHL, Wong SSY, Leung K-H, and Yuen K-Y (2005) Severe acute respiratory syndrome coronavirus-like virus in Chinese horseshoe bats. *Proc. Natl. Acad. Sci. USA* 102, 14040-14045.

Lawless MK, Barney S, Guthrie KI, Bucy TB, Petteway SR, and Merutka G (1996) HIV-1 membrane fusion mechanism: structural studies of the interactions between biological-active peptides from gp41. *Biochemistry* 35, 13697-13708.

Lenz O, Dittmar MT, Wagner A, Ferko B, Vorauer-Uhl K, Stiegler G, and Weissenhorn W (2005) Trimeric membrane-anchored gp41 inhibits HIV membrane fusion. *J. Biol. Chem.* 280, 4095-4101.

- Li H and Papadopoulos V (1998) Peripheral-type benzodiazepine receptor function in cholesterol transport. Identification of a putative cholesterol recognition/interaction amino acid sequence and consensus pattern. *Endocrinology* 139, 4991-4997.
- Li Y, McDonald AM, Dore GJ, and Kaldor JM (2000) Improving survival following AIDS in Australia, 1991-1996. *Aids* 14, 2349-2354.
- Li W, Moore MJ, Vasilieva N, Sui J, Wong SK, Berne MA, Somasundaran M, Sullivan JL, Luzuriaga K, Greenough TC, Choe H, and Farzan M (2003) Angiotensin-converting enzyme 2 is a functional receptor for the SARS coronavirus. *Nature* 426, 450-454.
- Li W, Shi Z, Yu M, Ren W, Smith C, Epstein JH, Wang H, Crameri G, Hu Z, Zhang H, et al. (2005) Bats are natural reservoirs of SARS-like coronaviruses. *Science* 310, 676-679.
- Lichtenberg D, Goñi FM, and Heerklotz H (2005) Detergent-resistant membranes should not be identified with membrane rafts. *Trends Biochem. Sci.* 30, 430-436.
- Lindgren M, Hällbrink M, Prochiantz A, and Langel Ü (2000) Cell-penetrating peptides. *Trends Pharmacol. Sci.* 21, 99-103.
- Liu S, Xiao G, Chen Y, He Y, Niu J, Escalante CR, Xiong H, Farmer J, Debnath AK, Tien P, and Jiang S (2004) Interaction between heptad repeat 1 and 2 regions in spike protein of SARS-associated coronavirus: implications for virus fusogenic mechanism and identification of fusion inhibitors. *Lancet* 363, 938-947.
- Liu S, Lu H, Niu J, Xu Y, Wu S, and Jiang S (2005) Different from the HIV fusion inhibitor C34, the anti-HIV drug fuzeon (T-20) inhibits HIV-1 entry by targeting multiple sites in gp41 and gp120. *J. Biol. Chem.* 280, 11259-11273.
- Liu S, Wu S, and Jiang S (2007a) HIV entry inhibitors targeting gp41: from polypeptides to small-molecule compounds. *Curr. Pharm. Design* 13, 143-162.
- Liu S, Jing W, Cheung B, Lu H, Sun J, Yan X, Niu J, Farmer J, Wu S, and Jiang S (2007b) HIV gp41 C-terminal heptad repeat contains multifunctional domains. Relation to mechanisms of action of anti-HIV peptides. *J. Biol. Chem.* 282, 9612-9620.

Lorizate M, Gómara MJ, de la Torre BG, Anfreu D, and Nieva JL (2006) Membrane-transferring sequences of the HIV-1 gp41 ectodomain assemble into an immunogenic complex. *J. Mol. Biol.* 360, 45-55.

Louie M and Markowitz M (2002) Goals and milestones during treatment of HIV-1 infection with antiretroviral therapy: a pathogenesis-based perspective. *Antiviral Res.* 55, 15-25.

Loura LMS and de Almeida RFM (2004) *Tópicos de biofísica de membranas*. Lidel, Lisboa, Portugal.

Lu M, Blacklow SC, and Kim PS (1995) A trimeric structural domain of the HIV-1 transmembrane glycoprotein. *Nature Struct. Biol.* 2, 1075-1082.

Lu M, Ji H, and Shen S (1999) Subdomain folding and biological activity of the core structure from human immunodeficiency virus type 1 gp41: implications for viral membrane fusion. *J. Virol.* 73, 4433-4438.

Maddon PJ, Dalgleish AG, McDougal JS, Clapham PR, Weiss RA, and Axel R (1986) The T4 gene encodes the AIDS virus receptor and is expressed in the immune system and the brain. *Cell* 47, 333-348.

Maeda K, Nakata H, Koh Y, Miyakawa T, Ogata H, Takaoka Y, Shibayama S, Sagawa K, Fukushima D, Moravek J, et al. (2004) Spirodiketopiperazine-based CCR5 inhibitor which preserves CC-chemokine/CCR5 interactions and exerts potent activity against R5 human immunodeficiency virus type 1 in vitro. *J. Virol.* 78, 8654-8662.

Mañes S, Mira E, Gómez-Moutón C, Lacalle RA, Keller P, Labrador JP, and Martínez-A C (1999) Membrane raft microdomains mediate front-rear polarity in migrating cells. *Embo J.* 18, 6211-6220.

Mañes S, del Real G, Lacalle RA, Lucas P, Gómez-Moutón C, Sánchez-Palomino S, Delgado R, Alcami J, Mira E, and Martínez-A C (2000) Membrane raft microdomains mediate lateral assemblies required for HIV-1 infection. *EMBO Rep.* 1, 190-196.

Markosyan RM, Cohen FS, and Melikyan GB (2003) HIV-1 envelope proteins complete their folding into six-helix bundles immediately after fusion pore formation. *Mol. Biol. Cell* 14, 926-938.

Marra MA, Jones SJM, Astell CR, Holt RA, Brooks-Wilson A, Butterfield YSN, Khattra J, Asano JK, Barber SA, Chan SY, et al. (2003) The genome sequence of the SARS-associated coronavirus. *Science* 300, 1399-1404.

Martín-Carbonero L (2004) Discontinuation of the clinical development of fusion inhibitor T-1249. *Aids Rev.* 6, 61-63.

Matsuzaki K (1999) Why and how are peptide-lipid interactions utilized for self-defense? Magainins and tachyplesins as archetypes. *Biochim. Biophys. Acta* 1462, 1-10.

Mattews T, Salgo M, Greenberg M, Chung J, DeMasi R, and Bolognesi D (2004) Enfuvirtide: the first therapy to inhibit the entry of HIV-1 into host CD4 lymphocytes. *Nat. Rev. Drug Discov.* 3, 215-225.

McDonald RI (1993) Temperature and ionic effects on the interaction of erythroid spectrin with phosphatidylserine membranes. *Biochemistry* 32, 6957-6964.

Meers P and Mealy T (1993) Calcium-dependent annexin V binding to phospholipids: stoichiometry, specificity, and the role of negative charge. *Biochemistry* 32, 11711-11721.

Melikyan GB, Markosyan RM, Hemmati H, Delmedico MK, Lambert DM, and Cohen FS (2000) Evidence that the transition of HIV-1 gp41 into a six-helix bundle, not the bundle configuration, induces membrane fusion. *J. Cell Biol.* 151, 413-423.

Melikyan GB, Egelhofer M, and von Laer D (2006) Membrane-anchored inhibitory peptides capture human immunodeficiency virus type 1 gp41 conformations that engage the target membrane prior to fusion. *J. Virol.* 80, 3249-3258.

Menger FM, Chlebowski ME, Galloway AL, Lu H, Seredyuk VA, Sorrells JL, and Zhang H (2005) A tribute to the phospholipid. *Langmuir* 21, 10336-10341.

Mobley PW, Pilpa R, Brown C, Waring AJ, and Gordon LM (2001) Membrane-perturbing domains of HIV type 1 glycoprotein 41. *Aids Res. Hum. Retrovir.* 17, 311-327.

Mocroft A, Katlama C, Johnson AM, Pradier C, Antunes F, Mulcahy F, Chiesi A, Phillips AN, Kirk O, and Lundgren JD (2000) AIDS across Europe, 1994-98: the EuroSIDA study. *Lancet* 356, 291-296.

Moore JP, Trkola A, and Dragic T (1997) Co-receptors for HIV-1 entry. *Curr. Opin. Immunol.* 9, 551-562.

Moore JP and Stevenson M (2000) New targets for inhibitors of HIV-1 replication. *Nat. Rev. Mol. Cell Biol.* 1, 40-49.

Moore JP and Doms RW (2003) The entry of entry inhibitors: a fusion of science and medicine. *Proc. Natl. Acad. Sci. USA* 100, 10598-10602.

Moreno MR, Pascual R, and Villalaín J (2004) Identification of membrane-active regions of the HIV-1 envelope glycoprotein gp41 using a 15-mer gp41-peptide scan. *Biochim. Biophys. Acta* 1661, 97-105.

Moreno MR, Giudici M, and Villalaín J (2006) The membranotropic regions of the endo and ecto domains of HIV gp41 envelope glycoprotein. *Biochim. Biophys. Acta* 1758, 111-123.

Muñoz-Barroso I, Durell S, Sakaguchi K, Appella E, and Blumenthal R (1998) Dilation of the human immunodeficiency virus-1 envelope glycoprotein fusion pore revealed by the inhibitory action of a synthetic peptide from gp41. *J. Cell Biol.* 140, 315-323.

Muñoz-Barroso I, Salzwedel K, Hunter E, and Blumenthal R (1999) Role of the membrane-proximal domain in the initial stages of human immunodeficiency virus type 1 envelope glycoprotein-mediated membrane fusion. *J. Virol.* 73, 6089-6092.

Munro S (2003) Lipid rafts: elusive or illusive? *Cell* 115, 377-388.

Muster T, Steindl F, Purtscher M, Trkola A, Klima A, Himmler G, Rucker F, and Katinger H (1993) A conserved neutralizing epitope on gp41 of human immunodeficiency virus type 1. *J. Virol.* 67, 6642-6647.

Nabel GJ (2005) Close to the edge: neutralizing the HIV-1 envelope. *Science* 308, 1878-1879.

Nagashima KA, Thompson DAD, Rosenfield SI, Maddon PJ, Dragic T, and Olson WC (2001) Human immunodeficiency virus type 1 entry inhibitors PRO 542 and T-20 are potentially synergistic in locking virus-cell and cell-cell fusion. *J. Infect. Dis.* 183, 1121-1125.

Nguyen DH and Hildreth JEK (2000) Evidence for budding of human immunodeficiency virus type 1 selectively from glycolipids-enriched membrane lipid rafts. *J. Virol.* 74, 3264-3272.

Nguyen DH and Taub D (2002) CXCR4 function requires membrane cholesterol: implications for HIV infection. *J. Immunol.* 168, 4121-4126.

Nieva JL and Agirre A (2003) Are fusion peptides a good model to study viral cell fusion? *Biochim. Biophys. Acta* 1614, 104-115.

Ofek G, Tang M, Sambor A, Katinger H, Mascola JR, Wyatt R, and Kwong PD (2004) Structure and mechanistic analysis of the anti-human immunodeficiency virus type 1 antibody 2F5 in complex with its gp41 epitope. *J. Virol.* 78, 10724-10737.

O'Hara BM and Olson WC (2002) HIV entry inhibitors in clinical development. *Curr. Opin. Pharmacol.* 2, 523-528.

Ono A and Freed EO (2001) Plasma membrane rafts play a critical role in HIV-1 assembly and release. *Proc. Natl. Acad. Sci. USA* 98, 13925-13930.

Otaka A, Nakamura M, Nameki D, Kodama E, Uchiyama S, Nakamura S, Nakano H, Tamamura H, Kobayashi Y, Matsuoka M, and Fujii N (2002) Remodeling of gp41-C34 peptide leads to highly effective inhibitors of the fusion of HIV-1 with target cells. *Angew. Chem. Int. Edit.* 41, 2938-2940.

O'Toole PJ, Wolfe C, Ladha S, and Cherry RJ (1999) Rapid diffusion of spectrin bound to a lipid surface. *Biochim. Biophys. Acta* 1419, 64-70.

Palella FJ, Delaney KM, Moorman AC, Loveless MO, Fuhrer J, Satten GA, Aschman DJ, Holmberg SD, and the HIV outpatient study investigators (1998) Declining morbidity and mortality among patients with advanced human immunodeficiency virus infection. *N. Eng. J. Med.* 338, 853-860.

Palfrey HC and Waseem A (1985) Protein kinase C in the human erythrocyte. Translocation to the plasma membrane and phosphorylation of bands 4.1 and 4.9 and other membrane proteins. *J. Biol. Chem.* 260, 16021-16029.

Parker CE, Deterding LJ, Hager-Braun C, Binley JM, Schülke N, Katinger H, Moore JP, and Tomer KB (2001) Fine definition of the epitope on the gp41 glycoprotein of human immunodeficiency virus type 1 for the neutralizing monoclonal antibody 2F5. *J. Virol.* 75, 10906-10911.

Pascual R, Contreras M, Fedorov A, Prieto M, and Villalaín J (2005a) Interaction of a peptide derived from the N-heptad repeat region of gp41 env ectodomain with model membranes. Modulation of phospholipid phase behaviour. *Biochemistry* 44, 14275-14288.

Pascual R, Moreno MR, and Villalaín J (2005b) A peptide pertaining to the loop segment of human immunodeficiency virus gp41 binds and interacts with model biomembranes: implications for the fusion mechanism. *J. Virol.* 79, 5142-5152.

Pécheur EI, Sainte-Marie J, Bienvenüe A, and Hoekstra D (1999) Peptides and membrane fusion: towards an understanding of the molecular mechanism of protein-induced fusion. *J. Membr. Biol.* 167, 1-17.

Peiris JSM, Lai ST, Poon LLM, Guan Y, Yam LYC, Lim W, Nicholls J, Yee WKS, Yan WW, Cheung MT, et al. (2003) Coronavirus as a possible cause of severe acute respiratory syndrome. *Lancet* 361, 1319-1325.

Peisajovich SG, Epanand RF, Pritsker M, Shai Y, and Epanand RM (2000) The polar region consecutive to the HIV fusion peptide participates in membrane fusion. *Biochemistry* 39, 1826-1833.

Peisajovich SG and Shai Y (2002) New insights into the mechanism of virus-induced membrane fusion. *Trends Biochem. Sci.* 27, 183-190.

Pellegrin I, Legrand E, Neau D, Pascal B, Masquelier B, Pellegrin J-L, Ragnaud J-M, Bernard N, and Fleury HJA (1996) Kinetics of appearance of neutralizing antibodies in 12 patients with primary or recent HIV-1 infection and relationship with plasma and cellular viral loads. *J. Acquir. Immune Def. Synd.* 11, 438-447.

Percherancier Y, Lagane B, Palnchenaukt T, Staropoli I, Altmeyer R, Virelizier J-L, Arenzana-Seisdedos F, Hoessli DC, and Bachelier F (2003) HIV-1 entry into T-cells is not dependent on CD4 and CCR5 localization to sphingolipid-enriched, detergent-resistant, raft membrane domains. *J. Biol. Chem.* 278, 3153-3161.

Persson S, Killian JA, and Lindblom G (1998) Molecular ordering of interfacially localized tryptophan analogs in ester- and ether-lipid bilayers studied by ²H-NMR. *Biophys. J.* 75, 1365-1371.

Phogat S, Wyatt RT, and Karlsson Hedestam GB (2007) Inhibition of HIV-1 entry by antibodies: potential viral and cellular targets. *J. Intern. Med.* 262, 26-43.

Pickl WF, Pimentel-Muiños FX, and Seed B (2001) Lipid rafts and pseudotyping. *J. Virol.* 75, 7175-7183.

Pike LJ (2004) Lipid rafts: heterogeneity on the high seas. *Biochem. J.* 378, 281-292.

Pilgrim AK, Pantaleo G, Cohen OJ, Fink LM, Zhou JY, Zhou JT, Bolognesi DP, Fauci AS, and Montefiori DC (1997) Neutralizing antibody responses to human immunodeficiency virus type 1 in primary infection and long-term-nonprogressive infection. *J. Infect. Dis.* 176, 924-932.

Popik W, Alce TM, and Au W-C (2002) Human immunodeficiency virus type 1 uses lipid raft-colocalized CD4 and chemokine receptors for productive entry into CD4⁺ T cells. *J. Virol.* 76, 4709-4722.

Prabakaran P, Xiao X, and Dimitrov DS (2004) A model of the ACE2 structure and function as a SARS-CoV receptor. *Biochem. Biophys. Res. Commun.* 314, 235-241.

Pralle A, Keller P, Florin E-L, Simons K, and Hörber JKH (2000) Sphingolipid-cholesterol rafts diffuse as small entities in the plasma membrane of mammalian cells. *J. Cell Biol.* 148, 997-1007.

Rabenstein M and Shin Y-K (1995) A peptide from the heptad repeat of human immunodeficiency virus gp41 shows both membrane binding and coiled-coil formation. *Biochemistry* 34, 13390-13397.

Rajendran L and Simons K (2005) Lipid rafts and membrane dynamics. *J. Cell Sci.* 118, 1099-1102.

Reeves JD, Gallo SA, Ahmad N, Miamidian JL, Harvey PE, Sharron M, Pöhlmann, Sfakianos JN, Derdeyn CA, Blumenthal R, Hunter E, and Doms RW (2002) Sensitivity of HIV-1 to entry inhibitors correlates with envelope/coreceptor affinity, receptor density, and fusion kinetics. *Proc. Natl. Acad. Sci. USA* 99, 16249-16254.

Reeves JD and Piefer AJ (2005) Emerging drug targets for antiretroviral therapy. *Drugs* 65, 1747-1766.

Richman DD, Wrin T, Little SJ, and Petropoulos CJ (2003) Rapid evolution of the neutralizing antibody response to HIV type 1 infection. *Proc. Natl. Acad. Sci. USA* 100, 4144-4149.

Rimsky LT, Shugars DC, and Matthews TJ (1998) Determinants of human immunodeficiency virus type 1 resistance to gp41-derived inhibitory peptides. *J. Virol.* 72, 986-993.

Robertson D (2003) US FDA approves new class of HIV therapeutics. *Nat. Biotech.* 21, 470-471.

Rodriguez N, Pincet F, and Cribier S (2005) Giant vesicles formed by gentle hydration and electroformation: a comparison by fluorescence microscopy. *Colloid Surf. B* 42, 125-130.

Root MJ, Kay MS, and Kim PS (2001) Protein design of an HIV-1 entry inhibitor. *Science* 291, 884-888.

Rota PA, Oberste MS, Monroe SS, Nix WA, Campagnoli R, Icenogle JP, Peñaranda S, Bankamp B, Maher K, Chen M et al. (2003) Characterization of a novel coronavirus associated with severe acute respiratory syndrome. *Science* 300, 1394-1399.

Ryu J-R, Jin B-S, Suh M-J, Yoo Y-S, Yoon SH, Woo E-R, and Yu YG (1999) Two interaction modes of the gp41-derived peptides with gp41 and their correlation with antimembrane fusion activity. *Biochem. Biophys. Res. Commun.* 265, 625-629.

Sackett K and Shai Y (2002) The HIV-1 gp41 N-terminal heptad repeat plays an essential role in membrane fusion. *Biochemistry* 41, 4678-4685.

Sackett K and Shai Y (2003) How structure correlates to function for membrane associated HIV-1 gp41 constructs corresponding to the N-terminal half of the ectodomain. *J. Mol. Biol.* 333, 47-58.

Sáez-Cirion A, Nir S, Lorizate M, Agirre A, Cruz A, Pérez-Gil J, and Nieva JL (2002) Sphingomyelin and cholesterol promote HIV-1 gp41 pretransmembrane sequence surface aggregation and membrane restructuring. *J. Biol. Chem.* 277, 21776-21785.

Sáez-Cirion A, Arrondo JLR, Gómara MJ, Lorizate M, Iloro I, Melikyan G, and Nieva JL (2003) Structural and functional roles of HIV-1 gp41 pretransmembrane sequence segmentation. *Biophys. J.* 85, 3769-3780.

Sainz Jr B, Rausch JM, Gallaher WR, Garry RF, and Wimley WC (2005a) Identification and characterization of the putative fusion peptide of the severe acute respiratory syndrome-associated coronavirus spike protein. *J. Virol.* 79, 7195-7206.

Sainz Jr B, Rausch JM, Gallaher WR, Garry RF, and Wimley WC (2005b) The aromatic domain of the coronavirus class I viral fusion protein induces membrane permeabilization: putative role during viral entry. *Biochemistry* 44, 947-958.

Salzwedel K, West JT, and Hunter E (1999) A conserved tryptophan-rich motif in the membrane-proximal region of the human immunodeficiency virus type 1 gp41 ectodomain is important for env-mediated fusion and virus infectivity. *J. Virol.* 73, 2469-2480.

Sánchez-Martínez S, Lorizate M, Katinger H, Kunert R, Basañez G, and Nieva JL (2006a) Specific phospholipid recognition by human immunodeficiency virus type-1 neutralizing anti-gp41 2F5 antibody. *FEBS Lett.* 580, 2395-2399.

Sánchez-Martínez S, Lorizate M, Katinger H, Kunert R, and Nieva JL (2006b) Membrane association and epitope recognition by HIV-1 neutralizing anti-gp41 2F5 and 4E10 antibodies. *Aids Res. Hum. Retrovir.* 22, 998-1006.

Santos NC, Prieto M, and Castanho MARB (1998) Interaction of the major epitope region of HIV protein gp41 with membrane model systems. A fluorescence spectroscopy study. *Biochemistry* 37, 8674-8682.

Santos NC, Prieto M, and Castanho MARB (2003) Quantifying molecular partition into model systems of biomembranes: an emphasis on optical spectroscopic methods. *Biochim. Biophys. Acta* 1612, 123-135.

Schibli DJ, Montelaro RC, and Vogel HJ (2001) The membrane-proximal tryptophan-rich region of the HIV glycoprotein, gp41, forms a well-defined helix in dodecylphosphocholine micelles. *Biochemistry* 40, 9570-9578.

Schols D, Claes S, Hatse S, Princen K, Vermeire K, De Clercq E, Skerlj R, Bridger G, Calandra G (2003) Anti-HIV activity profile of AMD070, an orally bioavailable CXCR4 antagonist. In Proceedings of the 14th international conference on antiviral research. Savannah, GA, USA, 27 April-1 May 2003; *Antiviral Res.* 57, A39.

Schütz GJ, Kada G, Ph.Pastushenko V, and Schindler H (2000) Properties of lipid microdomains in a muscle cell membrane visualized by single molecule microscopy. *Embo J.* 19, 892-901.

Shiratsuchi A, Umeda M, Ohba Y, and Nakanishi Y (1997) Recognition of phosphatidylserine on the surface of apoptotic spermatogenic cells and subsequent phagocytosis by sertoli cells of the rat. *J. Biol. Chem.* 272, 2354-2358.

Shnaper S, Sackett K, Gallo SA, Blumenthal R, and Shai Y (2004) The C- and the N-terminal regions of glycoprotein 41 ectodomain fuse membranes enriched and not enriched with cholesterol, respectively. *J. Biol. Chem.* 279, 18526-18534.

Si Z, Madani N, Cox JM, Chruma JJ, Klein JC, Schon A, Phan N, Wang L, Biorn AC, Cocklin S, et al. (2004) Small-molecule inhibitors of HIV-1 entry block receptor-induced conformational changes in the viral envelope glycoproteins. *Proc. Natl. Acad. Sci. USA* 101, 5036-5041.

Silvius JR (2003) Fluorescence energy transfer reveals microdomain formation at physiological temperatures in lipid mixtures modelling the outer leaflet of the plasma membrane. *Biophys. J.* 85, 1034-1045.

Simons K and Ikonen E (1997) Functional rafts in cell membranes. *Nature* 387, 569-572.

Simons K and Vaz WLC (2004) Model systems, lipid rafts, and cell membranes. *Annu. Rev. Biophys. Biomolec. Struct.* 33, 269-295.

Singer SJ and Nicolson GL (1972) The fluid mosaic model of the structure of cell membranes. *Science* 175, 720-731.

Snijder EJ, Bredenbeek PJ, Dobbe JC, Thiel V, Ziebuhr J, Poon LLM, Guan Y, Rozanov M, Spaan WJM, and Gorbalenya AE (2003) Unique and conserved features of genome and proteome of SARS-coronavirus, an early split-off from the coronavirus group 2 lineage. *J. Mol. Biol.* 331, 991-1004.

Spink CH, Manley S, and Breed M (1996) Thermodynamics of transfer of cholesterol from gel to fluid phases of phospholipid bilayer. *Biochim. Biophys. Acta* 1279, 190-196.

Stadler K, Massignani V, Eickmann M, Becker S, Abrignani S, Klenk H-D, and Rappuoli R (2003) SARS-beginning to understand a new virus. *Nat. Rev. Microbiol.* 1, 209-218.

Stiegler G, Kunert R, Purtscher M, Wolbank S, Voglauer R, Steindl F, and Katinger H (2001) A potent cross-clade neutralizing human monoclonal antibody against a novel epitope on gp41 of human immunodeficiency virus type 1. *Aids Res. Hum. Retrovir.* 17, 1757-1765.

Stolk LML and Lüers JFJ (2004) Increasing number of anti-HIV drugs but no definite cure. Review of anti-HIV drugs. *Pharm. World Sci.* 26, 133-136.

Suárez T, Gallaher WR, Agirre A, Goñi FM, and Nieva JL (2000a) Membrane interface-interacting sequences within the ectodomain of the human immunodeficiency virus type 1 envelope glycoprotein: putative role during viral fusion. *J. Virol.* 74, 8038-8047.

Suárez T, Nir S, Goñi FM, Saéz-Cirion A, and Nieva JL (2000b) The pre-transmembrane region of the human immunodeficiency virus type 1 glycoprotein: a novel fusogenic sequence. *FEBS Lett.* 477, 145-149.

Supekar VM, Bruckmann C, Ingallinella P, Bianchi E, Pessi A and Carfi A (2004) Structure of a proteolytically resistant core from the severe acute respiratory syndrome coronavirus S2 fusion protein. *Proc. Natl. Acad. Sci. USA* 101, 17958-17963.

Tagat JR, McCombie SW, Nazareno D, Labroli MA, Xiao Y, Steensma RW, Strizki JM, Baroudy BM, Cox K, Lachowicz J, et al. (2004) Piperazine-based CCR5 antagonists as HIV-1 inhibitors. IV. Discovery of 1-[(4,6-Dimethyl-5-pyrimidinyl)carbonyl]-4-[4-{2-methoxy-1(R)-4-(trifluoromethyl)-phenyl}ethyl-3(S)-methyl-1-piperazinyl]-4-methylpiperidine (Sch-417690/Sch-D), a potent, highly selective, and orally bioavailable CCR5 antagonist. *J. Med. Chem.* 47, 2405-2408.

Tamm LK and Han X (2000) Viral fusion peptides: a tool set to disrupt and connect biological membranes. *Biosci. Rep.* 20, 501-518.

Tamm LK, Han X, Li Y, and Lai AL (2002) Structure and function of membrane fusion peptides. *Biopolymers (Pep. Sci.)* 66, 249-260.

Tan K, Liu J-H, Wang J-H, Shen S, and Lu M (1997) Atomic structure of a thermostable subdomain of HIV-1 gp41. *Proc. Natl. Acad. Sci. USA* 94, 12303-12308.

Tan ELC, Ooi EE, Lin C-Y, Tan HC, Ling AE, Lim B, and Stanton LW (2004) Inhibition of SARS coronavirus infection in vitro with clinically approved antiviral drugs. *Emerg. Infect. Dis.* 10, 581-586.

To KF and Lo AWI (2004) Exploring the pathogenesis of severe acute respiratory syndrome (SARS): the tissue distribution of the coronavirus (SARS-CoV) and its putative receptor, angiotensin-converting enzyme 2 (ACE2). *J. Pathol.* 203, 740-743.

Tremblay CL, Giguel F, Kollmann C, Guan Y, Chou T-C, Baroudy BM, and Hirsch MS (2002) Anti-human immunodeficiency virus interactions of SCH-C (SCH 351125), a CCR5 antagonist, with other antiretroviral agents in vitro. *J. Virol.* 46, 1336-1339.

Tripet B, Howard MW, Jobling M, Holmes RK, Holmes KV, and Hodges RS (2004) Structural characterization of the SARS-coronavirus spike S fusion protein core. *J. Biol. Chem.* 279, 20836-20849.

Trivedi VD, Cheng S-F, Wu C-W, Karthikeyan R, Chen C-J, and Chang D-K (2003) The LLSGIV stretch of the N-terminal region of HIV-1 gp41 is critical for binding to a model peptide, T20. *Protein Eng.* 16, 311-317.

Trkola A, Pomales AB, Yuan H, Korber B, Maddon PJ, Allaway GP, Katinger H, Barbas III CF, Burton DR, Ho DD, and Moore JP (1995) Cross-clade neutralization of primary isolates of human immunodeficiency virus type 1 by human monoclonal antibodies and tetrameric CD4-IgG. *J. Virol.* 69, 6609-6617.

Turner BG and Summers MF (1999) Structural biology of HIV. *J. Mol. Biol.* 285, 1-32.

UNAIDS/WHO AIDS epidemic update: December 2006.
http://www.unaids.org/en/HIV_data/epi2006/default.asp (Accessed September 14, 2007).

Vaishnav YN and Wong-Staal F (1991) The biochemistry of AIDS. *Annu. Rev. Biochem.* 60, 577-630.

Veach SL, Polozov IV, Gawrisch K, and Keller SL (2004) Liquid domains in vesicles investigated by NMR and fluorescence microscopy. *Biophys. J.* 86, 2910-2922.

Vermeire K, Zhang Y, Princen K, Hatse S, Samala MF, Dey K, Choi H-J, Ahn Y, Sosoma A, Snoeck R, et al. (2002) CADA inhibits human immunodeficiency virus and human herpes virus 7 replication by down-modulation of the cellular CD4 receptor. *Virology* 302, 342-353.

Viard M, Parolini I, Sargiacomo M, Fecchi K, Ramoni C, Ablan S, Ruscetti FW, Wang JM, and Blumenthal R (2002) Role of cholesterol in human immunodeficiency virus type 1 envelope protein-mediated fusion with host cells. *J. Virol.* 76, 11584-11595.

Vincent N, Genin C, and Malvoisin E (2002) Identification of a conserved domain of the HIV-1 transmembrane protein gp41 which interacts with cholesteryl groups. *Biochim. Biophys. Acta* 1567, 157-164.

Webster RG (2004) Wet markets-a continuing source of severe acute respiratory syndrome and influenza? *Lancet* 363, 234-236.

Wei X, Decker JM, Liu H, Zhang Z, Arani RB, Kilby JM, Saag MS, Wu X, Shaw GM, and Kappes JC (2002) Emergence of resistant human immunodeficiency virus type 1 in patients receiving fusion inhibitor (T-20) monotherapy. *Antimicrob. Agents Chemother.* 46, 1896-1905.

Weiss RA (2000) Getting to know HIV. *Trop. Med. and Int. Health* 5, A10-A15.

Weissenhorn W, Dessen A, Harrison SC, Skehel JJ, and Wiley DC (1997) Atomic structure of the ectodomain from HIV-1 gp41. *Nature* 387, 426-430.

Weng Y and Weiss CD (1998) Mutational analysis of residues in the coiled-coil domain of human immunodeficiency virus type 1 transmembrane protein gp41. *J. Virol.* 72, 9676-9682.

White SH and Wimley WC (1998) Hydrophobic interactions of peptides with membrane interfaces. *Biochim. Biophys. Acta* 1376, 339-352.

White SH, Ladokhin AS, Jayasinghe S, and Hristova K (2001) How membranes shape protein structure. *J. Biol. Chem.* 276, 32395-32398.

Wong SK, Li W, Moore MJ, Choe H, and Farzan M (2004) A 193-amino acid fragment of the SARS coronavirus S protein efficiently binds angiotensin-converting enzyme 2. *J. Biol. Chem.* 279, 3197-3201.

World Health Organization: Severe acute respiratory syndrome (SARS): status of the outbreak and lessons for the immediate future. CSR/WHO May 2003. http://www.who.int/csr/media/sars_wha.pdf (Accessed October 25, 2007).

World Health Organization: Summary table of SARS cases by country, 1 November 2002 - 7 August 2003. http://www.who.int/csr/sars/country/2003_08_15/en/. (Accessed October 25, 2007).

Wieprecht T, Apostolov O, Beyermann M, and Seelig J (1999) Thermodynamics of the α -helix-coil transition of amphipathic peptides in a membrane environment: implications for the peptide-membrane binding equilibrium. *J. Mol. Biol.* 294, 785-794.

Wild C, Oas T, McDanal C, Bolognesi D, and Matthews T (1992) A synthetic peptide inhibitor of human immunodeficiency virus replication: correlation between solution structure and viral inhibition. *Proc. Natl. Acad. Sci. USA* 89, 10537-10541.

Wild CT, Shugars DC, Greenwell TK, McDanal CB, and Matthews TJ (1994a) Peptides corresponding to a predictive α -helical domain of human immunodeficiency virus type 1 gp41 are potent inhibitors of virus infection. *Proc. Natl. Acad. Sci. USA* 91, 9770-9774.

Wild C, Dubay JW, Greenwell T, Baird T, Oas T, McDanal C, Hunter E, and Matthews T (1994b) Propensity for a leucine zipper-like domain of human immunodeficiency virus type 1 gp41 to form oligomers correlates with a role in virus-induced fusion rather than assembly of the glycoprotein complex. *Proc. Natl. Acad. Sci. USA* 91, 12676-12680.

Wild C, Greenwell T, Shugars D, Rimsky-Clarke L, and Matthews T (1995) The inhibitory activity of an HIV type 1 peptide correlates with its ability to interact with a leucine zipper structure. *Aids Res. Hum. Retrovir.* 11, 323-325.

Wimley WC and White SH (1993) Membrane partitioning: Distinguishing bilayer effects from the hydrophobic effect. *Biochemistry* 32, 6307-6312.

Wimley WC and White SH (1996) Experimentally determined hydrophobicity scale for proteins at membrane interfaces. *Nat. Struct. Biol.* 3, 842-848.

Wyatt R and Sodroski J (1998) The HIV-1 envelope glycoproteins: fusogens, antigens, and immunogens. *Science* 280, 1884-1888.

Wyatt R, Kwong PD, Desjardins E, Sweet RW, Robinson J, Hendrickson, and Sodroski JG (1998) The antigenic structure of the HIV gp120 envelope glycoprotein. *Nature* 393, 705-711.

Xiao X, Chakraborti S, Dimitrov AS, Gramatikoff K, and Dimitrov DS (2003) The SARS-CoV S glycoprotein: expression and functional characterization. *Biochem. Biophys. Res. Commun.* 312, 1159-1164.

Xiao X and Dimitrov DS (2004) The SARS-CoV S glycoprotein. *Cell. Mol. Life Sci.* 61, 2428-2430.

Xu Y, Zhang X, Matsuoka M, and Hattori T (2000) The possible involvement of CXCR4 in the inhibition of HIV-1 infection mediated by DP178/gp41. *FEBS Lett.* 487, 185-188.

Xu Y, Lou Z, Liu Y, Pang H, Tien P, Gao GF, and Rao Z (2004) Crystal structure of severe acute respiratory syndrome coronavirus spike protein fusion core. *J. Biol. Chem.* 279, 49414-49419.

Yamamoto N, Yang R, Yoshinaka Y, Amari S, Nakano T, Cinatl J, Rabenau H, Doerr HW, Hunsmann G, Otaka A, et al. (2004) HIV protease inhibitor nelfinavir inhibits replication of SARS-associated coronavirus. *Biochem. Biophys. Res. Commun.* 318, 719-725.

Yau W-M, Wimley WC, Gawrisch K, and White SH (1998) The preference of tryptophan for membrane interfaces. *Biochemistry* 37, 14713-14718.

Yerly S, Kaiser L, Race E, Bru J-P, Clavel F and Perrin L (1999) Transmission of antiretroviral-drug-resistant HIV-1 strains. *Lancet* 354, 729-733.

Yeni P (2006) Update on HAART in HIV. *J. Hepatol.* 44, S100-103.

Yu ITS, Li Y, Wong TW, Tam W, Chan AT, Lee JHW, Leung DY, and Ho T (2004) Evidence of airborne transmission of the severe acute respiratory syndrome virus. *N. Engl. J. Med.* 350, 1731-1739.

Yuan W, Craig S, Si Z, Farzan M, and Sodroski J (2004) CD4-induced T-20 binding to human immunodeficiency virus type 1 gp120 blocks interaction with the CXCR4 coreceptor. *J. Virol.* 78, 5448-5457.

Zachowski A (1993) Phospholipids in animal eukaryotic membranes: transverse asymmetry and movement. *Biochem. J.* 294, 1-14.

Zanetti G, Briggs JAG, Grünewald K, Sattentau QJ, Fuller SD (2006) Cryo-electron tomographic structure of an immunodeficiency virus envelope complex in situ. *PLoS Pathog.* 2, 790-797.

Zaslhoff M (2000) Reconstructing one of nature's designs. *Trends Pharmacol. Sci.* 21, 236-238.

Zhang XW and Yap YL (2004) Old drugs as lead compounds for a new disease? Binding analysis of SARS coronavirus main proteinase with HIV, psychotic and parasite drugs. *Bioorg. Med. Chem.* 12, 2517-2521.

Zhu J, Xiao G, Xu Y, Yuan F, Zheng C, Liu Y, Yan H, Cole DK, Bell JI, Rao Z, Tien P, and Gao GF (2004) Following the rule: formation of the 6-helix bundle of the fusion core from severe acute respiratory syndrome coronavirus spike protein and identification of potent peptide inhibitors. *Biochem. Biophys. Res. Commun.* 319, 283-288.

Zhu P, Liu J, Bess Jr J, Chertova E, Lifson JD, Grisé H, Ofek GA, Taylor KA, and Roux KH (2006) Distribution and three dimensional structure of AIDS virus envelope spikes. *Nature* 441, 847-852.

Zolla-Pazner S (2004) Identifying epitopes of HIV-1 that induce protective antibodies. *Nat. Rev. Immunol.* 4, 199-210.

Zubay GL (1998) *Biochemistry* (4ed), McGraw-Hill Companies (Inc.), Dubuque, IA, USA.

Zwick MB, Labrijn AF, Wang M, Spencehauer C, Saphire EO, Binley JM, Moore JP, Stiegler G, Katinger H, Burton DR, and Parren PWHI (2001) Broadly neutralizing antibodies targeted to the membrane-proximal external region of human immunodeficiency virus type 1 glycoprotein gp41. *J. Virol.* 75, 10892-10905.

Zwick MB, Jensen R, Church S, Wang M, Stiegler G, Kunert R, Katinger H, and Burton DR (2005) Anti-Human immunodeficiency virus type 1 (HIV-1) antibodies 2F5 and 4E10 require surprisingly few crucial residues in the membrane-proximal external region of glycoprotein gp41 to neutralize HIV-1. *J. Virol.* 79, 1252-1261.